FACULTAD DE INGENIERIA U.N.A.M.
DIVISION DE EDUCACION CONTINUA

A LOS ASISTENTES A LOS CURSOS

Las autoridades de la Facultad de Ingeniería, por conducto del jefe de la División de Educación Continua, otorgan una constancia de asistencia a quienes cumplan con los requisitos establecidos para cada curso.

El control de asistencia se llevará a cabo a través de la persona que le entregó las notas. Las inasistencias serán computadas por las autoridades de la División, con el fin de entregarle constancia solamente a los alumnos que tengan un mínimo de 80% de asistencias.

Pedimos a los asistentes recoger su constancia el día de la clausura. Estas se retendrán por el periodo de un año, pasado este tiempo la DECFI no se hará responsable de este documento.

Se recomienda a los asistentes participar activamente con sus ideas y experiencias, pues los cursos que ofrece la División están planeados para que los profesores expongan una tesis, pero sobre todo, para que coordinen las opiniones de todos los interesados, constituyendo verdaderos seminarios.

Es muy importante que todos los asistentes llenen y entreguen su hoja de inscripción al inicio del curso, información que servirá para integrar un directorio de asistentes, que se entregará oportunamente.

Con el objeto de mejorar los servicios que la División de Educación Continua ofrece, al final del curso deberán entregar la evaluación a través de un cuestionario diseñado para emitir juicios anónimos.

Se recomienda llenar dicha evaluación conforme los profesores impartan sus clases, a efecto de no llenar en la última sesión las evaluaciones y con esto sean más fehacientes sus apreciaciones.

Atentamente
División de Educación Continua.

PALACIO DE MINERIA

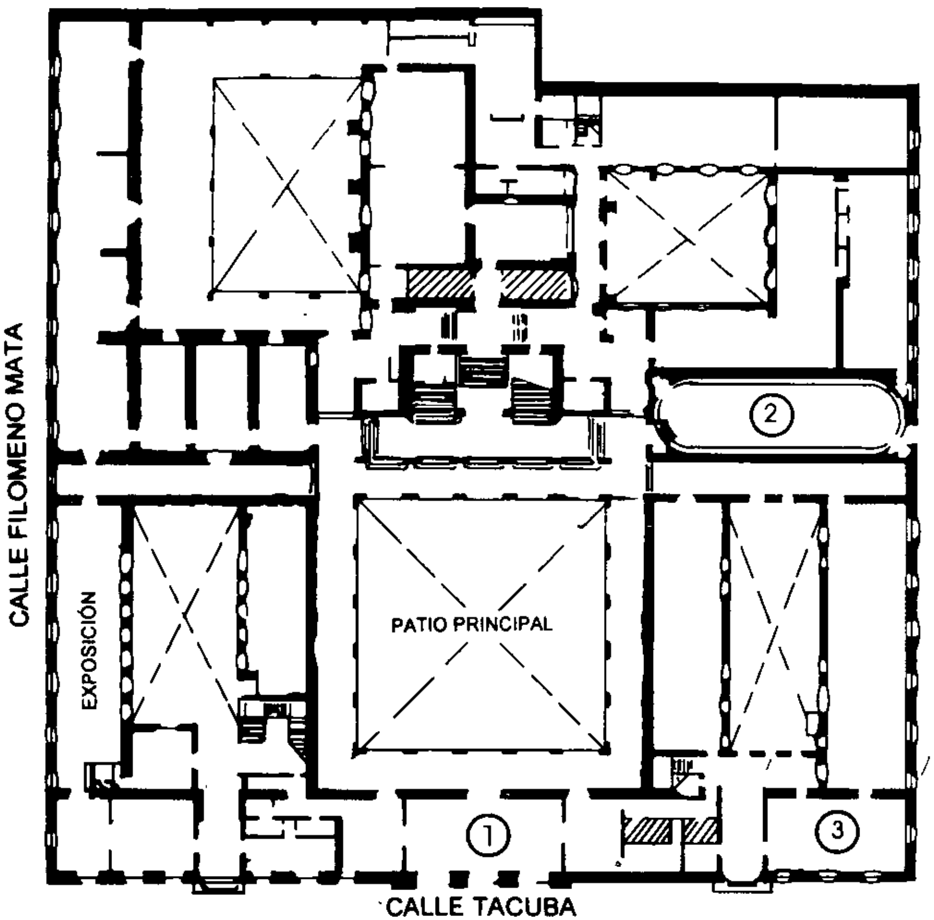

PLANTA BAJA

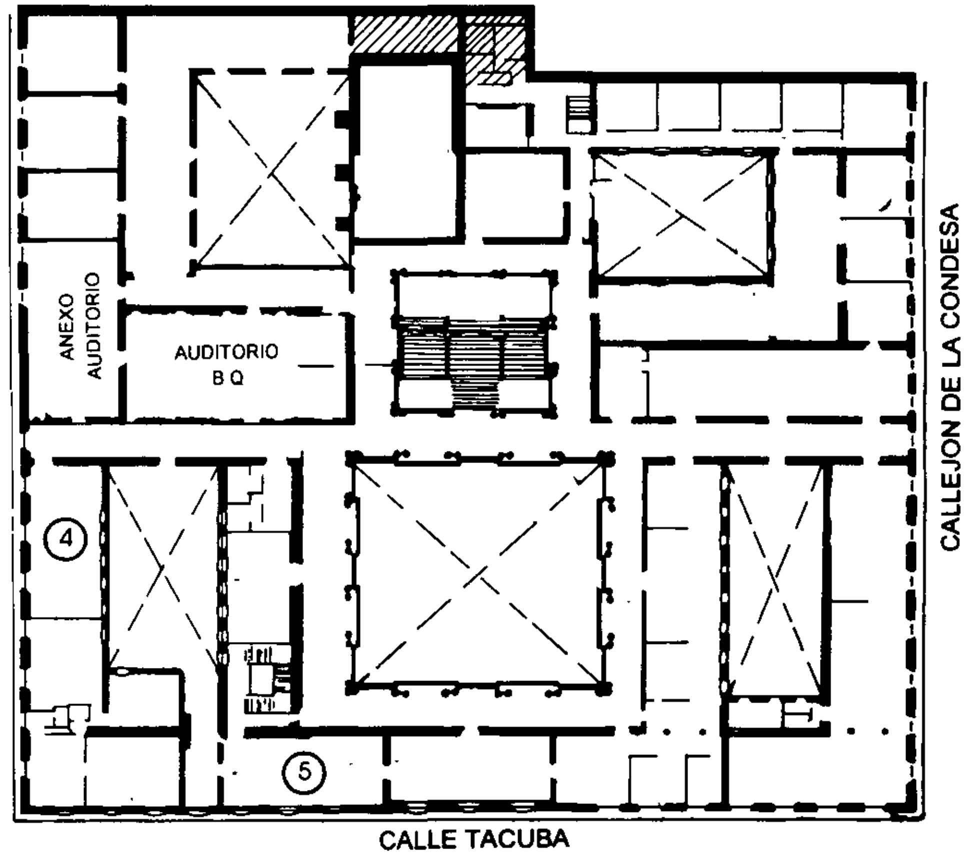

MEZZANINNE

PALACIO DE MINERIA

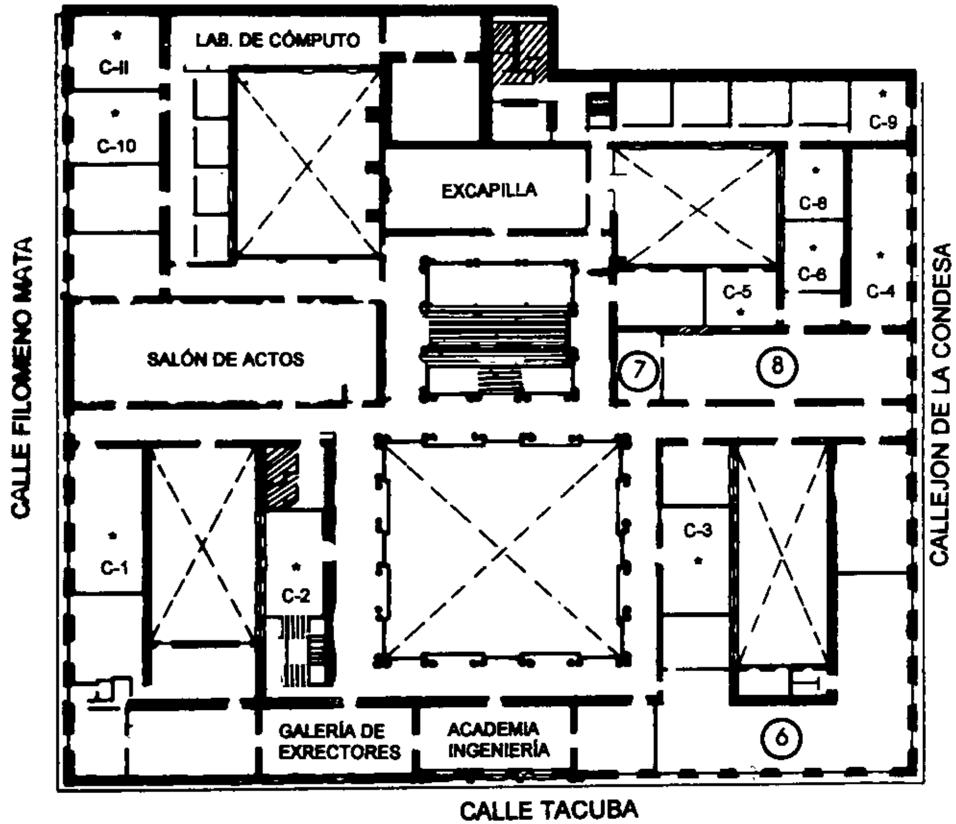

1er. PISO

GUÍA DE LOCALIZACIÓN

1. ACCESO
2. BIBLIOTECA HISTÓRICA
3. LIBRERÍA UNAM
4. CENTRO DE INFORMACIÓN Y DOCUMENTACIÓN "ING. BRUNO MASCANZONI"
5. PROGRAMA DE APOYO A LA TITULACIÓN
6. OFICINAS GENERALES
7. ENTREGA DE MATERIAL Y CONTROL DE ASISTENCIA
8. SALA DE DESCANSO

SANITARIOS

* AULAS

DIVISIÓN DE EDUCACIÓN CONTINUA
FACULTAD DE INGENIERÍA U.N.A.M.
CURSOS ABIERTOS

DIVISIÓN DE EDUCACIÓN CONTINUA

FACULTAD DE INGENIERIA U.N.A.M.
DIVISION DE EDUCACION CONTINUA

CURSOS ABIERTOS

XXV CURSO INTERNACIONAL DE INGENIERÍA SÍSMICA

MÓDULO III:

DISEÑO SÍSMICO DE PUENTES

TEMA

CIMENTACIONES RECTANGULARES

PALACIO DE MINERÍA
AGOSTO DE 1999

Palacio de Minería Calle de Tacuba 5 Primer piso Deleg. Cuauhtemoc 06000 Mexico, D.F. APDO. Postal M-2285
Telefonos 512-8955 512-5121 521-7335 521-1987 Fax 510-0573 521-4020 AL 26

CIMENTACIONES RECTANGULARES

$K_R = \alpha \beta K$

donde :

α = factor de forma
β = factor de desplante
K = coeficiente de rigidez para una cimentación circular

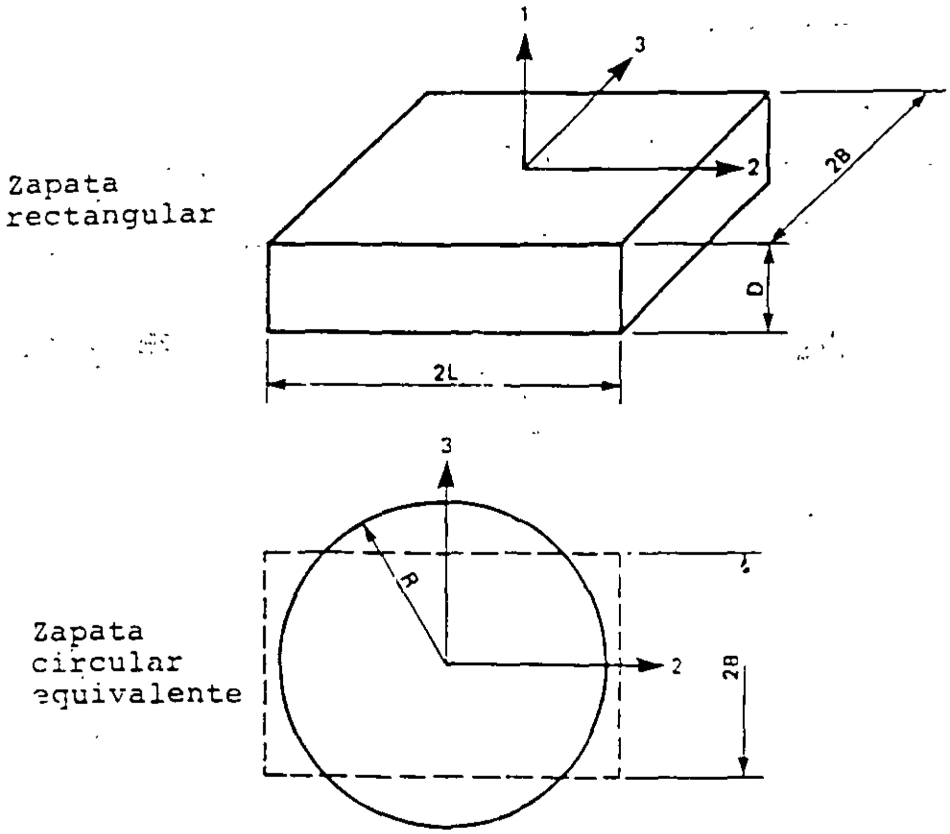

Radio equivalente

RADIOS EQUIVALENTES

TRASLACIÓN	$R_0 = \sqrt{4BL/\pi}$
ROTACIÓN (FLEXIÓN ALREDEDOR DE X)	$R_3 = \left[\frac{4BL\,(4B^2 + 4L^2)}{6\pi}\right]^{1/4}$
ROTACIÓN (FLEXIÓN ALREDEDOR DE Y)	$R_2 = \left[\frac{(2B)^3 + (2L)}{3\pi}\right]^{1/4}$
TORSIÓN	$R_1 = \left[\frac{(2B)\,(2L)^3}{3\pi}\right]^{1/4}$

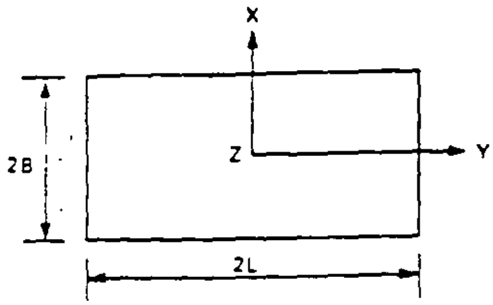

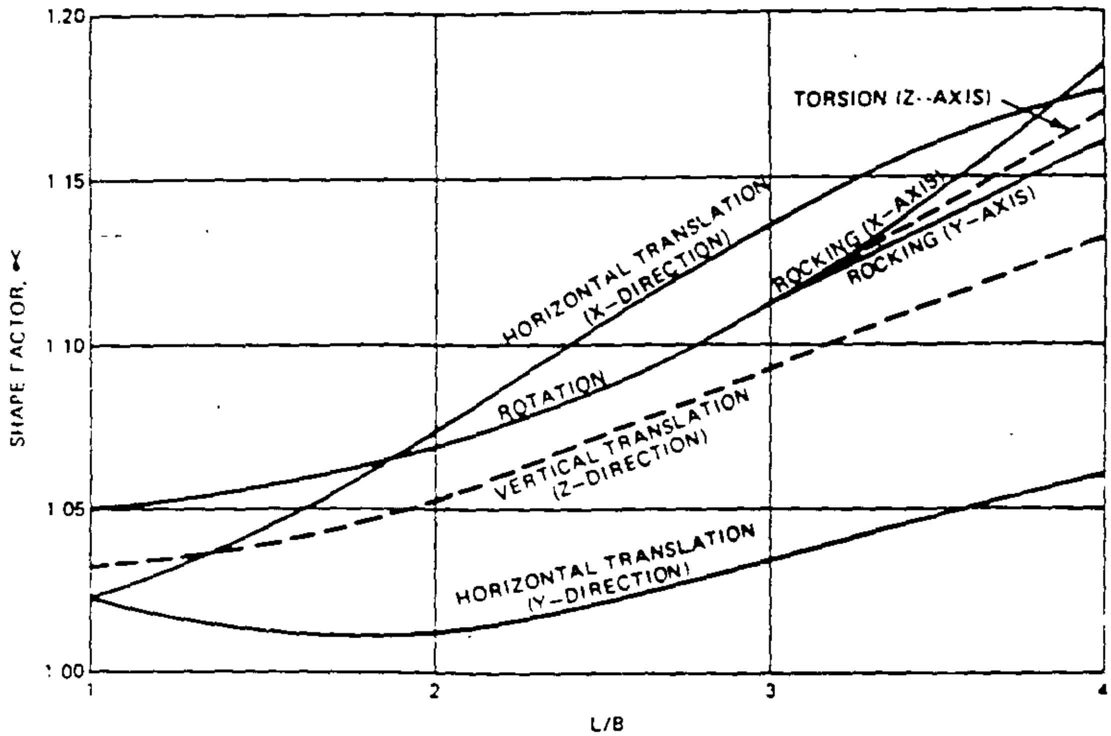

FACTOR DE FORMA

AEIC	Descripción: MODELO DE VOLADIZO	Hoja de
		Elaboró:
		Revisó:
		Fecha:

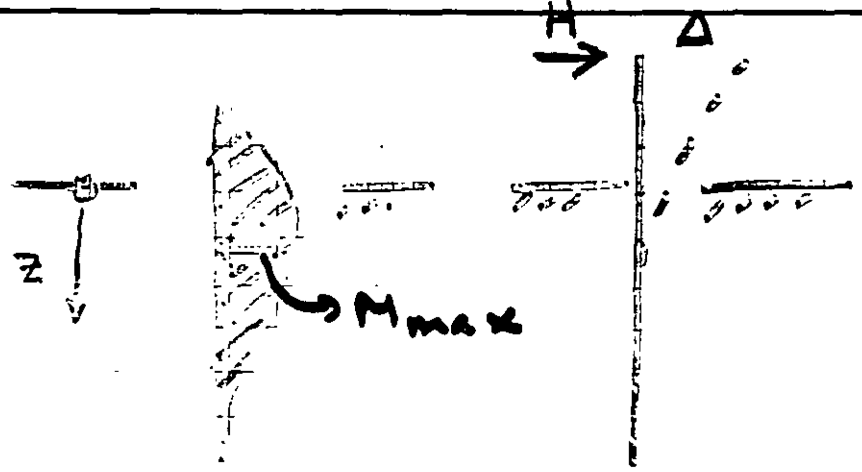

Momento deflexión

SISTEMA REAL

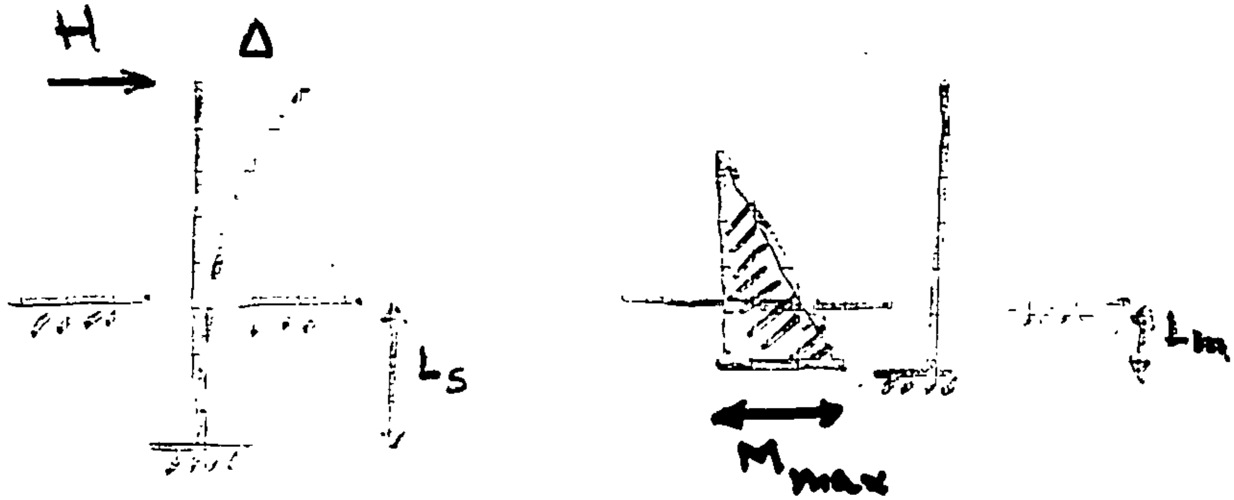

$L_s = 1.4R$ $L_m = 0.44R$

$L_s = 1.8R'$ $L_m = 0.78R'$

AEIC	Descripción: MOD LO DE VOLADIZO	Hoja de
		Elaboró:
		Revisó:
		Fecha:

$$R = \sqrt[4]{\frac{EI}{K_h}}$$ Suelos cohesivos

$$R' = \sqrt[5]{\frac{EI}{n_h}}$$ Suelos no cohesivos

$$n_h = \frac{d(K_h)}{dz}$$

K_h = módulo de reacción horizontal del suelo

$$K_h = K_h(N, c_u, \phi)$$

N = # de golpes

c_u = resistencia al cortante del suelo

ϕ = ángulo de fricción interna

EI = rigidez a flexión del pilote

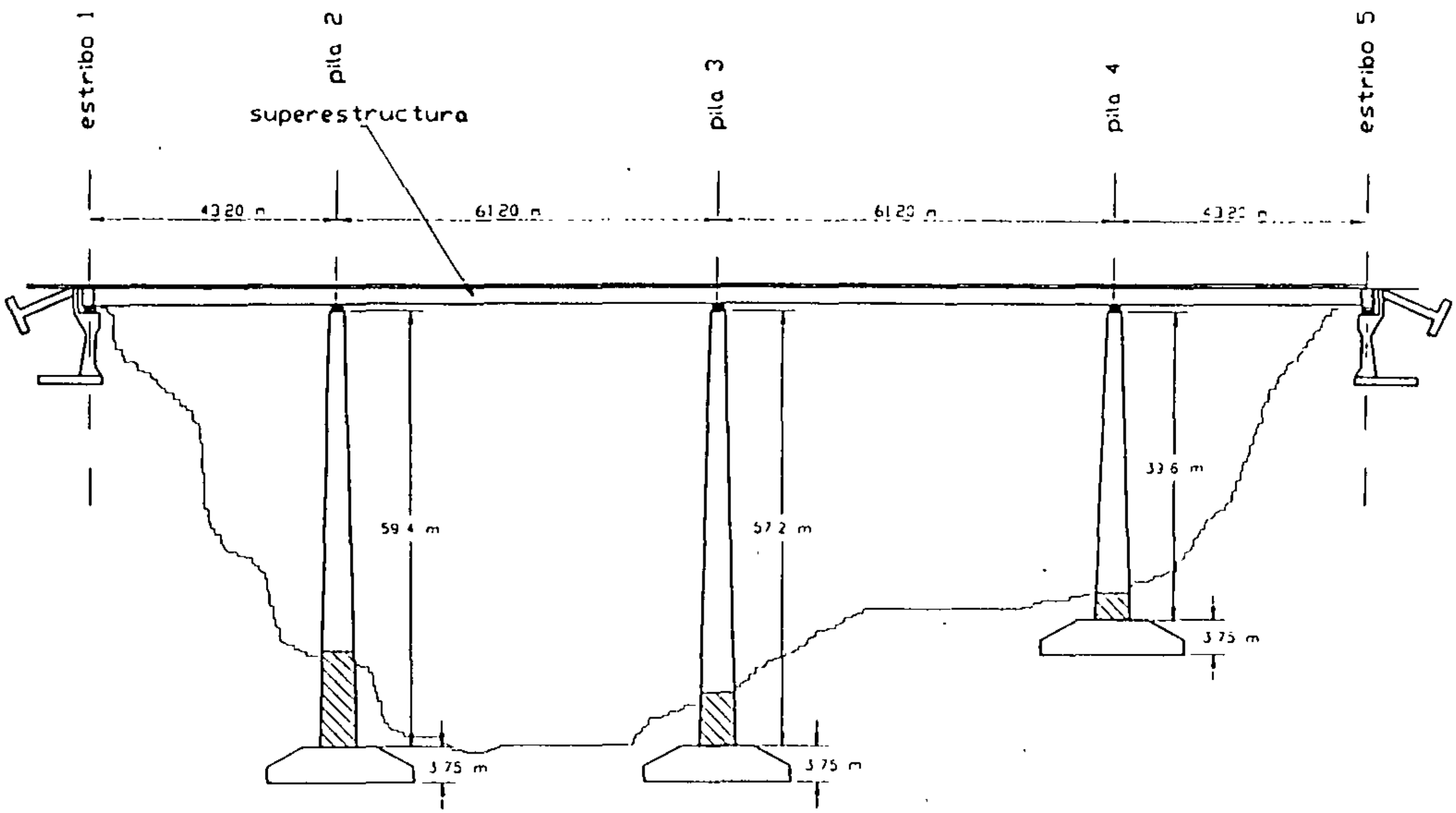
estribo 1
pila 2
pila 3
pila 4
estribo 5
superestructura
43.20 m
61.20 m
61.20 m
43.20 m
59.4 m
57.2 m
33.6 m
3.75 m
3.75 m
3.75 m

AEIC	Descripción: MODELO DE RES RTES N LA BASE	Hoja de
		Elaboró:
		Revisó:
		Fecha:

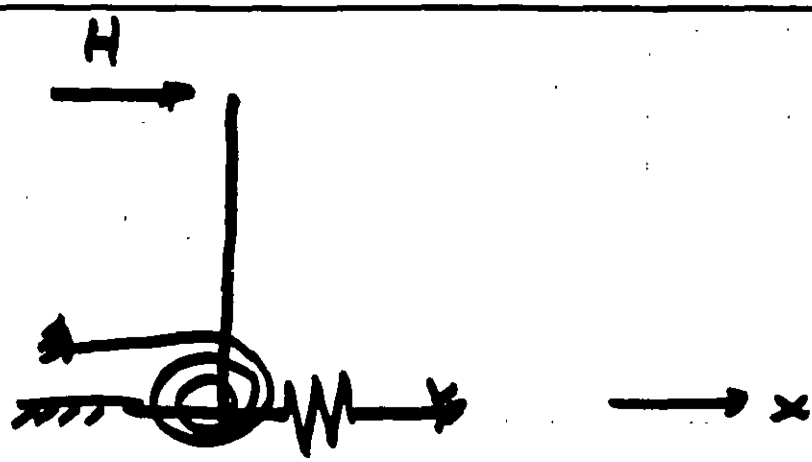

$$\begin{bmatrix} H \\ M \end{bmatrix} = \begin{bmatrix} K_{xx} & K_{x\theta} \\ K_{\theta x} & K_{\theta\theta} \end{bmatrix} \begin{Bmatrix} u_x \\ \theta \end{Bmatrix}$$

POULOS

BLANEY

KAYNIA

GOMEZ

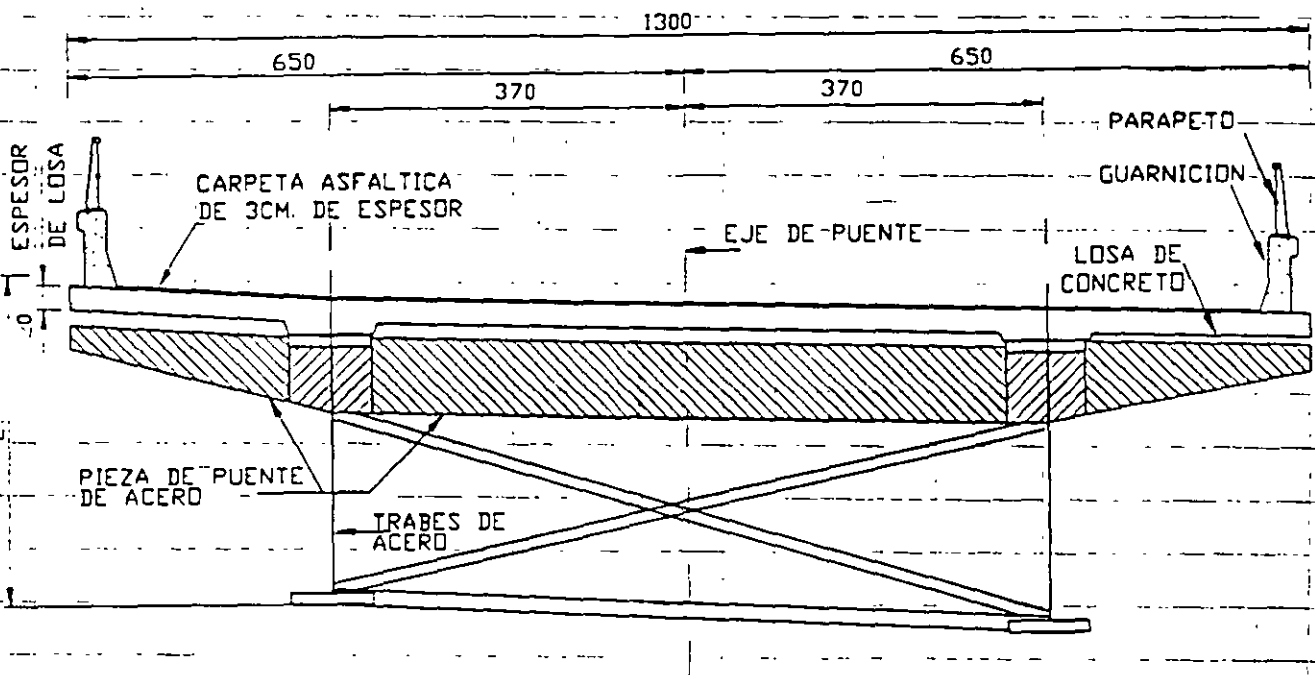

Dimensiones en cm

SECCION TRANSVERSAL DE LA COLUMNA

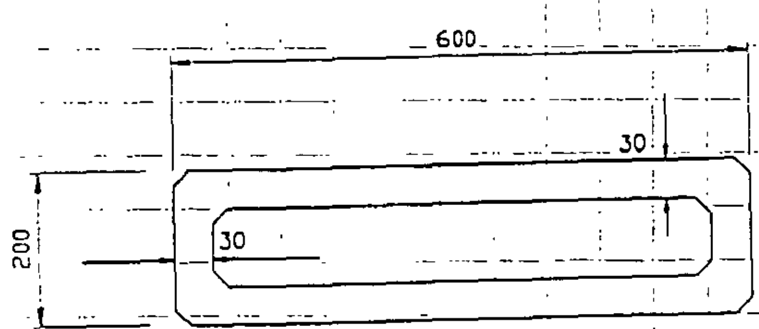

PARTE SUPERIOR

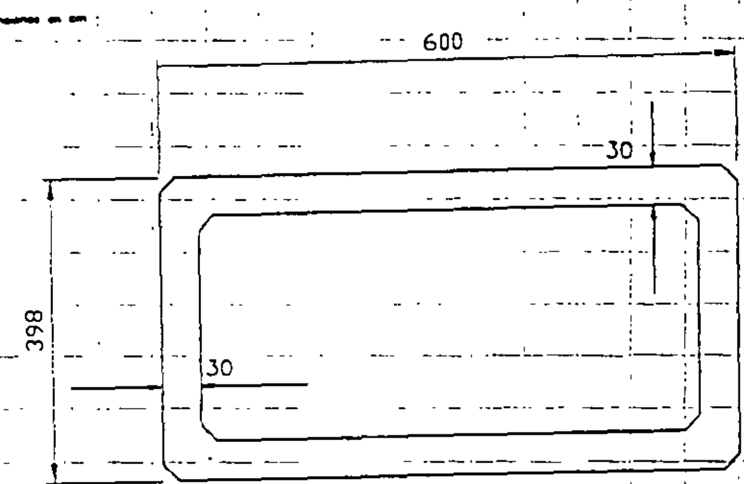

PARTE INFERIOR

METODO SIMPLIFICADO

ELEMENTO A DISEÑAR: Columna 2 del puente

PESO TOTAL: 774.18 ton

MASA TOTAL: 78.92 ton*s^2/m

$E = 14000\sqrt{250} = 2.2135 \times 10^5$ kg/cm^2 = 2.2135×10^6 ton/m^2

Rigidez lineal en el sentido de análisis

Rigidez lineal del marco en dirección longitudinal y transversal, considerando que la columna gira en su parte superior

$K_x = 856.03$

$K_y = 358.51$

Estos valores se determinaron con la expresión :

$$K = \frac{3EI}{H^3}$$

Rigidez lineal del marco en dirección longitudinal y transversal, sin considerar que gira la parte superior de la columna.

$K_x = 3500.12$

$K_y = 1434.04$

Estos valores se determinaron con la expresión :

$$K = \frac{12EI}{H^3}$$

Periodo natural de vibración

El periódo natural de vibración de la estructura se obtiene al aplicar la siguiente expresión :

$$T = 2\pi\sqrt{\frac{m}{K}}$$

donde ***m*** es la masa tributaria.

Con base en las rigideces calculadas anteriormente se obtienen los siguientes periodos, así como sus respectivos coeficientes de aceleración del terreno.

a) con los valores de rigideces que consideran giro en el extremo superior

$T_x = 1.89$ s $\quad a_o = 0.42$

$T_y = 2.95$ s $\quad a_o = 0.34$

b) con los valores de rigideces que <u>no</u> consideran giro en la parte superior de la columna

$T_x = 0.94$ s $\quad a_o = 0.60$

$T_y = 1.47$ s $\quad a_o = 0.48$

Fuerza lateral equivalente "P".

La fuerza lateral equivalente que se aplicará a la estructura se obtiene con la expresión :

$$P = \frac{a_o}{Q'} W$$

donde W es el peso de la masa tributaria, a_o es el coeficiente de aceleración del terreno y Q'es el factor de comportamiento sísmico. Con esta expresión se tiene que para:

$a_o = 0.42$ $P_x = 162.58$ ton
$a_o = 0.34$ $P_y = 131.61$ ton

$a_o = 0.60$ $P_x = 232.25$ ton
$a_o = 0.48$ $P_y = 185.80$ ton

Nota: Los coeficientes de aceleración del terreno se determinaron según el espectro de diseño correspondiente a la zona sísmica y al tipo de estructura.

DIAGRAMA DE MOMENTOS, METODO SIMPLIFICADO

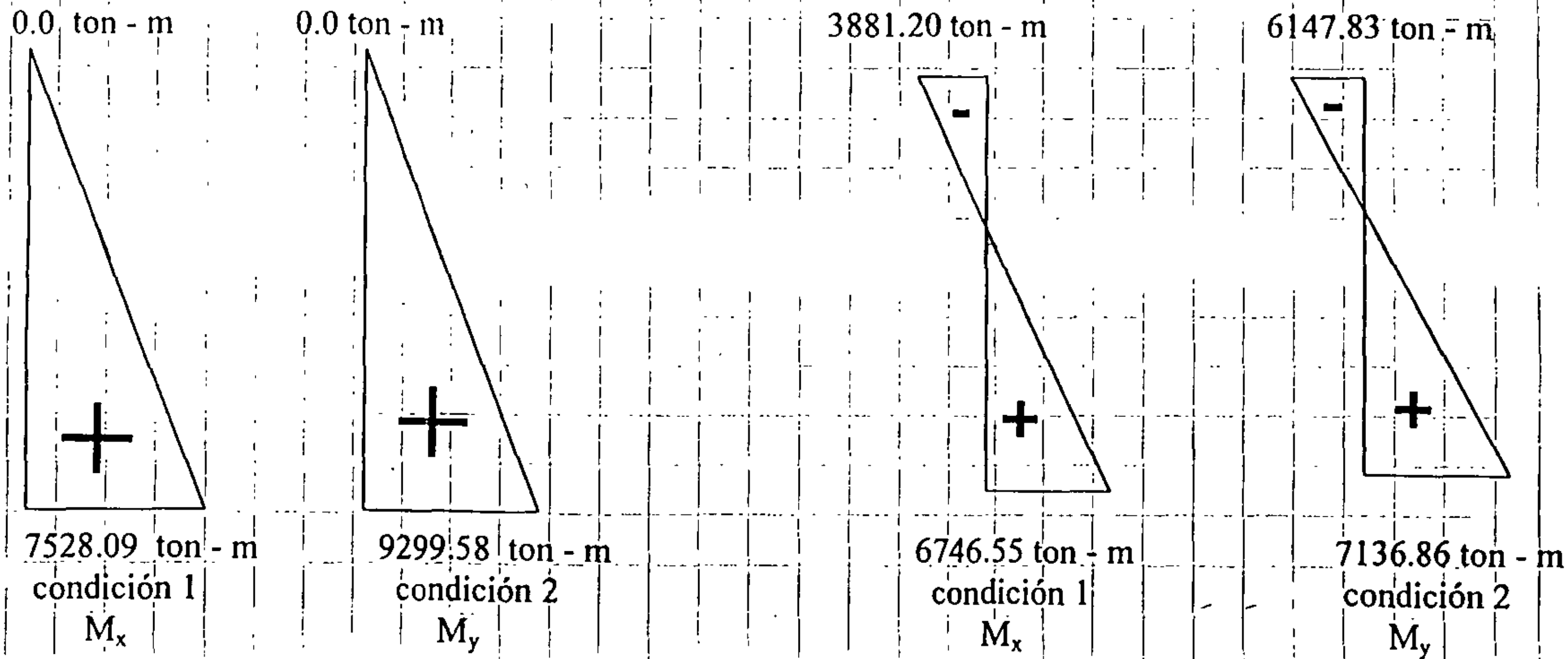

$$K = \frac{3EI}{H^3}$$

$$K = \frac{12EI}{H^3}$$

DIAGRAMA DE FUERZAS CORTANTES, METODO SIMPLIFICADO

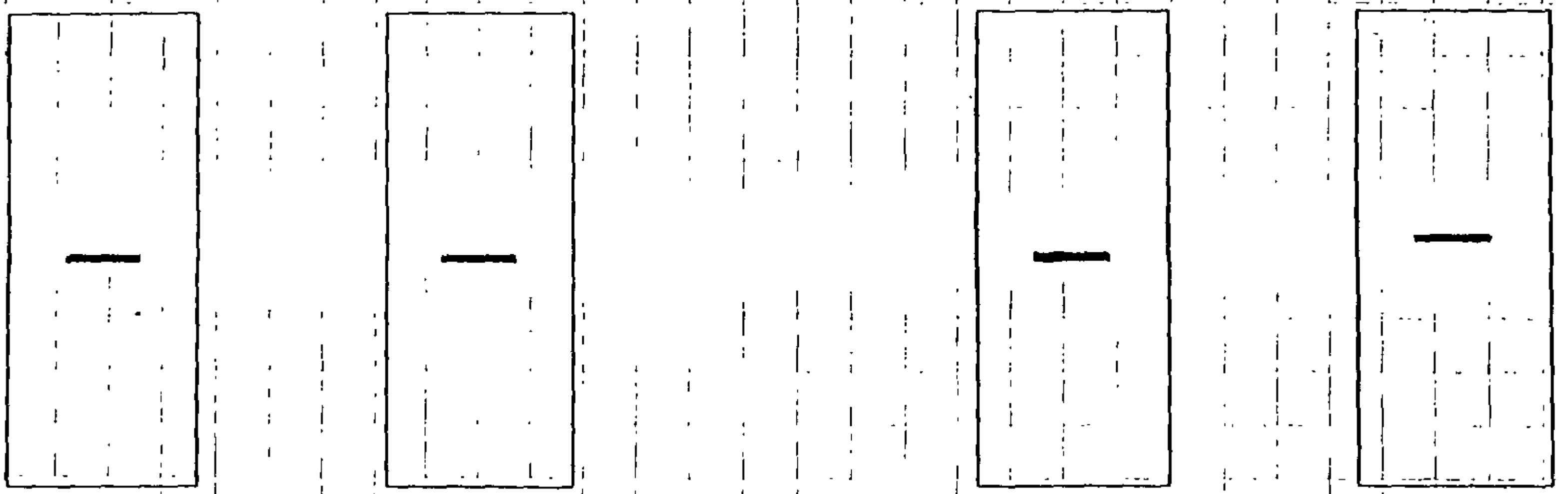

131.61 ton
condición 1
F_y

162.58 ton
condición 2
F_x

185.80 ton
condición 1
F_y

232.25 ton
condición 2
F_x

$$K = \frac{3EI}{H^3}$$

$$K = \frac{12EI}{H^3}$$

METODO DE LA CARGA UNIFORME

Características generales

LONGITUD TOTAL DEL PUENTE: 208.8 m

PENDIENTE LONGITUDINAL: -0.01

SUBESTRUCTURA: CONCRETO REFORZADO

SUPERESTRUCTURA: ACERO A-36

Características de los elementos estructurales

	ALTURA (m)	PESO (ton)
PILA 2	59.40	725.850
PILA 3	57.20	695.676
PILA 4	39.60	463.372

	LONGITUD (m)	PESO (ton)
SUPERESTRUCTURA	208.80	2641.278

PESO TOTAL: 4526.176 ton

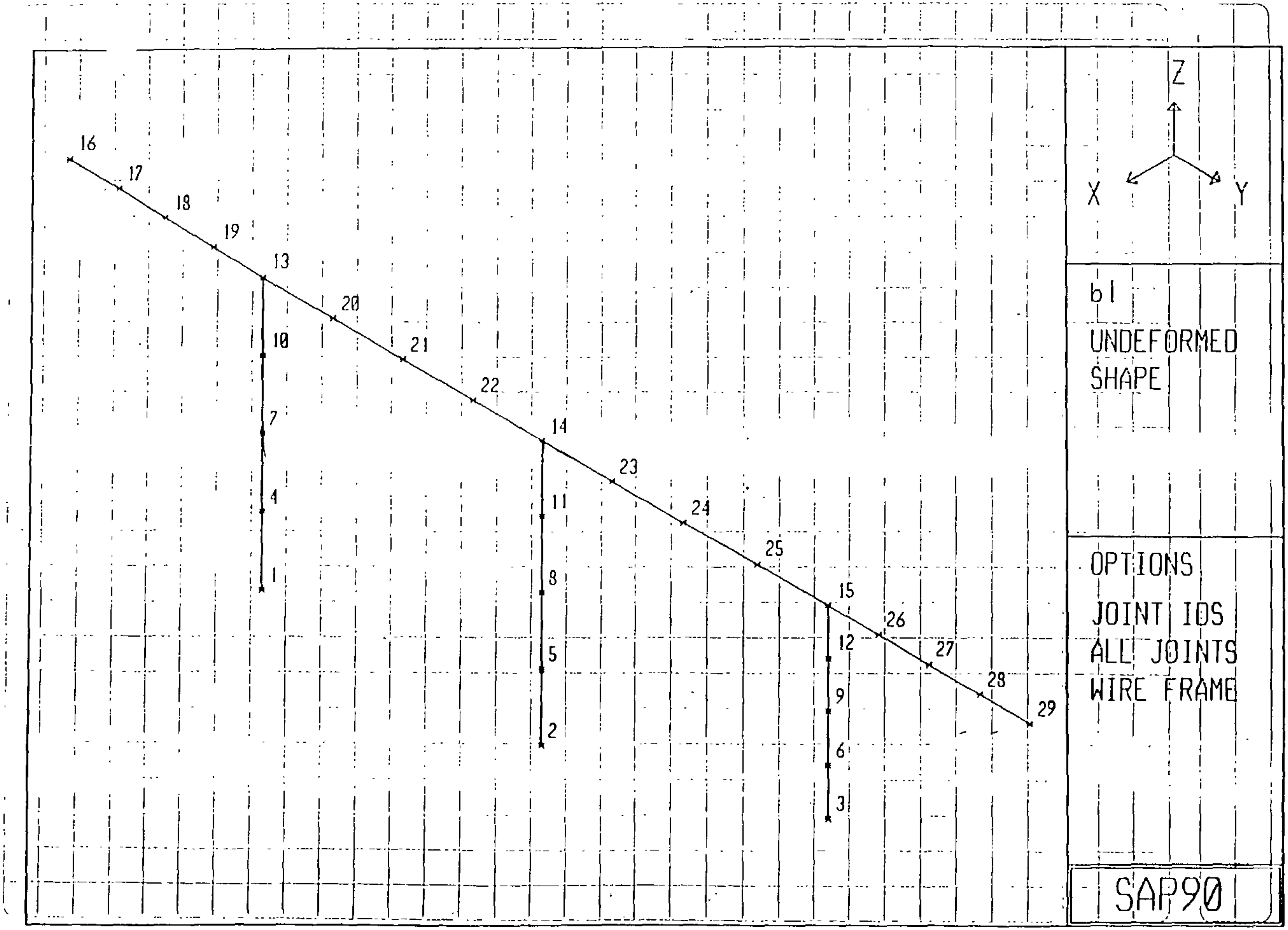
16
17
18
19
13
20
10
21
22
7
14
23
4
11
24
25
1
8
15
26
12
27
5
28
9
29
2
6
3
Z
X
Y
b1
UNDEFORMED
SHAPE
OPTIONS
JOINT IDS
ALL JOINTS
WIRE FRAME
SAP90

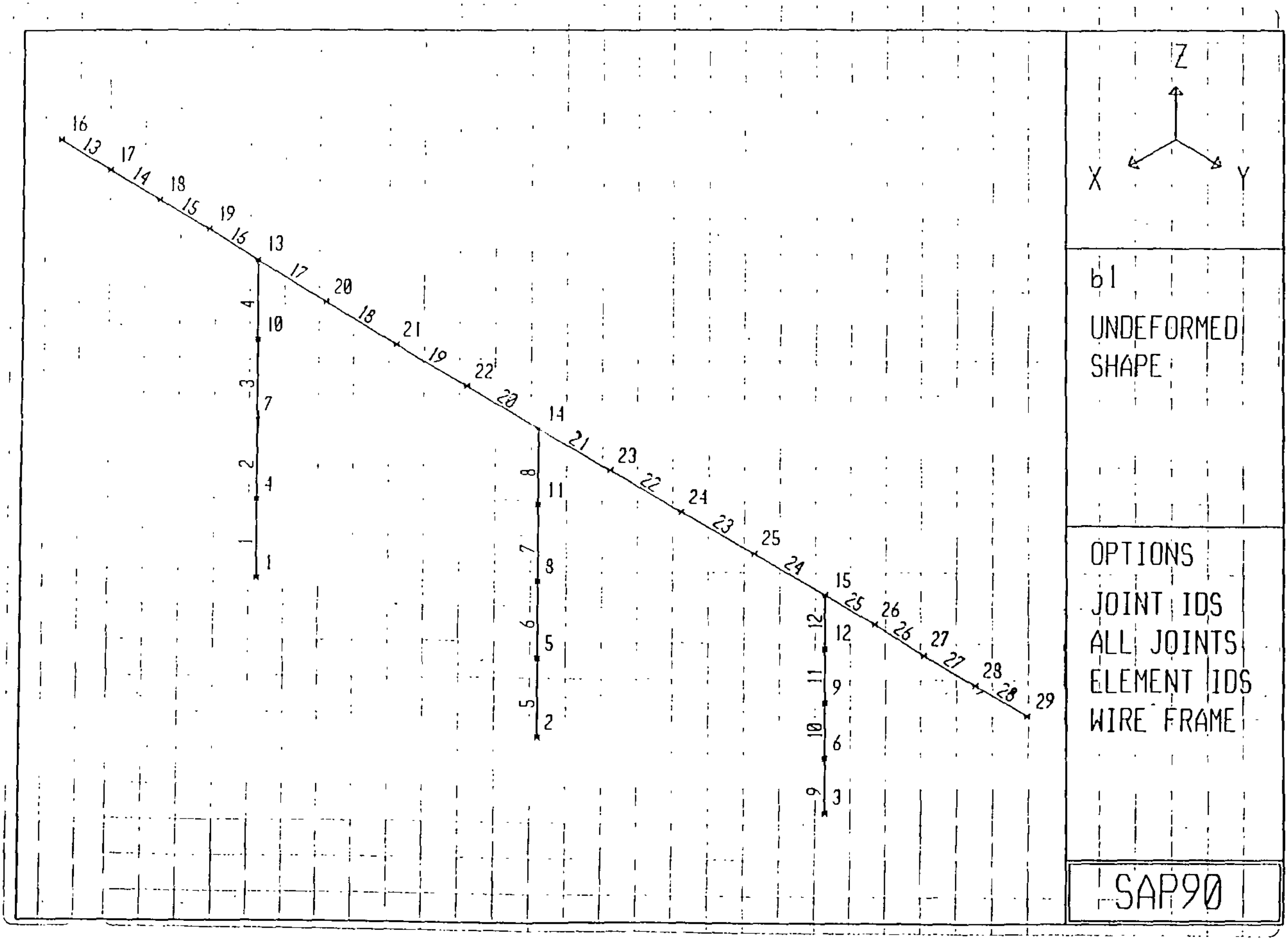

Z
X
Y
b1
UNDEFORMED SHAPE
OPTIONS
JOINT IDS
ALL JOINTS
ELEMENT IDS
WIRE FRAME
SAP90

Análisis transversal

1. RIGIDEZ DE LA ESTRUCTURA.

La rigidez de la estructura se calcula con:

$$K = \omega L / \Delta$$

donde:

K - Rigidez de la estructura, en ton/m.

ω - Carga uniformemente repartida sobre la superestructura; en ton/m.

L - Longitud de la superestructura; en m.

Δ - Desplazamiento máximo que sufre la estructura en la dirección de la carga uniformemente repartida; en m.

Se necesita obtener el valor de la carga uniformemente repartida (ω), que produzca un desplazamiento máximo unitario (Δ = 1 m), entonces:

Δ = 1 m

ω = 120.788 ton/m

L = 208.80 m

Por lo tanto el valor de la rigidez es:

$$\mathbf{K = 25\ 220.53\ \ ton/m}$$

2. PERIODO DE LA ESTRUCTURA.

El valor del periodo de la estructura se calcula con:

$$\mathbf{T = 2\pi\ [m\ /\ K]^{1/2}}$$

donde:

T – Periodo de la estructura; en s.

m – Masa de la superestructura; en ton- s^2 / m.

K – Rigidez de la estructura; en ton/m.

Para la masa m :

m = Peso de la superestructura / g = 2641.278 / 9.81

$$m = 269.243 \ \text{ton-}s^2 / m.$$
$$K = 25\ 220.53 \ \text{ton /m}$$

Por lo tanto el valor del periodo de la estructura es:

$$T = 0.649\ s$$

3. COEFICIENTE SISMICO.

Con el valor del periodo obtenido ($T = 0.649$ s), se entra al espectro de diseño para obtener el valor del coeficiente sísmico (α). Así:

$$\alpha = 0.721$$

4. FACTOR REDUCTIVO POR DUCTILIDAD.

a) $Q' = 1 + (Q - 1)\, T / T_a \quad ; \quad \text{si} \;\; T < T_a$

b) $Q' = Q \quad ; \quad \text{si} \;\; T > T_a$

En este caso : $\mathbf{Q' = Q}$ ya que $T = 0.649 > T_a = 0$

Donde Q = 2 debido a que la resistencia a las fuerzas laterales es suministrada por pilas de una sola columna de concreto reforzado (Manual de Diseño de Obras Civiles. CFE, Capítulo de Diseño por Sismo). Por lo tanto:

$$\mathbf{Q' = 2}$$

5. FUERZA LATERAL EQUIVALENTE.

La fuerza lateral equivalente se obtiene con:

$$\mathbf{P = (\alpha/Q')\ W}$$

donde:

α - Coeficiente Sísmico = 0.721

Q' – Factor reductivo por ductilidad = 2

W – Peso de la superestructura = 2641.278 ton

Por lo tanto el valor de la fuerza lateral equivalente es:

$$\mathbf{P = 952.1807\ ton}$$

La que se transforma a una fuerza uniformemente distribuida equivalente:

$$\omega_{eq.} = \mathbf{P / L}$$

donde:

P – Fuerza lateral = 952.1807 ton

L - Longitud del puente = 208.80 m

Por lo tanto:

$$\boxed{\omega_{eq.} = \mathbf{4.56\ ton / m}}$$

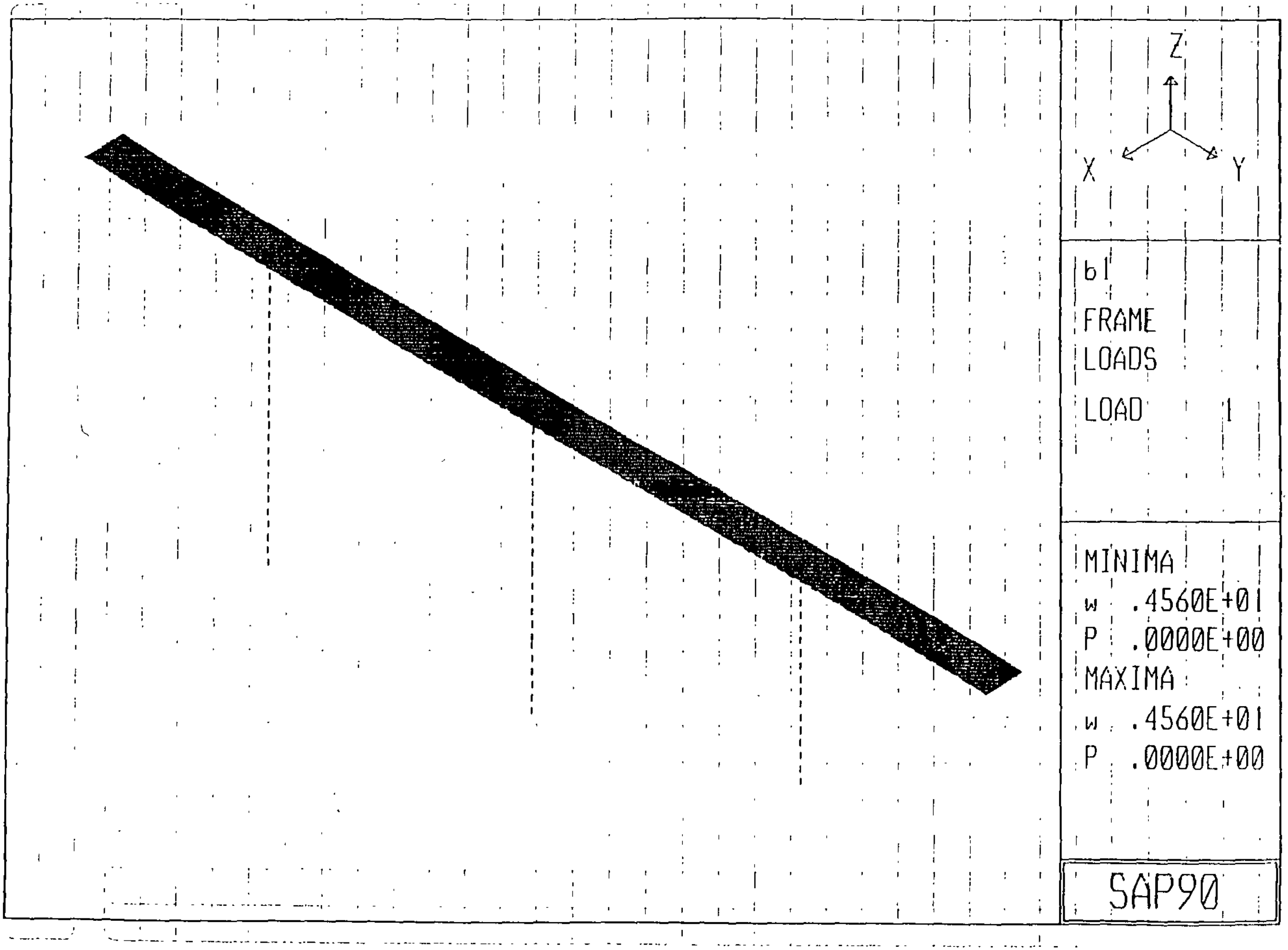
Z
X
Y
b1
FRAME
LOADS
LOAD 1
MINIMA
w .4560E+01
P .0000E+00
MAXIMA
w .4560E+01
P .0000E+00
SAP90

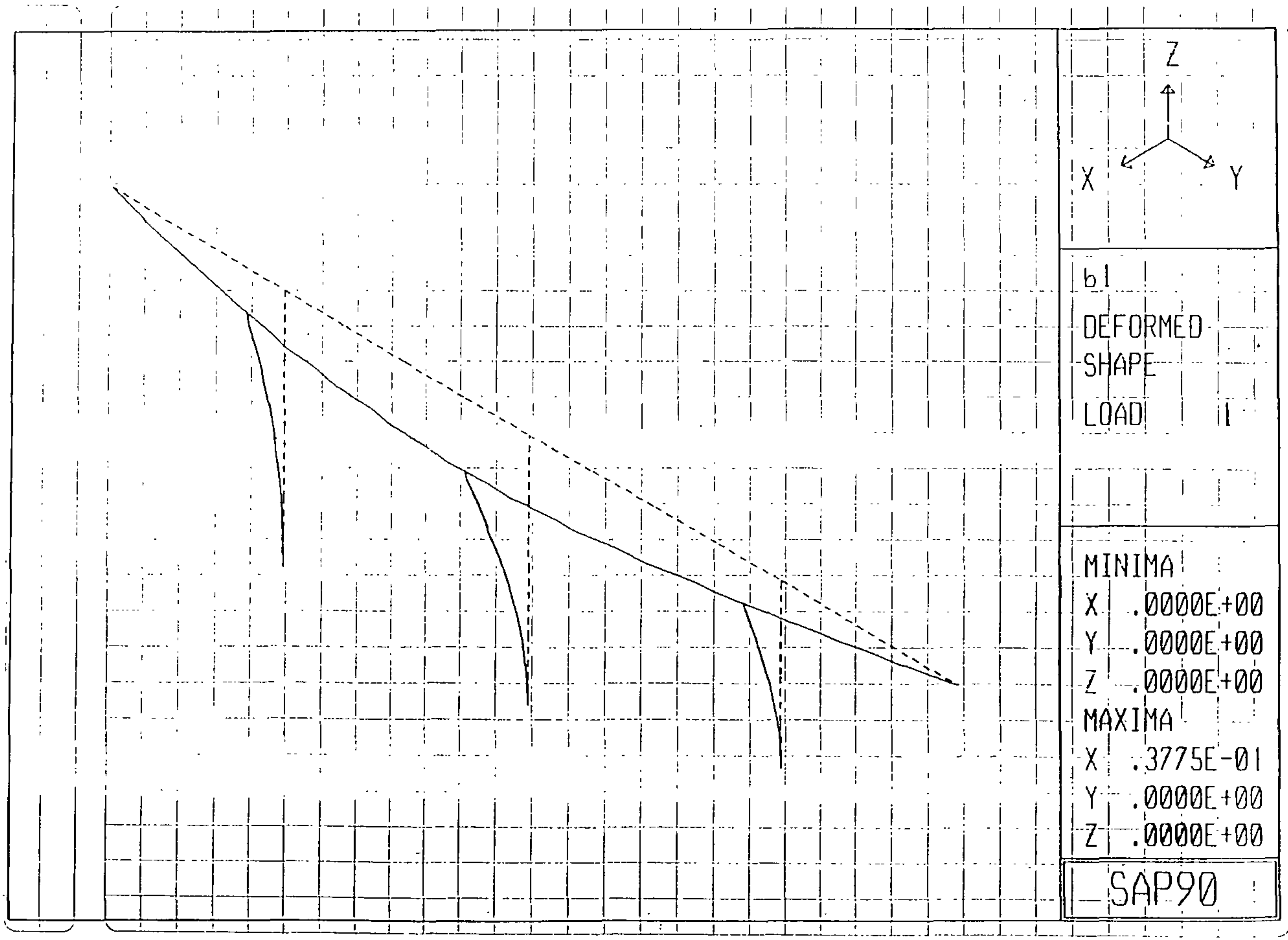
Z
X
Y
b1
DEFORMED
SHAPE
LOAD 1
MINIMA
X .0000E+00
Y .0000E+00
Z .0000E+00
MAXIMA
X .3775E-01
Y .0000E+00
Z .0000E+00
SAP90

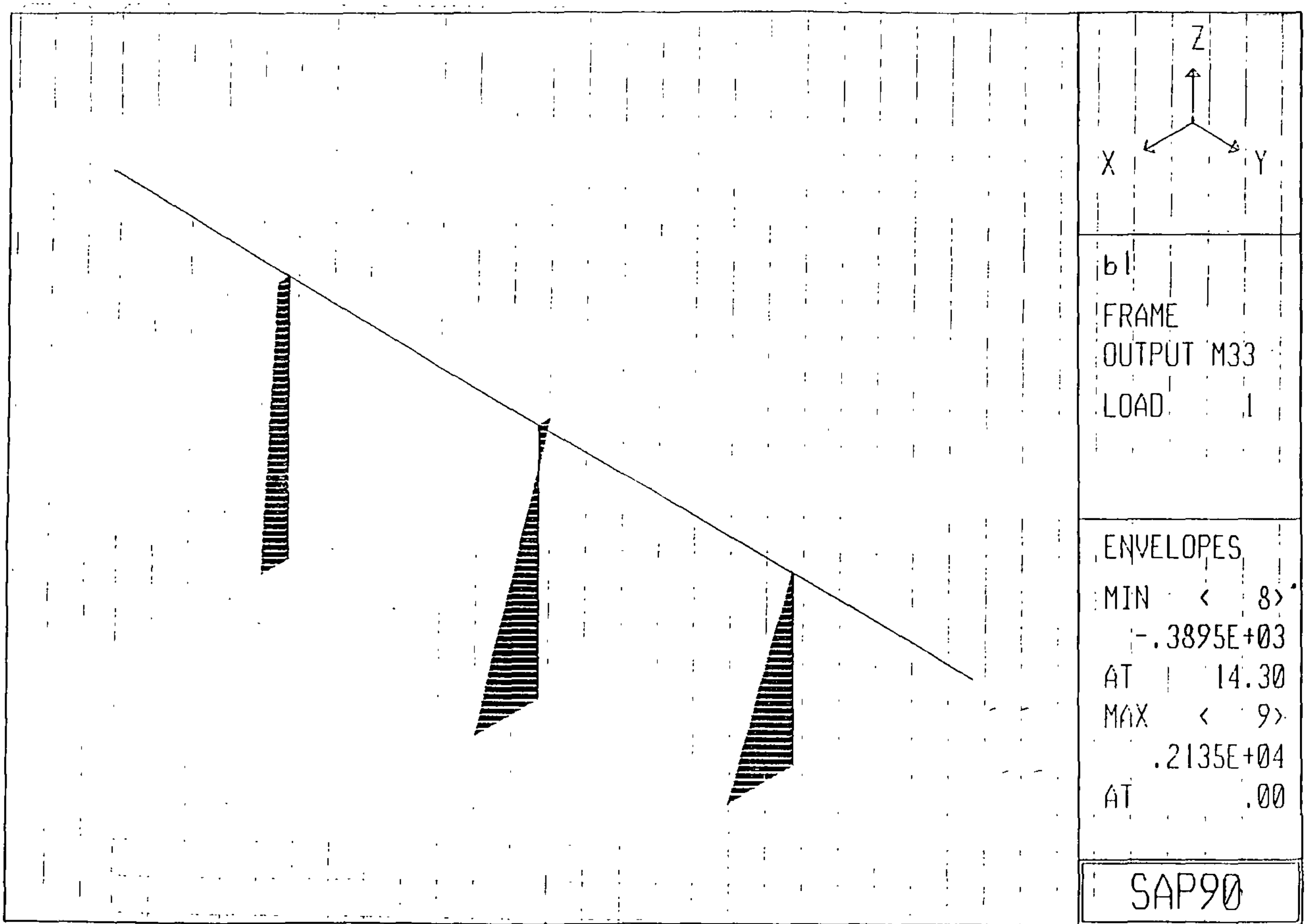
Z
X
Y
b1
FRAME
OUTPUT M33
LOAD 1
ENVELOPES
MIN < 8>
-.3895E+03
AT 14.30
MAX < 9>
.2135E+04
AT .00
SAP90

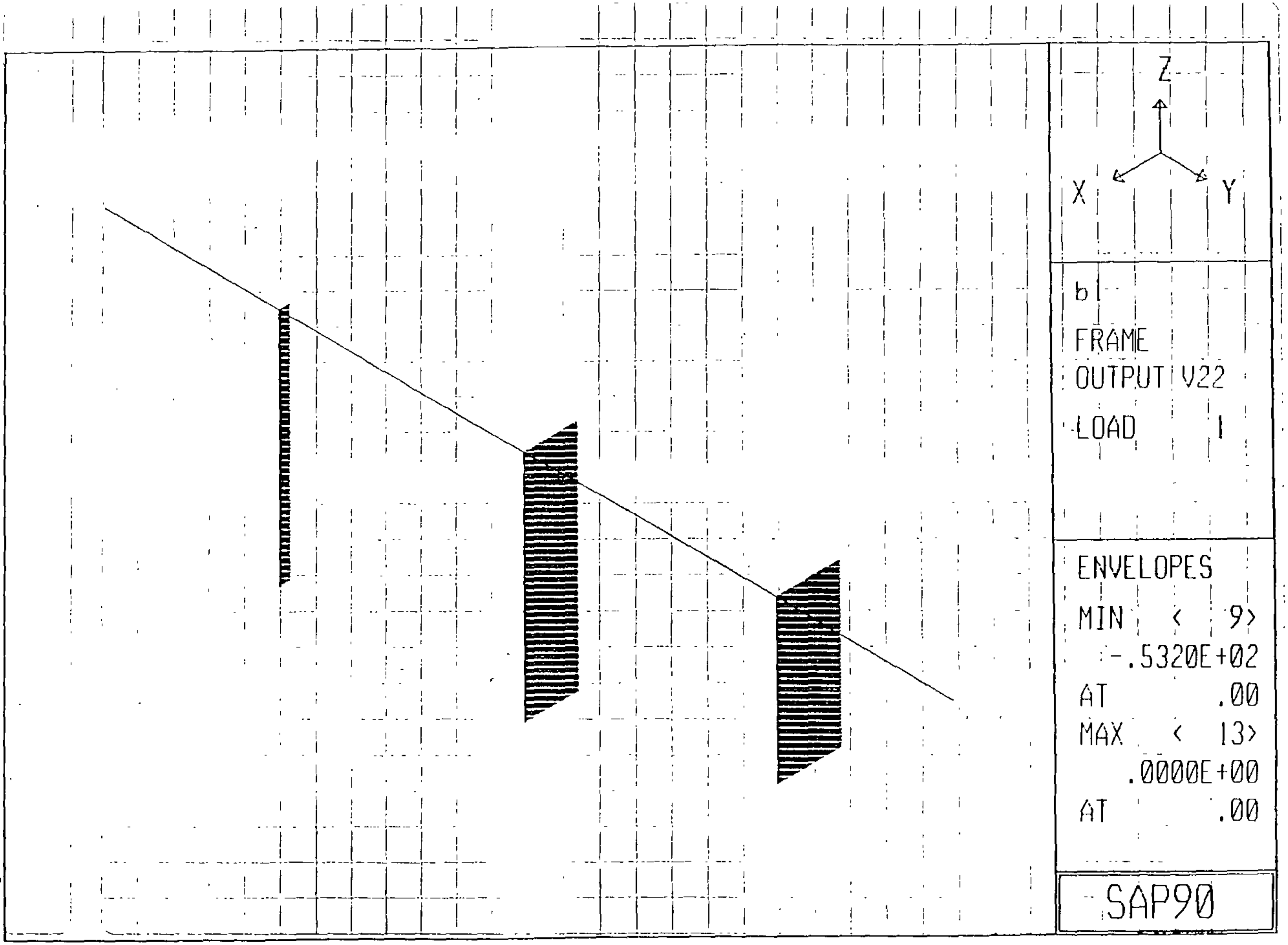
Z
X
Y
b1
FRAME
OUTPUT V22
LOAD 1
ENVELOPES
MIN < 9>
-.5320E+02
AT .00
MAX < 13>
.0000E+00
AT .00
SAP90

Análisis longitudinal

1. RIGIDEZ DE LA ESTRUCTURA.

La rigidez de la estructura se calcula con:

$$\mathbf{K = \omega L / \Delta}$$

donde:

K - Rigidez de la estructura, en ton/m.

ω - Carga uniformemente repartida sobre la superestructura; en ton/m.

L - Longitud de la superestructura; en m.

Δ - Desplazamiento máximo que sufre la estructura en la dirección de la carga uniformemente repartida; en m.

Se necesita obtener el valor de la carga uniformemente repartida (ω), que produzca un desplazamiento máximo unitario (Δ = 1m), entonces:

Δ = 1 m

ω = 19.6142 ton/m

L = 208.80 m

Por lo tanto el valor de la rigidez es:

$$K = 4\ 095.445 \text{ ton/m}$$

2. PERIODO DE LA ESTRUCTURA.

El valor del periodo de la estructura se calcula como:

$$T = 2\pi\ [m / K]^{1/2}$$

donde:

T – Periodo de la estructura; en s.

m – Masa de la superestructura; en ton- s^2 / m.

K – Rigidez de la estructura; en ton/m.

Para la masa m:

m = Peso de la superestructura / g = 2641.278 / 9.81

$$m = 269.243 \text{ ton-s}^2 / m$$

$$k = 4\ 095.445 \text{ ton / m}$$

Por lo tanto el valor del periodo de la estructura es:

$$T = 1.61 \text{ s}$$

3. COEFICIENTE SISMICO.

Con el valor del periodo obtenido (T = 1.61 s.), se entra al espectro de diseño para obtener el valor del coeficiente sísmico (α). Así:

$$\alpha = 0.458$$

4. FACTOR REDUCTIVO POR DUCTILIDAD.

a) $Q' = 1 + (Q - 1)\, T / T_a \quad ; \quad \text{si } T < T_a$

b) $Q' = Q \quad ; \quad \text{si } T > T_a$

En este caso : $\mathbf{Q' = Q}$ ya que $T = 0.75 > T_a = 0$

Donde $Q = 3$ debido a que la resistencia a las fuerzas laterales es suministrada por marcos de tres columnas de concreto reforzado (Manual de Diseño de Obras Civiles. CFE, Capítulo de Diseño por Sismo). Por lo tanto:

$$\mathbf{Q' = 3}$$

5. FUERZA LATERAL EQUIVALENTE.

La fuerza lateral equivalente se obtiene con:

$$\mathbf{P = (\alpha/Q')\ W}$$

donde:

α - Coeficiente Sísmico = 0.458

Q' – Factor reductivo por ductilidad = 3

W – Peso de la superestructura = 2641.278 ton.

Por lo tanto el valor de la fuerza lateral equivalente es:

$$P = 403.2351 \text{ ton}$$

La que se transforma a una fuerza uniformemente distribuida equivalente:

$$\omega_{eq.} = P / L$$

donde:

P – Fuerza lateral = 403.2351 ton

L – Longitud del puente = 208.80 m

Por lo tanto:

$$\boxed{\omega_{eq.} = 1.93 \text{ ton / m}}$$

METODO UNIMODAL DE ANÁLISIS

La ecuación que nos permite obtener la carga lateral debida a sismo es la siguiente (ec. A).

$$P_e(x) = C_s * \frac{\beta}{\gamma} * w(x) * v_s(x)$$

donde:

C_s = a/g, ordenada del espectro de diseño correspondiente, entrando al espectro de diseño con el periodo T

β = factor de distribución de desplazamientos debidos a la carga uniformemente repartida

γ = factor de desplazamiento máximo debido a la carga uniformemente repartida

w(x) = carga uniformemente repartida

$v_s(x)$ = distribución de desplazamientos

En primer término se aplica una carga uniformemente repartida p_o=1 t/m. El análisis del modelo, construido con el programa SAP90, proporciona la siguiente distribución de desplazamientos:

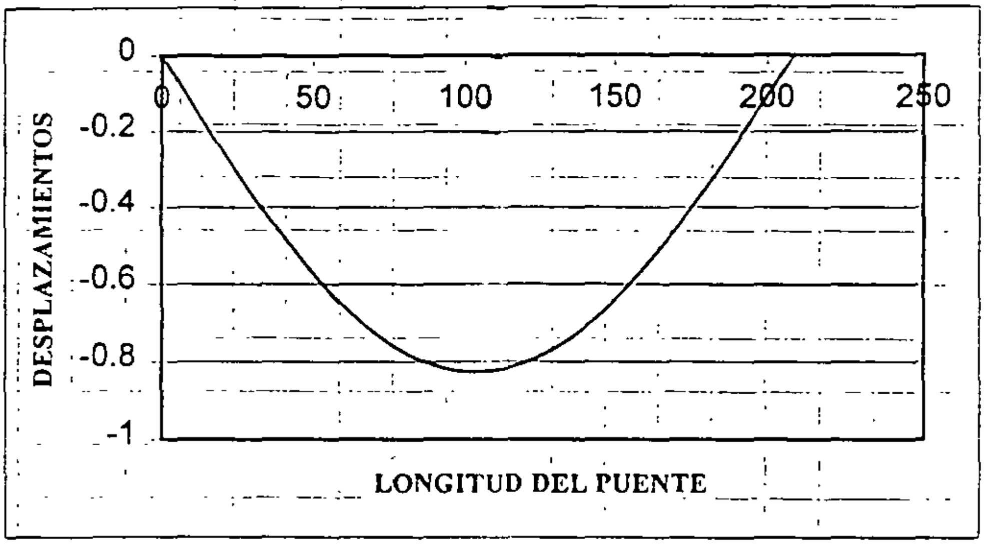

El factor se obtiene con la siguiente ecuación:

$$\alpha = \int_0^L v_s(x)dx$$

Integrando numéricamente para nuestro ejemplo

α=10.795/100)*(0+0.1386+0.2726+0.3981+0.5118+0.6476+0.7481+0.8089+
+0.8279+0.8053+0.7413+0.6389+0.5028+0.3903+0.2670+0.1357+0)

α = 0.8457

$$k_o = \frac{208.80}{0.008279} = 25220.43\,t/m$$

Periodo (T)

$$T = 2\pi\sqrt{\frac{W}{gk_o}}$$

W - Peso total

g - gravedad = 9.81 m/s^2

k_o - rigidez

$$T = 2\pi\sqrt{\frac{2641.20}{9.81 * 25220.43}}$$

T = 0.6492 s

Cálculo de Cs = a/g

Del espectro de diseño

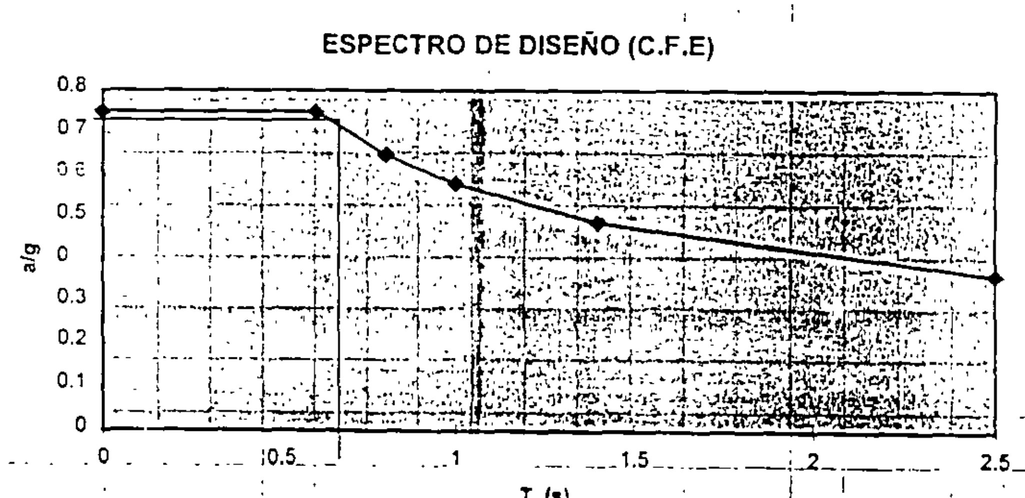

Cs= a/g = 0.72

Antes de proceder con la solución de la ec. A, necesitamos conocer lo siguiente:

Peso total (W). Este se obtiene con :

$$\mathbf{W = w * L}$$

donde

w = carga uniformemente repartida de (superestructura)

L = longitud total del puente

W = (12.65 t/m) * (208.80m)

W = 2641.32 t

Carga total lateral (P_o)

$$\mathbf{P_o = p_o * L}$$

p_o - carga unitaria uniformemente repartida

L - longitud total del puente

P_o = (1 t/m) * (208.80 m)

P_o = 208.80 t

Rigidez (k_o)

$$k_o = \frac{P_o}{\Delta}$$

P_o - Carga total lateral

Δ - desplazamiento máximo debido a la carga unitaria p_o=1 t/m

Cálculo de γ

$$\gamma = \int_0^L w(x)(v_s(x)^2)dx$$

w(x) - carga uniformemente repartida debida a la superestructura

$v_s(x)$ - distribución de desplazamientos unitarios

$v_s(x) = \Delta$

$\gamma = (12.65) * (0.008279)^2 * (208.80)$

$\gamma =$ **0.1810**

Cálculo de β

$$\beta = \int_0^L w(x)v_s(x)dx$$

$\beta = (12.65) * (0.008279) * (208.80)$

$\beta =$ **21.86**

Sustituimos en ecuación (A)

$$P_e(x) = 0.72 * \frac{21.86}{0.1810} * (12.65) * (0.008279)$$

$$\underline{\mathbf{P_e(x) = 9.11\ t/m}}$$

Considerando un factor de ductilidad Q´=2, La carga lateral por sismo que se aplicará al modelo será:

$$\omega = \frac{9.11}{2}$$

$$\boxed{\mathbf{\omega = 4.56\ t/m}}$$

DIAGRAMA DE MOMENTOS, METODO UNIMODAL

SIN CONSIDERAR EL PESO PROPIO DE LA ESTRUCTURA

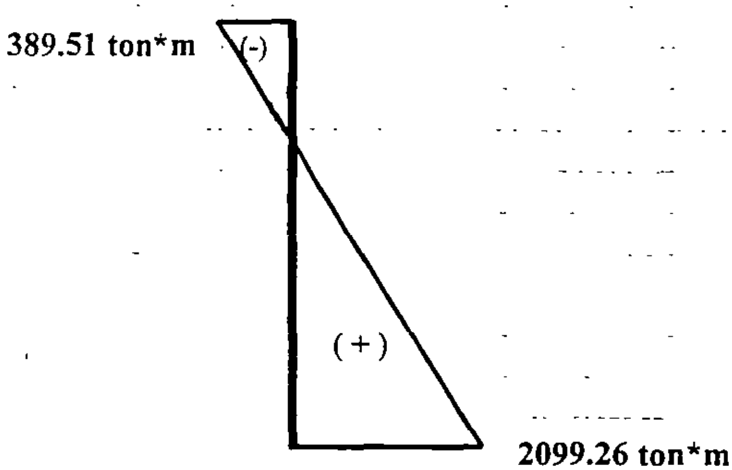

DIAGRAMA DE CORTANTES

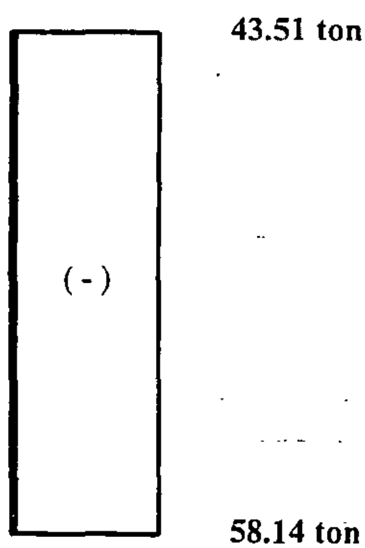

DIAGRAMA DE FUERZAS AXIALES

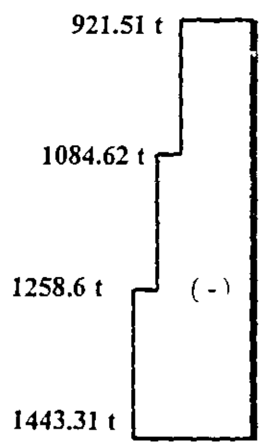

DIAGRAMA DE MOMENTOS TORSIONANTES

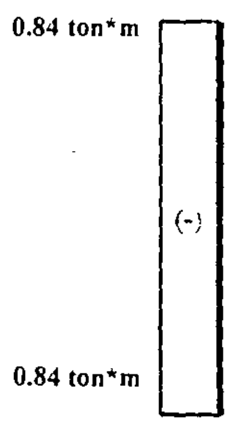

METODO UNIMODAL

DESPLAZAMIENTO MAXIMO EN LA PILA 2

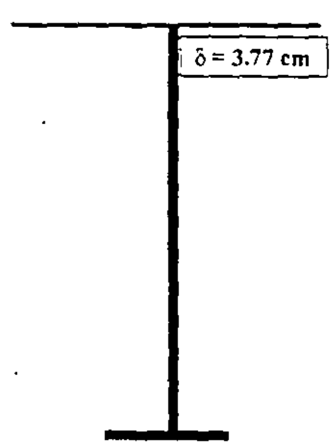

DIAGRAMA DE MOMENTOS, MÉTODO UNIMODAL

CONSIDERANDO PESO PROPIO DE LA ESTRUCTURA

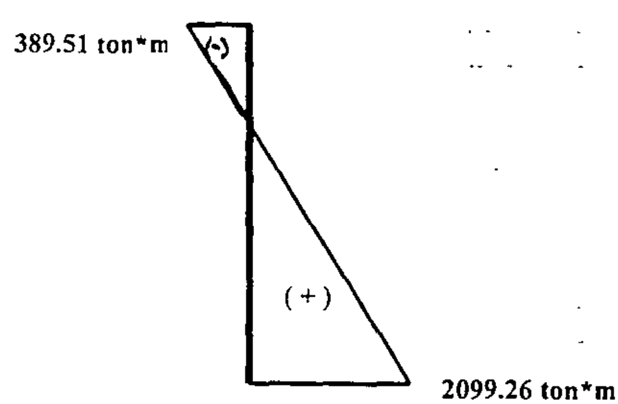

DIAGRAMA DE CORTANTES

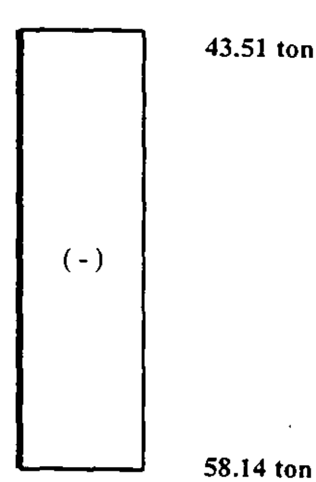

DIAGRAMA DE FUERZAS AXIALES

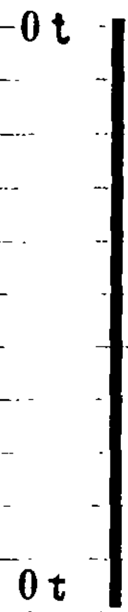

DIAGRAMA DE MOMENTOS TORSIONANTES

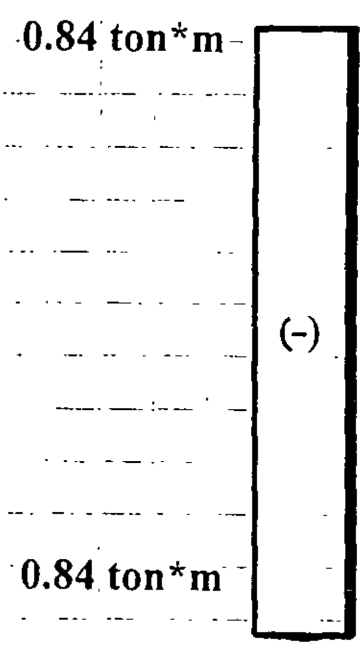

CUADRO COMPARATIVO PARA ANALISIS TRANSVERSAL				
	SIMPLIFICADO		ESTATICO	UNIMODAL
	SIN GIRO	CON GIRO		
PERIODO (seg)	1.17	2.36	0.649	0.649
CARGA EQUIVALENTE (ton/m)	31.45	21.73	6.093	9.18
MOMENTO FLEXIONANTE EN LA BASE DE LA PILA (ton-m)	-1141.98	-1242.96	-2805	-4226.14
FUERZA CORTANTE EN LA BASE DE LA PILA (ton)	-31.45	-21.73	-58.14	-87.59
DESPLAZAMIENTO MAXIMO (cm)	3.44	6.51	5.04	7.6

FACULTAD DE INGENIERIA U.N.A.M.
DIVISION DE EDUCACION CONTINUA

CURSOS ABIERTOS

XXV CURSO INTERNACIONAL DE INGENIERÍA SÍSMICA

MÓDULO III:

DISEÑO SÍSMICO DE PUENTES

TEMA

SISMOLOGÍA

M. EN I. MARTHA SUÁREZ LÓPEZ
PALACIO DE MINERÍA
AGOSTO DE 1999

DISEÑO SISMICO DE PUENTES

TEMA 2 SISMOLOGIA

Profesora : M. en I. Martha Suárez López
Instituto de Ingeniería, UNAM

MEXICO

CONCEPTOS BÁSICOS

Foco y epicentro

Desde la formación del sistema solar, los elementos que constituyen a la Tierra comenzaron a acumularse los más pesados en su centro y los más ligeros en la superficie, de tal manera que su estructura quedó constituida por capas de diferentes densidades. La parte más superficial llamada corteza, se divide en corteza oceánica formada por rocas máficas (basalto y gabro) que tiene un espesor promedio de 10 km; y en corteza continental constituida por materiales más ligeros como andesitas y en mayor cantidad por rocas siálicas (granitos) formando espesores promedio de 40 km. La corteza se apoya sobre rocas ultramáficas rígidas y más densas (peridotitas) que constituyen a la litosfera (con 100 km de espesor) la cual se divide en siete placas mayores (en total unas doce placas) conocidas como placas tectónicas (fig. 1), que se apoyan a su vez en rocas parcialmente derretidas debido al calor y a la presión a la que están sometidas. Estas últimas forman parte de la astenosfera (fig 2). El calor producido por el decaimiento radiactivo de los elementos del interior de la Tierra, genera corrientes de convección ocasionando que estas placas rígidas de la litosfera 'naveguen' sobre la astenosfera a una velocidad medible de varios centímetros por año. El continuo y lento movimiento de las placas produce concentración de esfuerzos en algunas zonas de las fronteras donde se atascan y no permite el deslizamiento entre ellas. Un sismo se genera cuando se libera la energía acumulada en esas zonas, esto es, cuando la energía que se acumula es mayor que la que pueden resistir las rocas que constituyen a la corteza y/o la litosfera, produciendo un súbito rompimiento y consecuente deslizamiento. Al lugar en donde se produce esa ruptura se le llama foco. A su proyección en la superficie se le conoce como epicentro. Algunos sismos se generan también cuando hay erupciones volcánicas, deslizamientos de taludes o, incluso, son generados por algunas explosiones realizadas por el hombre.

Los movimientos entre placas son de tres tipos:

Divergentes.- Cuando las placas tectónicas se separan una de la otra. Es aquí donde se genera continuamente corteza oceánica.

Convergentes o de subducción.- Cuando dos placas tectónicas chocan una con la otra y debido a ello, una de ellas se hunde. En estas zonas se destruye la corteza oceánica. El 90% de los sismos ocurren a lo largo de estas fronteras.

Transcurrentes.- Es la frontera en la cual no se crea ni se destruye la corteza.

En las zonas de transcurrencia y divergencia ocurren el 5% de los sismos, el otro 5% se genera en zonas alejadas de las fronteras entre placas.

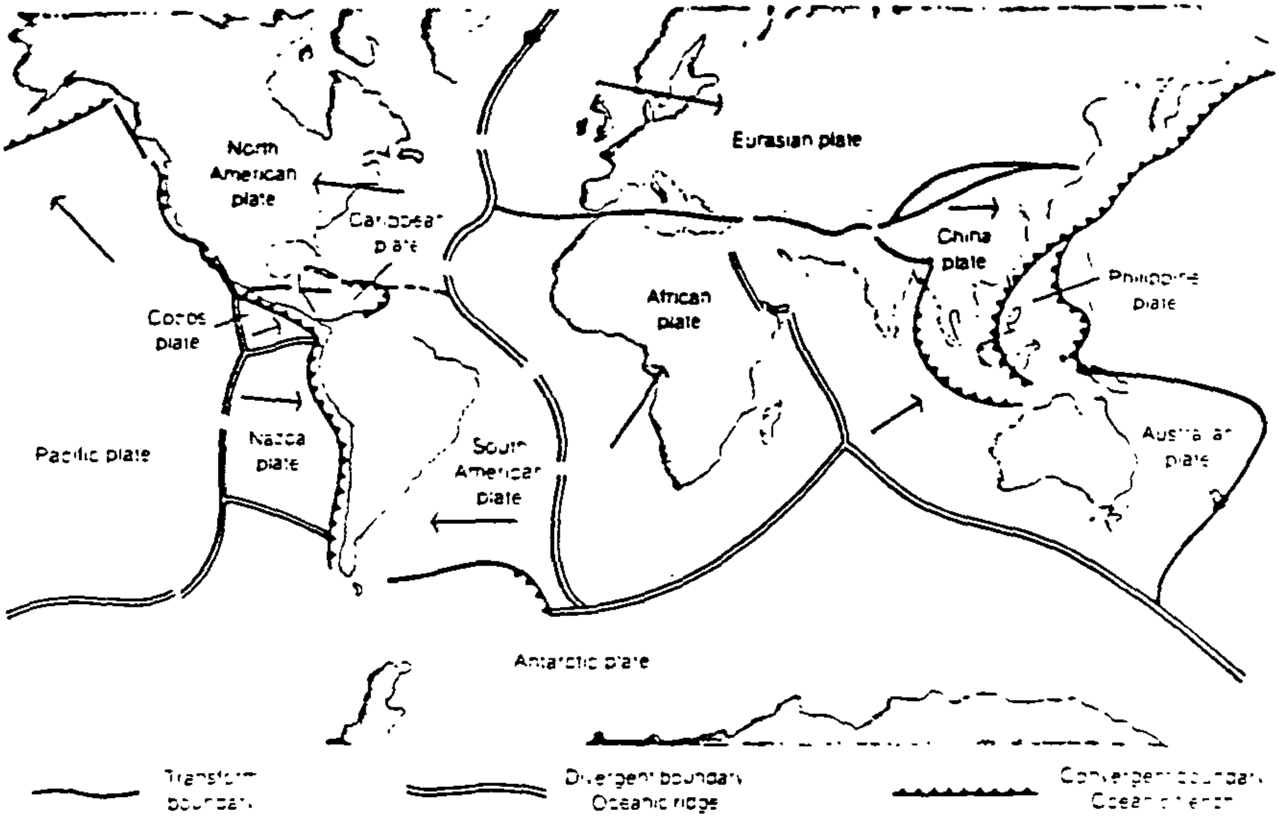

Fig. 1 Placas tectónicas de la Tierra. Las flechas indican la dirección en la que se mueven las placas (Alt, 1982).

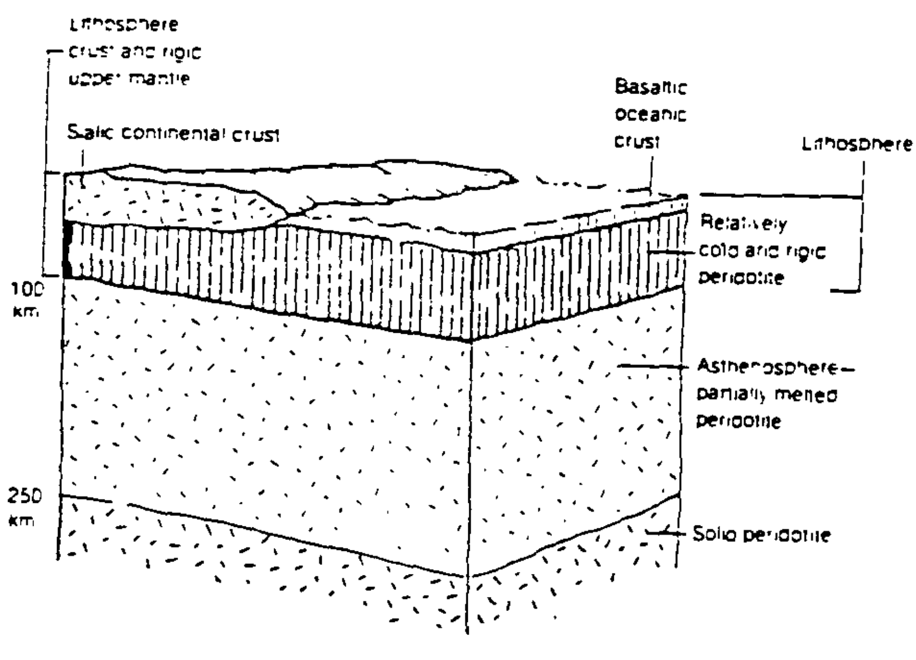

Fig. 2 Sección esquemática de la parte externa de la Tierra (Alt, 1982).

Propagación de ondas (ondas P, S y superficiales)

Cuando se libera energía, una buena parte de esta lo hace en forma de ondas. Estas son perturbaciones que se propagan de un punto a otro en un medio. La propagación se lleva a cabo a una determinada velocidad y el tipo de onda que se produce depende de la naturaleza de los enlaces que existen entre los puntos por los que se propaga. Estas son de varios tipos. Se les clasifica en ondas de cuerpo o superficiales dependiendo si la propagación se realiza en el interior del material o en las fronteras de este, respectivamente. En su estudio se toman en cuenta las hipótesis de la teoría de la elasticidad que relacionan a las fuerzas externas que actúan en un medio con sus fuerzas internas que se manifiestan mediante cambios de tamaño y forma que sufre éste. Las deformaciones que experimenta un elemento infinitesimal cuando es sometido a esfuerzos están dadas por

$$e_{ij}=\frac{1}{2}\left[u_{i,j}+u_{j,i}\right] \tag{1}$$

donde u_i es el desplazamiento del cuerpo en la dirección x_i. La coma indica derivación con respecto a la dirección señalada. La ley de Hooke o ley de la proporcionalidad entre esfuerzos y deformaciones se puede expresar como

$$\sigma_{ij}=\lambda e_{kk}\delta_{ij}+2\mu e_{ij} \tag{2}$$

siendo δ_{ij} la delta de Kronecker (=1 si $i=j$; =0 si $i\neq j$), i,j,k = 1, 2,3 y λ, μ las constantes de Lamé. Empleando la segunda ley de Newton y despreciando las fuerzas de cuerpo, la ecuación de movimiento en la dirección x_i puede expresarse de la forma

$$\rho\ddot{u}_j=\sigma_{ij,j} \tag{3}$$

Utilizando las relaciones de elasticidad (1) y (2) la ec (3) se transforma en

$$\rho\ddot{u}=(\lambda+\mu)\nabla(\nabla u)+\mu\nabla^2 u \tag{4}$$

Las ondas de cuerpo se dividen en:

Ondas longitudinales que se propagan en la misma dirección del movimiento generando compresiones y dilataciones en el material. A estas ondas se les conoce también como ondas *P* o primarias pues son las primeras en ser detectadas por un observador o instrumento. Su velocidad de propagación (α) es mayor y se calcula como:

$$\alpha=\sqrt{\frac{\lambda+2\mu}{\rho}}$$

donde λ y μ son las constantes de Lamé y ρ es la densidad del material.

Ondas de corte que tienen un movimiento perpendicular a la dirección del movimiento generando esfuerzos de corte en el material por el que se propagan. Por esta misma razón, este tipo de ondas no se transmite por fluidos. Son las segundas en ser detectadas, por ello se les conoce como ondas *S* o secundarias. Se propagan con una velocidad β dada por

$$\beta=\sqrt{\frac{\mu}{\rho}}$$

En la fig. 3 se presenta un diagrama de cómo se propagan este tipo de ondas. Las oscilaciones longitudinales producidas por las ondas *P* son simétricas con respecto a la dirección de propagación, en cambio las oscilaciones de las ondas transversales (ondas *S*) dependen del plano que cruza la dirección de propagación en el cual se efectua el movimiento transversal. Al rumbo que tienen las ondas de corte en ese plano se le denomina *polarización*. Para el estudio de las ondas *S* su movimiento puede descomponerse en una componente horizontal (ondas polarizadas horizontalmente o *SH*) y en una vertical (ondas polarizadas verticalmente o *SV*). En la fig 4 se ilustra este concepto.

Las ondas superficiales se dividen en ondas de Rayleigh cuyo movimiento es circular parecido al de las olas de aguas profundas en el oceano, y ondas de Love que tienen un movimiento parecido al de las ondas *S* pero que disminuye de amplitud cuando se aleja de la frontera del material por el cual se propagan (ver fig. 3). Ambos tipos de ondas tienen una velocidad de propagación menor que las ondas de cuerpo y son las que en un sismograma presentan las mayores amplitudes.

Si se supone que las ondas son periodicas con dependencia temporal dada por $e^{i\omega t}$ donde $i = (-1)^{1/2}$ y ω = frecuencia angular, el movimiento dilatacional asociado a las ondas *P* que viajan a una velocidad α queda descrito por

$$(\lambda+2\mu)\nabla^2(\nabla u)+\rho\omega^2\nabla u=0$$

y el asociado a las ondas *S* que tienen una velocidad de propagación β está dado por

$$\mu\nabla^2(\nabla\times u)+\rho\omega^2\nabla\times u=0$$

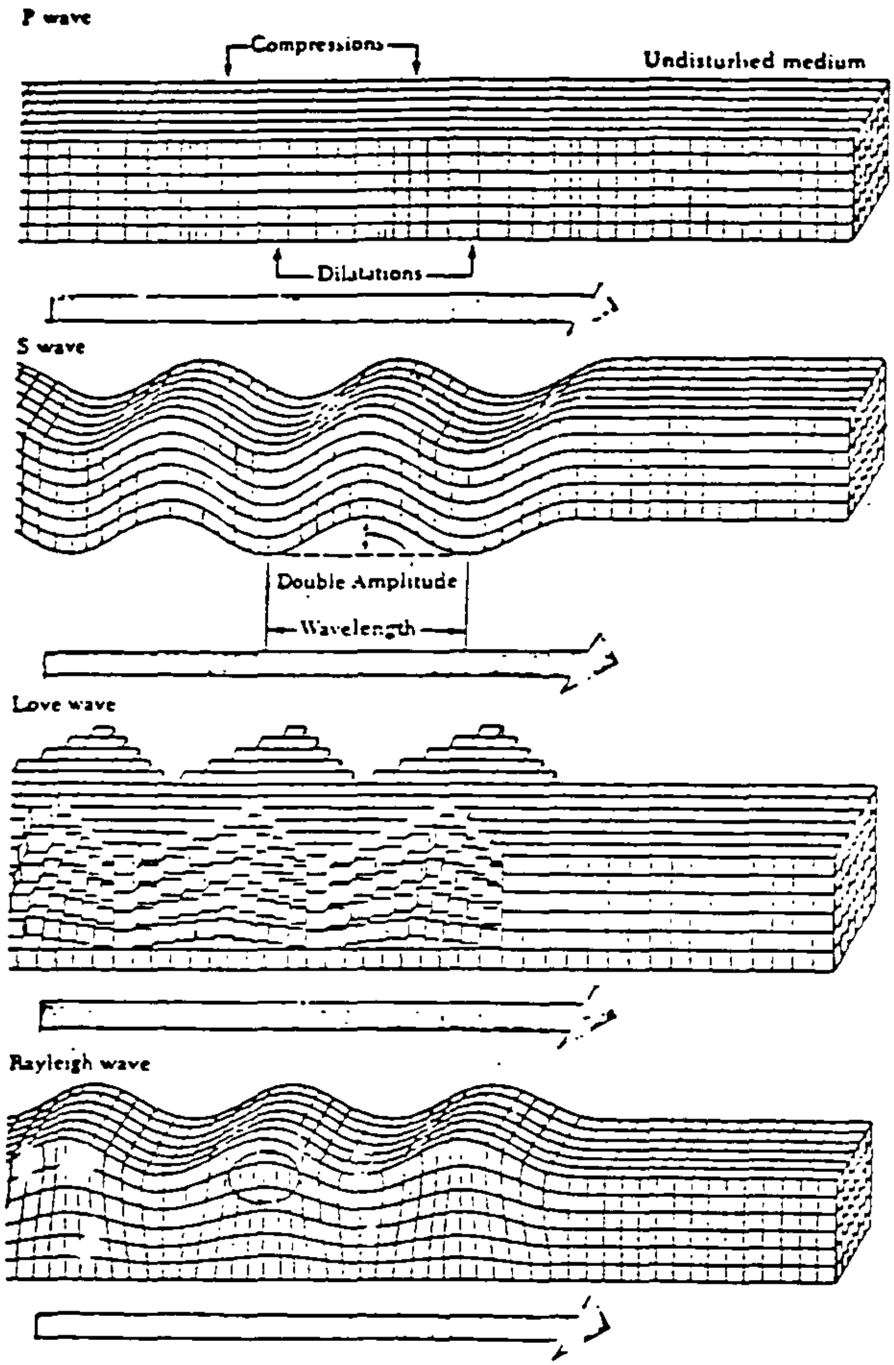

Fig. 3 Diagrama que ilustra las formas del movimiento de las partículas de la Tierra cerca de la superficie cuando se propagan los cuatro tipos de onda (Bolt, 1976).

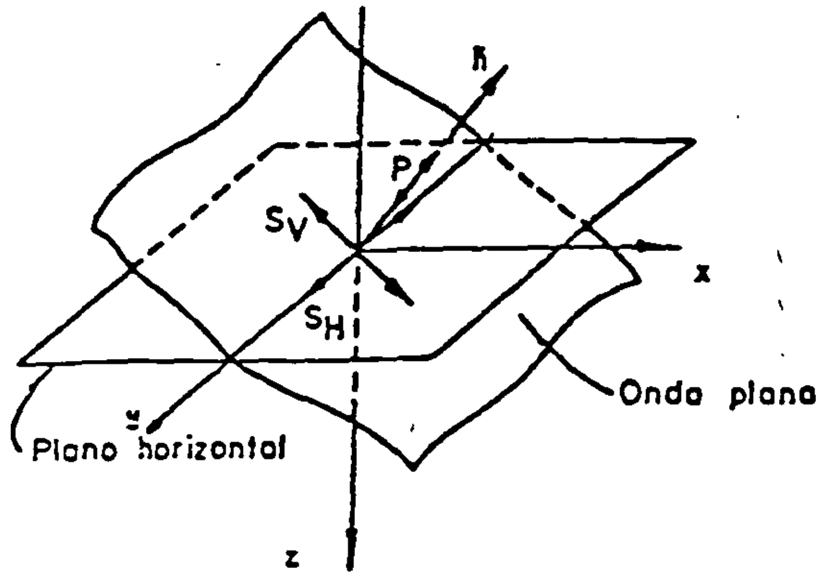

Fig. 4 Frente de onda plano. Polarización de las ondas *S* en ondas *SH* y *SV*.

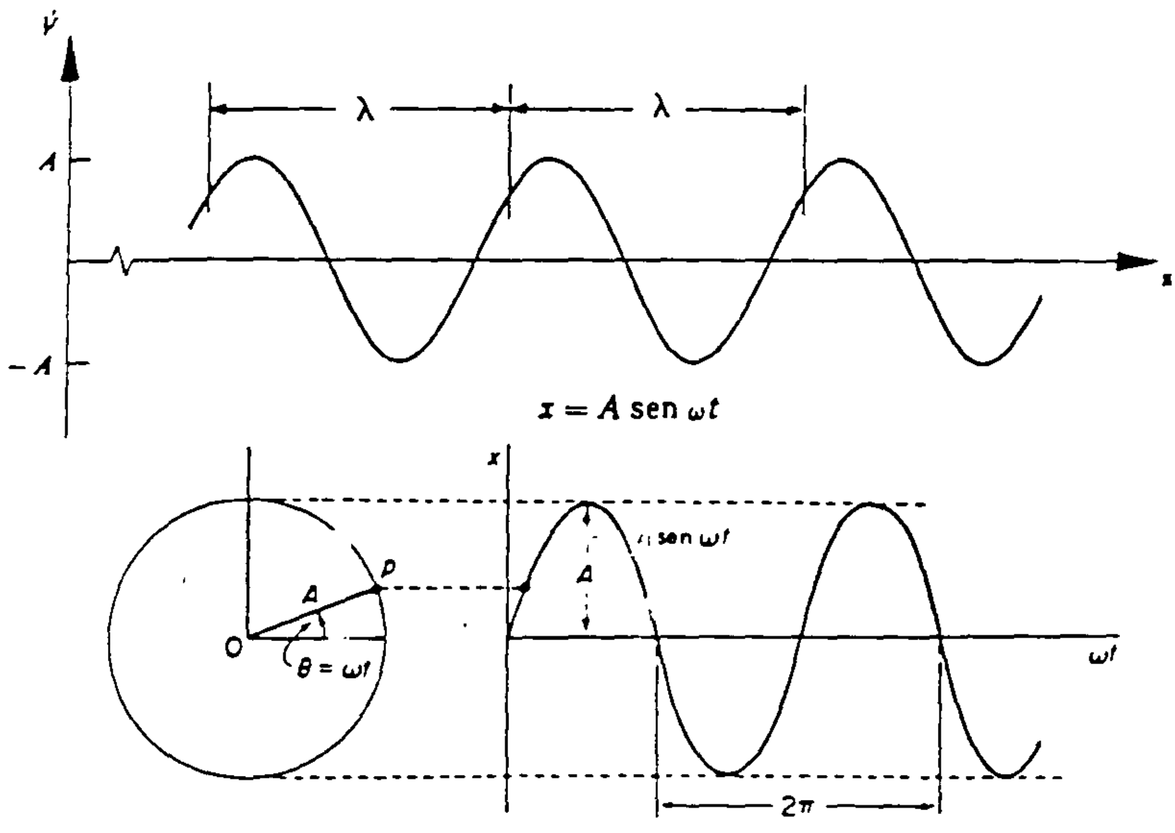

Fig. 5 Onda monocromática. *A* representa la amplitud de onda y *λ* su longitud de onda. *ω* es la velocidad angular o frecuencia angular del movimiento armónico que tiene una partícula *p* que se mueve describiendo un círculo.

La ec (4) proporciona una regla general que debe cumplir toda función que describa un movimiento ondulatorio. Esta función puede ser un pulso o una señal registrada en un sismograma. Para facilitar la interpretación y manejo matemático en el estudio de la propagación de una señal arbitraria, se considera que esta se puede representar como la suma de un conjunto de funciones armónicas (principio de superposición) que cumplen con la ecuación de onda (ec (4)) y observar la acción de cada sumando por separado. Basándose en el desarrollo en series de Fourier (Newland, 1980), una señal se remplaza por la suma de funciones trigonométricas seno y coseno. Esta forma de representar señales facilita mucho la interpretación de los fenómenos en la propagación de ondas pues en estas funciones es fácil identificar el periodo $T\ (=\lambda/\beta)$, la fase y la longitud de onda λ y obtener su relación con la frecuencia ($f=1/T$ o frecuencia angular $\omega=2\pi f$) y velocidad de propagación o velocidad de fase ($\beta=\lambda f$); además su empleo en forma de funciones exponenciales facilita mucho el manejo matemático. En la fig. 5 se presenta la trayectoria que tiene una partícula con movimiento armónico y la nomenclatura de algunas de las características del movimiento comentadas arriba. Por esta razón, en el estudio de la propagación de ondas sísmicas se trabaja con espectros de frecuencia. De esta manera su manejo e interpretación es más sencillo. Los espectros se obtienen al pasar la serie de tiempo del movimiento al dominio de la frecuencia por medio de la transformada de Fourier (espectro de Fourier) que se basa en los conceptos descritos arriba. Con base en estas ideas es posible pasar del dominio de la frecuencia, al del tiempo. Las transformadas de Fourier que se utilizan son (Newland, 1980)

$$F(\omega)=\int_{-\infty}^{\infty} f(t)\, e^{-i\omega t}dt \tag{9}$$

$$f(t)=\frac{1}{2\pi}\int_{-\infty}^{\infty} F(\omega)\, e^{i\omega t}d\omega \tag{10}$$

donde $F(\omega)$ y $f(t)$ son funciones que representan al espectro de Fourier y a la señal respectivamente.

Reflexión, refracción y difracción

Cuando una onda plana (que se propaga con un frente de onda plano a lo largo de líneas paralelas denominadas rayos) incide con amplitud A_2 y ángulo α_2 en una frontera que divide a dos medios (medio 1 y medio 2), parte de su energía (A_2') se refleja con el mismo ángulo con el que incidió (ángulo γ_2), y la otra parte (A_1) penetra en el otro medio modificando su dirección en un ángulo γ_1 con respecto a un plano vertical (ver fig 6). El ángulo γ_1 (ángulo de refracción) está relacionado con el ángulo de incidencia (γ_2) y la velocidad de propagación en los medios 1 y 2 de la siguiente manera (ley de Snell),

$$\frac{sen\gamma_2}{c_2} = \frac{sen\gamma_1}{c_1} \qquad (11)$$

donde c_1 y c_2 son las velocidades de propagación en los medios 1 y 2, respectivamente. Otra manera de interpretar este resultado consiste en reconocer que la velocidad de fase aparente a lo largo de la interfaz de todas las ondas involucradas en la reflexión y refracción se conserva. Las amplitudes A_1 y A_2' con las que se propaga dependeran de las condiciones de compatibilidad (o condiciones de frontera) de igualdad de desplazamientos y esfuerzos en cualquier punto ubicado en la frontera de ambos medios.

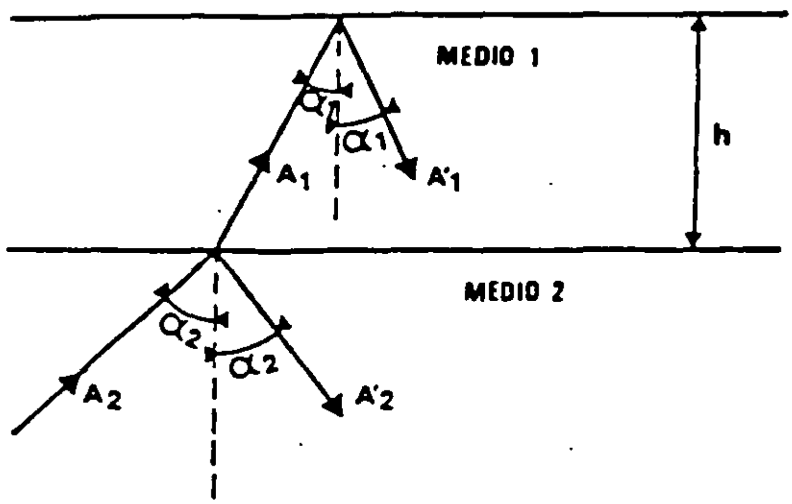

Fig. 6 Reflexión y refracción de una onda que incide con un ángulo γ_2 y una amplitud A_2 en un medio 1.

Un fenómeno importante en la propagación de ondas es la difracción. Muchos de los fenómenos que se observan en la realidad son debidos a esta y no pueden ser explicados considerando que las ondas se propagan únicamente en forma rectilínea de acuerdo con las leyes de la óptica geométrica. La difracción es la desviación en la dirección de los trayectos de las ondas pues estas tienden a bordear los obstáculos que impiden a una parte de un frente de onda continuar propagándose (fig. 7). La primera interpretación ondulatoria de la difracción se debe a Thomas Young quién decía que "la difusión de la amplitud (de las ondas) está acompañada de la variación de la fase de oscilación. De esta manera, a medida que se propaga el frente ondulatorio tiene lugar una nivelación o una 'disipación' de la distribución heterogénea de la amplitud en el frente ondulatorio" (Landsberg, 1976). Young partía del concepto de la propagación rectilínea de las ondas, concepto que tiempo atrás había introducido

Huygens. Sin embargo, fue Fresnel quién le dió un sentido físico al completarlo con la idea de la interferencia de las ondas.

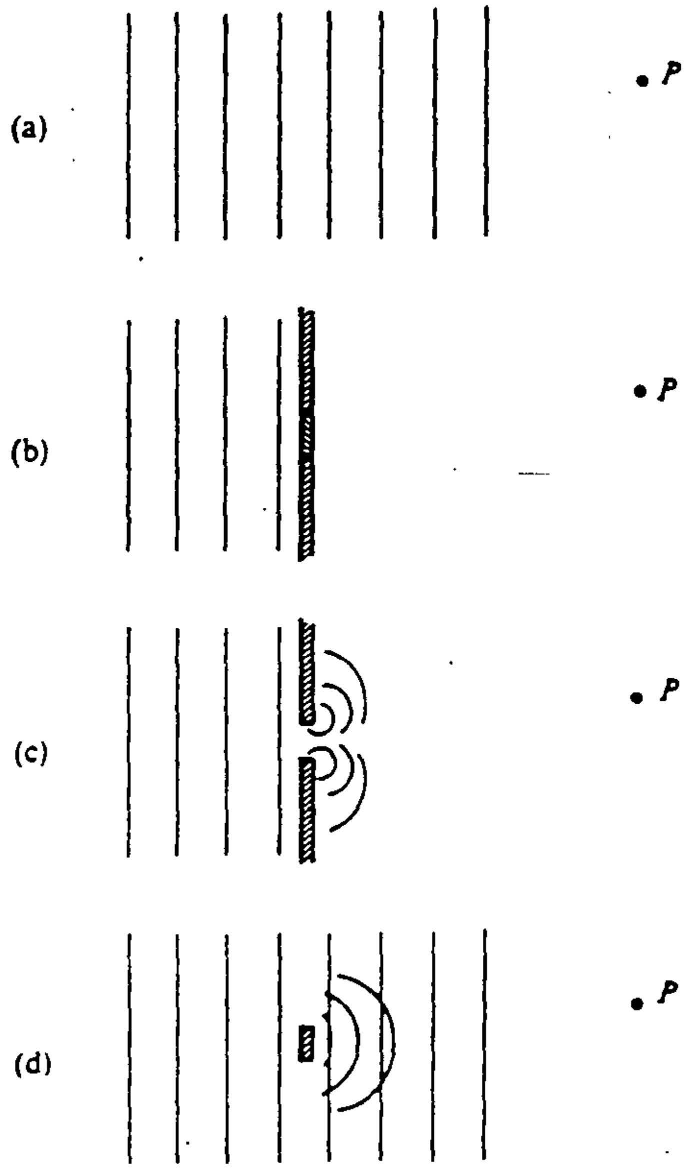

Fig. 7 Propagación de izquierda a derecha de ondas planas a un punto de observación P (a) sin presencia de obstáculos, (b) con bloqueo total al campo de ondas, (c) Bloqueo parcial con una pantalla permitiendo el paso de la onda por un orificio, (d) bloqueo parcial debido a la presencia de un objeto de dimensiones finitas.

El fenómeno de la difracción depende de la longitud de onda λ, de las dimensiones del obstáculo d y de la posición y distancia a la que se encuentre un observador. Los parámetros de una onda que se ven afectados son su amplitud y su fase. El problema se reduce a encontrar esos valores. Es conveniente considerar a la difracción como ondas emitidas por fuentes ficticias ubicadas en los lugares donde se genera y aplicar los conceptos de la teoría de rayos para estas ondas. Esto implica que el punto en donde se miden sus efectos se encuentra lejos de la fuente o que las ondas que se analizan son de alta frecuencia. Considérese por ejemplo un frente de onda al que se le interpone una pantalla opaca que tiene dos orificios (fig. 8); para un observador ubicado lejos de la pantalla, la amplitud y forma de las ondas que le lleguen estarán dadas por la suma de las ondas consideradas en forma independiente "emitidas" desde cada orificio. La fase con la que llegan al punto de observación depende de las distancias entre los orificios y el ángulo que forman con respecto al observador. La diferencia de fases entre las ondas emitidas por los distindos orificios está dada por

$$\alpha(\theta) = kd\, sen\theta \tag{12}$$

donde $k = \omega/c$, ω = frecuencia circular y c = velocidad de propagación. La amplitud total de la onda $A(\theta)$ que llega a un observador ubicado a un ángulo θ con respecto a la normal de la pantalla, se obtiene al sumar las amplitudes $A_c(\theta)$ de las ondas emitidas por cada fuente (que se consideran iguales) tomando en cuenta su diferencia de fases $\alpha(\theta)$. En una pantalla que tenga varios orificios separados una distancia d uno de otro, la amplitud $A(\theta)$, siendo escalar, admite una construcción geométrica, y se obtiene como se indica en la fig. 9, resultando

$$A(\theta) = A_c(\theta)\left|\frac{sen[1/2N\alpha(\theta)]}{sen[1/2\alpha(\theta)]}\right|$$

donde N = número de orificios. Si se define a la intensidad $\Phi(\theta)^2 = (A(\theta)/A_c(\theta))^2$, se puede obtener su variación dependiendo de λ, de la distancia d y de θ. En la fig. 10 se presenta la variación de la intensidad de un frente de onda cuando atravieza 2 y 5 orificios (Main, 1978).

De acuerdo al principio de Huygens se puede obtener el campo total difractado debido a la presencia de una ranura de dimensión a en una pantalla (fig. 11) considerando la suma de los campos de ondas emitidos por un número finito de fuentes ubicadas a lo largo de la ranura. Si se tienen muchas fuentes, el diagrama correspondiente para el cálculo de la amplitud $A(\theta)$ dá por resultado un arco de ángulo β (fig. 12) donde A_{max} es la longitud del arco. Considerándo que el radio del arco es igual a A_{max}/β o a $A_c/(2sen\beta/2)$ donde A_c es la amplitud de las ondas emitidas por cada fuente. La intensidad $\Phi(\theta)^2$ se obtiene como

$$\Phi(\theta)^2 = \left(\frac{A_c}{A_{max}}\right)^2 = \left|\frac{sen\beta/2}{\beta/2}\right|^2$$

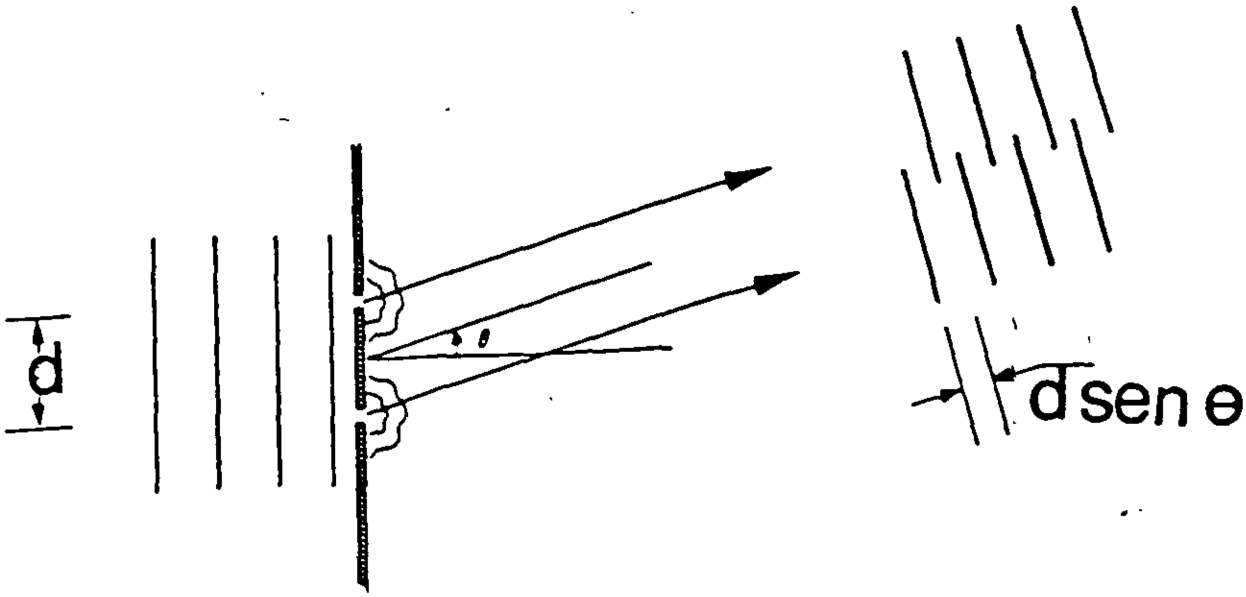

Fig. 8 Difracción de ondas que inciden en la cara izquierda de la pantalla. Para un observador ubicado a gran distancia y a un ángulo θ con respecto al centro de la pantalla, las ondas difractadas que le llegan se pueden considerar como ondas planas que se encuentran desfasadas debido a la diferencia de distancias que recorren (Main, 1978).

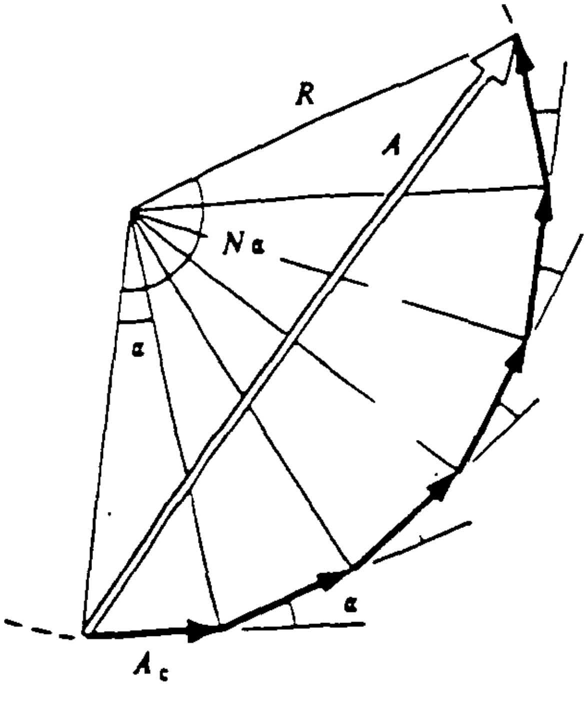

Fig. 9 Cálculo de la amplitud $A(\theta)$para un punto ubicado a un ángulo θ con respecto a la normel de la pantalla, que en este caso contiene N orificios. α es la diferencia de fases entre dos orificios consecutivos.

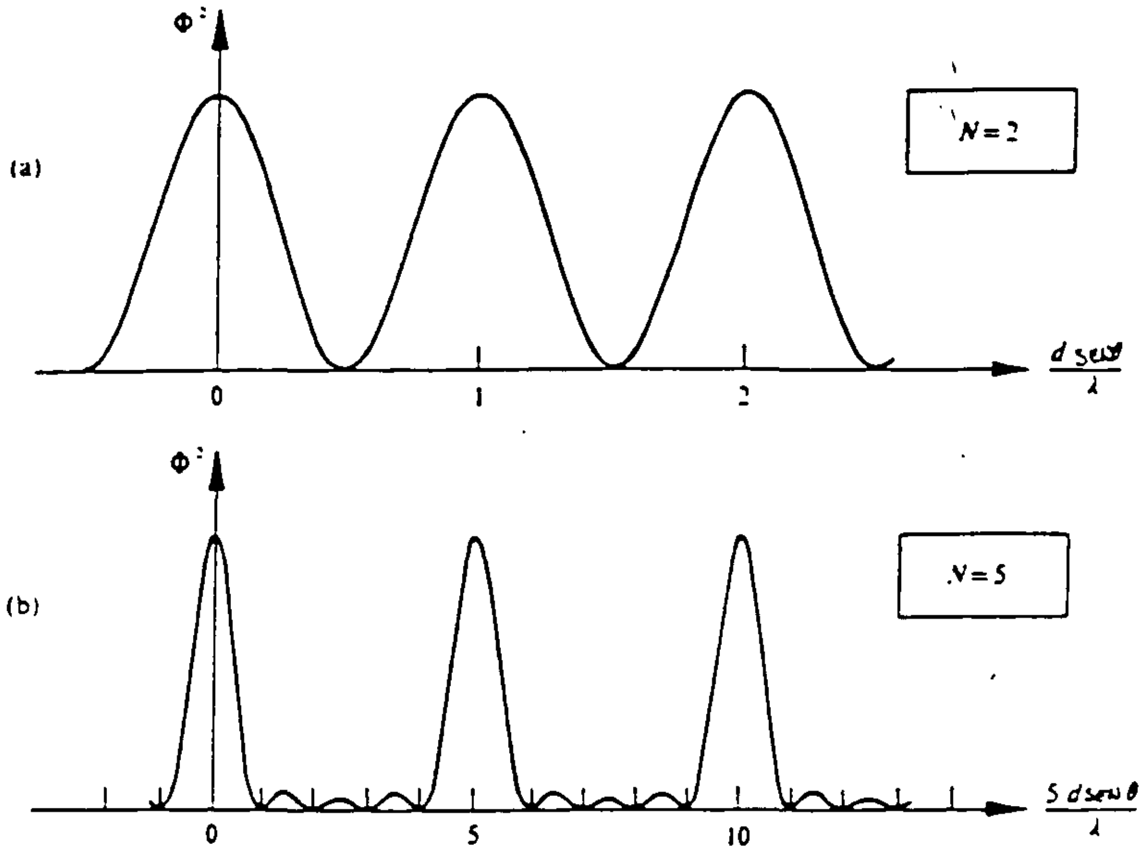

Fig. 10 Gráficas de intensidad Φ^2 contra fase σ de las ondas dofractadas debido a la presencia de una pantalla con (a) dos orificios y (b) cinco orificios.

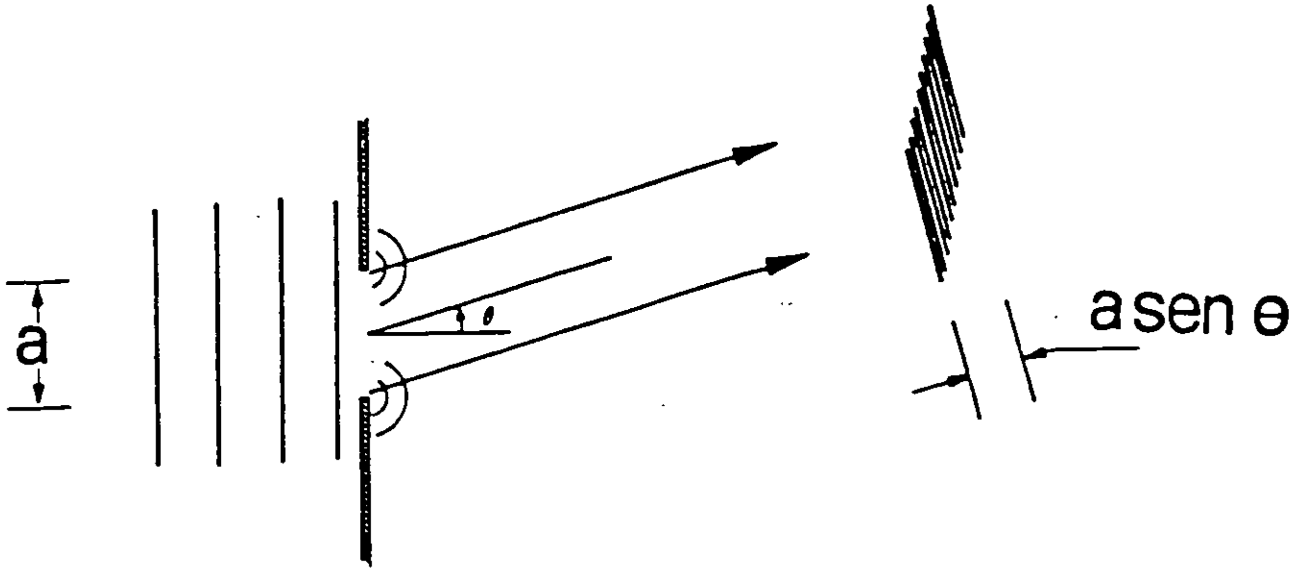

Fig. 11 Difracción provocada por la presencia de una ranura de dimensión *a* en una pantalla. Para considerar la difracción en este caso se colocan varias fuentes distribuídas a lo largo de ra ranura. El patrón de ondas planas que generan las fuentes se presenta a la derecha cuando el observador está ubicado a gran distancia. En la figura sólo se dibujaron las fuentes de los extremos de la ranura (Maiin, 1978).

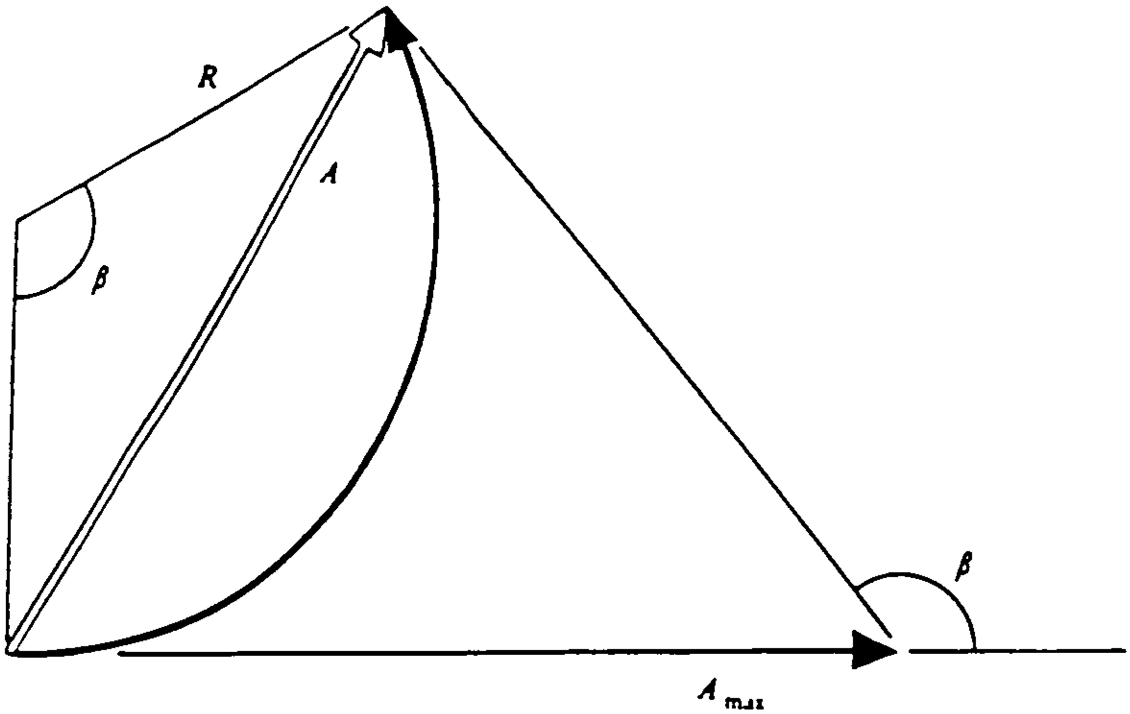

Fig. 12 Diagrama de vectores para el cálculo de amplitud $A(\theta)$. La diferencia de fases $\beta(\theta)$ entre el primero y el último vector está dada por $ka\text{sen}\theta$.

La intensidad tiene valores nulos cuando $\beta(\theta)=2\pi,4\pi,6\pi,\ldots$, esto es cuando $\theta = m\pi/ka=\lambda/a$, donde m es par. De aquí que la difracción sea más importante cuando es más pequeña la ranura de la pantalla y/o cuando la longitud de onda es grande (frecuencias pequeñas).

El número de fuentes necesarias para la construcción adecuada de un frente de onda plano dependerá de la longitud de onda. Esto es, el número de fuentes se deberá incrementar cuando la longitud de onda crezca, por esta razón, mientras más fuentes se consideren por longitud de onda, se tendrá mayor exactitud en los cálculos. La amplitud correspondiente a cada fuente se obtendrá de la solución de sistemas de ecuaciónes que se forman al considerar las condiciones de frontera del problema que se analice.

Sismómetros y acelerómetros

El detectar y registrar las ondas sísmicas implica un problema interesante, ¿como medir el movimiento cuando el punto de referencia utilizado es el que se mueve? La solución consiste básicamente en suspender un peso de un resorte, el cual a su vez está sujeto a una base. El soporte o base es asegurado al cuerpo cuyo movimiento se va a medir. El movimiento relativo entre la masa y la base, registrado en un cilindro que gira o a algún otro dispositivo colocado dentro del instrumento, indicará el movimiento del cuerpo. Los sismómetros son los intrumentos más antiguos que se utilizan para registrar las vibraciones del terreno. Los acelerómetros miden las aceleraciones del terreno. Escencialmente utilizan el mismo principio de los sismómetros pero en lugar de tener resortes blandos, usan resortes muy duros con el fin de obtener una frecuencia natural muy alta. Considérese por ejemplo la fig. 13. Utilizando la segunda ley de Newton ($\sum F=ma$) se tiene:

$$-k(x1-x2)-c(\dot{x}1-\dot{x}2)=m\ddot{x}1 \qquad (15)$$

El movimiento relativo está dado por $x1\text{-}x2=x$. Si la vibración a la que se somete la el sistema (fig. 13) está dada por $x2=A\text{sen}(\omega t)$, sustituyendo en la ec. 15:

$$m\ddot{x}+c\dot{x}+kx=mA\omega^2 sen\,\omega t$$

La solución de esta ecuación diferencial está dada por:

$$x_p=\frac{A}{\sqrt{\frac{1}{r^4}-\frac{2-4\xi}{r^2}+1}}\text{sen}(\omega t-\phi) \qquad (17)$$

donde $\xi=c/2m\omega_n$, $\omega_n^2=k/m$, $r=\omega/\omega_n$, $\Phi=\tan^{-1}c\omega/(k\text{-}m\omega^2)$. Si ω_n es muy pequeña (la masa m es muy grande), entonces $x_p=A$, lo que implica que el sistema estaría midiendo la amplitud del movimiento. Si por otro lado ω_n es muy grande (la rigidez k es muy grande), entonces $x_p=Ar^2=A\omega^2/\omega_{n2}$; donde $A\omega^2$ es una medida de la aceleración, por tanto, el movimiento relativo es una medida de la aceleración.

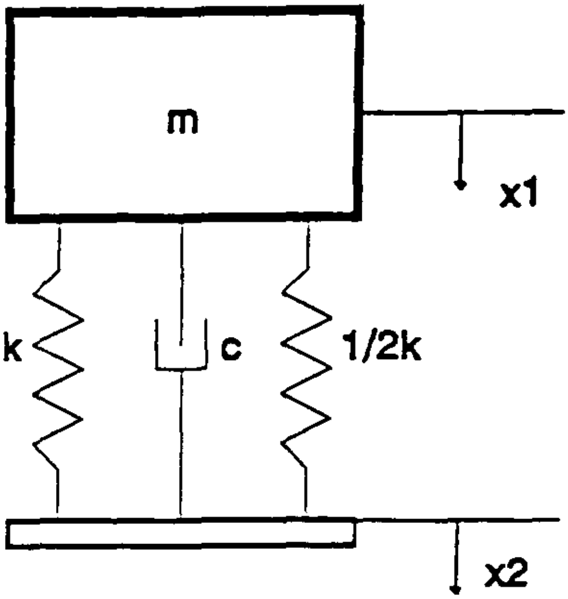

Fig. 13 Sistema de un grado de libertad. Forma esquemática para representar un sismógrafo o un acelerógrafo.

Con base en la diferencia del tiempo de arribo entre las ondas *P* y las ondas *S*, se puede determinar la distancia en la que ocurrió la liberación de la energía. Se necesitan por lo menos dos aparatos (sismógrafos o acelerógrafos) cercanos al foco, para determinar la profundidad en la que se localizó; y tres aparatos para determinar la ubicación del epicentro (fig. 14).

Magnitud e intensidad

Los sismólogos estiman la violencia local del movimiento de tierra usando la *Escala Modificada de Intensidad de Mercalli* en donde se mide que tan severos fueron los daños, en grados. Los terremotos menos intensos sólo pueden ser detectados por instrumentos y no causan daño; de ahí, los terremotos se miden en escala creciente de daños hasta el grado más alto que implica a aquellos sismos que causan la destrucción total de todas las estructuras.

Como es de esperar, los mapas de curvas de igual intensidad en general muestran progresivamente menor daño cuando se incrementa la distancia del epicentro. Sin embargo, los daños tienden a ser más severos en zonas donde los sedimentos del suelo son blandos o no están consolidados. Tomando en cuenta que la intensidad de un sismo no resuelve el problema de conocer que tan grande fue un terremoto debido a que un sismo fuerte a cierta distancia puede producir los mismos daños que uno pequeño en un área cerca al epicentro; y además de que la escala de intensidad no contribuye a la investigación de temblores cuyos epicentros se localizan en el oceano o en lugares inhabitados donde no se puede registrar el daño estructural, los sismólogos requirieron de una escala que midiera el grado de los temblores en términos de la cantidad de energía liberada.

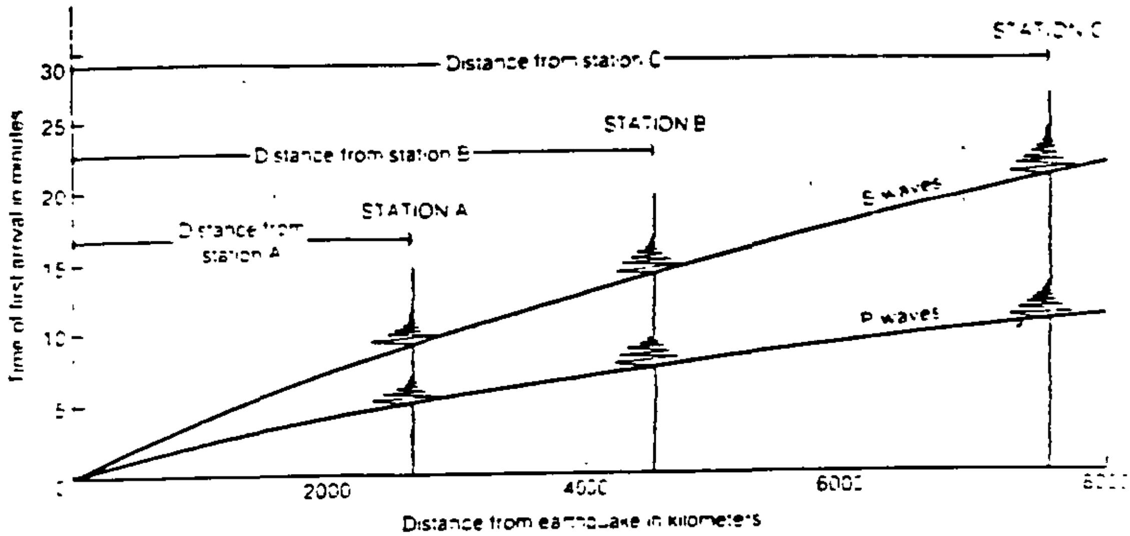

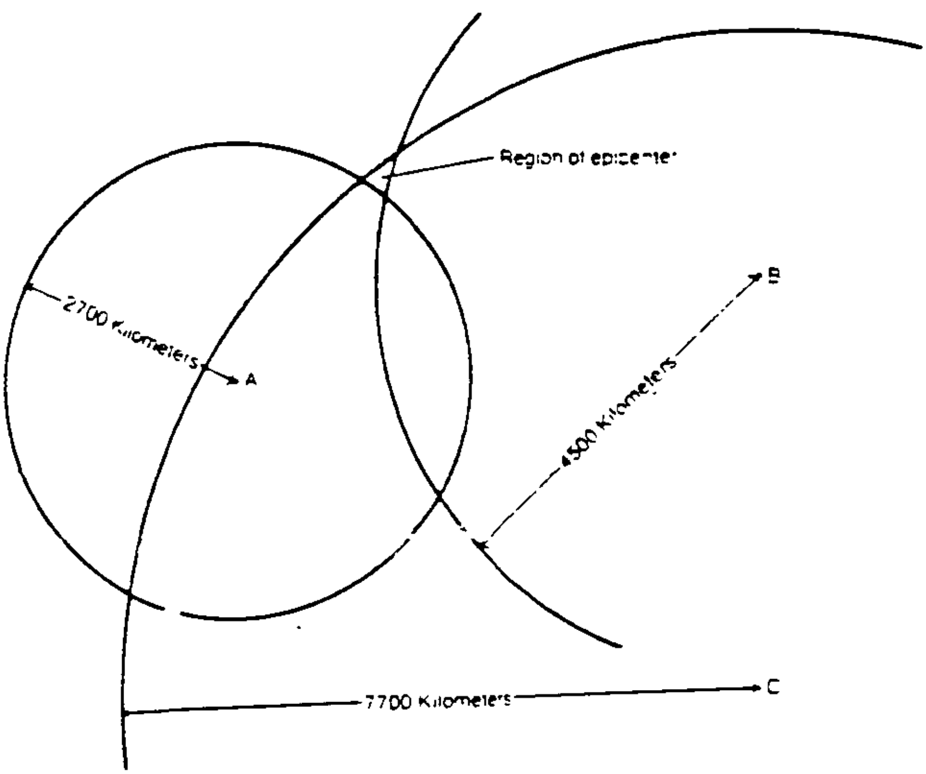

Fig. 14 El intervalo de tiempo de llegada entre las ondas *P* y las ondas *S* se incrementa con la distancia, haciendo posible dibujar un círculo con el radio apropiado desde el sismograma hasta el posible lugar donde se localiza el foco. Para poder determinar el la ubicación del epicentro se requieren tres sismógrafos (Main, 1982).

Los sismólogos generalmente usan la *Escala de Magnitud de Richter* en la cual un brinco de un número entero a otro refleja una diferencia de diez veces la amplitud del movimiento, y aproximadamente una diferencia de treinta veces la cantidad de energía liberada en el foco. Un sismo con una magnitud en la escala de Richter mayor a 5.5 puede causar daños estructurales; magnitudes mayores que 6 son generalmente destructivos si se generan en zonas pobladas. Los terremotos más grandes detectados tienen magnitudes de 8.9. Muchos sismólogos sospechan que los sismos de esta magnitud son los más grandes que se pueden generar, pues creen que la litosfera es demasiado débil para aguantar esfuerzos mayores sin sufrir desplazamientos.

Estructura interna de la Tierra

Los sismógrafos ubicados en cualquier parte del globo terráqueo registran a partir de un gran terremoto, una larga serie de vibraciones de las cuales, sólo pocas, provienen directamente del foco. Las demás son ondas reflejadas de la superficie de la Tierra o de las fronteras entre sus diferentes capas en su interior. El contacto con los diferentes tipos de roca, hacen que las ondas se propaguen con distintas velocidades. La investigación de los diferentes trayectos que siguen las ondas ha dado lugar a la interpretación de la estructura y composición de la Tierra.

El más simple y persistente eco proviene de la frontera entre la corteza terrestre y la litosfera a la cual se le dá el nombre de discontinuidad de Mohorovicic o, más sencillamente, discontinuidad Moho. Esta se localiza aproximadamente entre los 40 y 50 km si se mide en la corteza continental y a los 10 km de profundidad si se mide en la corteza oceánica.

Entre los 100 y 250 km de profundidad, las ondas sísmicas disminuyen su velocidad de propagación de manera considerable y una buena parte del componente de las ondas de corte desaparece. Esto sugiere que esta zona de baja velocidad de propagación está formada por rocas parcialmente derretidas. A esta zona se le conoce como astenosfera.

Los sismógrafos que reciben las vibraciones de los terremotos grandes generalmente registran un eco que proviene de una profundidad de aproximadamente 2900 km que aparentemente refleja la superficie del núcleo de la Tierra. Este núcleo crea una *zona de sombra* en el lado opuesto de la Tierra al lugar donde se generó el sismo debido a la refracción y reflexión de las ondas. Sin embargo, cerca del centro de esta zona de sombra en el área directamente opuesta al foco, se registran fuertes vibraciones causadas por un enfocamiento de energía que el núcleo genera, actuando como un lente que se encuentra embebido en el planeta. Estas vibraciones son causadas por ondas longitudinales habiendo ausencia total de las ondas de corte, lo que sugiere que, al menos la parte externa del núcleo es líquida (fig. 15).

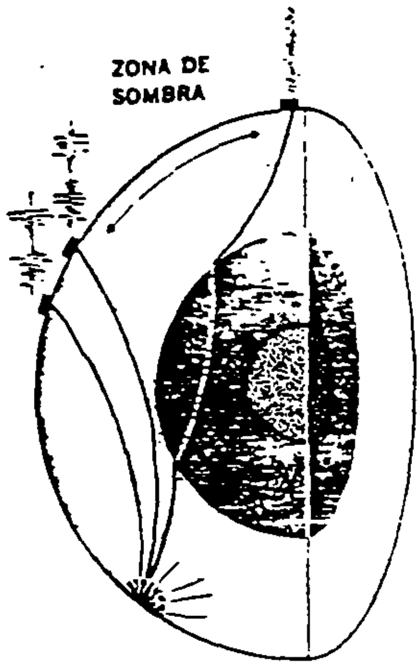

Fig. 15 La zona de sombra es una área donde las ondas no llegan por la desviación que sufren debido a la presencia del núcleo. Sin embargo, algunas ondas sísmicas atraviezan el núcleo y aparecen enfocadas en un área directamente opuesta a donde se generó el sismo.

EFECTOS SÍSMICOS EN PUENTES

Los efectos que los sismos producen en los puentes o en cualquier estructura van a depender de las características del sismo, del suelo donde se cimenta la estructura y de la estructura misma.

Para poder llevar a cabo un diseño adecuado de la cimentación de la estructura se requiere:

a) Evaluar el comportamiento esfuerzo-deformación de los suelos (o rocas) bajo la carga dinámica esperada en la práctica.

b) Desarrollar métodos que permitan conocer los efectos de las fuerzas de inercia y con ello conocer el comportamiento de las masas de suelo y de los sistemas suelo-estructura.

c) Predecir la intensidad, duración y contenido de frecuencias de los sismos que se puedan presentar, con base en los eventos detectados en la zona con anterioridad.

d) Evaluar la potencialidad de falla por licuación del suelo.

e) Investigar la posibilidad de deslizamientos de taludes durante un terremoto.

Todo ello con el propósito de asegurarse de que:

a) Las amplitudes de las vibraciones que se generen no sean excesivas.

b) Los esfuerzos/deformaciones inducidos en estructuras vecinas, sean pequeñas.

c) No haya peligro de una acumulación permanente de deformaciones debidas a la compactación dinámica en estratos arenosos.

Para determinar las propiedades dinámicas del suelo se recurre tanto a pruebas de campo como las de laboratorio. En las tablas I, II y III se presentan algunas de las pruebas utilizadas para determinar los parámetros dinámicos del suelo. Con estos parámetros se podrán obtener las impedancias dinámicas que están relacionadas con la fuerza dinámica (R) y el desplazamiento que se genera en el suelo (u) de la siguente manera: $k = R/u$, donde $u = u_1 + iu_2$, $i_2 = -1$; por consiguiente $k = k_1 + ik_2$. $k_1(\omega)$ depende de las características de rigidez del sistema (el cual no depende de ω; notese que las propiedades del suelo de módulo de cortante, coeficiente de Poisson y amortiguamiento son en escencia independientes de ω) y de las características de inercia del suelo (que son proporcionales a ω^2). $k_2(\omega)$ representa el amortiguamiento del sistema que engloba una parte independiente de la frecuencia reflejando el amortiguamiento histerético del suelo, y otra parte dependiente de la frecuencia que representa al amortiguamiento viscoso.

Para llevar a cabo los estudios de propagación de ondas en suelos y/o estructuras generalmente se recurre a modelos que son sujetos a hipótesis fuertes pero simplifican enormemente el problema, lo que permite entender, en general, el comportamiento del modelo real y tomar decisiones respecto a su diseño.

Modelos unidimensionales

En estos modelos se aceptan las hipótesis de que los materiales por los cuales se propagan las ondas son elásticos y homogeneos; además, la dirección de propagación de ondas es en una sóla dirección, lo que implica que las fronteras entre los medios que constituyen al modelo, son paralelas y la incidencia de ondas perpendicular a estas fronteras.

Como ejemplo considerese una barra por la cual se propagan ondas longitudinales (fig. 16) que generan esfuerzos (σ) y desplazamientos (u) que están en función del tiempo y de la posición en la cual son medidos. El equilibrio dinámico de un elemento infinitesimal de la barra está dado por

$$\frac{\partial \sigma_x}{\partial x}+\rho \ddot{u}_x=0 \tag{18}$$

Aplicando la ley de Hooke

$$\sigma_x=Ee_x=E\left(-\frac{\partial u_x}{\partial x}\right) \tag{19}$$

donde E es el módulo de elasticidad, de ahí que

$$\frac{\partial^2 u_x}{\partial x^2}=\frac{1}{\alpha^2}\ddot{u}_x \tag{20}$$

Esta es la ecuación de onda para modelos unidimensionales cuando se propagan ondas longitudinales. La obtención de la ecuación de onda para otros tipos de ondas es análoga. Cualquier función que cumpla con la ecuación de onda (ec. 20) y con las condiciones de frontera que impone el modelo, representa la solución del problema analizado. Estas funciones van a ser de la forma

$$u_x=f_a(x+ct)+f_b(x-ct) \tag{21}$$

donde c es la velocidad con la que se propagan las ondas en el medio. $f(x \pm ct)$ representa a las ondas propagándose en la dirección $\mp x$.

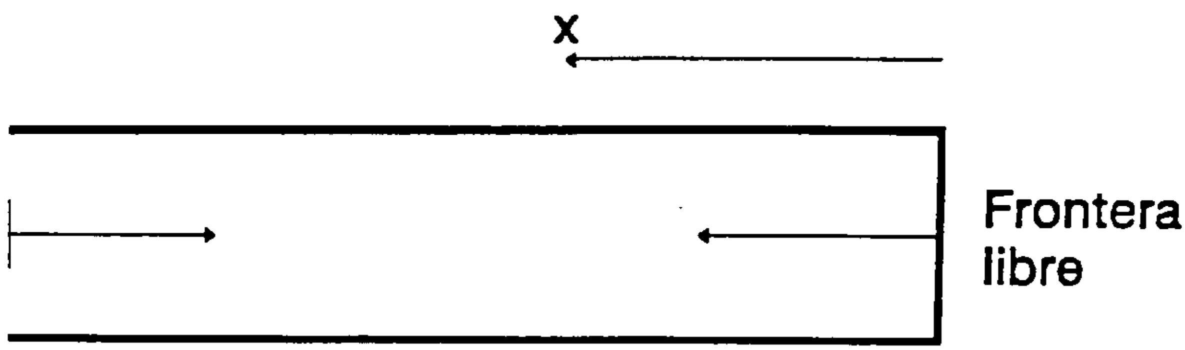

Fig. 16 Barra longitudinal por donde se propagan las ondas, con un extremo libre. Las ondas inciden de izquierda a derecha.

Cuando se considera en el modelo una frontera libre (fig. 17) las condiciones de frontera son $\sigma_x=0$ en $x=0$. Si la solución de la ecuación de onda es

$$u = Be^{i\omega t}e^{-i\frac{\omega}{c}x} + Ae^{i\omega t}e^{i\frac{\omega}{c}x} \tag{22}$$

donde A y B son las amplitudes de las ondas incidentes y reflejadas, respectivamente, se tiene que en $x=0$ aplicando las condiciones de frontera

$$-\frac{i\omega}{c}B + \frac{i\omega}{c}A = 0 \tag{23}$$

$$A = B$$

Si ahora se considera una frontera fija, las condiciones de fronera son $u=0$ en $x=0$ de donde se obtiene que $A=-B$ y, por consiguiente

$$u = Ae^{i\omega t}\left[e^{i\frac{\omega}{c}x} - e^{-i\frac{\omega}{c}x}\right] = 2Asen\left(\frac{\omega}{c}x\right)e^{i\omega t} \tag{24}$$

y $\sigma = 2\sigma_{inc}$ en $x=0$.

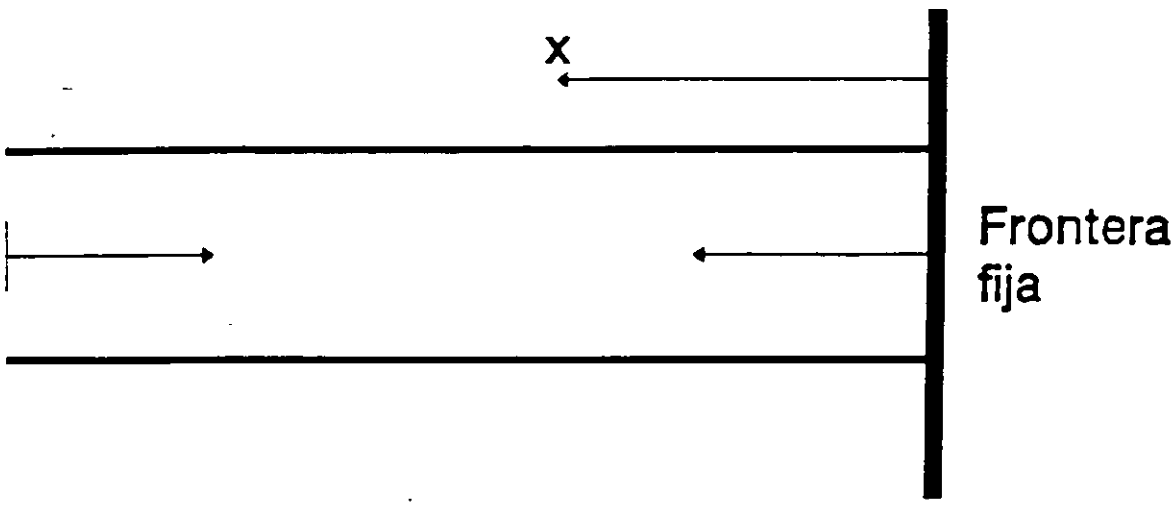

Fig. 17 Barra longitudinal por donde se propagan las ondas, con un extremo fijo. Las ondas inciden de izquierda a derecha.

Cuando la propagación de ondas se lleva a cabo entre dos medios (fig. 18) se deben considerar dos ecuaciones de onda (una para cada medio). La solución general es de la forma

$$u_1 = u_{inc} + u_{ref} = A_{inc} e^{i\omega t} e^{i\frac{\omega}{c_1}x} + A_{ref} e^{i\omega t} e^{-i\frac{\omega}{c_1}x}$$
$$u_2 = u_{trans} = B_{trans} e^{i\omega t} e^{i\frac{\omega}{c_2}x} \tag{25}$$

Las condiciones de frontera en $x=0$ son $u_1 = u_2$ y $\sigma_1 = \sigma_2$, de ahí se obtiene

$$A_{inc} + A_{ref} = B_{trans}$$
$$A_{inc} - A_{ref} = \frac{\rho_2 c_2}{\rho_1 c_1} B_{trans} \tag{26}$$

de donde

$$B_{trans} = \frac{2}{1 + \frac{\rho_2 c_2}{\rho_1 c_1}} \cdot A_{inc}$$
$$A_{ref} = \frac{1 - \frac{\rho_2 c_2}{\rho_1 c_1}}{1 + \frac{\rho_2 c_2}{\rho_1 c_1}} \cdot A_{inc} \tag{27}$$

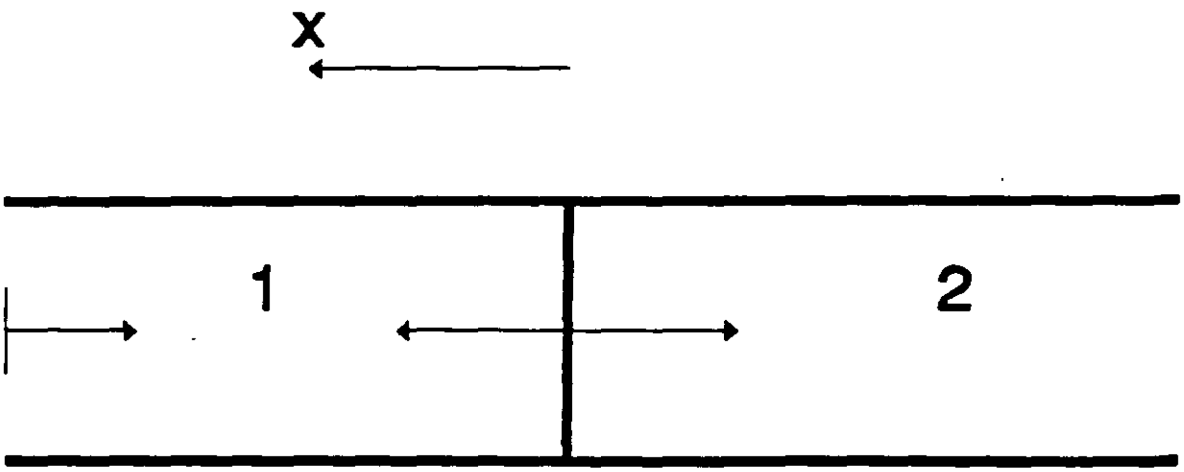

Ilustr. 4

Fig. 18 Barra longitudinal compuesta por dos materiales con propiedades del suelo por donde se propagan las ondas, con un extremo fijo. Las ondas inciden de izquierda a derecha.

Los modelos bi y tridimensionales tienen la particularidad de que las ondas se propagan en dos o más direcciones debido a la presencia de fronteras u obstáculos que, incluso pueden dar origen a la difracción de ondas. Al final de estas notas se presenta un artículo en el cual se analiza un caso particular de propagación de ondas en modelos bidimensionales (Suarez y Sánchez-Sesma, 1994).

GEOLOGÍA Y CONDICIONES LOCALES

Cuando se registra la señal de un sismo cuyo epicentro se localiza a varios kilómetros de distancia, el registro que se obteniene es generalmete diferente al de alguna estación localizada directamente sobre el foco del sismo, debido a que las ondas viajan a través de distintos materiales con diferentes velocidades de propagación y configuraciones varias que provocan que éstas modifiquen su trayecto, velocidad y amplitud (efectos de trayecto). Cuando las ondas atraviesan los suelos o formaciones locales del sitio, sufren también modificaciones adicionales (efectos de sitio o condiciones locales). En la fig. 19 se presentan estos conceptos. Considerando efectos lineales únicamente, si se conoce la señal antes y despues de ser afectada por las condiciones locales, la contribución de los efectos de sitio se obtiene al efectuar la división de los espectros de Fourier de la señal ubicada en el sitio, con aquella que no se afectó por las condiciones locales. Al espectro que se obtiene de esta manera se le conoce con el nombre de función de transferencia o cociente espectral. De esta manera, cuando se tiene cualquier incidencia de ondas se puede obtener la respuesta del sitio al multiplicar su espectro de Fourier por la función de transferencia.

Una hipótesis adicional que se hace es considerar planas a las ondas que se propagan dentro de medios homogéneos e isótropos. Esta hipótesis implica que se puede identificar el lugar geométrico de los puntos que se encuentran en una misma fase donde se localiza un frente de onda recto (fig. 20). Si la fuente de una perturbación es muy pequeña y la onda se propaga en un medio isótropo, entonces el frente de onda tendrá una superficie esférica con el centro en la fuente. Si la distancia r a la fuente es muy grande, el frente de onda se puede considerar con buena aproximación como plano (fig. 21). A la dirección con la que se propagan los frentes de onda se le representa por rayos que son líneas perpendiculares a estos. Anexo a estas notas se presenta un artículo en donde se plantea la importancia de considerar las condiciones locales cuando se estudia la respuesta sísmica de un sitio (Sánchez-Sesma *et al*, 1987).

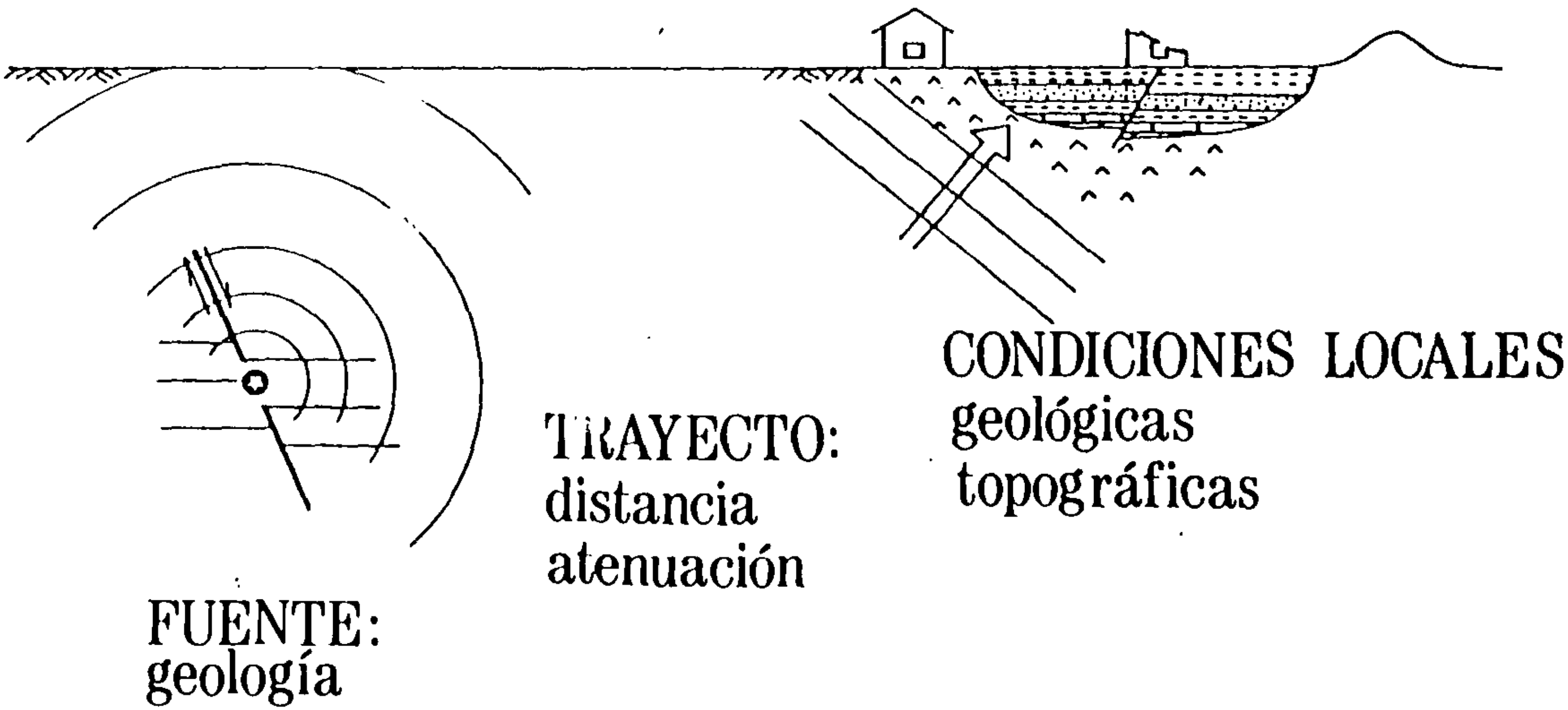

Fig. 19 Elementos que influyen en la propagación de ondas sísmicas. Fuente, trayecto y condiciones locales (modificada a partir de Chávez-García, 1987)

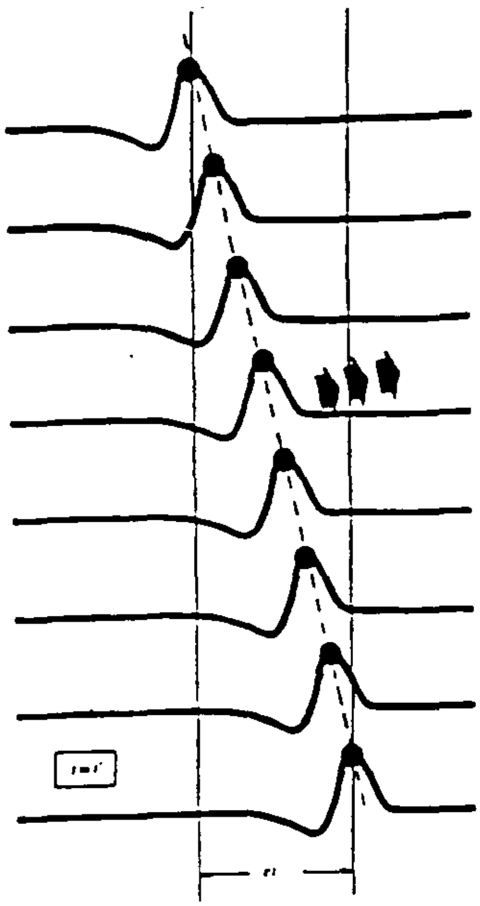

Fig. 20 Frente de ondas (línea a trazos) que pasa por los puntos indicados por un círculo lleno en un tiempo $t = t'$. Las flechas indican la dirección de la propagación del frente de onda.

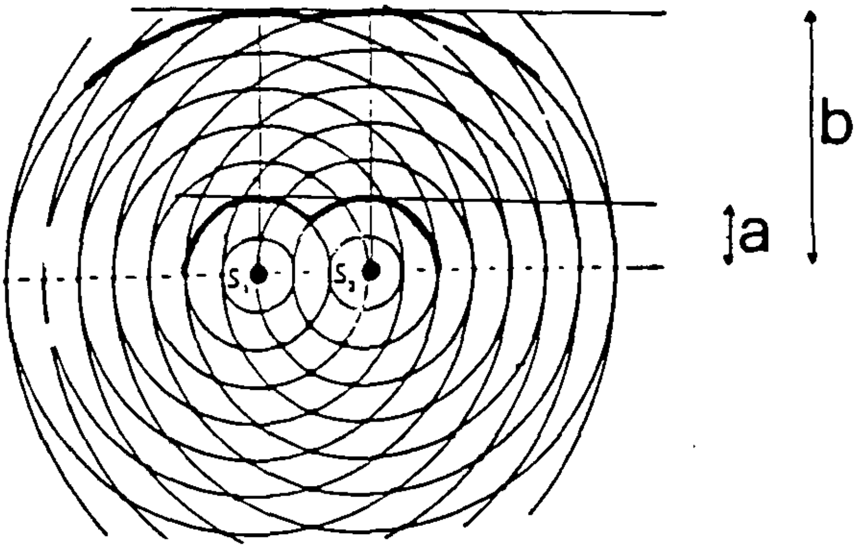

Fig. 21 Un frente de onda a una distancia *b* puede considerarse más cercanamente representado por un frente de onda plano que el ubicado a una distancia menor *a*. En la figura se presentan los campos generados por dos fuentes (S_1 y S_2).

REFERENCIAS

Alt (1982), "Physical Geology", *Wadsworth Publishing Company.*

Bolt B A (1976), "Nuclear Explosions and earthquakes", *W. H. Freeman and Company.*

Chávez-García F J (1987). "Evaluation de risque sismique à Thessalsniki", Trabajo presentado para la obtención del grado D E A, *Université Joseph Fourier de Grenoble,* Francia.

Main G I (1978), "Vibrations and waves in Physics", *Cambridge University Press,* Cambrigde, London, New York, Melbourne.

Newland D E (1980), "An introduction to random vibrations and spectral analysis", *Longman,* London.

Sánchez-Sesma F J, Pérez-Rocha L E, Suarez M, Bravo M A, "El modelado de la respuesta sísmica del valle de México", *Simposio de la SMMS,* 1987.

Suarez M y Sánchez-Sesma F J, "Amplificación local del movimiento en depósitos sedimentarios usando modelos simplificados", *Ingeniería Sismica,*48, pp 11-21, 1994.

FACULTAD DE INGENIERIA U.N.A.M.
DIVISION DE EDUCACION CONTINUA

CURSOS ABIERTOS

XXV CURSO INTERNACIONAL DE INGENIERÍA SÍSMICA

MÓDULO III:

DISEÑO SÍSMICO DE PUENTES

TEMA

RIESGO SÍSMICO Y DINÁMICA ESTRUCTURAL

DR. JAIME GARCÍA PÉREZ
PALACIO DE MINERÍA
AGOSTO DE 1999

Palacio de Minería Calle de Tacuba 5 Primer piso Deleg. Cuauhtémoc 06000 México D.F. APDO. Postal M-2285
Teléfonos 512-8955 512-5121 521-7335 521-1987 Fax 510-0573 521-4020 AL 26

DISEÑO SISMICO DE PUENTES

TEMA 3 RIESGO SISMICO Y DINAMICA ESTRUCTURAL

Profesor : Dr. Jaime García Pérez
Instituto de Ingeniería, UNAM

MEXICO

Chapter 6

SEISMICITY

LUIS ESTEVA
Instituto de Ingeniería, Universidad Nacional Autónoma de México, Mexico

6.1 ON SEISMICITY MODELS

Rational formulation of engineering decisions in seismic areas requires quantitative descriptions of seismicity. These descriptions should conform with their intended applications: in some instances, simultaneous intensities during each earthquake have to be predicted at several locations, while in others it suffices to make independent evaluations of the probable effects of earthquakes at each of those locations.

The second model is adequate for the selection of design parameters of individual components of a regional system (the structures in a region or country) when no significant interaction exists between response or damage of several such individual components, or between any of them and the system as a whole. In other words, it applies when the damage — or negative utility — inflicted upon the system by an earthquake can be taken simply as the addition of the losses in the individual components.

The linearity between monetary values and utilities implied in the second model is not always applicable. Such is the case, for instance, when a significant portion of the national wealth or of the production system is concentrated in a relatively narrow area, or when failure of life-line components may disrupt emergency and relief actions just after an earthquake. Evaluation of risk for the whole regional system has then to be based on seismicity models of the first type, that is, models that predict simultaneous intensities at several locations during each event; for the purpose of decision making, nonlinearity between monetary values and utilities can be accounted for by means of adequate scale transformations. These models are also of interest to insurance companies, when the probability distribution of the maximum loss in a given region during a given time interval is to be estimated.

Whatever the category to which a seismic risk problem belongs, it requires the prediction of probability distributions of certain ground motion characteristics (such as peak ground acceleration or velocity, spectral density, response or Fourier spectra, duration) at a given site during a single shock or of maximum values of some of those characteristics in earthquakes occurring during given time intervals. When the reference interval tends to infinity, the probability distribution of the maximum value of a given characteristic approaches that of its maximum *possible* value. Because different systems or subsystems are sensitive to different ground motion characteristics, the term *intensity characteristic* will be used throughout this chapter to mean a particular parameter or set of parameters of an earthquake motion, in terms of which the response is to be predicted. Thus, when dealing with the failure probability of a structure, intensity can be alternatively measured — with different degrees of correlation with structural response — by the ordinate of the response spectrum for the corresponding period and damping, the peak ground acceleration, or the peak ground velocity.

In general, local instrumental information does not suffice for estimating the probability distributions of maximum intensity characteristics, and use has to be made of data on subjective measures of intensities of past earthquakes, of models of *local seismicity*, and of expressions relating characteristics with magnitude and site to source distance. Models of local seismicity consist, at least, of expressions relating magnitudes of earthquakes generated in given volumes of the earth's crust with their return periods. More often than not, a more detailed description of local seismicity is required, including estimates of the maximum magnitude that can be generated in these volumes, as well as probabilistic (stochastic process) models of the possible histories of seismic events (defined by magnitudes and coordinates).

This chapter deals with the various steps to be followed in the evaluation of seismic risk at sites where information other than direct instrumental records of intensities has to be used: identifying potential sources of activity near the site, formulating mathematical models of local seismicity for each source, obtaining the contribution of each source to seismic risk at the site and adding up contributions of the various sources and combining information obtained from local seismicity of sources near the site with data on instrumental or subjective intensities observed at the site.

The foregoing steps consider use of information stemming from sources of different nature. Quantitative values derived therefrom are ordinarily tied to wide uncertainty margins. Hence they demand probabilistic evaluation, even though they cannot always be interpreted in terms of relative frequencies of outcomes of given experiments. Thus, geologists talk of the maximum magnitude that can be generated in a given area, assessed by looking at the dimensions of the geological accidents and by extrapolating the observations of other regions which available evidence allows to brand as similar to the one of interest; the estimates produced are obviously uncertain, and the degree of uncertainty should be expressed together with the most probable value. Following nearly parallel lines, some geophysicists estimate the energy that can be liberated by a single shock in a given area by making quantitative assumptions about source dimensions, dislocation amplitude and stress drop, consistent with tectonic models of the region and, again, with comparisons with areas of similar tectonic characteristics.

Uncertainties attached to estimates of the type just described are in general extremely large: some studies relating fault rupture area, stress drop, and magnitude (Brune, 1968) show that, considering not unusually high stress drops, it does not take very large source dimensions to get magnitudes 8.0 and greater, and those studies are practically restricted to the simplest types of fault displacement. It is not clear, therefore, that realistic bounds can always be assigned to potential magnitudes in given areas or that, when this is feasible, those bounds are sufficiently low, so that designing structures to withstand the corresponding intensities is economically sound, particularly when occurrence of those intensities is not very likely in the near future. Because uncertainties in maximum feasible magnitudes and in other parameters defining magnitude-recurrence laws can be as significant as their mean values when trying to make rational seismic design decisions, those uncertainties have to be explicitly recognized and accounted for by means of adequate probabilistic criteria. A corollary is that geophysically based estimates of seismicity parameters should be accompanied with corresponding uncertainty measures.

Seismic risk estimates are often based only on statistical information (observed magnitudes and hypocentral coordinates). When this is done, a wealth of relevant geophysical information is neglected, while the probabilistic prediction of the future is made to rely on a sample that is often small and of little value, particularly if the sampling period is short as compared with the desirable return period of the events capable of severely damaging a given system.

The criterion advocated here intends to unify the foregoing approaches and rationally to assimilate the corresponding pieces of information. Its philosophy consists in using the geological, geophysical, and all other available non-statistical evidence for producing a set of alternate assumptions concerning a mathematical (stochastic process) model of seismicity in a given source area. An initial probability distribution is assigned to the set of hypotheses, and the statistical information is then used to improve that probability assignment. The criterion is based on application of *Bayes theorem*, also called the *theorem of the probabilities of hypotheses*. Since estimates of risk depend largely on conceptual models of the geophysical processes involved, and these are known with different degrees of uncertainty in different zones of the earth's crust, those estimates will be derived from stochastic process models with uncertain forms or parameters. The degree to which these uncertainties can be reduced depends on the limitations of the state of the art of geophysical sciences and on the effort that can be put into compilation and interpretation of geophysical and statistical information. This is an economical problem that should be handled, formally or informally, by the criteria of decision making under uncertainty.

6.2 INTENSITY ATTENUATION

Available criteria for the evaluation of the contribution of potential seismic sources to the risk at a site make use of *intensity attenuation* expressions that relate intensity characteristics with magnitude and distance from site to source. Depending on the application envisaged, the intensity characteristic to be predicted can be expressed in a number of manners, ranging from a subjective index, such as the *Modified Mercalli intensity*, to a combination of one or more quantitative measures of ground shaking (see Chapter 1).

A number of expressions for attenuation of various intensity characteristics with distance have been developed, but there is little agreement among most of them (Ambraseys, 1973). This is due in part to discrepancies in the definitions of some parameters, in the ranges of values analyzed, in the actual wave propagation properties of the geological formations lying between source and site, in the dominating shock mechanisms, and in the forms of the analytical expressions adopted a priori.

Most intensity attenuation studies concern the prediction of earthquake characteristics on rock or firm ground, and assume that these characteristics, properly modified in terms of frequency dependent soil amplification factors, should constitute the basis for estimating their counterparts on soft ground. Observations about the influence of soil properties on earthquake damage support the assumption of a strong correlation between type of local ground and intensity in a given shock. Attempts to analytically predict the characteristics of motions on soil given those on firm ground or on bedrock have not been too successful, however (Crouse, 1973; Hudson and Udwadia, 1973; Salt, 1974), with the exception of some peculiar cases, like Mexico City (Herrera et al., 1965), where local conditions favor the fulfillment of the assumptions implied by usual analytical models. The following paragraphs concentrate on prediction on intensities on firm ground; the influence of local soil is discussed in Chapter 4.

6.2.1 *Intensity attenuation on firm ground*

When isoseismals (lines joining sites showing equal intensity) of a given shock are based only on intensities observed on homogeneous ground conditions, such as *firm ground* (compact soils) or bedrock, they are roughly elliptical and the orientations of the corresponding axes are often correlated with local or regional geological trends (Figs. 6.1–6.3). In some regions – for instance near major faults in the western United States – those trends are well defined and the correlations are clear enough as to permit prediction of intensity in the near and far fields in terms of magnitude and distance to the generating fault or to the centroid of the energy liberating volume. In other regions, such as the eastern United States and most of Mexico, isoseismals seem to elongate systematically in a direction that is a function of the epi-

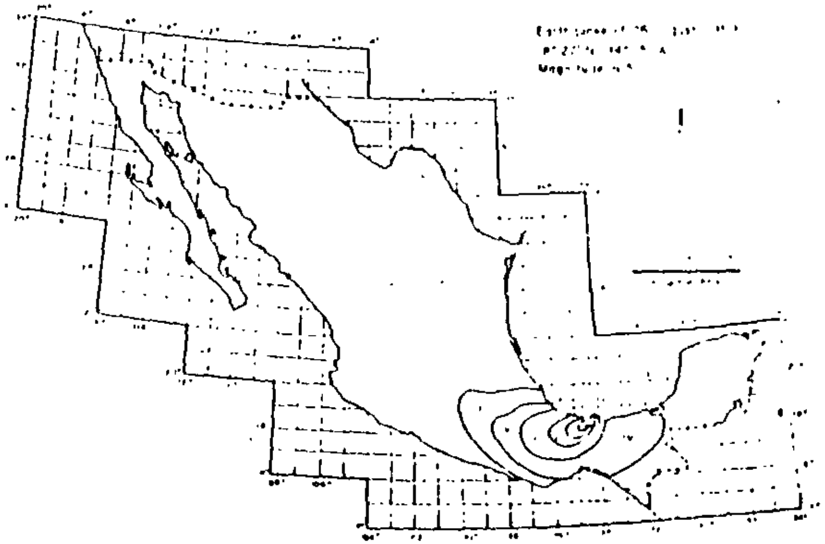

Fig. 6.1 Isoseismals of an earthquake in Mexico (After Figueroa, 1963.)

central coordinates (Bollinger, 1973; Figueroa, 1963). In that case, intensity should be expressed as a function of magnitude and coordinates of source and site. For most areas in the world, intensity has to be predicted in terms of simple – and cruder – expressions that depend only on magnitude and distance from site to instrumental hypocenter. This stems from inadequate knowledge of geotectonic conditions and from limited information concerning the volume where energy is liberated in each shock.

A comparison of the rates of attenuation of intensities on firm ground for shocks on western and eastern North America has disclosed systematic differences between those rates (Milne and Davenport, 1969). This is the source of a basic, but often unavoidable, weakness of most intensity-attenuation expressions, because they are based on heterogeneous data, recorded in different zones, and the very nature of their applications implies that the less is known about possible systematic deviations in a given zone, as a consequence of the meagerness of local information, the greater weight is given to predictions with respect to observations.

6.2.1.1 *Modified Mercalli intensities*

An analysis of the Modified Mercalli intensities on firm ground reported for earthquakes occurring in Mexico in the last few decades leads to the fol-

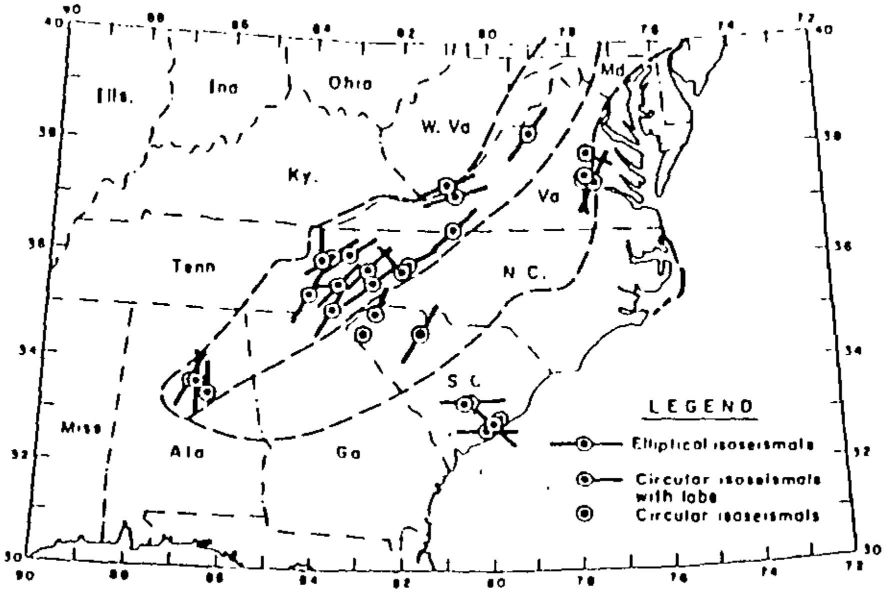

Fig. 6.2. Elongation of isoseismals in the southeastern United States. (After Bollinger, 1973.)

lowing expression relating magnitude M, hypocentral distance R (in kilometers) and intensity I (Esteva, 1968).

$$I = 1.45\,M - 5.7 \log_{10} R + 7.9 \tag{6.1}$$

The prediction error, defined as the difference between observed and computed intensity, is roughly normally distributed, with a standard deviation of 2.01, which means that there is a probability of 60% that an observed intensity is more than one degree greater or smaller than its predicted value.

6.2.1.2 Peak ground accelerations and velocities

A few of the available expressions will be described. Their comparison will show how cautiously a designer intending to use them should proceed.

Housner studied the attenuation of peak ground accelerations in several regions of the United States and presented his results graphically (1969) in terms of fault length (in turn a function of magnitude), shapes of isoseismals and areas experiencing intensities greater than given values (Fig. 6.4 and 6.5).

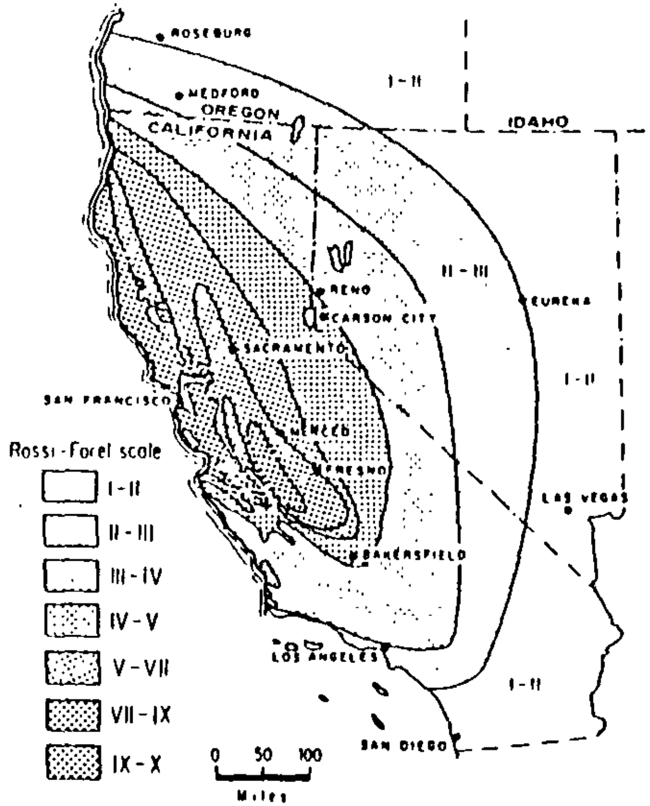

Fig. 6.3. Isoseismals in California. (After Bolt, 1970.)

He showed that intensities attenuate faster with distance on the west coast than in the rest of the country. This comparison is in agreement with Milne and Davenport (1969), who performed a similar analysis for Canada. From observations of strong earthquakes in California and in British Columbia, they developed the following expression for a, the peak ground acceleration, as a fraction of gravity:

$$a/g = 0.0069\,e^{1.64M}/(1.1\,e^{1.1M} + R^2) \tag{6.2}$$

Here, R is epicentral distance in kilometers. The acceleration varies roughly as $e^{1.64M} R^{-2}$ for large R, and as $e^{0.54M}$ where R approaches zero. This reflects to some extent the fact that energy is released not at a single point but from a finite volume. A later study by Davenport (1972) led him

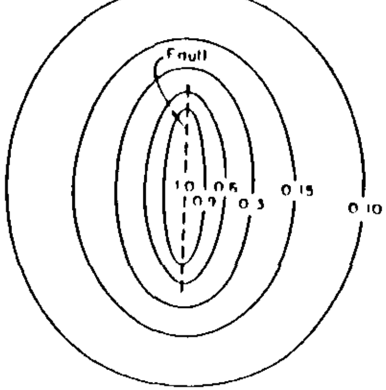

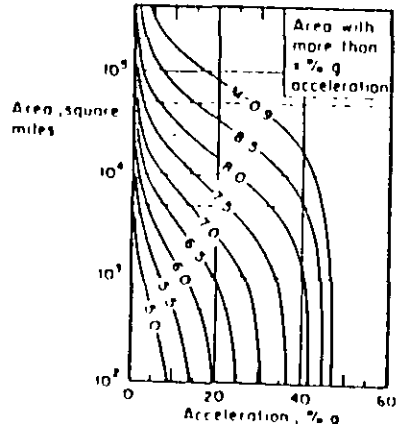

Fig. 6.4 Idealized contour lines of intensity of ground shaking. (After Housner, 1969.)

Fig. 6.5 Area in square miles experiencing shaking of x %g or greater for shocks of different magnitudes. (After Housner, 1969.)

to propose the expression:

$$a/g = 0.279\, e^{0.8M}/R^{1.64} \tag{6.3}$$

The statistical error of this equation was studied by fitting a lognormal probability distribution to the ratios of observed to computed accelerations. A standard deviation of 0.74 was found in the natural logarithms of those ratios.

Esteva and Villaverde (1973), on the basis of accelerations reported by Hudson (1971, 1972a,b), derived expressions for peak ground accelerations and velocities, as follows:

$$a/g = 5.7\, e^{0.8M}/(R + 40)^2 \tag{6.4}$$

$$v = 32\, e^{M}/(R + 25)^{1.7} \tag{6.5}$$

Here v is peak ground velocity in cm/sec and the other symbols mean the same as above. The standard deviation of the natural logarithm of the ratio of observed to predicted intensity is 0.64 for accelerations and 0.74 for velocities. If judged by this parameter, eqs. 6.3 and 6.4 seem equally reliable. However, as shown by Fig. 6.6, their mean values differ significantly in some ranges.

With the exception of eq. 6.2, all the foregoing attenuation expressions are products of a function of R and a function of M. This form, which is acceptable when the dimensions of the energy-liberating source are small com-

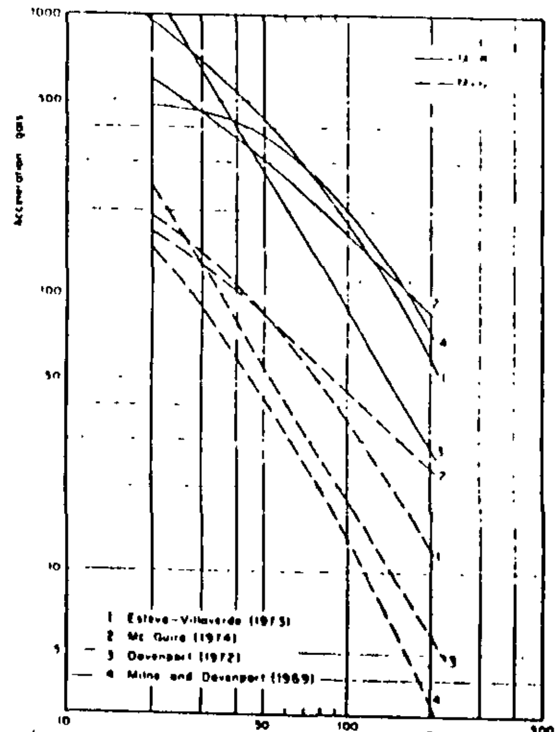

Fig. 6.6. Comparison of several attenuation expressions.

pared with R, is inadequate when dealing with earthquake sources whose dimensions are of the order of moderate hypocentral distances, and often greater than them. Although equation errors (probability distributions of the ratio of observed to predicted intensities) have been evaluated by Davenport (1972) and Esteva and Villaverde (1973), their dependence on M and R has not been analyzed. Because seismic risk estimates are very sensitive to the attenuation expressions in the range of large magnitudes and short distances, more detailed studies should be undertaken, aiming at improving those expressions in the mentioned range, and at evaluating the influence of M and R on equation error. Information on strong motion records will probably be scanty for those studies, and hence they will have to be largely based on analytical or physical models of the generation and propagation of seismic waves. Although significant progress has been lately attained in this direction (Trifunac, 1973) the results from such models have hardly influenced the practice of seismic risk estimation because they have remained either unknown to or imperfectly appreciated by engineers in charge of the corresponding decisions

6.2.1.3 Response spectra

Peak ground acceleration and displacement are fairly good indicators of the response of structures possessing respectively very high and very small natural frequencies. Peak velocity is correlated with the response of intermediate-period systems, but the correlation is less precise than that tying the former parameters; hence, it is natural to formulate seismic risk evaluation and engineering design criteria in terms of spectral ordinates.

Response spectrum prediction for given magnitude and hypocentral or site-to fault distance usually entails a two-step process, according to which peak ground acceleration, velocity and displacement are initially estimated and then used as reference values for prediction of the ordinates of the response spectrum. Let the second step in the process be represented by the operation $y_s = \alpha y_g$, where y_s is an ordinate of the response spectrum for a given natural period and damping ratio, and y_g is a parameter (such as peak ground acceleration or velocity) that can be directly obtained from the time-history record of a given shock regardless of the dynamic properties of the systems whose response is to be predicted. For given M and R, y_g is random and so is $y_s/y_g = \alpha$; the mean and standard deviation of y_s depend on those of y_g and α and on the coefficient of correlation of the latter variables. As shown above, y_g can only be predicted within wide uncertainty limits, often wider than those tied to y_s (Esteva and Villaverde, 1973). The coefficient of variation of y_s given M and R can be smaller than that of y_g only if α and y_g are negatively correlated, which is often the case: the greater the deviation of an observed value of y_g with respect to its expectation for given M and R, the lower is likely to be α. In other words, it seems that in the intermediate range of natural periods the expected values of spectral ordinates for given damping ratios can be predicted directly in terms of magnitude and focal distance with narrower (or at most equal) margins of uncertainty than those tied to predicted peak ground velocities. For the ranges of very short or very long natural periods, peak amplitudes of ground motion and spectral ordinates approach each other and their standard errors are therefore nearly equal

McGuire (1974) has derived attenuation expressions for the conditional values (given M and R) of the mean and of various percentiles of the probability distributions of the ordinates of the response spectra for given natural periods and damping ratios. Those expressions have the same form as eqs 6.4 and 6.5, but their parameters show that the rates of attenuation of spectral ordinates differ significantly from those of peak ground accelerations or velocities. For instance, McGuire finds that peak ground velocity attenuates in proportion to $(R + 25)^{-1.20}$, while the mean of the pseudovelocity for a natural period of 1 sec and a damping ratio of 2% attenuates in proportion to $(R + 25)^{-0.59}$. These results stem from the way that frequency content changes with R and lead to the conclusion that the ratio of spectral velocity should be taken as a function of M and R.

TABLE 6.1

McGuire's attenuation expressions $y = b_1 10^{b_2 M}(R + 25)^{-b_3}$

y	b_1	b_2	b_3	$V(y)$ = coeff. of var. of y
a gals	472.3	0.278	1.301	0.548
v cm/sec	5.64	0.401	1.202	0.696
d cm	0.393	0.434	0.885	0.883
Undamped spectral pseudovelocities				
T = 0.1 sec	11.0	0.278	1.346	0.941
0.5	3.05	0.391	1.001	0.636
1.0	0.631	0.378	0.519	0.768
2.0	0.0768	0.469	0.419	0.989
5.0	0.0834	0.561	0.897	1.344
5% damped spectral pseudovelocities				
T = 0.1 sec	10.09	0.233	1.341	0.651
0.5	5.74	0.356	1.197	0.591
1.0	0.432	0.399	0.701	0.703
2.0	0.122	0.466	0.675	0.941
5.0	0.0706	0.557	0.938	1.193

Table 6.1 summarizes McGuire's attenuation expressions and their coefficients of variation for ordinates of the pseudovelocity spectra and for peak ground acceleration, velocity and displacement. Similar expressions were derived by Esteva and Villaverde (1973), but they are intended to predict only the maxima of the expected acceleration and velocity spectra, regardless of the periods associated with those maxima. No analysis has been performed of the relative validity of McGuire's and Esteva and Villaverde's expressions for various ranges of M and R.

6.3 LOCAL SEISMICITY

The term *local seismicity* will be used here to designate the degree of seismic activity in a given volume of the earth's crust; it can be quantitatively described according to various criteria, each providing a different amount of information. Most usual criteria are based on upper bounds to the magnitudes of earthquakes that can originate in a given seismic source, on the amount of energy liberated by shocks per unit volume and per unit time or on more detailed statistical descriptions of the process.

6.3.1 Magnitude-recurrence expressions

Gutenberg and Richter (1954) obtained expressions relating earthquake magnitudes with their rates of occurrence for several zones of the earth. Their results can be put in the form:

$$\lambda = \alpha e^{-\beta M} \tag{6.6}$$

where λ is the mean number of earthquakes per unit volume and per unit time having magnitude greater than M and α and β are zone-dependent constants; α varies widely from point to point, as evidenced by the map of epicenters shown in Fig. 6.7, while β remains within a relatively narrow range, as shown in Fig. 6.8. Equation 6.6 implies a distribution of the energy liberated per shock which is very similar to that observed in the process of microfracturing of laboratory specimens of several types of rock subjected to gradually increasing compressive or bending strain (Mogi, 1962; Scholz, 1968). The values of β determined in the laboratory are of the same order as those obtained from seismic events, and have been shown to depend on the heterogeneity of the specimens and on their ability to yield locally. Thus, in heterogeneous specimens made of brittle materials many small shocks precede a major fracture, while in homogeneous or plastic materials the number of small shocks is relatively small. These cases correspond to large and small β-values, respectively. No general relationship is known to the writer between β and geotectonic features of seismic provinces: complexity of crustal structure and of stress gradients precludes extrapolation of laboratory results; and statistical records for relatively small zones of the earth are not, as a rule, adequate for establishing local values of β. Figure 6.8 shows that for very high magnitudes the observed frequency of events is lower than predicted by eq. 6.6. In addition, Rosenblueth (1969) has shown that β cannot be smaller than 3.46, since that would imply an infinite amount of energy liberated per unit time. However, Fig. 6.8 shows that the values of β which result from fitting expressions of the form 6.6 to observed data are smaller than 3.46; hence, for very high values of M (above 7, approximately) the curve should bend down, in accordance with statistical evidence.

Expressions alternative to eq. 6.6 have been proposed, attempting to represent more adequately the observed magnitude-recurrence data (Rosenblueth, 1964, Merz and Cornell, 1973). Most of these expressions also fail to recognize the existence of an upper bound to the magnitude that can be generated in a given source. Although no precise estimates of this upper bound can yet be obtained, recognition of its existence and of its dependence on the geotectonic characteristics of the source is inescapable. Indeed, the prac-

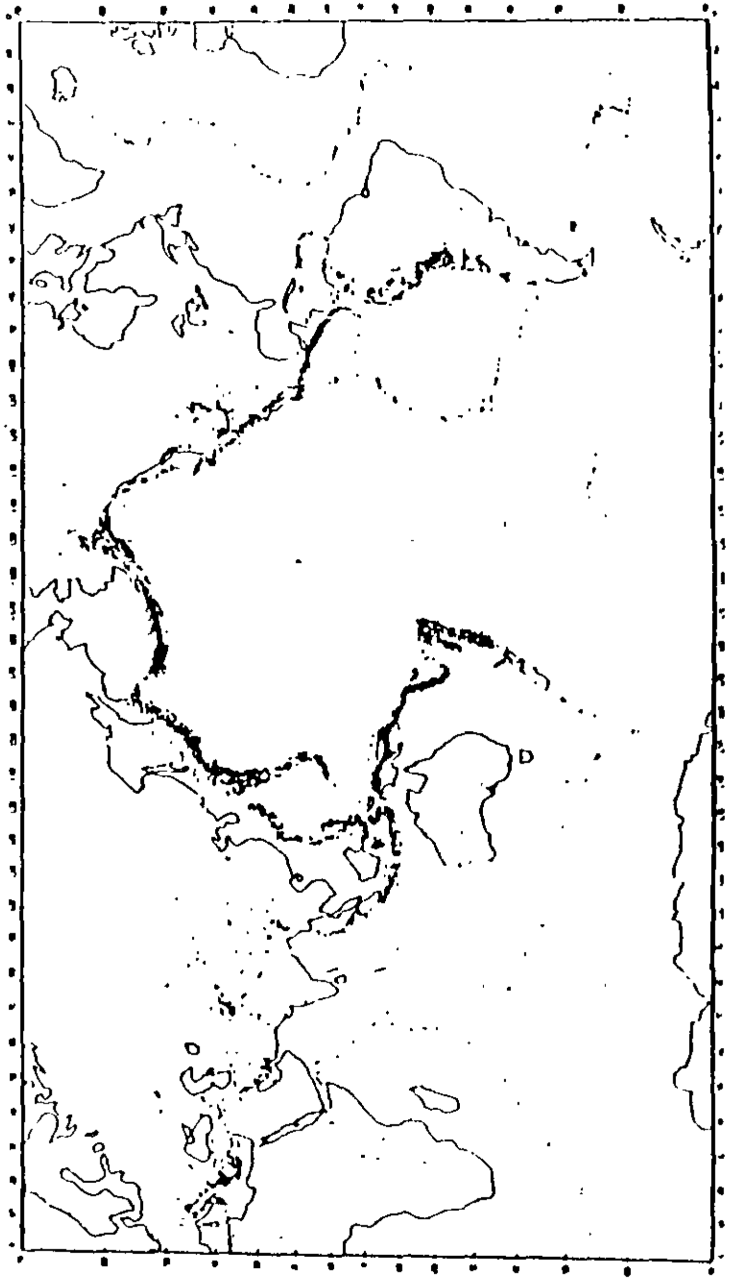

Fig. 6.7. Map showing epicenters for the interval 1961—1967. (After Newmark and Rosenblueth, 1971.)

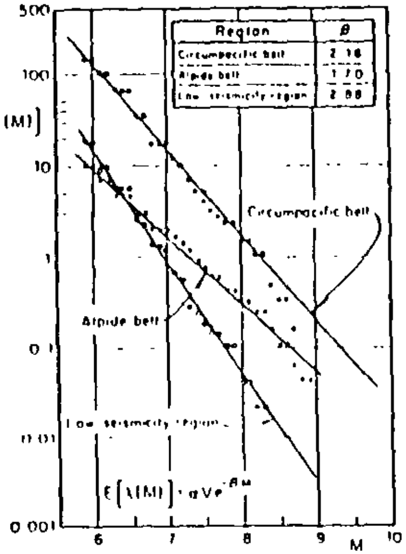

Fig. 6.8. Seismicity of macrozones. (After Esteva, 1968.)

tice of seismic zoning in the Soviet Union has been based on this concept (Gzovsky, 1962; Ananiin et al., 1968) and in many countries design spectra for very important structures, such as nuclear reactors or large dams, are usually derived from the assumption of a maximum credible intensity at a site; that intensity is ordinarily obtained by taking the maximum of the intensities that result at the site when at each of the potential sources an earthquake with magnitude equal to the maximum feasible value for that source is generated at the most unfavourable location within the same source. When this criterion is applied no attention is usually paid to the uncertainty in the maximum feasible magnitude nor to the probability that an earthquake with that magnitude will occur during a given time period. The need to formulate seismic-risk-related decisions that account both for upper bounds to magnitudes and for their probabilities of occurrence suggests adoption of magnitude recurrence expressions of the form:

$$
\begin{aligned}
\lambda &= \lambda_L G^*(M) && \text{for } M_L < M < M_U \\
&= \lambda_L && \text{for } M < M_L \\
&= 0 && \text{for } M > M_U
\end{aligned}
\tag{6.7}
$$

where M_L = lowest magnitude whose contribution to risk is significant, M_U

= maximum feasible magnitude, and $G^*(M)$ = complementary cumulative probability distribution of magnitudes every time that an event ($M > M_L$) occurs. A particular form of $G^*(M)$ that lends itself to analytical derivations is:

$$
G^*(M) = A_0 + A_1 \exp(-\beta M) - A_2 \exp[-(\beta - \beta_1)M]
\tag{6.8}
$$

where:

$$A_0 = A\beta_1 \exp[-\beta(M_U - M_L)]$$

$$A_1 = A(\beta - \beta_1)\exp(\beta M_L)$$

$$A_2 = A_\beta \exp(-\beta_1 M_U + \beta M_L)$$

$$A = [\beta\{1 - \exp[-\beta_1(M_U - M_L)]\} - \beta_1\{1 - \exp[-\beta(M_U - M_L)]\}]^{-1}$$

As M tends to M_L from above, eq. 6.7 approaches eq. 6.6. Adoption of adequate values of M_U and β_1 permits satisfying two additional conditions: the maximum feasible magnitude and the rate of variation of λ in its vicinity. When $\beta_1 \to \infty$, eq. 6.8 tends to an expression proposed by Cornell and Vanmarcke (1969).

Yegulalp and Kuo (1974) have applied the theory of extreme values to estimating the probabilities that given magnitudes are exceeded in given time intervals. They assume those probabilities to fit an extreme type-III distribution given by:

$$
\begin{aligned}
F_{M_{max}}(M|t) &= \exp[-C(M_U - M)^k t] && \text{for } M \leq M_U \\
&= 0 && \text{for } M > M_U
\end{aligned}
\tag{6.9}
$$

Here $F_{M_{max}}(M|t)$ indicates the probability that the maximum magnitude observed in t years is smaller than M, M_U has the same meaning as above, and C and K are zone-dependent parameters. This distribution is consistent with the assumption that earthquakes with magnitudes greater than M take place in accordance with a Poisson process with mean rate λ equal to $C(M_U - M)^k$. Equation 6.9 produces magnitude recurrence curves that fit closely the statistical data on which they are based for magnitudes above 5.2 and return periods from 1 to 60 years, even though the values of M_U that result from pure statistical analysis are not reliable measures of the upper bound to magnitudes, since in many cases they turn out inadmissibly high.

For low magnitudes, only a fraction of the number of shocks that take place is detected. As a consequence, λ-values based on statistical information lie below those computed according to eqs. 6.6 and 6.8 for M smaller than about 5.5. In addition, Fig. 6.9, taken from Yegulalp and Kuo (1974), shows that the numbers of detected shocks fit the extreme type III in eq. 6.9 better than the extreme type-I distribution implied by eq. 6.6., coupled with the assumption of Poisson distribution of the number of events. It is not

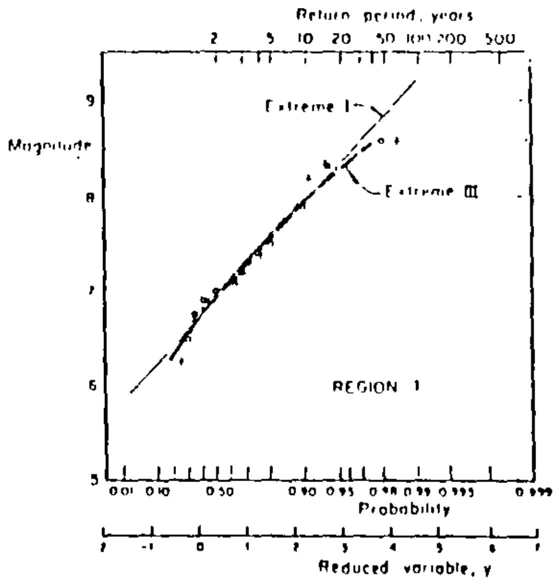

Fig. 6.9 Magnitude statistics in the Aleutian Islands region (After Yegulalp and Kuo, 1974.)

clear what portion of the deviation from the extreme type I distribution is due to the low values of the detectability levels and what portion comes from differences between the actual form of variation of λ with M and that given by eq. 6.6. The problem deserves attention because estimates of expected losses due to nonstructural damage may be sensitive to the values of λ for small magnitudes (say below 5.5) and because the evaluation of the level of seismic activity in a region is often made to depend on the recorded numbers of small magnitude shocks and on assumed detectability levels, i.e. of ratios of numbers of detected and occurred earthquakes (Kaila and Narain 1971; Kaila et al., 1972, 1974).

None of the expressions for λ presented in this chapter possess the desirable property that its applicability over a number of non-overlapping regions of the earth's crust implies the validity of an expression of the same form over the addition of those regions, unless some restrictions are imposed on the parameters of each λ. For instance, the addition of expressions like 6.6 gives place to an expression of the same form only if β is the same for all terms in the sum. Similar objections can be made to eq. 6.8. In what follows these forms will be preserved, however, as their accuracy is consistent with

the amount of available information and their adoption offers significant advantages in the evaluation of regional seismicity, as shown later.

6.3.2 Variation with depth

Depth of prevailing seismic activity in a region depends on its tectonic structure. For instance, most of the activity in the western coast of the United States and Canada consists of shocks with hypocentral depths in the range of 20–30 km. In other areas, such as the southern coast of Mexico, seismic events can be grouped into two ensembles: one of small shallow shocks and one of earthquakes with magnitudes comprised in a wide range, and with depths whose mean value increases with distance from the shoreline (Fig. 6.10). Figure 6.11 shows the depth distribution of earthquakes with magnitude above 5.9 for the whole circum-Pacific belt.

6.3.3 Stochastic models of earthquake occurrence

Mean exceedance rates of given magnitudes are expected averages during long time intervals. For decision-making purposes the times of earthquake occurrence are also significant. At present those times can only be predicted within a probabilistic context.

Let t_i ($i = 1, ..., n$) be the unknown times of occurrence of earthquakes generated in a given volume of the earth's crust during a given time interval, and let M_i be the corresponding magnitudes. For the moment it will be assumed that the risk is uniformly distributed throughout the given volume, and hence no attention will be paid to the focal coordinates of each shock.

Classical methods of time-series analysis have been applied by different researchers attempting to devise analytical models for random earthquake sequences. The following approaches are often found in the literature:

(a) Plotting of histograms of waiting times between shocks (Knopoff, 1964; Aki, 1963).

(b) Evaluation of Poisson's index of dispersion, that is of the ratio of the sample variance of the number of shocks to its expected value (Vere-Jones, 1970; Shlien and Toksöz, 1970). This index equals unity for Poisson processes, is smaller for nearly periodic sequences, and is greater than one when events tend to cluster.

(c) Determination of autocovariance functions, that is, of functions representing the covariance of the numbers of events observed in given time intervals, expressed in terms of the time elapsed between those intervals (Vere-Jones, 1970; Shlien and Toksöz, 1970). The autocovariance function of a Poisson process is a Dirac delta function. This feature is characteristic for the Poisson model since it does not hold for any other stochastic process.

(d) The hazard function $h(t)$, defined so that $h(t)\,dt$ is the conditional probability that an event will take place in the interval $(t, t + dt)$ given that

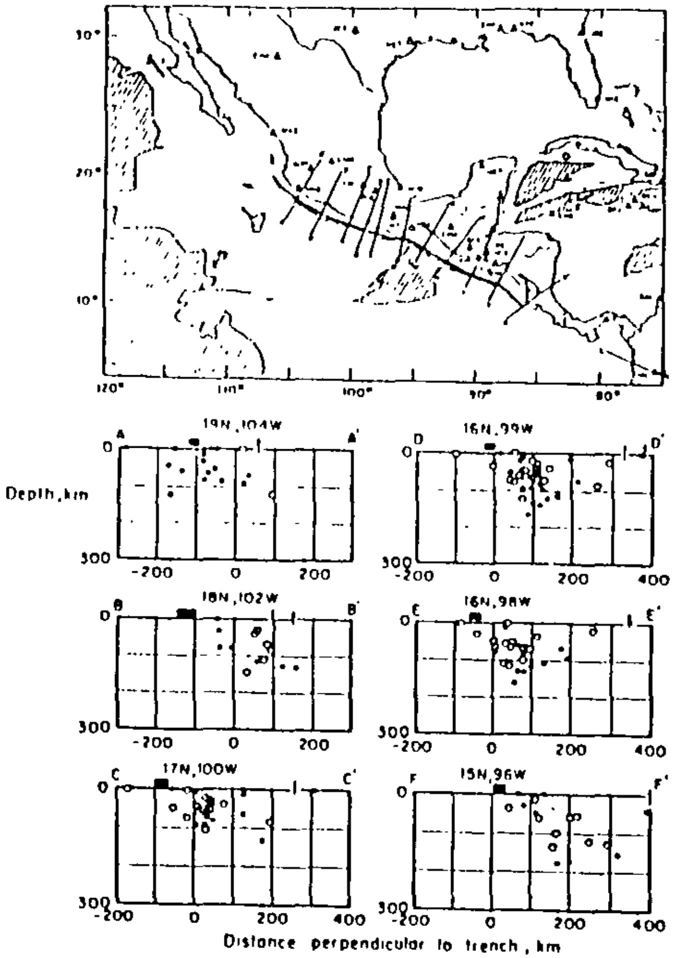

Fig. 6.10. Earthquake hypocenters projected onto a series of vertical sections through Mexico (After Molnar and Sykes, 1969.)

no events have occurred before t. If $F(t)$ is the cumulative probability distribution of the time between events:

$$h(t) = f(t)/[1 - F(t)] \tag{6.10}$$

where $f(t) = \partial F(t)/\partial t$.

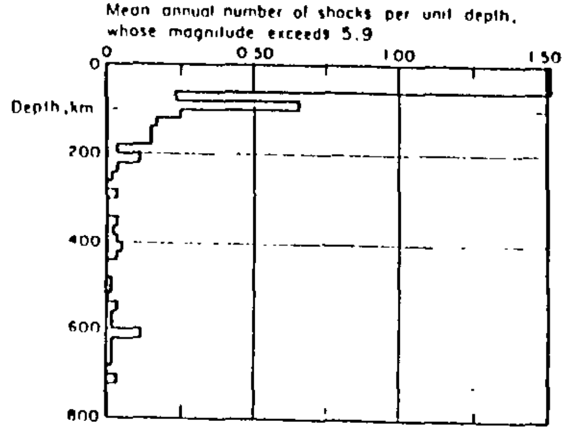

Fig. 6.11. Variation of seismicity with depth. Circum Pacific Belt. (After Newmark and Rosenblueth, 1971.)

For the Poisson model, $h(t)$ is a constant equal to the mean rate of the process.

6.3.3.1 Poisson model

Most commonly applied stochastic models of seismicity assume that the events of earthquake occurrence constitute a Poisson process and that the M_i's are independent and identically distributed. This assumption implies that the probability of having N earthquakes with magnitude exceeding M during time interval $(0, t)$ equals:

$$p_N = [\exp(-\nu_M t)(\nu_M t)^N]/N! \tag{6.11}$$

where ν_M is the mean rate of exceedance of magnitude M in the given volume. If N is taken equal to zero in eq. 6.11, one obtains that the probability distribution of the maximum magnitude during time interval t is equal to $\exp(-\nu_M t)$. If ν_M is given by eq. 6.6, the extreme type-I distribution is obtained.

Some weaknesses of this model become evident in the light of statistical information and of an analysis of the physical processes involved: the Poisson assumption implies that the distribution of the waiting time to the next event is not modified by the knowledge of the time elapsed since the last one, while physical models of gradually accumulated and suddenly released energy call for a more general renewal process such that, unlike what happens in the Poisson process, the expected time to the next event decreases as time goes on (Esteva, 1974). Statistical data show that the Poisson assumption may be acceptable when dealing with large shocks throughout the world (Ben-Menahem, 1960), implying lack of correlation between seismicities of different regions; however, when considering small volumes of the earth, of the order of those that can significantly contribute to seismic risk at a site, data often contradict Poisson's model, usually because of clustering of earthquakes in time: the observed numbers of short intervals between events are significantly higher than predicted by the exponential distribution, and values of Poisson's index of dispersion are well above unity (Figs 6.12 and 6.13). In some instances, however, deviations in the opposite direction have been observed: waiting times tend to be more nearly periodic, Poisson's index of dispersion is smaller than one, and the process can be represented by a renewal model. This condition has been reported, for instance, in the southern coast of Mexico (Esteva 1974), and in the Kamchatka and Pamir—Hindu Kush regions (Gaisky, 1966 and 1967). The models under discussion also fail to account for clustering in space (Tsuboi, 1958; Gajardo and Lomnitz, 1960), for the evolution of seismicity with time, and for the systematic shifting of active sources along geologic accidents (Allen, Chapter 3 of this book). On account of its simplicity, however, the Poisson process model provides a valuable tool for the formulation of some seismic-risk-related decisions, particularly of those that are sensitive only to magnitudes of events having very long return periods.

6.3.3.2 Trigger models

Statistical analysis of waiting times between earthquakes does not favor the adoption of the Poisson model or of other forms of renewal processes, such as those that assume that waiting times are mutually independent with lognormal or gamma distributions (Shlien and Toksöz, 1970). Alternative models have been developed, most of them of the 'trigger type' (Vere Jones, 1970), i.e. the overall process of earthquake generation is considered as the superposition of a number of time series, each having a different origin, where the origin times are the events of a Poisson process. In general, let N be the number of events that take place during time interval $(0, t)$, τ_m = origin time of the mth series, $W_m(t, \tau_m)$ the corresponding number of events up to instant t, and n_t the random number of time series initiated in the interval $(0, t)$. The total number of events that occur before instant t is then:

$$N = \sum_{m}^{n_t} W_m(t, \tau_m) \tag{6.12}$$

If origin times are distributed according to a homogeneous Poisson process with mean rate ν, and all W_m's are identically distributed stochastic processes with respect to $(t - \tau_m)$, it can be shown (Parzen, 1962) that the mean and variance of N can be obtained from:

$$E(N) = \nu \int_0^t E[W(t, \tau)]d\tau \tag{6.13}$$

12

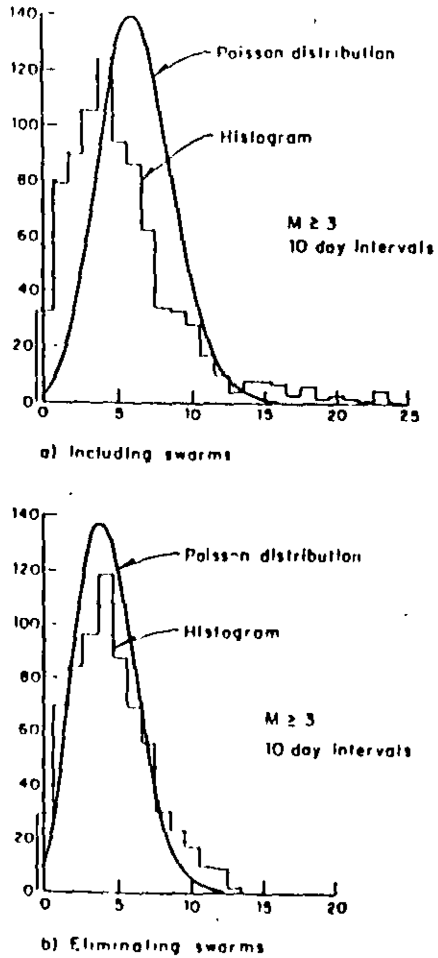

Fig. 6.12 Evaluation of Poisson process assumption. (After Knopoff, 1964.)

$$\text{var}(N) = \nu \int_0^t E[W^2(t, \tau)]d\tau \tag{6.14}$$

Parzen (1962) gives also an expression for the probability generating function $\psi_N(Z; t)$ of the distribution of N in terms of $\psi_W(Z; t, \tau)$, the general

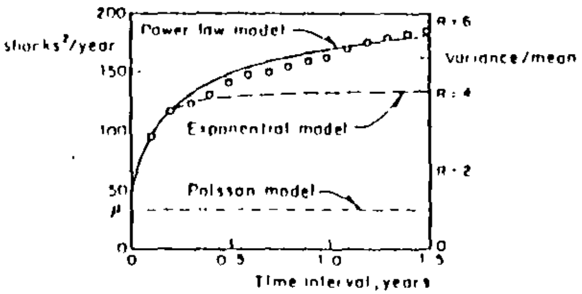

Fig. 6.13. Variance–time curve for New Zealand shallow shocks. (After Vere-Jones, 1966.)

ing function of each of the component processes:

$$\psi_N(Z;t) = \exp\left[-\nu t + \nu\int_0^t \psi_W(Z;t,\tau)\mathrm{d}\tau\right] \tag{6.15}$$

where:

$$\psi_W(Z,t,\tau) = \sum_{n=0}^{\infty} Z^n P\{W(t,\tau) = n\} \tag{6.16}$$

and the probability mass function of N can be obtained from $\psi_N(Z;t)$ by recalling that:

$$\psi_N(Z;t) = \sum_{n=0}^{\infty} Z^n P\{N = n\}$$

expanding ψ_N in power series of Z, and taking $P(N = n)$ equal to the coefficient of Z^n in that expansion. For instance, if it is of interest to compute $P(N = 0)$, expansion of $\psi_N(Z;t)$ in a Taylor's series with respect to $Z = 0$ leads to:

$$\psi_N(Z;t) = \psi_N(0;t) + Z\psi_N'(0;t) + \frac{Z^2}{2!}\psi_N''(0;t) + \ldots \tag{6.17}$$

where the prime signifies derivative with respect to Z. From the definition of ψ_N, $P(N = 0) = \psi_N(0,t)$.

Because the component processes of 'trigger'-type time series appear overlapped in sample histories, their analytical representation usually entails study of a number of alternative models, estimation of their parameters, and comparison of model and sample properties — often second-order properties (Cox and Lewis, 1966).

Vere-Jones models. Applicability of some general 'trigger' models to represent local seismicity processes was discussed in a comprehensive paper by Vere-Jones (1970), who calibrated them mainly against records of seismic activity in New Zealand. In addition to simple and compound Poisson processes (Parzen, 1962), he considered Neyman-Scott and Bartlett-Lewis models, both of which assume that earthquakes occur in clusters and that the number of events in each cluster is stocastically independent of its origin time. In the Neyman-Scott model, the process of clusters is assumed stationary and Poisson, and each cluster is defined by p_ν, the probability mass function of its number of events, and $\Lambda(t)$, the cumulative distribution function of the time of an event corresponding to a given cluster, measured from the cluster origin. The Bartlett-Lewis model is a special case of the former, where each cluster is a renewal process that ends after a finite number of renewals. In these models the conditional probability of an event taking place during the interval $(t, t + \mathrm{d}t)$, given that the cluster consists of N shocks, is equal to $N\lambda(t)\mathrm{d}t$, where $\lambda(t) = \partial\Lambda(t)/\partial t$.

Because clusters overlap in time they cannot easily be identified and separated. Estimation of process parameters is accomplished by assuming different sets of those parameters and evaluating the corresponding goodness of fit with observed data.

Various alternative forms of Neyman-Scott's model were compared by Vere-Jones with observed data on the basis of first- and second-order statistics: hazard functions, interval distributions (in the form of power spectra) and variance time curves. The statistical record comprises about one thousand New Zealand earthquakes with magnitudes greater than 4.5, recorded from 1942 to 1961. Figures 6.13–6.15 show results of the analysis for shallow New Zealand shocks as well as the comparison of observed data with sev-

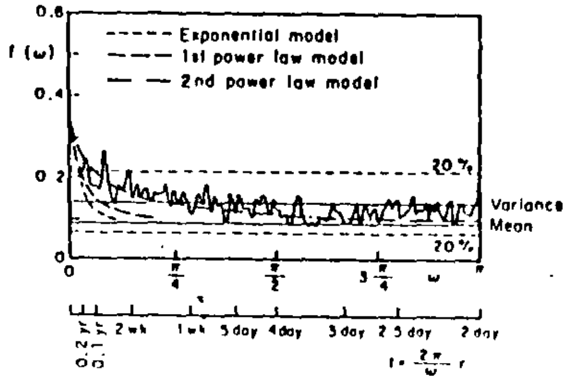

Fig. 6.14. Smoothed periodogram for New Zealand shallow shocks. (After Vere-Jones, 1966.)

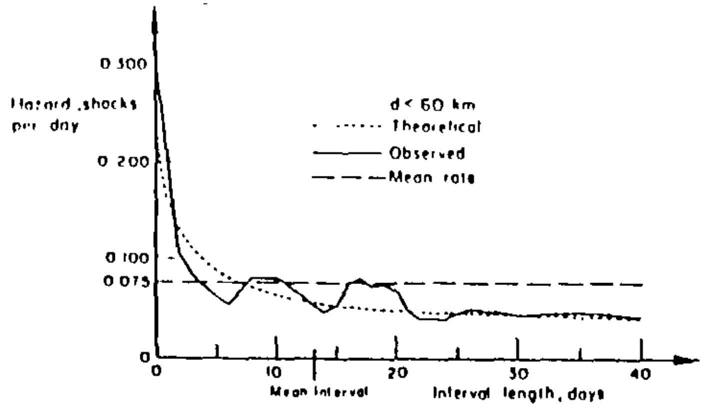

Fig. 6.15. Hazard function for New Zealand shallow shocks. (After Vere-Jones, 1970.)

eral alternative models. The process of cluster origins is Poisson in all cases, but the distributions of cluster sizes (N) and of times of events within clusters differ among the various instances in the Poisson model no clustering takes place (the distribution of N is a Dirac delta function centered at $N = 1$) while in the exponential and in the power-law models the distribution of N is extremely skewed towards $N = 1$, and $\Lambda(t)$ is taken respectively as $1 - e^{-\lambda t}$

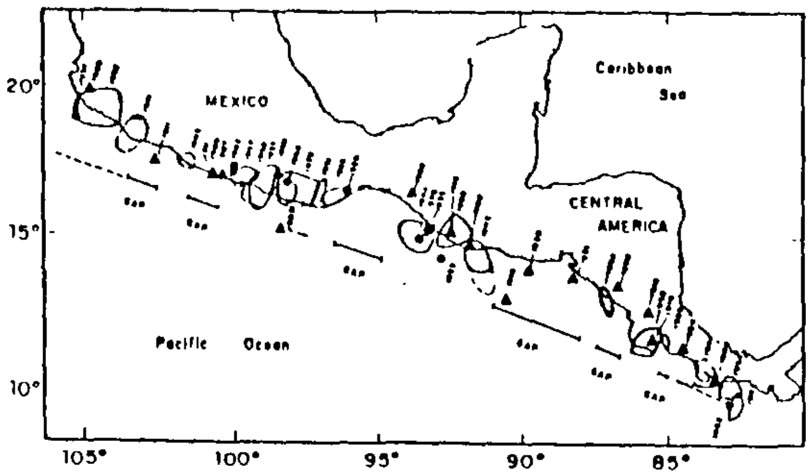

Fig. 6.16. Rupture zones and epicenters of large shallow Middle American earthquakes of this century. (After Kelleher et al., 1973.)

and $1 - [c/(c + t)]^{\lambda}$ for $t \geq 0$, and as zero for $t < 0$, where λ, c, and δ are positive parameters. In Figs. 6.13–6.15, $\delta = 0.25$, $c = 2.3$ days, and $\lambda = 0.061$ shocks/day. The significance of clustering is evidenced by the high value of Poisson's dispersion index in Fig. 6.13, while no significant periodicity can be inferred from Fig. 6.14. Both figures show that the power-law model provides the best fit to the statistics of the samples. A similar analysis for New Zealand's deep shocks shows much less clustering: Poisson's dispersion index equals 2, and the hazard function is nearly constant with time.

Still, data reported by Gaisky (1967) have hazard functions that suggest models where the cluster origins as well as the clusters themselves may be represented by renewal processes. Mean return periods are of the order of several months, and hence these processes do not correspond, at least in the time scale, to the process of alternate periods of activity and quiescense of some geological structures cited by Kelleher et al. (1973), which have led to the concept of 'temporal seismic gaps', discussed below.

Simplified trigger models. Shlien and Toksöz (1970) proposed a simple particular case of the Neyman-Scott process; they lumped together all earthquakes taking place during non-overlapping time intervals of a given length and defined them as clusters for which $\lambda(t)$ was a Dirac delta function. Working with one-day intervals, they assumed the number of events per cluster to be distributed in accordance with the discrete Pareto law and applied a maximum-likelihood criterion to the information consisting of 35 000 earthquakes reported by the USCGS from January 1971 to August 1968. The model proposed represents reasonably well both the distribution of the number of earthquakes in one-day intervals and the dispersion index. However, owing to the assumption that no cluster lasts more than one day, the model fails to represent the autocorrelation function of the daily numbers of shocks for small time lags. The degree of clustering is shown to be a regional function, and to diminish with the magnitude threshold value and with the focal depth.

Aftershock sequences. The trigger processes described have been branded as reasonable representations of regional seismic activity, even when aftershock sequences and earthquake swarms are suppressed from statistical records, however arbitrary that suppression may be. The most significant instances of clustering are related, however, to aftershock sequences which often follow shallow shocks and only rarely intermediate and deep events. Persistence of large numbers of aftershocks for a few days or weeks has propitiated the detailed statistical analysis of those sequences since last century. Omori (1894) pointed out the decay in the mean rate of aftershock occurrence with t, the time elapsed since the main shock; he expressed that rate as inversely proportional to $t + q$, where q is an empirical constant. Utsu (1961) proposed a more general expression, proportional to $(t + c)^{-\zeta}$ where ζ is a constant; Utsu's proposal is consistent with the power-law expression for $\Lambda(t)$ presented above.

Lomnitz and Hax (1966) proposed a clustering model to represent aftershock sequences; it is a modified version of Neyman and Scott's model, where the process of cluster origins is non-homogeneous Poisson with mean rate decaying in accordance with Omori's law, the number of events in each cluster has a Poisson distribution, and $A(t)$ is exponential. All the results and methods of analysis described by Vere-Jones (1970) for the stationary process of cluster origins can be applied to the nonstationary case through a transformation of the time scale. Fitting of parameters to four aftershock sequences was accomplished through use of the second-order information of the sample defined on a transformed time scale. By applying this criterion to earthquake sets having magnitudes above different threshold values it was noticed that the degree of clustering decreases as the threshold value increases.

The magnitude of the main shock influences the number of aftershocks and the distribution of their magnitudes and, although the rate of activity decreases with time, the distribution of magnitudes remains stable throughout each sequence (Lomnitz, 1966; Utsu, 1962; Drakopoulos, 1971). Equation 6.6 represents fairly well the distribution of magnitudes observed in most aftershock sequences. Values of β range from 0.9 to 3.9 and decrease as the depth increases. Since values of β for regular (main) earthquakes are usually estimated from relatively small numbers of shocks generated throughout crust volumes much wider than those active during aftershock sequences, no relation has been established among β-values for series of both types of events. The parameters of Utsu's expression for the decay of aftershock activity with time have been estimated for several sequences, for instance those following the Aleutian earthquake of March 9, 1957, the Central Alaska earthquake of April 7, 1958, and the Southeastern Alaska earthquake of July 10, 1958 (Utsu, 1962), with magnitudes equal to 8.3, 7.3, and 7.9, respectively; c (in days) was 0.37, 0.40, and 0.01, while ζ was 1.05, 1.05 and 1.13, respectively. The relationship of the total number of aftershocks whose magnitude exceeds a given value with the magnitude of the main shock was studied by Drakopoulos (1971) for 140 aftershock sequences in Greece from 1912 to 1968. His results can be expressed by $N(M) = A \exp(-\beta M)$, where $N(M)$ is the total number of aftershocks with magnitude greater than M, and A is a function of M_0, the magnitude of the main shock:

$$A = \exp(3.62\,\beta + 1.1 M_0 - 3.46) \tag{6.18}$$

Formulation of stochastic process models for given earthquake sequences is feasible once this relationship and the activity decay law are available for the source of interest. For seismic-risk estimation at a given site the spatial distribution of aftershocks may be as significant as the distribution of magnitudes and the time variation of activity, particularly for sources of relatively large dimensions.

6.3.3.3 Renewal process models

The trigger models described are based on information about earthquakes with magnitudes above relatively low thresholds recorded during time intervals of at most ten years. The degrees of clustering observed and the distributions of times between clusters cannot be extrapolated to higher magnitude thresholds and longer time intervals without further study.

Available information shows beyond doubt that significant clustering is the rule, at least when dealing with shallow shocks. However, there is considerable ground for discussion on the nature of the process of cluster origins during intervals of the order of one century or longer. While lack of statistical data hinders the formulation of seismicity models valid over long time intervals, qualitative consideration of the physical processes of earthquake generation may point to models which at least are consistent with the state of knowledge of geophysical sciences. Thus, if strain energy stored in a region grows in a more or less systematic manner, the hazard function should grow with the time elapsed since the last event, and not remain constant as the Poisson assumption implies. The concept of a growing hazard function is consistent with the conclusions of Kelleher et al. (1973) concerning the theory of periodic activation of *seismic gaps*. This theory is partially supported by results of nearly qualitative analysis of the migration of seismic activity along a number of geological structures. An instance is provided by the southern coast of Mexico, one of the most active regions in the world. Large shallow shocks are generated probably by the interaction of the continental mass and the subductive oceanic Cocos plate that underthrusts it and by compressive or flexural failure of the latter (Chapter 2). Seismological data show significant gaps of activity along the coast during the present century and not much is known about previous history (Fig. 6.16). Along these gaps, seismic-risk estimates based solely on observed intensities are quite low, although no significant difference is evident in the geological structure of these regions with respect to the rest of the coast, save some transverse faults which divide the continental formation into several blocks. Without looking at the statistical records a geophysicist would assign equal risk throughout the area. On the basis of seismicity data, Kelleher et al. have concluded that activity migrates along the region, in such a manner that large earthquakes tend to occur at seismic gaps, thus implying that the hazard function grows with time since the last earthquake. Similar phenomena have been observed in other regions; of particular interest is the North Anatolian fault where activity has shifted systematically along it from east to west during the last forty years (Allen, 1969).

Conclusions relative to activation of seismic gaps are controversial because the observation periods have not exceeded one cycle of each process. Nevertheless, those conclusions point to the formulation of stochastic models of seismicity that reflect plausible features of the geophysical processes.

These considerations suggest the use of renewal-process models to represent sequences of individual shocks or of clusters. Such models are characterized because times between events are independent and identically distributed. The Poisson process is a particular renewal model for which the distribution of the waiting time is exponential. Wider generality is achieved, without much loss of mathematical tractability, if inter-event times are supposed to be distributed in accordance with a gamma function:

$$f_1(t) = \frac{\nu}{(h-1)!}(\nu t)^{h-1}\,e^{-\nu t} \tag{6.19}$$

which becomes the exponential distribution when $h = 1$. If $h < 1$, short intervals are more frequent and the coefficient of variation is greater than in the Poisson model; if $h > 1$, the reverse is true. Shlien and Toksöz (1970) found that gamma models were unable to represent the sequences of individual shocks they analyzed; but these authors handled time intervals at least an order of magnitude shorter than those referred to in this section.

On the basis of hazard function estimated from sequences of small shocks in the Hindu-Kush, Vere Jones (1970) deduces the validity of 'branching renewal process' models, in which the intervals between cluster centers, as well as those between cluster members, constitute renewal processes.

Owing to the scarcity of statistical information, reliable comparisons between alternate models will have to rest partially on simulation of the process of storage and liberation of strain energy (Burridge and Knopoff, 1967; Veneziano and Cornell, 1973).

6.3.4 Influence of the seismicity model on seismic risk

Nominal values of investments made at a given instant increase with time when placing them at compound interest rates, i.e. when capitalizing them. Their real value — and not only the nominal one — will also grow, provided the interest rate overshadows inflation. Conversely, for the purpose of making design decisions, nominal values of expected utilities and costs inflicted upon in the future have to be converted into present or actualized values, which can be directly compared with initial expenditures. Descriptions of seismic risk at a site are insufficient for that purpose unless the probability distributions of the times of occurrence of different intensities — or magnitudes at neighbouring sources — are stipulated; this entails more than simple magnitude-recurrence graphs or even than maximum feasible magnitude estimates.

Immediately after the occurrence of a large earthquake, seismic risk is abnormally high due to aftershock activity and to the probability that damage inflicted by the main shock may have weakened natural or man-made structures if emergency measures are not taken in time. When aftershock activity has ceased and damaged systems have been repaired, a normal risk level is attained, which depends on the probability-density functions of the waiting times to the ensuing damaging earthquakes.

For the purpose of illustration, let it be assumed that a fixed and deterministically known damage D_0 occurs whenever a magnitude above a given value is generated at a given source. If $f(t)$ is the probability-density function of the waiting time to the occurrence of the damaging event, and if the risk level is sufficiently low that only the first failure is of concern, the expected value of the actualized cost of damage is (see Chapter 9):

$$\bar{D} = D_0 \int_0^{\infty} e^{-\gamma t} f(t)\,dt \tag{6.20}$$

where γ is the discount (or compound interest) coefficient and the overbar denotes expectation. If the process is Poisson with mean rate ν, then $f(t)$ is exponential and $\bar{D} \cong D_0\ \nu/\gamma$; however, if damaging events take place in clusters and most of the damage produced by each cluster corresponds to its first event, the computation of $\bar{D}$ should make use of the mean rate ν corresponding to the clusters, instead of that applicable to individual events. Table 6.II shows a comparison of seismic risk determined under the alternative assumptions of a Poisson and a gamma model ($k = 2$), both with the same mean return period, k/ν (Esteva, 1974). Three descriptions of risk are presented as functions of the time t_0 elapsed since the last damaging event: T_1, the expected time to the next event, measured from instant t_0; the expected value of the present cost of failure computed from eq. 6.20, and the hazard function (or mean failure rate). Since clustering is neglected, risk of aftershock occurrence must be either included in D_0 or superimposed on that displayed in the table.

This table shows very significant differences among risk levels for both processes. At small values of t_0, risk is lower for the gamma process, but it

TABLE 6.II

Comparison of Poisson and gamma processes

$t_0\,\nu/k$	$\bar{T}_1\,\nu/k$	Poisson process, $k = 1$: D/D_0, $\gamma k/\nu = 10$	$\gamma k/\nu = 100$	hk/ν	$T_1\,\nu/k$	Gamma process, $k = 2$: D/D_0, $\gamma k/\nu = 10$	$\gamma k/\nu = 100$	hk/ν
0					1.0	0.0278	0.0001	0
0.1					0.92	0.0511	0.0036	0.367
0.2					0.86	0.0675	0.0059	0.667
0.5					0.75	0.0973	0.0100	1.333
1	1.0	0.0909	0.0099	1.0	0.67	0.120	0.0132	2.000
2					0.60	0.139	0.0158	2.667
5					0.54	0.154	0.0179	3.333
10					0.52	0.160	0.0187	3.633
					0.50	0.167	0.0196	4.000

grows with time, until it outrides that for the Poisson process, which remains constant. The differences shown clearly affect engineering decisions.

6.4 ASSESSMENT OF LOCAL SEISMICITY

Only exceptionally can magnitude recurrence relations for small volumes of the earth's crust and statistical correlation functions of the process of earthquake generation be derived exclusively from statistical analysis of recorded shocks. In most cases this information is too limited for that purpose and it does not always reflect geological evidence. Since the latter, as well as its connection with seismicity, is beset with wide uncertainty margins, information of different nature has to be evaluated, its uncertainty analyzed, and conclusions reached consistent with all pieces of information. A probabilistic criterion that accomplishes this is presented here: on the basis of geotectonic data and of conceptual models of the physical processes involved, a set of alternate assumptions can be made concerning the functions in question (magnitude recurrence, time, and space correlation) and an initial probability distribution assigned thereto; statistical information is used to judge the likelihood of each assumption, and a posterior probability distribution is obtained. How statistical information contibutes to the posterior probabilities of the alternate assumptions depends on the extent of that information and on the degree of uncertainty implied by the initial probabilities. Thus, if geological evidence supports confidence in a particular assumption or range of assumptions, statistical information should not greatly modify the initial probabilities. If, on the other hand, a long and reliable statistical record is available, it practically determines the form and parameters of the mathematical model selected to represent local seismicity.

6.4.1 Bayesian estimation of seismicity

Bayesian statistics provide a framework for probabilistic inference that accounts for prior probabilities assigned to a set of alternate hypothetical models of a given phenomenon as well as for statistical samples of events related to that phenomenon. Unlike conventional methods of statistical inference, Bayesian methods give weight to probability measures obtained from samples or from other sources; numbers, coordinates and magnitudes of earthquakes observed in given time intervals serve to ascertain the probable validity of each of the alternative models of local seismicity that can be postulated on the grounds of geological evidence. Any criterion intended to weigh information of different nature and different degrees of uncertainty should lead to probabilistic conclusions consistent with the degree of confidence attached to each source of information. This is accomplished by Bayesian methods.

Let H_i ($i = 1, \ldots, n$) be a comprehensive set of mutually exclusive assumptions concerning a given, imperfectly known phenomenon and let A be the observed outcome of such a phenomenon. Before observing outcome A we assign an initial probability $P(H_i)$ to each hypothesis. If $P(A|H_i)$ is the probability of A in case hypothesis H_i is true, then Bayes' theorem (Raiffa and Schlaifer, 1968) states that:

$$P(H_i|A) = P(H_i)\frac{P(A|H_i)}{\sum_i P(H_i)P(A|H_i)} \tag{6.21}$$

The first member in this equation is the (posterior) probability that assumption H_i is true, given the observed outcome A.

In the evaluation of seismic risk, Bayes' theorem can be used to improve initial estimates of $\lambda(M)$ and its variation with depth in a given area as well as those of the parameters that define the shape of $\lambda(M)$ or; equivalently, the conditional distribution of magnitudes given the occurrence of an earthquake. For that purpose, take $\lambda(M)$ as the product of a rate function $\lambda_L = \lambda(M_L)$ by a shape function $G^*(M,B)$, equal to the conditional complementary distribution of magnitudes given the occurrence of an earthquake with $M > M_L$, where M_L is the magnitude threshold of the set of statistical data used in the estimation, and B is the vector of (uncertain) parameters $B_1, \ldots, B_r$ that define the shape of $\lambda(M)$. For instance, if $\lambda(M)$ is taken as given by eq. 6.8, B is a vector of three elements equal respectively to β, β_1, and M_U; if eq. 6.9 is adopted, B is defined by k and M_U.

The initial distribution of seismicity is in this case expressed by the initial joint probability density function of λ_L and B: $f'(\lambda_L, B)$. The observed outcome A can be expressed by the magnitudes of all earthquakes generated in a given source during a given time interval. For instance, suppose that N earthquakes were observed during time interval t and that their magnitudes were $m_1, m_2, \ldots, m_N$. Bayes' expression takes the form:

$$f''(\lambda_L, B|m_1, \ldots, m_N; t) = f'(\lambda_L, B)\frac{P[m_1, m_2, \ldots, m_N; t|\lambda_L, B]}{\int\int P[m_1, m_2, \ldots, m_N, t|l, b] f'(l, b)\,dl\,db} \tag{6.22}$$

where $f''(.)$ is the posterior probability density function, and l and b are dummy variables that stand for all values that may be taken by λ_L and B, respectively. Estimation of λ_L can usually be formulated independently of that of the other parameters. The observed fact is then expressed by N_L, the number of earthquakes with magnitude above M_L during time t, and the following expression is obtained, as a first step in the estimation of $\lambda(M)$:

$$f''(\lambda_L|N_L; t) = f'(\lambda_L)\frac{P(N_L; t|\lambda_L)}{\int P(N_L; t|l) f'(l)\,dl} \tag{6.23}$$

6.4.1.1 Initial probabilities of hypothetical models

Where statistical information is scarce, seismicity estimates will be very sensitive to initial probabilities assigned to alternative hypothetical models, the opinions of geologists and geophysicists about probable models, about the parameters of these models, and the corresponding margins of uncertainty should be adequately interpreted and expressed in terms of a function f', as required by equations similar to 6.22 and 6.23. Ideally, these opinions should be based on the formulation of potential earthquake sources and on their comparison with possibly similar geotectonic structures. This is usually done by geologists, more qualitatively than quantitatively, when they estimate M_U. Initial estimates of λ_L are seldom made, despite the significance of this parameter for the design of moderately important structures (see Chapter 9).

Analysis of geological information must consider local details as well as general structure and evolution. In some areas it is clear that all potential earthquake sources can be identified by surface faults, and their displacements in recent geological times measured. When mean displacements per unit time can be estimated, the order of magnitude of creep and of energy liberated by shocks and hence of the recurrence intervals of given magnitudes can be established (Wallace, 1970, Davies and Brune, 1971), the corresponding uncertainty evaluated, and an initial probability distribution assigned. The fact that magnitude recurrence relations are only weakly correlated with the size of recent displacements is reflected in large uncertainties (Petrushevsky, 1966).

Application of the criterion described in the foregoing paragraph can be unfeasible or inadequate in many problems, as in areas where the abundance of faults of different sizes, ages, and activity, and the insufficient accuracy with which focal coordinates are determined preclude a differentiation of all sources. Regional seismicity may then be evaluated under the assumption that at least part of the seismic activity is distributed in a given volume rather than concentrated in faults of different importance. The same situation would be faced when dealing with active zones where there is no surface evidence of motions. Hence, consideration of the overall behavior of complex geological structures is often more significant than the study of local details.

Not much work has been done in the analysis of the overall behavior of large geological structures with respect to the energy that can be expected to be liberated per unit volume and per unit time in given portions of those structures. Important research and applications should be expected, however, since, as a result of the contribution of plate-tectonics theory to the understanding of large-scale tectonic processes, the numerical values of some of the variables correlated with energy liberation are being determined, and can be used at least to obtain orders of magnitude of expected activity along plate boundaries. Far less well understood are the occurrence of shocks in apparently inactive regions of continental shields and the behavior of complex continental blocks or regions of intense folding, but even there some

progress is expected in the study of accumulation of stresses in the crust.

Knowledge of the geological structure can serve to formulate initial probability distributions of seismicity even when quantitative use of geophysical information seems beyond reach. Initial probability distributions of local seismicity parameters λ_L, B in the small volumes of the earth's crust that contribute significantly to seismic risk at a site, can be assigned by comparison with the average seismicity observed in wider areas of similar tectonic characteristics, or where the extent and completeness of statistical information warrant reliable estimates of magnitude-recurrence curves (Esteva, 1969). In this manner we can, for instance, use the information about the average distribution of the depths of earthquakes of different magnitudes throughout a seismic province to estimate the corresponding distribution in an area of that province, where activity has been low during the observation interval, even though there might be no apparent geophysical reason to account for the difference. Similarly, the expected value and coefficient of variation of λ_L in a given area of moderate or low seismicity (as a continental shield) can be obtained from the statistics of the motions originated at all the supposedly stable or aseismic regions in the world.

The significance of initial probabilities in seismic risk estimates, against the weight given to purely statistical information, becomes evident in the example of Fig. 6.16: if Kelleher's theory about activation of seismic gaps is true, risk is greater at the gaps than anywhere else along the coast; if Poisson models are deemed representative of the process of energy liberation, the extent of statistical information is enough to substantiate the hypothesis of reduced risk at gaps. Because both models are still controversial, and represent at most two extreme positions concerning the properties of the actual process, risk estimates will necessarily reflect subjective opinions.

6.4.1.2 Significance of statistical information

Estimation of λ_L. Application of eq. 6.23 to estimate λ_L independently of other parameters will be first discussed, because it is a relatively simple problem and because λ_L is usually more uncertain than M_U and much more so than β.

A model as defined by eq. 6.19 will be assumed to apply. If the possible assumptions concerning the values of λ_L constitute a continuous interval, the initial probabilities of the alternative hypotheses can be expressed in terms of a probability-density function of λ_L. If, in addition, a certain assumption is made concerning the form of this probability-density function, only the initial values of $E(\lambda_L)$ and $V(\lambda_L)$ have to be assumed. It is advantageous to assign to $\nu = h/E(T)$ a gamma distribution. Then, if ρ and μ are the parameters of this initial distribution of ν, if h is assumed to be known, and if the observed outcome is expressed as the time t_n elapsed during $n + 1$ consecutive events (earthquakes with magnitude $>M_L$), application of eq. 6.23 leads to the conclusion that the posterior probability function of ν is also gamma, now with parameters $\rho + nk$ and $\mu + t_n$. The initial and the posterior expected values of ν are respectively equal to ρ/μ, and to $(\rho + nk)/(\mu + t_n)$. When initial uncertainty about ν is small, ρ and μ will be large and the initial and the posterior expected values of ν will not differ greatly. On the other hand, if only statistical information were deemed significant, ρ and μ should be given very small values in the initial distribution, and $E(\nu)$, and hence λ_L, will be practically defined by n, k, and t_n. This means that the initial estimates of geologists should not only include expected or most probable values of the different parameters, but also statements about ranges of possible values and degrees of confidence attached to each.

In the case studied above only a portion of the statistical information was used. In most cases, especially if seismic activity has been low during the observation interval, significant information is provided by the durations of the intervals elapsed from the initiation of observations to the first of the $n + 1$ events considered, and from the last of these events until the end of the observation period. Here, application of eq. 6.23 leads to expressions slightly more complicated than those obtained when only information about t_n is used.

The particular case when the statistical record reports no events during *at least* an interval $(0, t_0)$ comes up frequently in practical problems. The probability-density function of the time T_1 from t_0 to the occurrence of the first event must account for the corresponding shifting of the time axis. Furthermore, if the time of occurrence of the last event before the origin is unknown, the distribution of the waiting time from $t = 0$ to the first event coincides with that of the *excess life* in a renewal process at an arbitrary value of t that approaches infinity (Parzen, 1962). For the particular case when the waiting times constitute a gamma process, T_1 is measured from $t = 0$, T is the waiting time between consecutive events, and it is known that $T_1 > t_0$, the conditional density function of $\tau_1 = (T_1 - t_0)/E(T)$ is given by eq. 6.24 (Esteva, 1974), where $u_0 = t_0/E(T)$:

$$f_{\tau_1}(u|T_1 > t_0) = \frac{\sum_{m=1}^{k} \frac{k}{(m-1)!} [k(u + u_0)]^{m-1}}{\sum_{m=1}^{k} \sum_{n=1}^{m} \frac{1}{(n-1)!} (ku_0)^{n-1}} e^{-ku} \tag{6.24}$$

Consider now the implications of Bayesian analysis when applied to one of the seismic gaps in Fig. 6.16, under the conditions implicit in eq. 6.24. An initial set of assumptions and corresponding probabilities was adopted as described in the following. From previous studies referring to all the southern coast of Mexico, local seismicity in the gap area (measured in terms of λ for $M > 6.5$) was represented by a gamma process with $k = 2$. An initial

probability density function for ν was adopted such that the expected value of $\lambda(6.5)$ for the region coincided with its average throughout the complete seismic province. Two values of ρ were considered: 2 and 10, which correspond to coefficients of variation of 0.71 and 0.32, respectively. Values in Table 6.III were obtained for the ratio of the final to the initial expected values of ν, in terms of u_0.

The last two columns in the table contain the ratios of the computed values of $E''(T_1)$ and $E'(T)$ when ν is taken as equal respectively to its initial or to its posterior expected value. This table shows that, for $\rho = 10$, that is, when uncertainty attached to the geologically based assumptions is low, the expected value of the time to the next event keeps decreasing, in accordance with the conclusions of Kelleher et al. (1973). However, as time goes on and no events occur, the statistical evidence leads to a reduction in the estimated risk, which shows in the increased conditional expected values of T_1. For $\rho = 2$, the geological evidence is less significant and risk estimates decrease at a faster rate.

6.4.1.3 Bayesian estimation of jointly distributed parameters

In the general case, estimation of B will consist in the determination of the posterior Bayesian joint probability function of its components, taking as statistical evidence the relative frequencies of observed magnitudes. Thus, if event A is described as the occurrence of N shocks, with magnitudes $m_1, ..., m_N$, and b_i $(i = 1, ..., r)$ are values that may be adopted by the components of vector B being estimated, eq. 6.21 becomes:

$$f''_B(b_1, ..., b_r|A) = \frac{f'_B(b_1, ..., b_r)P(A|b_1, ..., b_r)}{\int ... \int f'_B(u_1, ..., u_r)P(A|u_1, ..., u_r)\mathrm{d}u_1, ..., \mathrm{d}u_r} \tag{6.25}$$

where $P(A|u_1, ..., u_r)$ is proportional to:

$$\prod_{i=1}^{N} g(m_i|u_1, ..., u_r)$$

and $g(m) = -\partial G^*(m)/\partial m$.

Closed-form solutions for f'' as given by eq. 6.25 are not feasible in general. For the purpose of evaluating risk, however, estimates of the posterior first and second moments of f'' can be obtained from eq. 6.25, making use of available first-order approximations (Benjamin and Cornell, 1970; Rosenblueth, 1975). Thus, the posterior expected value of B_i is given by $\int f''_{B_i}(u)\, u\, \mathrm{d}u$, where $f''_{B_i}(u_i) = \int ... \int f''_B(u_1, ..., u_r)\, \mathrm{d}u_1, ..., \mathrm{d}u_n$ and the multiple integral is of order $r - 1$, because it is not extended to the dominion of B_i. Hence:

$$E''(B_i) = \frac{E'_B[B_iP(A|B_1, ..., B_r)]}{E'_B[P(A|B_1, ..., B_r)]} \tag{6.26}$$

TABLE 6.III

Bayesian estimates of seismicity in one seismic gap

$u_0 = t_0/E'(T)$	$E''(\nu)/E'(\nu)$		$E''(T_1 \mid T_1 > t_0)/E'(T)$	
	$\rho = 2$	$\rho = 10$	$\rho = 2$	$\rho = 10$
0	1.0	1.0	0.75	0.75
0.1	0.95	0.99	0.76	0.71
0.5	0.75	0.91	0.91	0.71
1	0.58	0.87	1.11	0.73
5	0.20	0.51	3.11	1.05
10	0.11	0.36	5.17	1.55
20	0.06	0.22	10.50	2.18

where E' and E'' stand for initial and posterior expectation, and subscript B means that expectation is taken with respect to all the components of B. Likewise, the following *posterior moments* can be obtained:

Covariance of B_i and B_j

$$\mathrm{Cov}''(B_i, B_j) = \frac{E'_B[B_i B_j P(A \mid B_1, ..., B_r)]}{E'_B[P(A \mid B_1, ..., B_r)]} - E''(B_i)E''(B_j) \tag{6.27}$$

Expected value of $\lambda(M)$

$$E''[\lambda(M)] = E''(\lambda_1)E''[G^*(M, B)]$$
$$= E''(\lambda_1)\frac{E'_B[G^*(M; B)P(A \mid B_1, ..., B_r)]}{E'_B[P(A \mid B_1, ..., B_r)]} \tag{6.28}$$

Marginal distributions. The posterior expectation of $\lambda(M)$ is in some cases all that is required to describe seismicity for decision-making purposes. Often, however, uncertainty in $\lambda(M)$ must also be acounted for. For instance, the probability of exceedance of a given magnitude during a given time interval has to be obtained as the expectation of the corresponding probabilities over all alternative hypotheses concerning $\lambda(M)$. In this manner it can be shown that, if the occurrence of earthquakes is a Poisson process and the Bayesian distribution of λ_L is gamma with mean $\bar{\lambda}_L$ and coefficient of variation V_L, the marginal distribution of the number of earthquakes is negative binomial with mean $\bar{\lambda}_L$. In particular, the marginal probability of zero events during time interval t — equivalently, the complementary distribution function of the waiting time between events — is equal to $(1 + t/t'')^{-r''}$, where $r'' = V_L^{-2}$ and $t'' = r''/\bar{\lambda}_L$. The marginal probability-density function of the waiting time, that should be substituted in eq. 6.20, is $\bar{\lambda}_L(1 + t/t'')^{-r''-1}$, which tends to the exponential probability function as r'' and t'' tend to infinity (and $V_L \to 0$) while their ratio remains equal to $\bar{\lambda}_L$.

Bayesian uncertainty tied to the joint distribution of all seismicity parameters $(\lambda_L, B_1, ..., B_r)$ can be included in the computation of the probability of occurrence of a given event Z by taking the expectation of that probability with respect to all parameters:

$$P(Z) = E_{\lambda_L, B}[P(Z); \lambda_L, B_1, ..., B_r)] \tag{6.29}$$

When the joint distribution of λ_L, B stems from Bayesian analysis of an initial distribution and an observed event, A, this equation adopts the form:

$$P''(Z) = \frac{E'_{\lambda_L, B}[P(Z \mid \lambda_L, B)P(A \mid \lambda_L, B)]}{E'_{\lambda_L, B}[P(A \mid \lambda_L, B)]} \tag{6.30}$$

where ′ and ″ stand for initial and posterior, respectively.

Spatial variability. Figure 6.17 shows a map of geotectonic provinces of Mexico, according to F. Mooser. Each province is characterized by the large-scale features of its tectonic structure, but significant local perturbations to the overall patterns can be identified. Take for instance zone 1, whose seismotectonic features were described above, and are schematically shown in Fig. 6.18 (Singh, 1975): the Pacific plate underthrusts the continental block and is thought to break into several blocks, separated by faults transverse to the coast, that dip at different angles. The continental mass is also

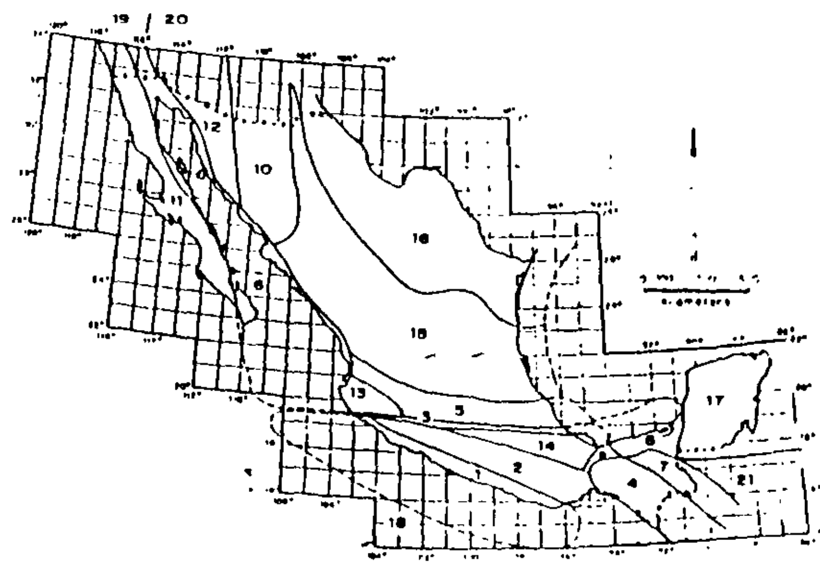

Fig. 6.17. Seismotectonic provinces of Mexico. (After F. Mooser.)

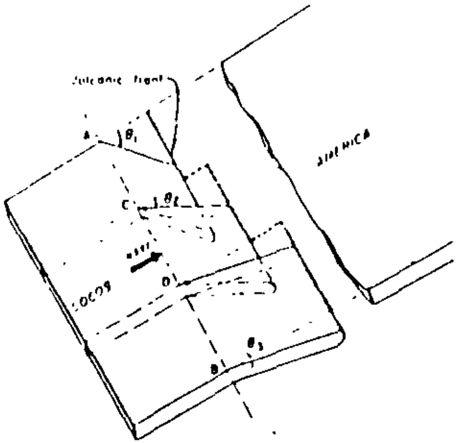

$\theta_1 > \theta_2 > \theta_3$

Fig. 6.18. Schematic drawing of the segmenting of Cocos plate as it subducts below American plate. (After Singh, 1974.)

made up of several large blocks. Seismic activity at the underthrusting plate or at its interface with the continental mass is characterized by magnitudes that may reach very high values and by the increase of mean hypocentral depth with distance from the coast; small and moderate shallow shocks are generated at the blocks themselves. Variability of statistical data along the whole tectonic system was discussed above and is apparent in Fig. 6.10. Bayesian estimation of local seismicity averaged throughout the system is a matter of applying eq. 6.21 or any of its special forms (eqs. 6.22 and 6.23), taking as statistical evidence the information corresponding to the whole system. However, seismic risk estimates are sensitive to values of local seismicity averaged over much smaller volumes of the earth's crust; hence the need to develop criteria for probabilistic inference of possible patterns of space variability of seismicity along tectonically homogeneous zones.

On the basis of seismotectonic information, the system under consideration can first be subdivided into the underthrusting plate and the subsystem of shallow sources; each subsystem can then be separately analyzed. Take for instance the underthrusting plate and subdivide it into s sufficiently small equal-volume subzones. Let ν_L be the rate of exceedance of magnitude M_L throughout the main system, ν_{L_i} the corresponding rate at each subzone, and define p_i as ν_{L_i}/ν_L, with p_i independent of ν_L (p_i is equal to the probability that an earthquake known to have been generated in the overall system originated at subzone i). Initial information about possible space variability of

ν_{L_i} can be expressed in terms of an initial probability distribution of p_i and of the correlation among p_i and p_j for any i and j. Because $\Sigma \nu_{L_i} = \nu_L$, one obtains $\Sigma p_i = 1$. This imposes two restrictions on the initial joint probability distribution of the p_i's: $E'(p_i) = 1$, var$'$ $\Sigma p_i = 0$. If all p_i's are assigned equal expectations and all pairs p_i, p_j, $i \neq j$ are assumed to possess the same correlation coefficient $\rho_{ij} = \rho'$, the restrictions mentioned lead to $E'(p_i) = 1/s$ and $\rho' = -1/(s-1)$. Posterior values of $E(p_i)$ and ρ_{ij} are obtained according to the same principles that led to eqs. 6.25–6.28. Statistical evidence is in this case described by N, the total number of earthquakes generated in the system, and n_i ($i = 1, \ldots, s$) the corresponding numbers for the subzones. Given the p_i's, the probability of this event is the multinomial distribution:

$$P[A|p_1, \ldots, p_s] = \frac{N!}{n_1!, \ldots, n_s!} p_1^{n_1} \ldots p_s^{n_s} \tag{6.31}$$

If the correlation coefficients among seismicities of the various subzones can be neglected, each p_i can be separately estimated. Because p_i has to be comprised between 0 and 1, it is natural to assign it a beta initial probability distribution, defined by its parameters n_i' and N_i', such that $E'(p_i) = n_i'/N_i'$ and var$'(p_i) = n_i'(N_i' - n_i')/[N_i'^2(N_i' + 1)]$ (Raiffa and Schlaifer, 1968). The parameters of the posterior distribution will be:

$$n_i'' = n_i' + n_i, N_i'' = N_i' + N$$

Take for instance a zone whose prior distribution of λ_L is assumed gamma with expected value λ_L' and coefficient of variation V_L'. Suppose that, on the basis of geological evidence and of the dimensions involved, it is decided to subdivide the zone into four subzones of equal dimensions; a-priori considerations lead to the assignment of expected values and coefficients of variation of p_i for those subzones, say $E'(p_i) = 0.25$, $V'(p_i) = 0.25$ ($i = 1, \ldots, 4$). From previous considerations for $s = 4$ take $\rho_{ij}' = -1/3$ for $i \neq j$. Suppose now that, during a given time interval t, ten earthquakes were observed in the zone, of which 0, 1, 3, and 6 occurred respectively in each subzone. If the Poisson process model is adopted, λ_L' and V_L' can be expressed in terms of a fictitious number of events $n' = V_L'^{-2}$ occurred during a fictitious time interval $t' = n'/\bar{\lambda}_L'$; after observing n earthquakes during an interval t, the Bayesian mean and coefficient of variation of λ_L will be $\bar{\lambda}_L'' = (n' + n)/(t' + t)$, $V_L'' = (n' + n)^{-1/2}$ (Esteva, 1968). Hence:

$$\lambda_L'' = (V_L'^{-2} + 10)/(V_L'^{-2} \bar{\lambda}_L'^{-1} + t), \quad V_L'' = (V_L'^{-2} + 10)^{-1/2}$$

Local deviations of seismicity in each subzone with respect to the average λ_L can be analyzed in terms of p_i ($i = 1, \ldots, 4$); Bayesian analysis of the proportion in which the ten earthquakes were distributed among the subzones proceeds according to:

$$E''(p_i|A) = \frac{E'[p_i P(A|p_1, \ldots, p_4)]}{E'[P(A|p_1, \ldots, p_4)]} \tag{6.32}$$

The expectations that appear in this equation have to be computed with respect to the initial joint distribution of the p_i's. In practice, adequate approximations are required. For instance, Benjamin and Cornells' (1970) first-order approximation leads to $E''(p_1) = 0.226$, $E''(p_4) = 0.294$.

If correlation among subzone seismicities is neglected, and statistical information of each subzone is independently analyzed, when the p_i's are assigned beta probability-density functions with means and coefficients of variation as defined above, one obtains $E''(p_1) = 0.206$, $E''(p_4) = 0.311$, which are not very different from those formerly obtained; however, when $E'(p_i) = 0.25$ and $V'(p_i) = 0.5$, the first criterion leads to $E''(p_i) = 0.206$, $E''(p_4) = 0.311$, while the second produces 0.131 and 0.416, respectively. Part of the difference may be due to neglect of p'_{ij}, but probably a significant part stems from inaccuracies of the first order approximation to the expectations that appear in eq. 6.32; alternate approximations are therefore desirable.

Incomplete data. Statistical information is known to be fairly reliable only for magnitudes above threshold values that depend on the region considered, its level of activity, and the quality of local and nearby seismic instrumentation. Even incomplete statistical records may be significant when evaluating some seismicity parameters; their use has to be accompanied by estimates of detectability values, that is, of ratios of the numbers of events recorded to total numbers of events in given ranges (Esteva, 1970; Kaila and Narain, 1971).

6.5 REGIONAL SEISMICITY

The final goal of local seismicity assessment is the estimation of regional seismicity, that is, of probability distributions of intensities at given sites, and of probabilistic correlations among them. These functions are obtained by integrating the contributions of local seismicities of nearby sources, and hence their estimates reflect Bayesian uncertainties tied to those seismicities. In the following, regional seismicity will be expressed in terms of mean rates of exceedance of given intensities; more detailed probabilistic descriptions would entail adoption of specific hypotheses concerning space and time correlations of earthquake generation.

6.5.1 *Intensity-recurrence curves*

The case when uncertainty in seismicity parameters is neglected will be discussed first. Consider an elementary seismic source with volume dV and local seismicity $\lambda(M)$ per unit volume, distant R from a site S, where intensity-recurrence functions are to be estimated. Every time that a magnitude M shock is generated at that source, the intensity at S equals:

22

$$Y = \epsilon Y_p = \epsilon b_1 \exp(b_2 M) g(R) \qquad (6.33)$$

(see eqs. 6.4 and 6.5), where ϵ is a random factor and Y and Y_p stand for actual and predicted intensities, b_1 and b_2 are given constants, and $g(R)$ is a function of hypocentral distance. The probability that an earthquake originating at the source will have an intensity greater than y is equal to the probability that $\epsilon Y_p > y$. If Y_p is expressed in terms of M and randomness in ϵ is accounted for, one obtains:

$$\nu(y) = \int_{\alpha_U}^{\alpha_L} \nu_p(y/u) f_\epsilon(u) \mathrm{d}u \qquad (6.34)$$

where ν and ν_p are respectively mean rates at which actual and predicted intensities exceed given values, $\alpha_U = y/y_U$, $\alpha_L = y/y_L$, y_U, and y_L are the predicted intensities that correspond to M_U and M_L, and f_ϵ the probability-density function of ϵ. If eq. 6.33 is assumed to hold:

$$\nu_p(y) = K_0 + K_1 y^{-r_1} - K_2 y^{-r_2} \qquad (6.35)$$

where:

$$K_i = [b_1 g(R)]^{r_i} A_i \lambda_L \mathrm{d}V \quad (i = 0, 1, 2) \qquad (6.36)$$

$$r_0 = 0, \quad r_1 = \beta/b_2, \quad r_2 = (\beta - \beta_1)/b_2 \qquad (6.37)$$

Substitution of eq. 6.35 into 6.34, coupled with the assumption that $\ln \epsilon$ is normally distributed with mean m and standard deviation σ leads to:

$$\nu(y) = c_0 K_0 + c_1 K_1 y^{-r_1} - c_2 K_2 y^{-r_2} \qquad (6.38)$$

where:

$$c_i = \exp(Q_i) \left[\phi\left(\frac{\ln \alpha_L - u_i}{\sigma}\right) - \phi\left(\frac{\ln \alpha_U - u_i}{\sigma}\right) \right] \qquad (6.39)$$

ϕ is the standard normal cumulative distribution function, $Q_i = 1/2\, \sigma^2 r_i^2 + m r_i$, and $u_i = m + \sigma^2 r_i$. Similar expressions have been presented by Merz and Cornell (1973) for the special case of eq. 6.8 when $\beta_1 \to \infty$ and for a quadratic form of the relation between magnitude and logarithm of exceedance rate. Closed-form solutions in terms of incomplete gamma functions are obtained when magnitudes are assumed to possess extreme type-III distributions (eq. 6.9).

Intensity-recurrence curves at given sites are obtained by integration of the contributions of all significant sources. Uncertainties in local seismicities can be handled by describing regional seismicity in terms of means and variances of $\nu(y)$ and estimating these moments from eq. 6.34 and suitable first and second-moment approximations. Influence of these uncertainties in design decisions has been discussed by Rosenblueth (in preparation).

6.5.2 Seismic probability maps

When intensity-recurrence functions are determined for a number of sites with uniform local ground conditions the results are conveniently represented by sets of seismic probability maps, each map showing contours of intensities that correspond to a given return period. For instance, Figs. 6.19 and 6.20 show peak ground velocities and accelerations that correspond to 100 years return period on firm ground in Mexico. These maps form part of a set that was obtained through application of the criteria described in this chapter. Because the ratio of peak ground accelerations and velocities does not remain constant throughout a region, the corresponding design spectra will not only vary in scale but also in shape (frequency content), in other words, seismic risk will usually have to be expressed in terms of at least the values of two parameters (for instance, as in this case, peak ground accelerations and velocities that correspond to various risk levels (return periods)).

6.5.3 Microzoning

Implicit in the above criteria for evaluation of regional seismicity is the adoption of intensity attenuation expressions valid on firm ground. Scatter of actual intensities with respect to predicted values was ascribed to differences in source mechanisms, propagation paths, and local site conditions; at least the latter group of variables can introduce systematic deviations in the

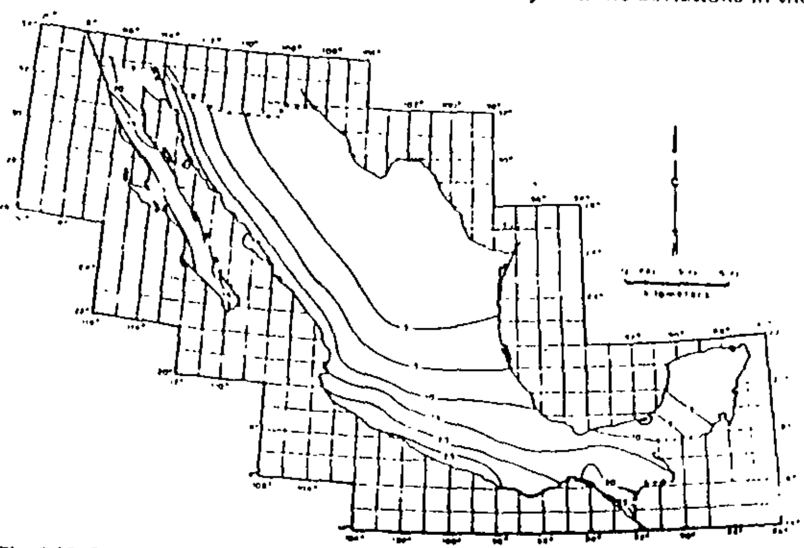

Fig. 6.19 Peak ground velocities with return period of 100 years (cm/sec).

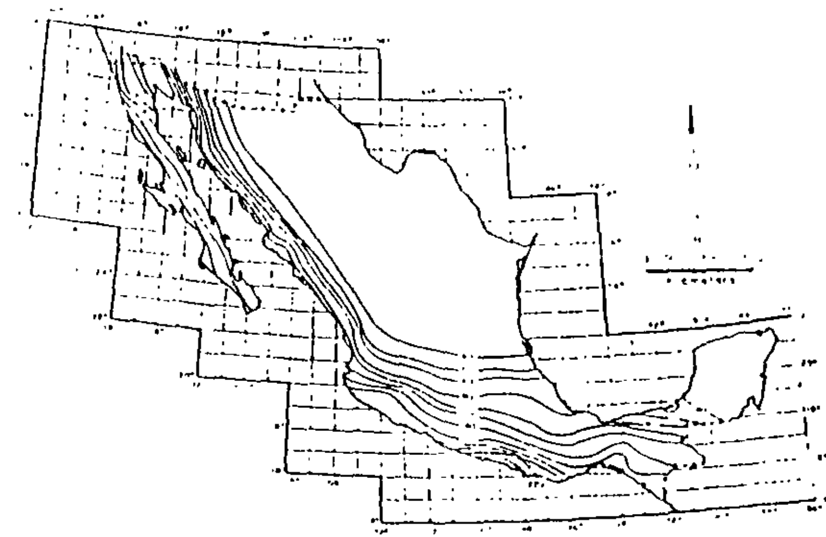

Fig. 6.20 Peak ground accelerations with return period of 100 years (cm/sec^2).

ratio of actual to predicted intensities; and geological details may significantly alter local seismicity in a small region, as well as energy radiation patterns, and hence regional seismicity in the neighbourhood. These systematic deviations are the matter of microzoning, that is, of local modification of risk maps similar to Figs. 6.19 and 6.20.

Most of the effort invested in microzoning has been devoted to study of the influence of local soil stratigraphy on the intensity and frequency content of earthquakes (see Chapter 4). Analytical models have been practically limited to response analysis of stratified formations of linear or nonlinear soils to vertically traveling shear waves. The results of comparing observed and predicted behavior have ranged from satisfactory (Herrera et al., 1965) to poor (Hudson and Udwadia, 1972). Topographic irregularities, as hills or slopes of firm ground formations underlying sediments, may introduce significant systematic perturbations in the surface motion, as a consequence of wave focusing or dynamic amplification. The latter effect was probably responsible for the exceptionally high accelerations recorded at the abutment of Pacoima dam during the 1971 San Fernando earthquake.

Present practice of microzoning determines seismic intensities or design parameters in two steps. First the values of those parameters on firm ground are estimated by means of suitable attenuation expressions and then they are amplified according to the properties of local soil; but this implies an arbitrary decision to which seismic risk is very sensitive: selecting the boundary between soil and firm ground. A specially difficult problem stems when trying to fix that boundary for the purpose of predicting the motion at the top of a hill or the slope stability of a high cliff (Rukos, 1974).

It can be concluded that rational formulation of microzoning for seismic risk is still in its infancy and that new criteria will appear that will probably require intensity attenuation models which include the influence of local systematic perturbations. Whether these models are available or the two step process described above is acceptable, intensity-recurrence expressions can be obtained as for the unperturbated case, after multiplying the second member of eq. 6.34 by an adequate intensity dependent corrective factor.

REFERENCES

Aki, K., 1963. *Some Problems in Statistical Seismology*. University of Tokyo, Geophysical Institute.

Allen, C.R., 1969. Active faulting in northern Turkey. *Calif. Inst. Tech., Div. Geol. Sci., Contrib.* 1577.

Allen, C.R., St. Amand, P., Richter, C.F. and Nordquist, J.M., 1965. Relationship between seismicity and geologic structure in the southern California region. *Bull. Seism. Soc. Am.*, 55 (4): 753–797.

Ambraseys, N.N., 1973. Dynamics and response of foundation materials in epicentral regions of strong earthquakes. *Proc. 5th World Conf. Earthquake Eng., Rome.*

Anonin, I.V., Bune, V.I., Vvedenskaia, N.A., Kirillova, I.V., Reisner, G.I. and Shelpo, V.N., 1968. *Methods of Compiling a Map of Seismic Regionalization on the Example of the Caucasus*. C. Yu. Schmidt Institute of the Physics of the Earth, Academy of Sciences of the USSR, Moscow.

Benjamin, J.R. and Cornell, C.A., 1970. *Probability, Statistics and Decision for Civil Engineers*. McGraw-Hill, New York.

Ben Menahem, A., 1960. Some consequences of earthquake statistics for the years 1918–1955. *Gerlands Beitr. Geophys.*, 69: 68–72.

Bollinger, G.A., 1973. Seismicity of the southeastern United States. *Bull. Seismol. Soc. Am.*, 63: 1785–1808.

Bolt, B.A., 1970. Causes of earthquakes. In: R.L. Wiegel (editor), *Earthquake Engineering*. Prentice Hall, Englewood Cliffs.

Brune, J.N., 1968. Seismic moment, seismicity and rate of slip along major fault zones. *J. Geophys. Res.*, 73: 777–784.

Burridge, R. and Knopoff, L., 1967. Model and theoretical seismicity. *Bull. Seismol. Soc. Am.*, 57: 341–371.

Cornell, C.A. and Vanmarcke, E.H., 1969. The major influences on seismic risk. *Proc. 4th World Conf. Earthquake Eng. Santiago.*

Crouse, C.B., 1973. Engineering studies of the San Fernando earthquake. *Calif. Inst. Technol., Earthquake Eng. Res. Lab.* Rep. 73 04.

Cox, D.F. and Lewis, P.A.W., 1966. *The Statistical Analysis of Series of Events*. Methuen, London.

Davenport, A.G., 1972. A statistical relationship between shock amplitude, magnitude and epicentral distance and its application to seismic zoning. *Univ. Western Ontario, Faculty Eng. Sci.*, BLWT 4 72.

Davies, G.F. and Brune, J.N., 1971. Regional and global fault slip rates from seismicity. *Nature*, 229: 101–107.

Drakopoulos, J.C., 1971. A statistical model on the occurrence of aftershocks in the area of Greece. *Bull. Int. Inst. Seismol. Earthquake Eng.*, 8: 17–39.

Esteva, L., 1968. Bases para la formulación de decisiones de diseño sísmico. *Natl. Univ. Mexico, Inst. Eng. Rep.* 182.

Esteva, L., 1969. Seismicity prediction: a bayesian approach. *Proc. 4th World Conf. Earthquake Eng. Santiago.*

Esteva, L., 1970. Consideraciones prácticas en la estimacion bayesiana de riesgo sísmico. *Natl. Univ. Mexico, Inst. Eng., Rep.* 248.

Esteva, L., 1974. Geology and probability in the assessment of seismic risk. *Proc. 2nd Int. Congr. Int. Assoc. Eng. Geol., Sao Paulo.*

Esteva, L. and Villaverde, R., 1973. Seismic risk, design spectra and structural reliability. *Proc. 5th World Conf. Earthquake Eng., Rome*, pp. 2586–2597.

Figueroa, J., 1963. Isosistas de macrosismos mexicanos. *Ingenieria*, 33 (1): 45–68.

Gaisky, V.N., 1966. The time distribution of large, deep earthquakes from the Pamir–Hindu-Kush. *Dokl. Akad. Nauk Tadjik S.S.R.*, 9 (8): 18–21.

Gaisky, V.N., 1967. On similarity between collections of earthquakes, the connections between them, and their tendency to periodicity. *Fiz. Zemli*, 7: 20–28 (English transl., pp. 432–437).

Gajardo, E. and Lomnitz, C., 1960. Seismic provinces of Chile. *Proc. 2nd World Conf. Earthquake Eng., Tokyo*, pp. 1529–1540.

Gutenberg, B. and Richter, C.F., 1954. *Seismicity of the Earth*. Princeton University Press, Princeton.

Gzovsky, M.G., 1962. Tectonophysics and earthquake forecasting. *Bull. Seismol. Soc. Am.*, 52 (3): 485–505.

Herrera, I., Rosenblueth, E. and Rascón, O.A., 1965. Earthquake spectrum prediction for the Valley of Mexico. *Proc. 3rd Int. Conf. Earthquake Eng., Auckland and Wellington*, I: 61–74.

Housner, G.W., 1969. Engineering estimates of ground shaking and maximum earthquake magnitude. *Proc. 4th World Conf. Earthquake Eng., Santiago.*

Hudson, D.E., 1971. *Strong Motion Instrumental Data on the San Fernando Earthquake of February 9, 1971*. California Institute of Technology, Earthquake Engineering Research Laboratory.

Hudson, D.E., 1972a. Local distributions of strong earthquake ground shaking. *Bull. Seismol. Soc. Am.*, 62 (6).

Hudson, D.E., 1972b. *Analysis of Strong Motion Earthquake Accelerograms, III, Response Spectra, Part A*. California Institute of Technology, Earthquake Engineering Research Laboratory.

Hudson, D.E. and Udwadia, F.E., 1973. Local distribution of strong earthquake ground motions. *Proc. 5th World Conf. Earthquake Eng., Rome*, pp. 691–700.

Kaila, K.L. and Narain, H., 1971. A new approach for preparation of quantitative seismicity maps as applied to Alpide Belt–Sunda Arc and adjoining areas. *Bull. Seismol. Soc. Am.*, 61 (5): 1275–1291.

Kaila, K.L., Gaur, V.K. and Narain, H., 1972. Quantitative seismicity maps of India. *Bull. Seismol. Soc. Am.*, 62 (5): 1119–1132.

Kaila, K.L., Rao, N.M. and Narain, H., 1974. Seismotectonic maps of southwest Asia region comprising eastern Turkey, Caucasus, Persian Plateau, Afghanistan and Hindukush. *Bull. Seismol. Soc. Am.*, 64 (3): 657–669.

Kelleher, J., Sykes, L. and Oliver, J., 1973. Possible criteria for predicting earthquake locations and their application to major plate boundaries of the Pacific and the Caribbean. *J. Geophys. Res.*, 78 (14): 2547–2585.

Knopoff, L., 1964. The statistics of earthquakes in southern California. *Bull. Seismol. Soc. Am.*, 54: 1871–1873.

Lomnitz, C., 1966. Magnitude stability in earthquake sequences. *Bull. Seismol. Soc. Am.*, 56: 247–249.

Lomnitz, C. and Hax, A., 1966. Clustering in aftershock sequences. In: J.S. Steinhart and T. Jefferson Smith (editors), *The Earth Beneath the Continents*. Am. Geophys. Union, pp. 502–508.

carga estática
(métodos de
análisis estructural)

carga dinámica

Dinámico → variación en el tiempo

carga dinámica
- prescrita (determinista)
- aleatoria (estocéstica)

PERIODICA

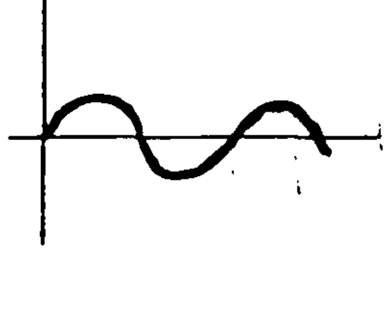

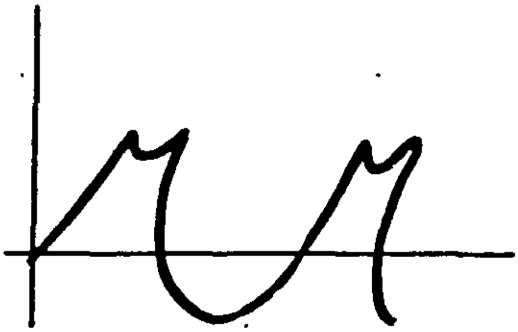

barcos.

No periódica

bombas

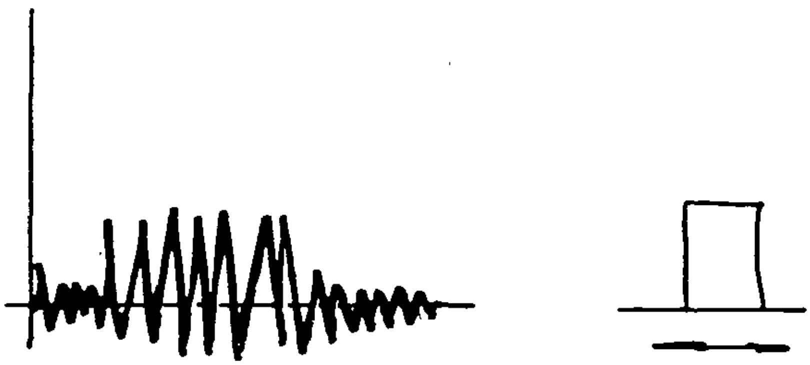

sismo.

1 grado de libertad.

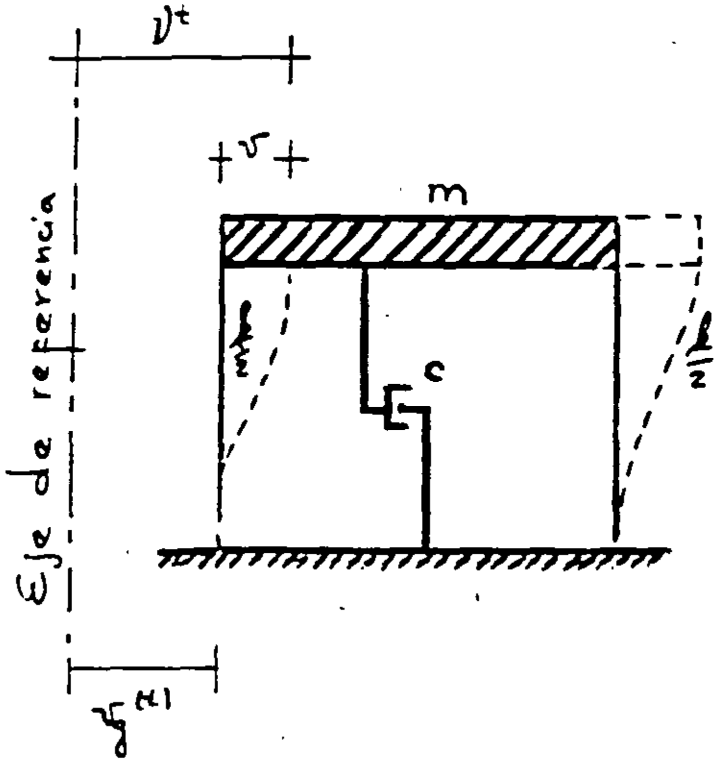

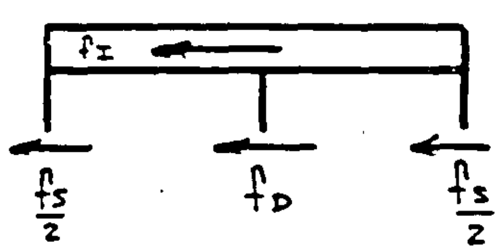

ECUACIONES DE MOVIMIENTO

métodos

Equilibrio

$$f_I + f_D + f_S = p(t)$$

$$f_S = k v$$
$$f_I = m \ddot{v}$$
$$f_D = c \dot{v}$$

Análisis de trabajo virtual

$$-f_I \delta v - f_D \delta v - f_S \delta v + p(t) \delta v = 0$$

Hamilton

$$T = \tfrac{1}{2} m \dot{v}^2$$
$$V = \tfrac{1}{2} k v^2$$

$$m\ddot{v}(t)+c\,\dot{v}(t)+k\,v(t)=p(t)$$

Respuesta de vibraciones libres.

no amortiguado

$$m\,\ddot{v}(t)+k\,v(t)=0$$

$$\ddot{v}(t)+\frac{k}{m}\,v(t)=0$$

$$\ddot{v}(t)+\omega^2 v(t)=0 \qquad \omega^2=\frac{k}{m}$$

Resolviendo

$$v(t)=\underbrace{C\ \cos\omega t + D}_{\text{constantes}}\ \text{sen}\ \omega t$$

Si $v(0)$ - $\quad t=0$
$\dot{v}(0)$ -

$$v(t)=v(0)\cos\omega t+\frac{\dot{v}(0)}{\omega}\ \text{sen}\ \omega t$$

o bien

$$v(t) = \rho \cos(\omega t - \theta)$$

$$f = \frac{\omega}{2\pi}$$

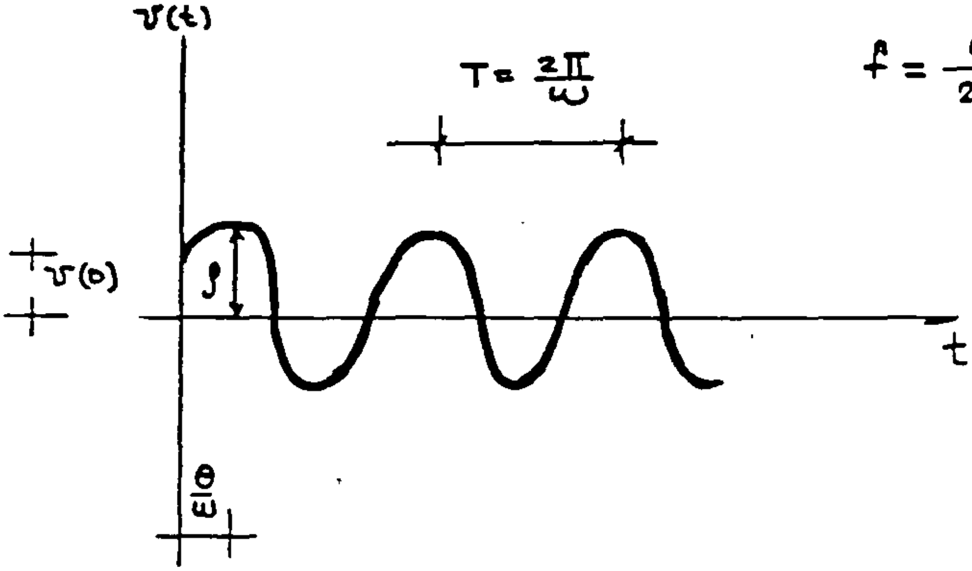

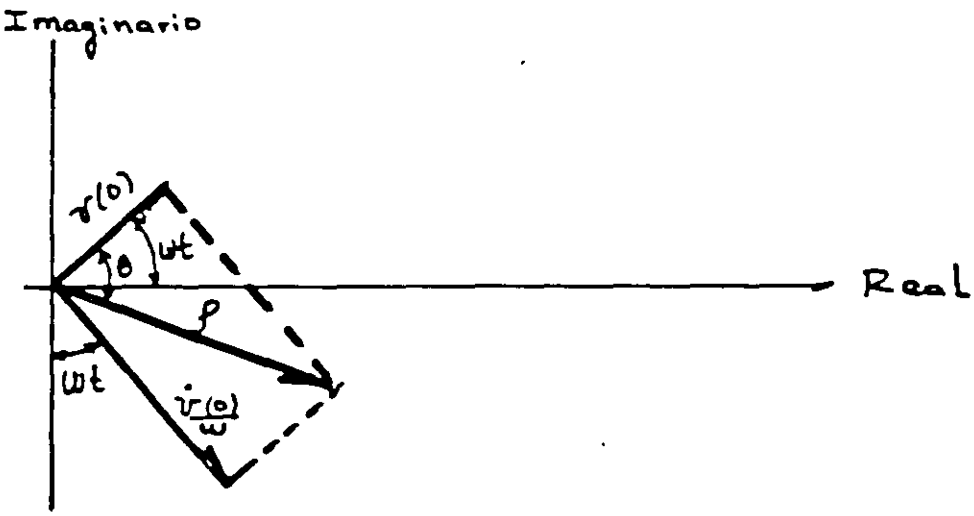

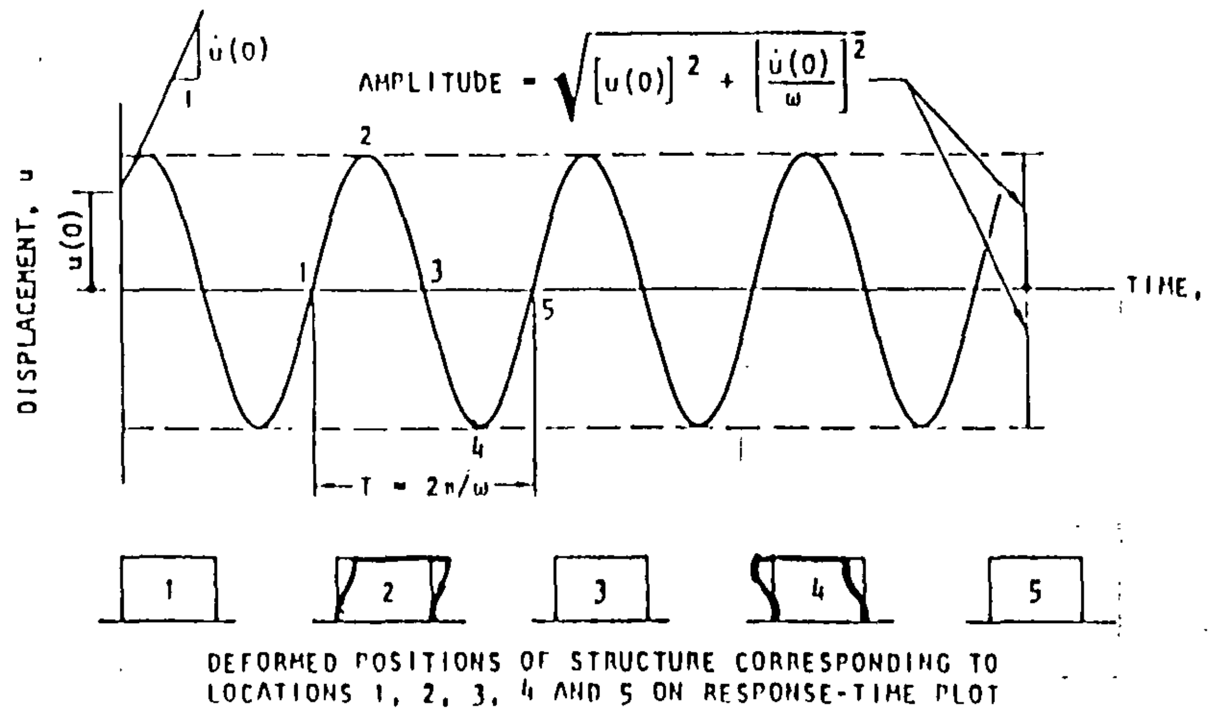

Figure 8 Free vibration of an undamped structure

amortiguado

$$m\ddot{v}(t) + c\dot{v}(t) + k\,v(t) = 0$$

$$\ddot{v}(t) + \frac{c}{m}\dot{v}(t) + \frac{k}{m}v(t) = 0$$

$$\ddot{v}(t) + 2\gamma\omega\dot{v}(t) + \omega^2 v(t) = 0$$

$$2\gamma\omega = \frac{c}{m}$$

$$\gamma = \frac{c}{2m\omega} = \frac{c}{2\sqrt{km}}$$

$c_c = 2\sqrt{km}$ amortiguamiento crítico

Resolviendo:

$\gamma > 1$

$v(t) = c_1 e^{s_1 t} + c_2 e^{s_2 t}$ sobreamortiguado

$\gamma = 1$

$v(t) = c_1 e^{st} + c_2 t e^{st}$

crítico

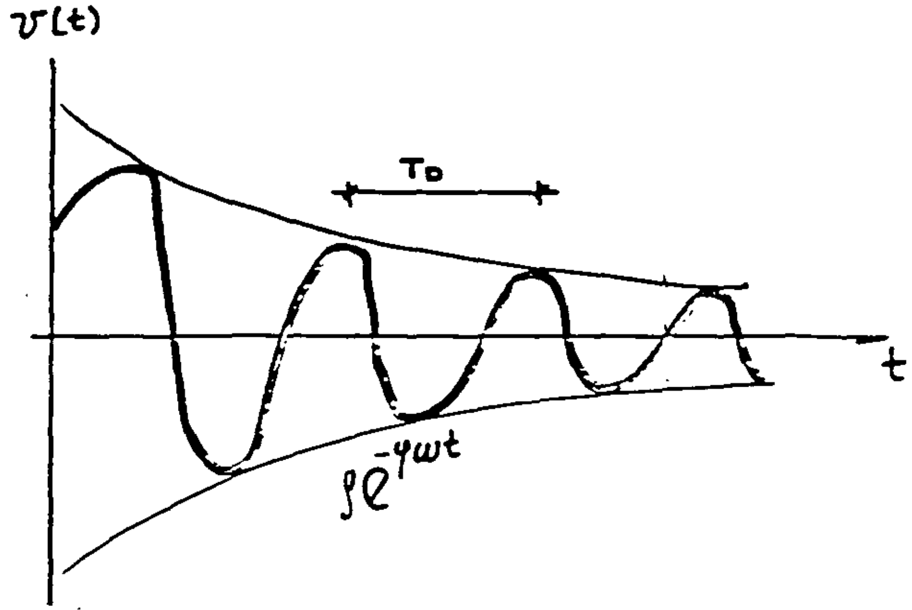

cálculo del amortiguamiento

$$\frac{v_t}{v_{t+nT_D}} = \frac{\rho e^{-\gamma\omega t}\cos(\omega_D t - e)}{\rho e^{-\gamma\omega(t+nT_D)}\cos[\omega_D(t+nT_D)-e]}$$

$$\frac{2\pi n\gamma}{\sqrt{1-\gamma^2}} = \ln\frac{v_t}{v_{t+nT_D}}$$

$\gamma < 1$ subamortiguado.

$$\omega_D = \omega \sqrt{1 - \gamma^2}$$

$$v(t) = e^{-\gamma \omega t} \left[A \cos \omega_D t + B \operatorname{sen} \omega_D t \right]$$

constantes.

Si

$$\left. \begin{array}{l} v(0) \\ \dot{v}(0) \end{array} \right. \longrightarrow t = 0$$

$$v(t) = e^{-\gamma \omega t} \left[v(0) \cos \omega_D t + \frac{\dot{v}(0) + \gamma \omega v(0)}{\omega_D} \sin \omega_D t \right]$$

$$v(t) = \rho \, e^{-\gamma \omega t} \cos (\omega_D t - \theta)$$

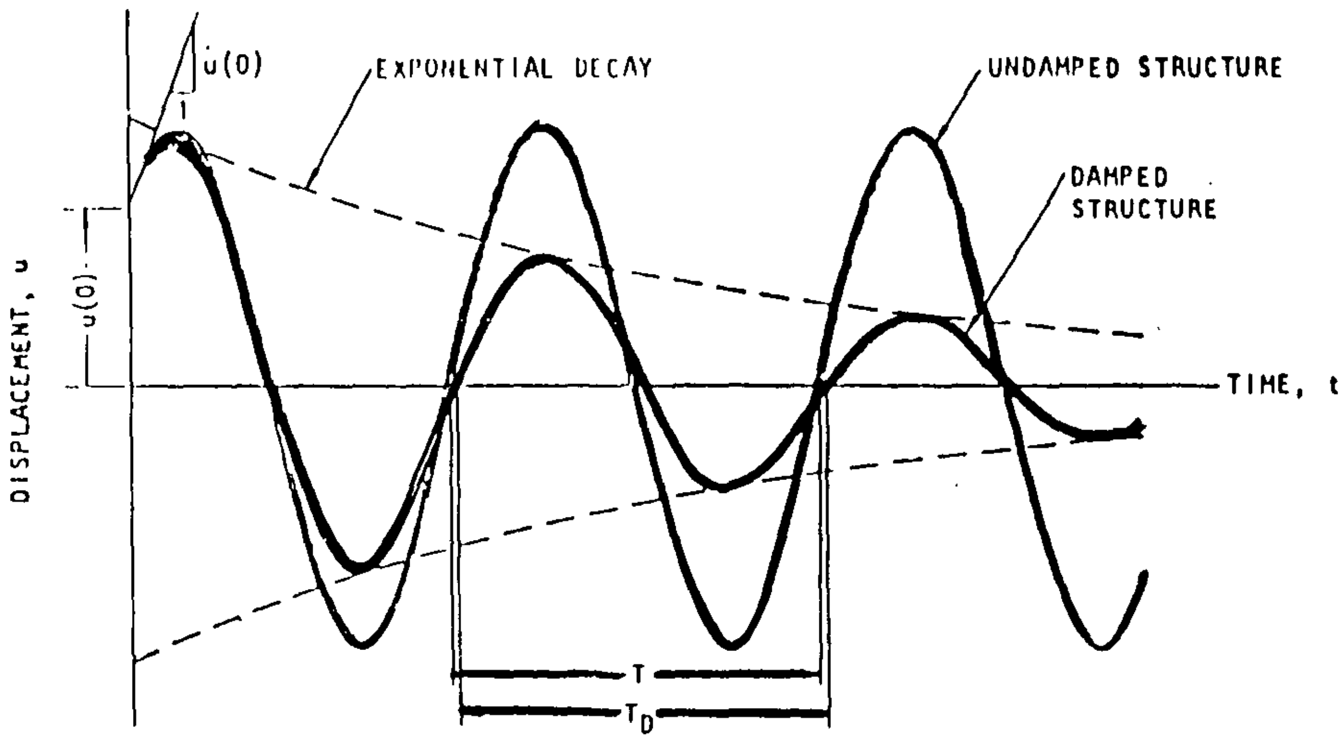

Figure 9. Effect of damping on free vibration

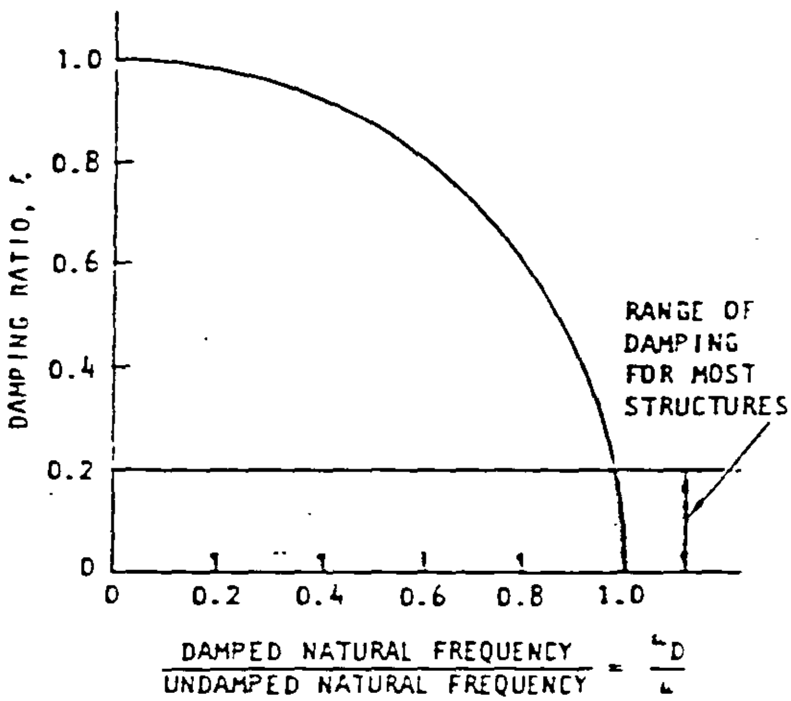

Figure 10. Effect of damping on natural frequency of vibration

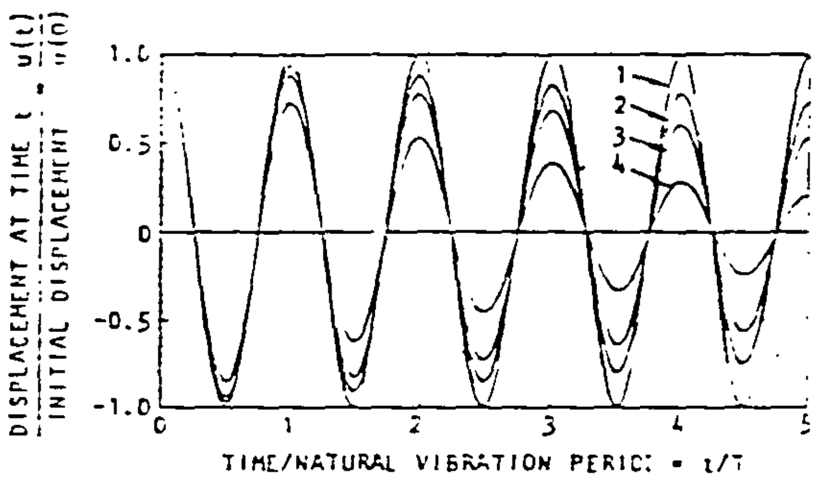

Figure 11. Effect of damping on free vibration. Curves 1, 2, 3, and 4 are for damping ratios of 0, 1, 2, and 5 percent, respectively

VIBRACIONES FORZADAS.

no amortiguadas

$$m\ddot{v}(t) + k\,v(t) = F$$

$$\ddot{v}(t) + \frac{k}{m}\,v(t) = \frac{F}{m}$$

$$\ddot{v}(t) + \omega^2\,v(t) = F/m$$

$$v(t) = v_c(t) + v_p(t)$$

$$v_c(t) = C\cos\omega t + D\,\mathrm{sen}\,\omega t$$

$$v_p(t) = F/k$$

$v(0)$
$\dot{v}(0)$ para $t=0$

$$v(t) = F/k\,(1-\cos\omega t)$$

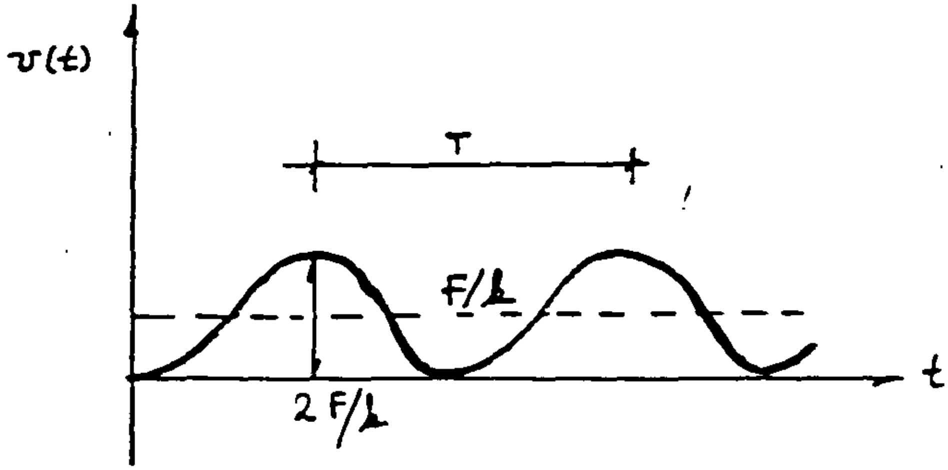

Caso II

$$F(t) = P_o \operatorname{sen} \bar{\omega} t$$

$$m\ddot{v}(t) + k\, v(t) = P_o \operatorname{sen} \bar{\omega} t$$

$$\ddot{v}(t) + \frac{k}{m} v(t) = \frac{P_o}{m} \operatorname{sen} \bar{\omega} t$$

$$v(t) = v_o(t) + v_p(t)$$

$$v_c(t) = C \cos \omega t + D \operatorname{sen} \omega t$$

$$v_p(t) = \frac{P_o}{k} \underbrace{\frac{\omega^2}{\omega^2 - \bar{\omega}^2}}_{\text{f.a.}} \operatorname{sen} \bar{\omega} t$$

$$\frac{1}{1 - \left(\frac{\bar{\omega}}{\omega}\right)^2}$$

para $t=0$

$v(0)$

$\dot{v}(0)$

$$v(t)=\frac{P_o}{k}\,\frac{1}{1-\bar{\omega}^2/\omega^2}\Big(\overset{\text{estacionaria}}{\operatorname{Sen}\bar{\omega}t}-\underset{\text{transitoria}}{\frac{\bar{\omega}}{\omega}\operatorname{sen}\omega t}\Big)$$

$$v(t)\Big|_{\bar{\omega}=\omega}$$

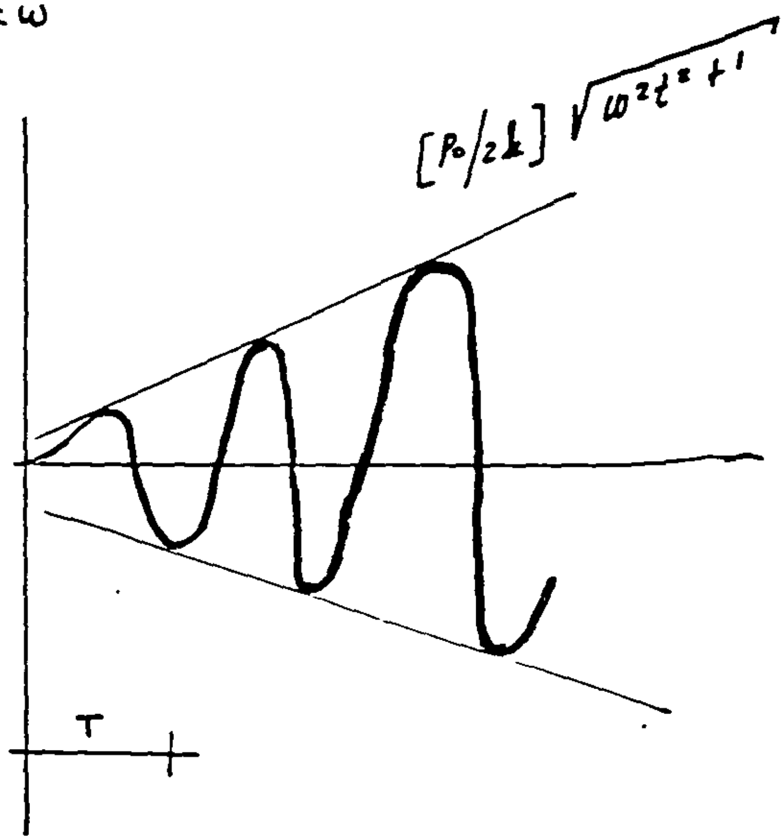

amortiguados

$$m\ddot{v}(t) + c\,\dot{v}(t) + k\,v(t) = P_o \operatorname{sen} \bar{\omega} t$$

$$v(t) = v_c(t) + v_p(t)$$

libre

$$v_c(t) = e^{-\gamma\omega t}\left[A\cos\omega_o t + B\operatorname{sen}\omega_o t\right]$$

$$v_p(t) = -\frac{2\gamma\omega\bar{\omega}\,\frac{P_o}{m}}{(\omega^2-\bar{\omega})^2 + (2\gamma\omega\bar{\omega})^2}\cos\bar{\omega}t +$$

$$+\frac{(\omega^2-\bar{\omega}^2)\,\frac{P_o}{m}}{(\omega^2-\bar{\omega}^2)^2 + (2\gamma\omega\bar{\omega})^2}\operatorname{sen}\bar{\omega}t$$

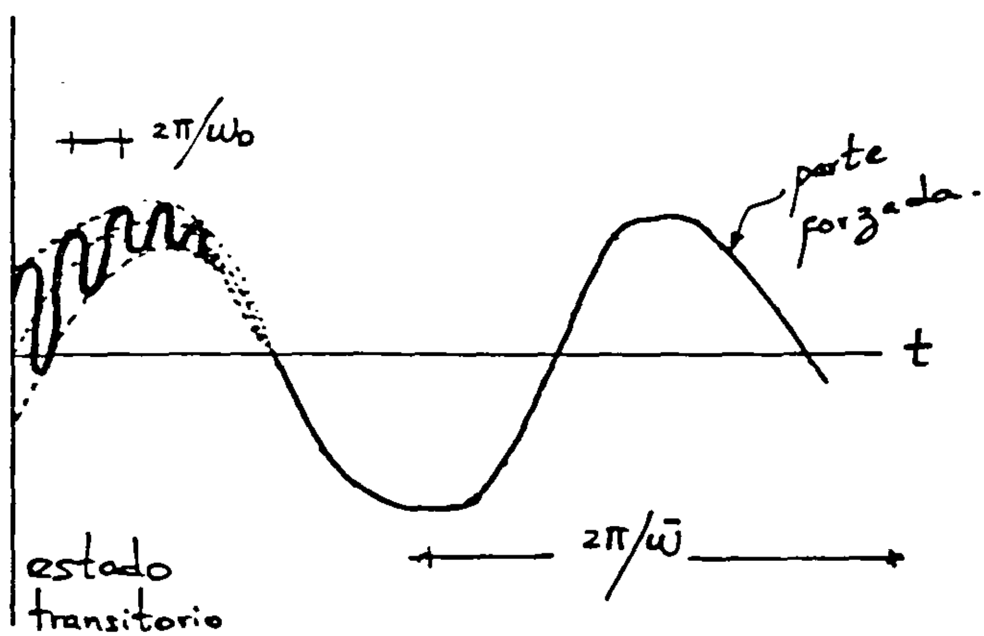

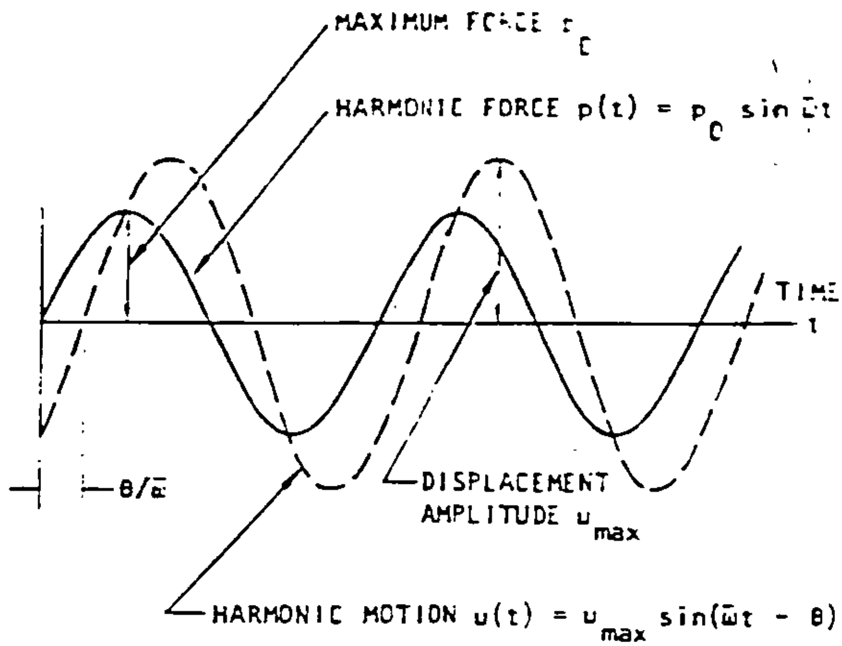

Figure 14. Steady state motion due to harmonic force

factor de amplificación

$$D = \frac{\rho}{P_0/k} = \frac{1}{\sqrt{\left(1 - \frac{\bar{\omega}^2}{\omega^2}\right)^2 + \left(2\varphi \frac{\bar{\omega}}{\omega}\right)^2}}$$

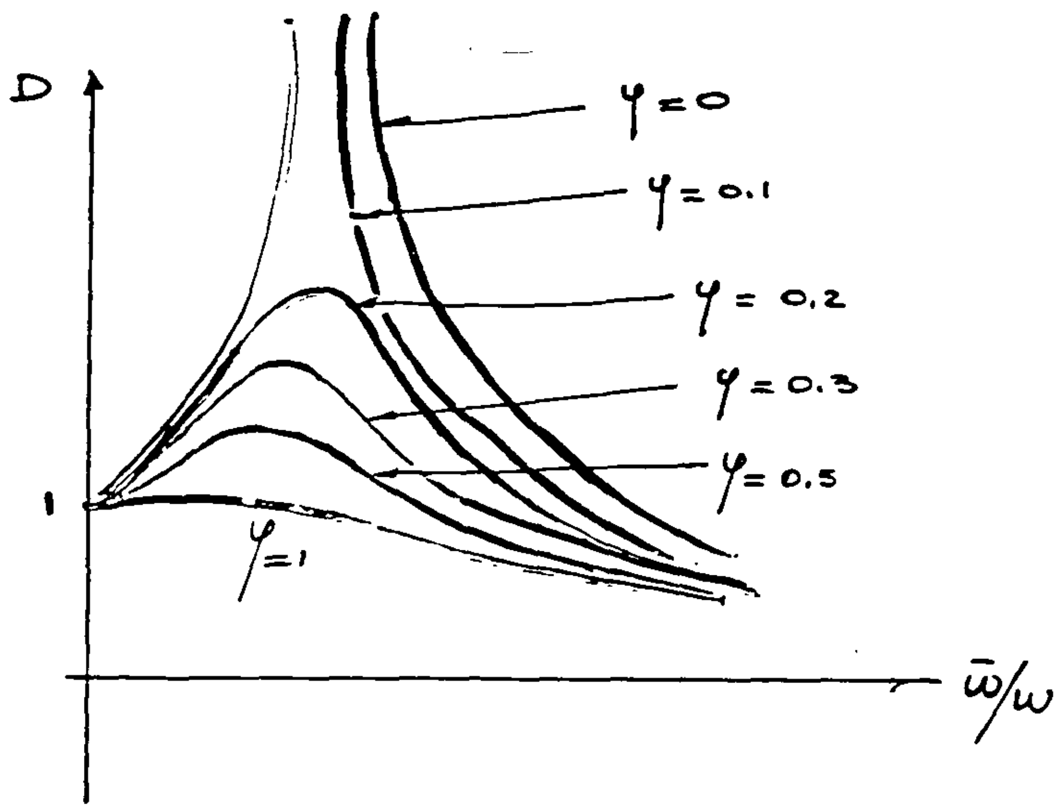

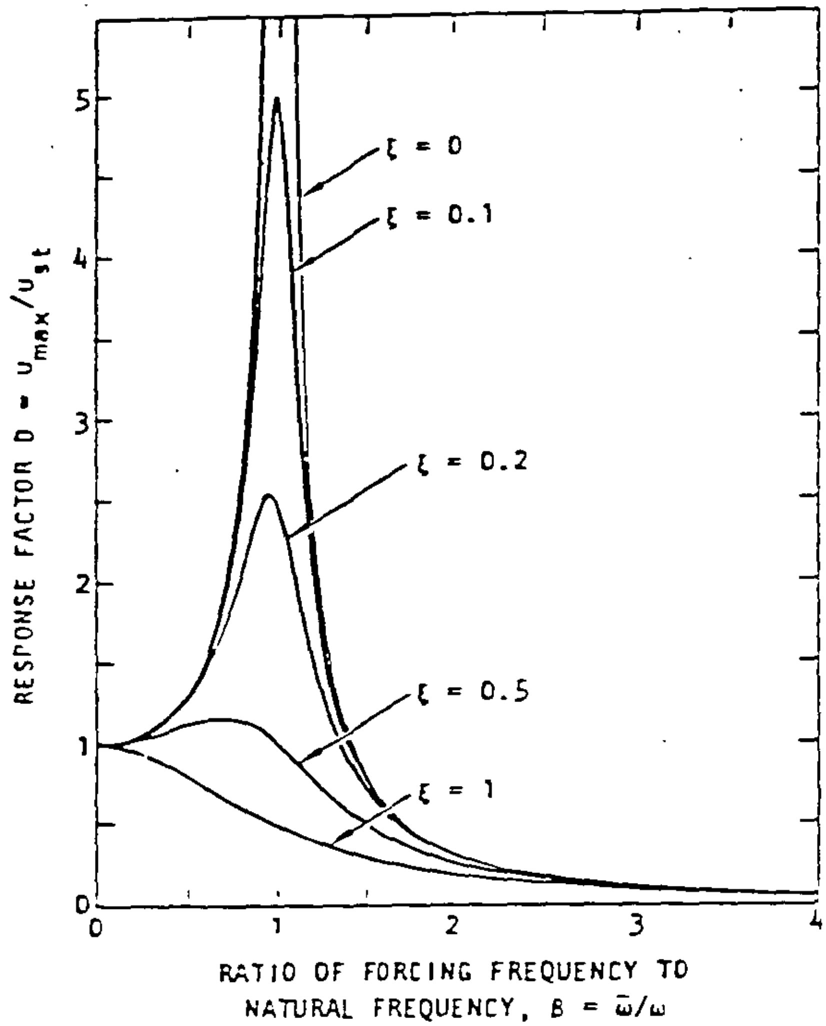

Figure 15. Response factor for a one-story structure subjected to harmonic force

FACULTAD DE INGENIERIA U.N.A.M.
DIVISION DE EDUCACION CONTINUA

CURSOS ABIERTOS

XXV CURSO INTERNACIONAL DE INGENIERÍA SÍSMICA

MÓDULO III:

DISEÑO SÍSMICO DE PUENTES

TEMA

ANÁLISIS SÍSMICO DE PUENTES

DR. ROBERTO GÓMEZ MARTÍNEZ
PALACIO DE MINERÍA
AGOSTO DE 1999

Palacio de Minería Calle de Tacuba 5 Primer piso Deleg. Cuauhtémoc 06000 México D.F. APDO. Postal M-2285
Teléfonos 512-8955 512-5121 521-7335 521-1987 Fax 510-0573 521-4020 AL 26

ANALISIS SÍSMICO DE PUENTES

Roberto Gómez Martínez
Instituto de Ingeniería, UNAM

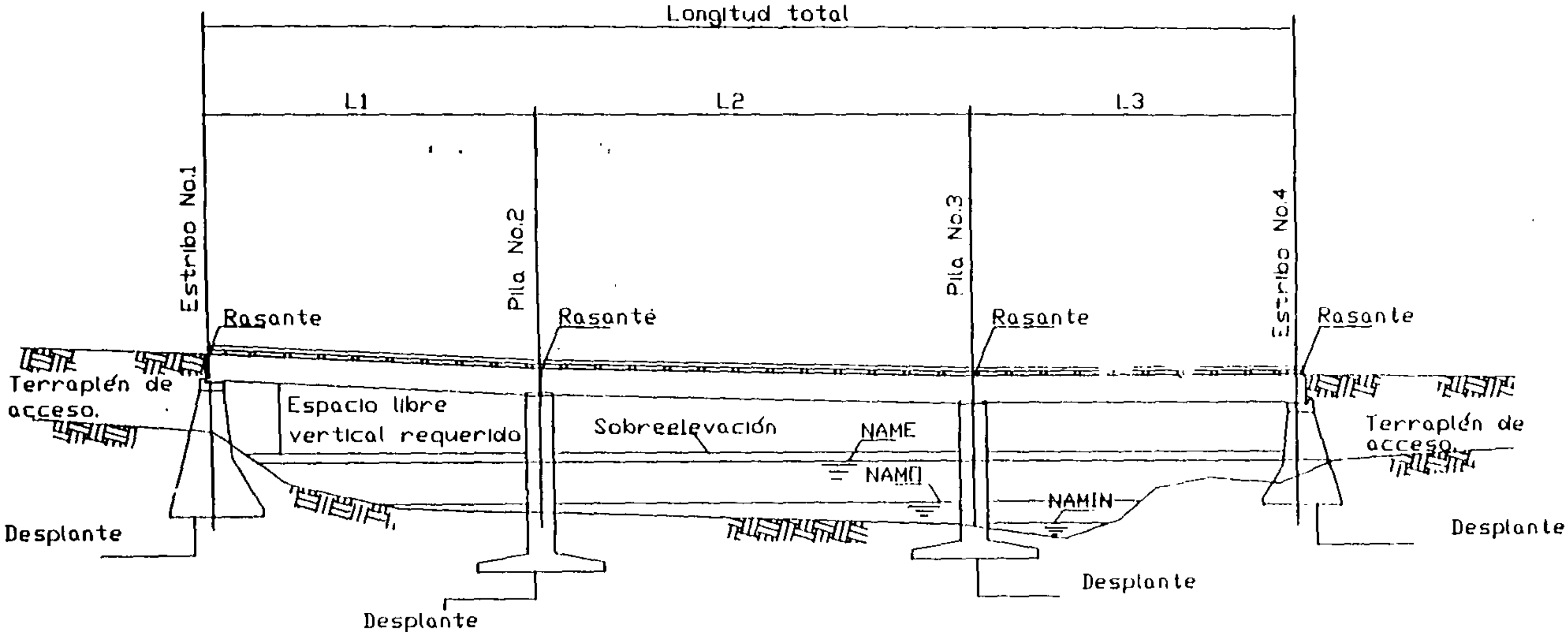

Longitud total
L1
L2
L3
Estribo No.1
Pila No.2
Pila No.3
Estribo No.4
Rasante
Rasante
Rasante
Rasante
Terraplén de acceso.
Espacio libre vertical requerido
Sobreelevación
NAME
NAMO
NAMIN
Terraplén de acceso.
Desplante
Desplante
Desplante
Desplante

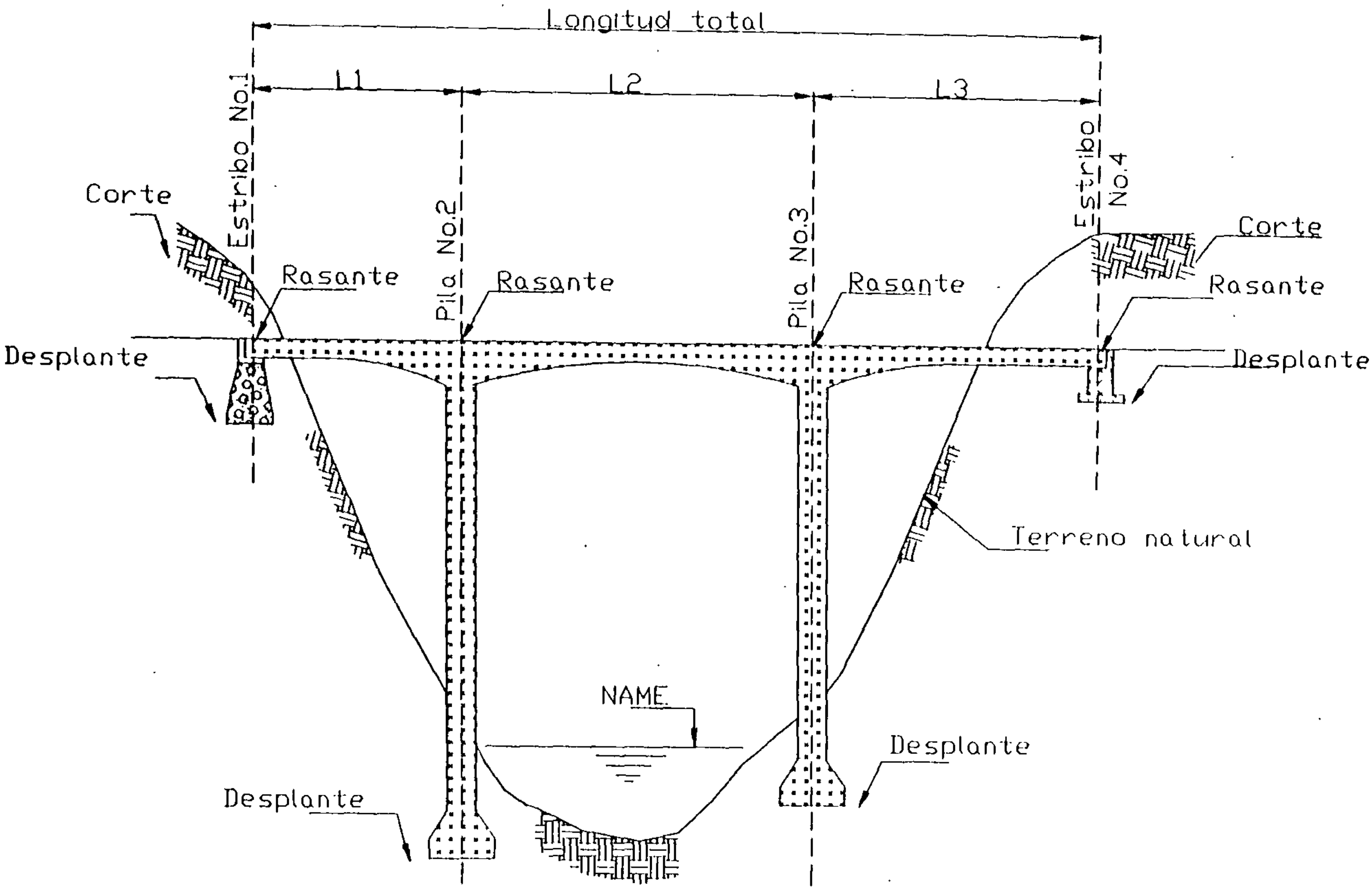
Longitud total
L1
L2
L3
Estribo No.1
Pila No.2
Pila No.3
Estribo No.4
Corte
Corte
Rasante
Rasante
Rasante
Rasante
Desplante
Desplante
Desplante
Desplante
Terreno natural
NAME

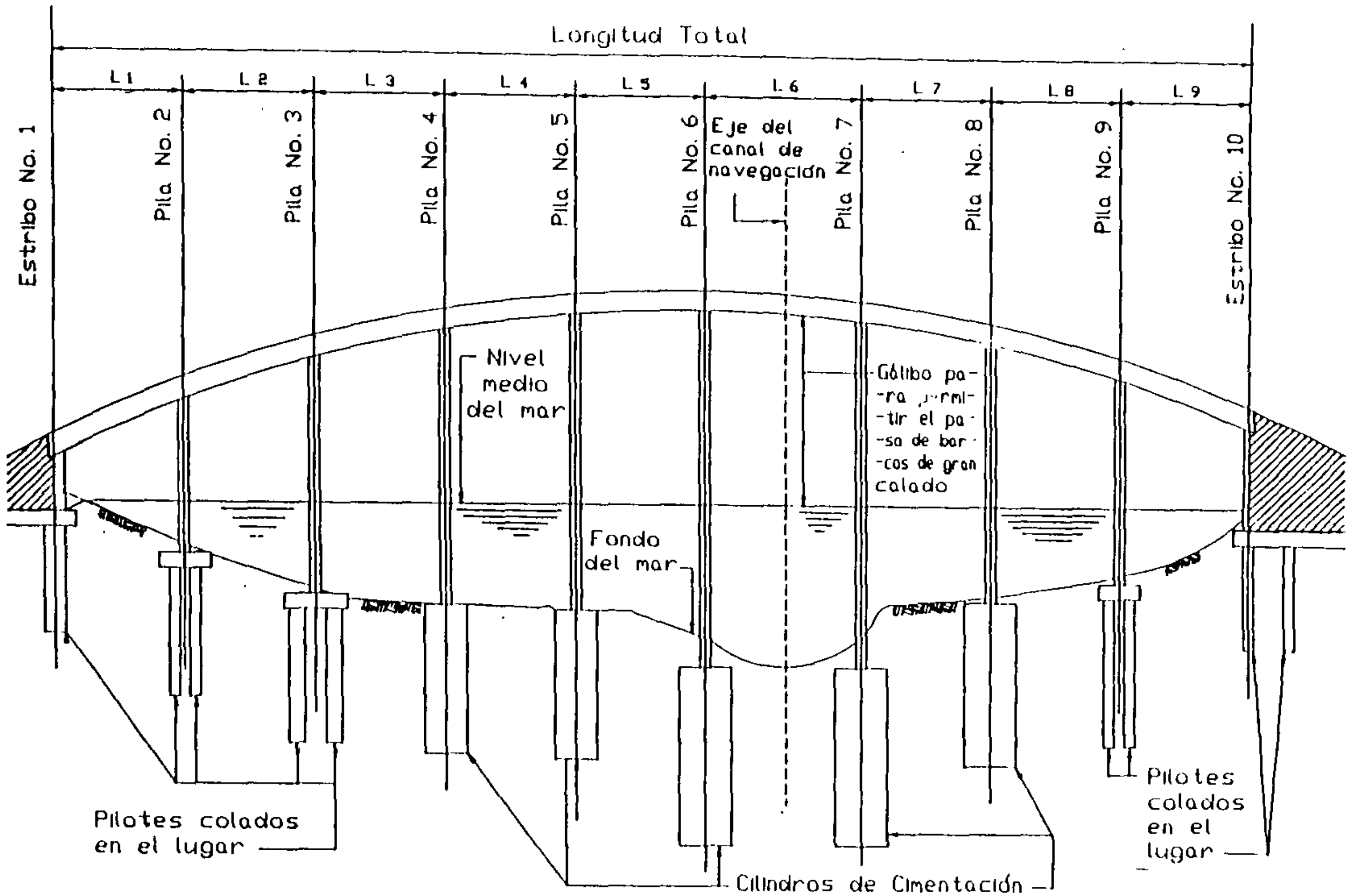

Longitud Total
L 1
L 2
L 3
L 4
L 5
L 6
L 7
L 8
L 9
Estribo No. 1
Pila No. 2
Pila No. 3
Pila No. 4
Pila No. 5
Pila No. 6
Pila No. 7
Pila No. 8
Pila No. 9
Estribo No. 10
Eje del canal de navegación
Nivel medio del mar
Gálibo para permitir el paso de barcos de gran calado
Fondo del mar
Pilotes colados en el lugar
Cilindros de Cimentación
Pilotes colados en el lugar

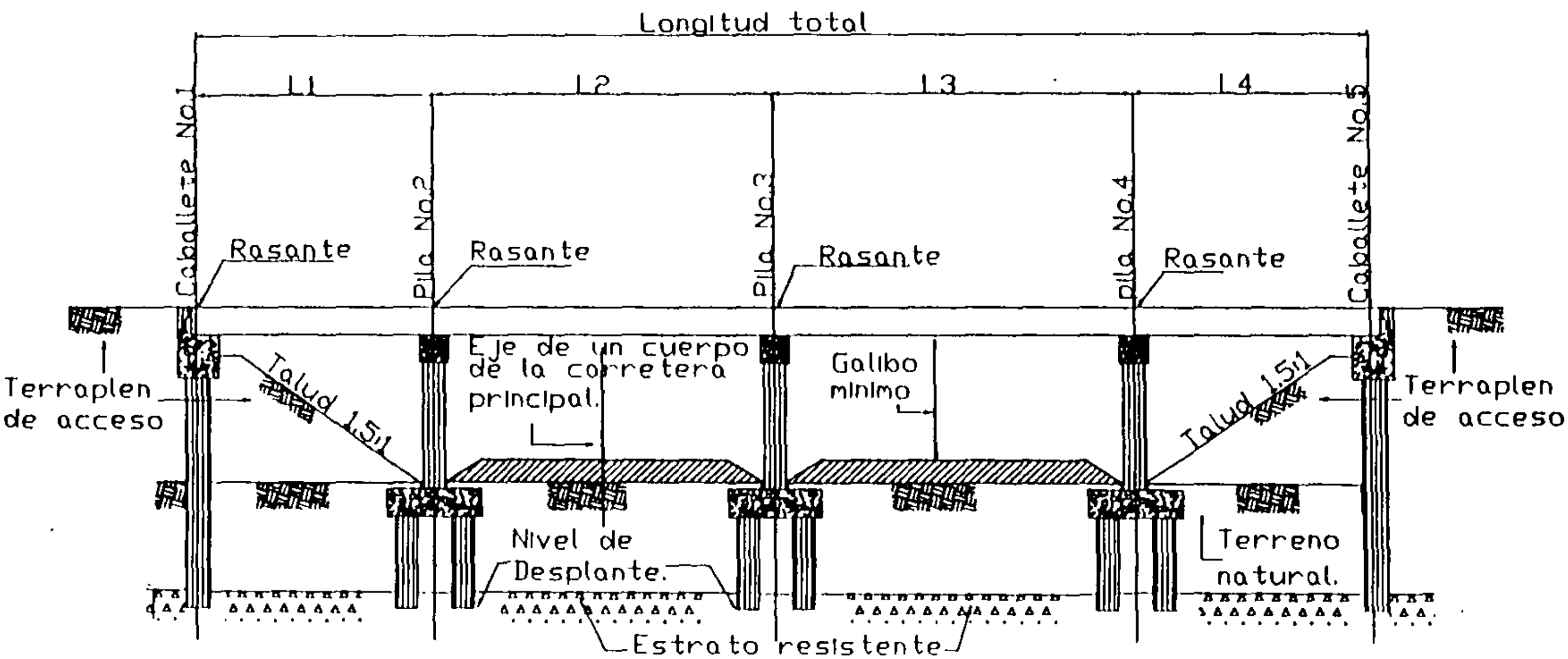
Longitud total
L1
L2
L3
L4
Caballete No.1
Pila No.2
Pila No.3
Pila No.4
Caballete No.5
Rasante
Rasante
Rasante
Rasante
Eje de un cuerpo de la carretera principal.
Galibo minimo
Terraplen de acceso
Terraplen de acceso
Talud 1.5:1
Talud 1.5:1
Nivel de Desplante.
Terreno natural.
Estrato resistente

CARGAS

Carga viva

- superestructura

Carga sísmica

- subestructura
- conexiones

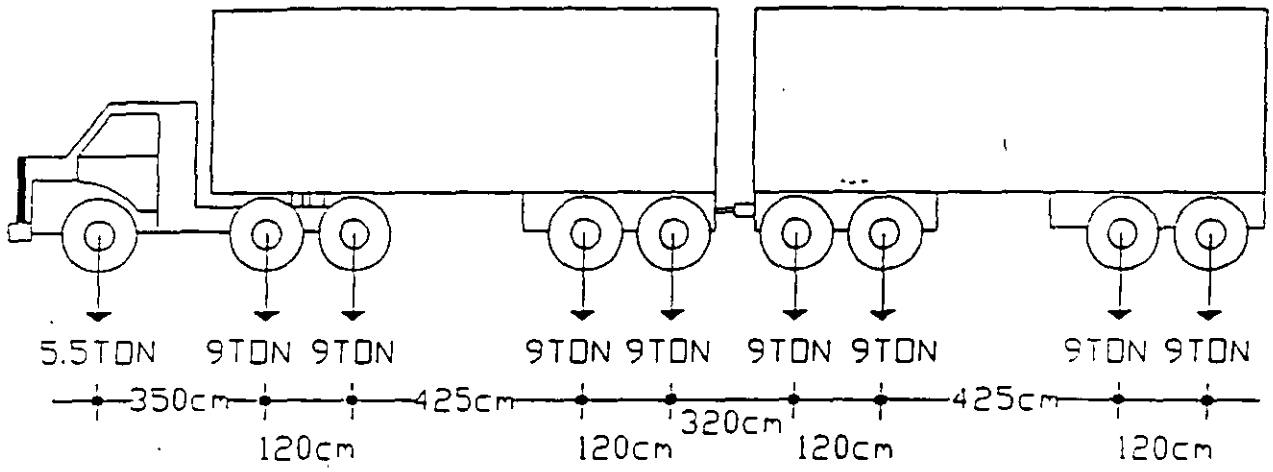

(a) T3-S2-R4

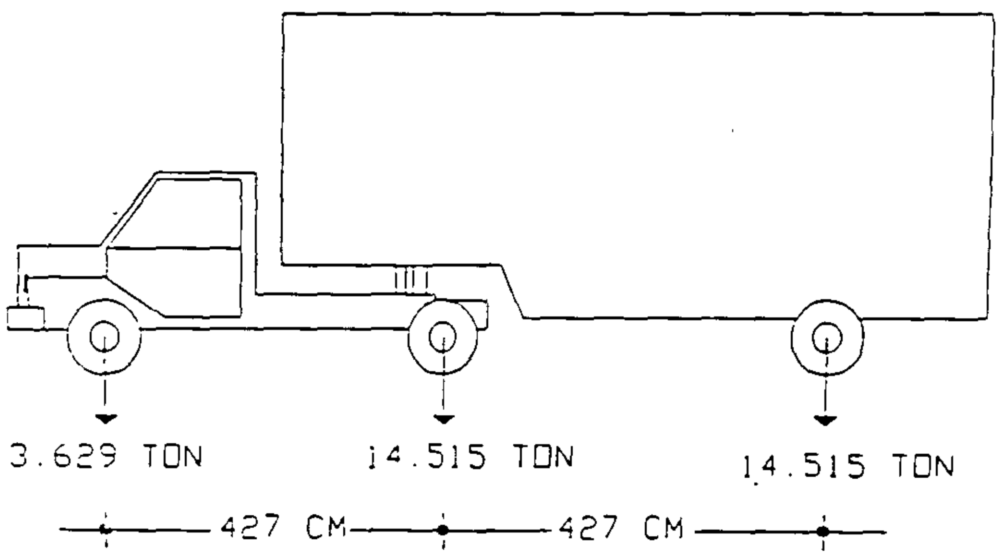

(b) HS-20

Fig 2. CARGAS Y DISTANCIAS ENTRE EJES

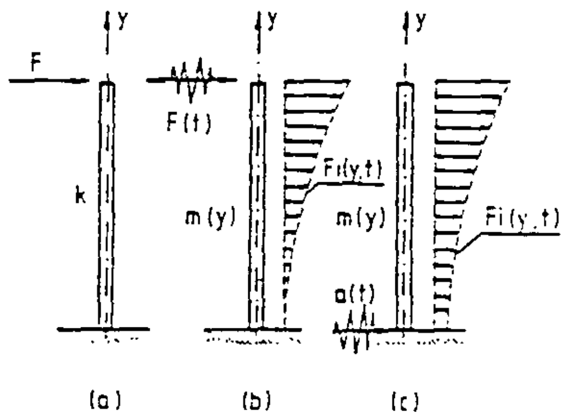

CARGAS ESTATICA, DINAMICA Y SISMICA

(a) estática, (b) dinámica;
(c) sísmica

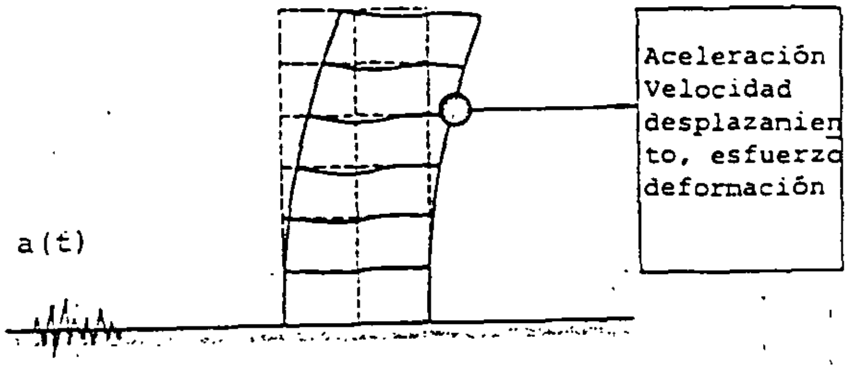

RESPUESTA SISMICA

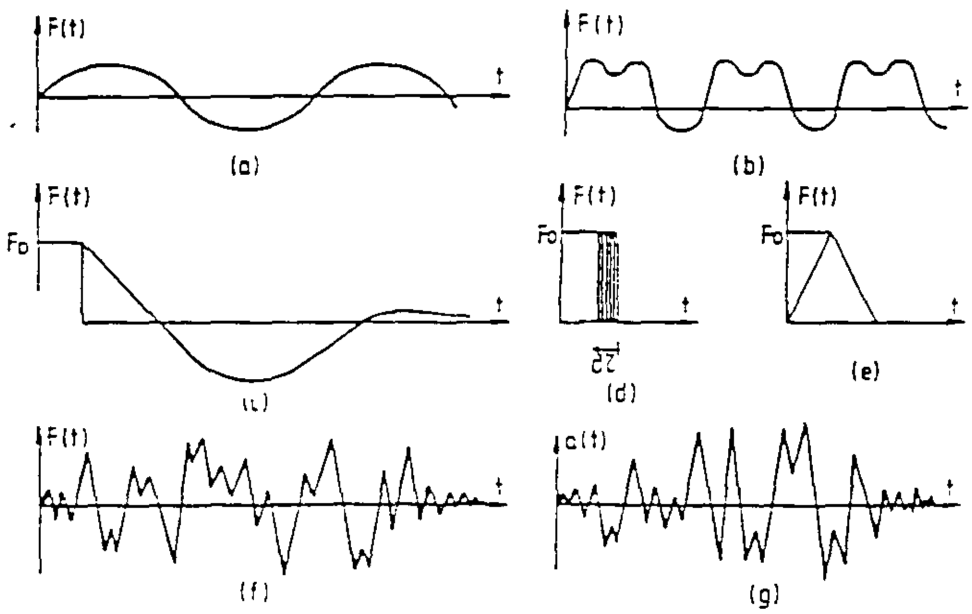

CARGAS DINAMICAS TIPICAS

(a) armónica, (b) periódica; (c) cuasi-periódica
(d), (e) impulsos; (f) carga dinámica general;
(g) sísmica

FORMA ESTRUCTURAL

* SIMPLE
* SIMETRICA
* INTEGRAL

ANALISIS ESTATICO

$F = (f_i)\ (f_c))\ (f_s)\ (f_z)\ \ (W_{trib.})$

ANALISIS DINAMICO

- análisis modal espectral
- análisis en el dominio del tiempo
- análisis no lineal

PUENTES ESPECIALES

- Geometría no convencional

- Tipo no convencional

TIPO NO CONVENCIONAL

- Suspendidos
- Atirantados
- Arco

GEOMETRIA NO CONVENCIONAL

- Curvatura excesiva
- Esviajamiento excesivo
- Pilas muy altas
- Pilas de diferente altura
- Claros contínuos muy largos
- Claros discontínuos muy largos
- Subestructuras en aguas profundas

- Claros mayores
- Requisitos estéticos

* * * * * *

- Nuevos materiales
- Análisis por computadora

MODELO MATEMATICO

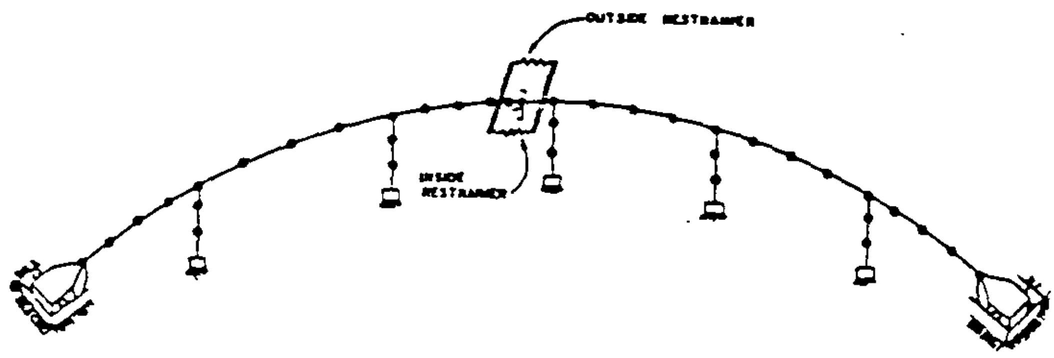

IDEALIZACION DE LA ESTRUCTURA

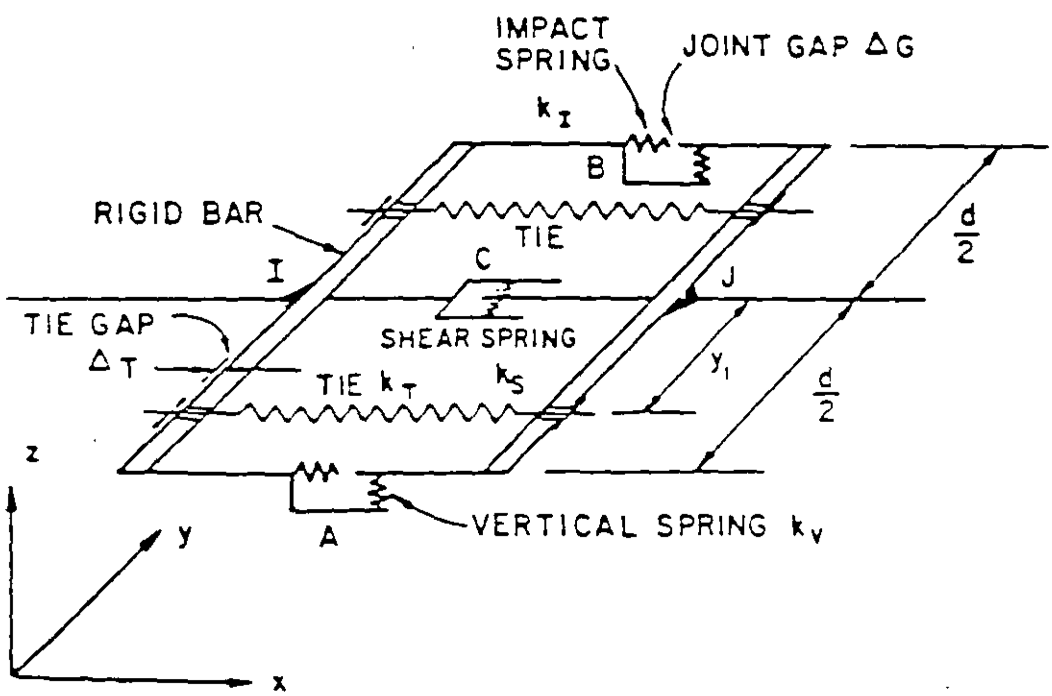

IDEALIZACION DE ARTICULACIONES

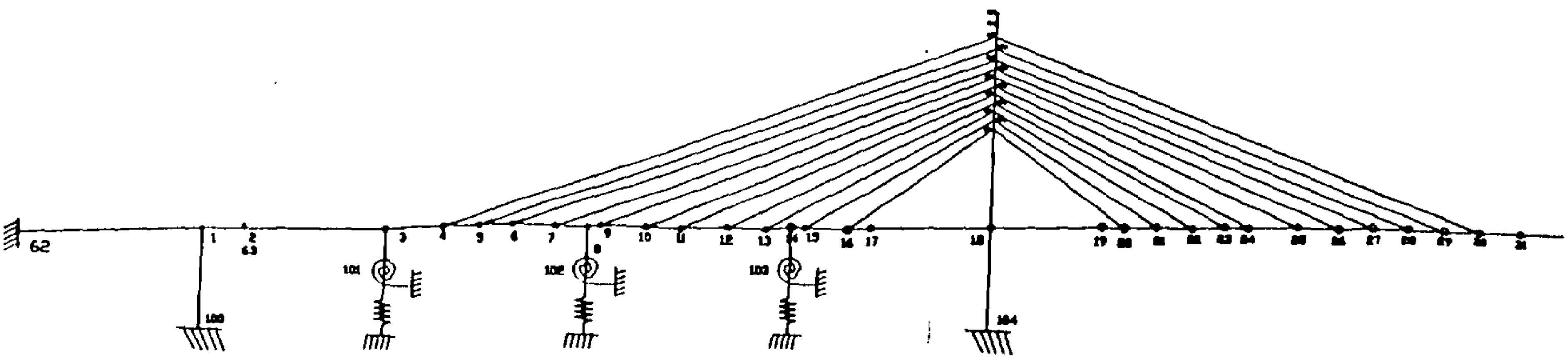

Fig 3. Finite element model

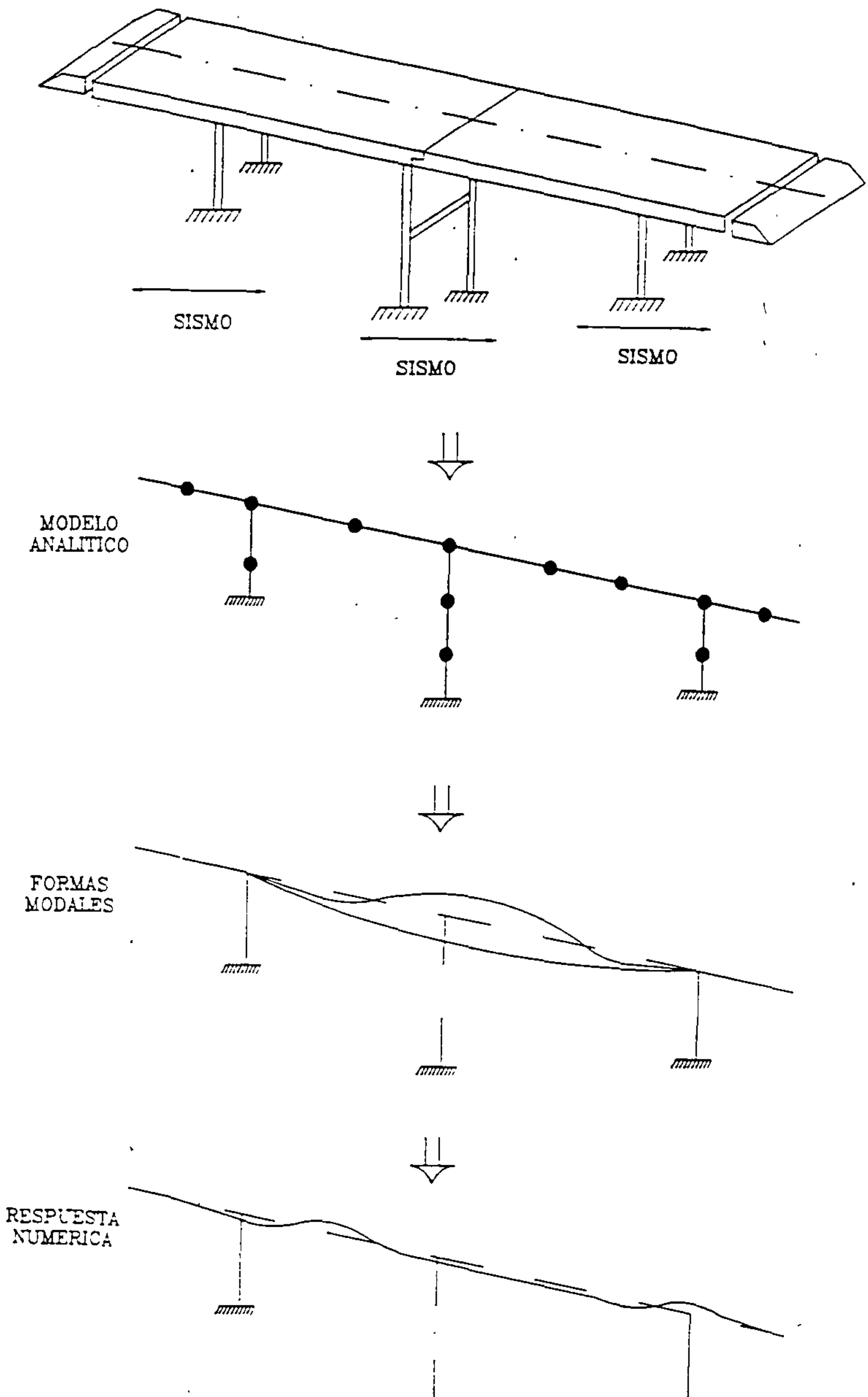

SISMO
SISMO
SISMO
MODELO
ANALITICO
FORMAS
MODALES
RESPUESTA
NUMERICA

RIGIDEZ

- SUPERESTRUCTURA
- APOYOS
- SUBESTRUCTURA
- CIMENTACION

COMBINACION ORTOGONAL DE FUERZAS SISMICAS

PENDULO

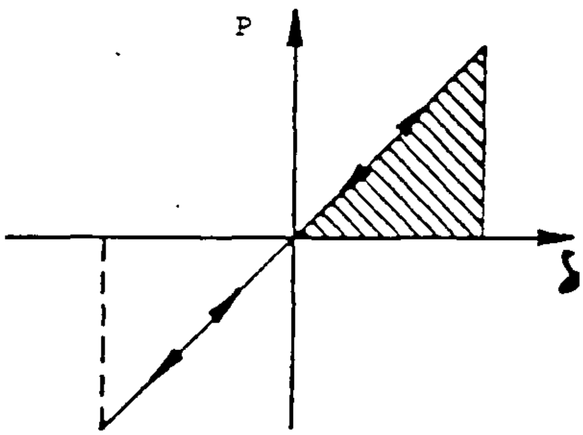

CARGA DESPLAZAMIENTO, RANGO ELASTICO

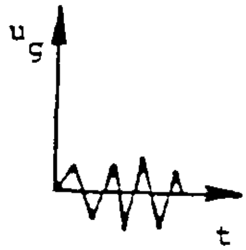

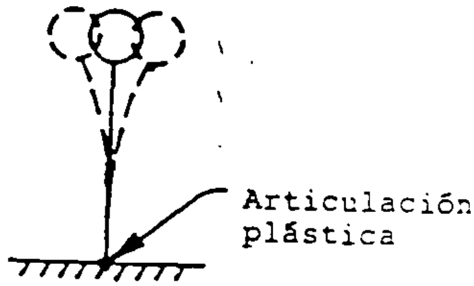

PENDULO CON ARTICULACION PLASTICA

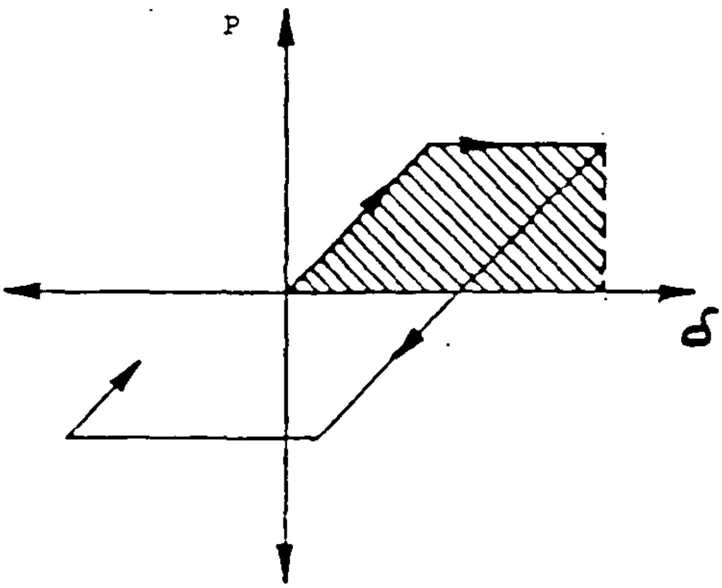

CARGA-DESPLAZAMIENTO, RANGO ELASTO-PLASTICO

DUCTILIDAD

- Desplazamiento
- Curvatura

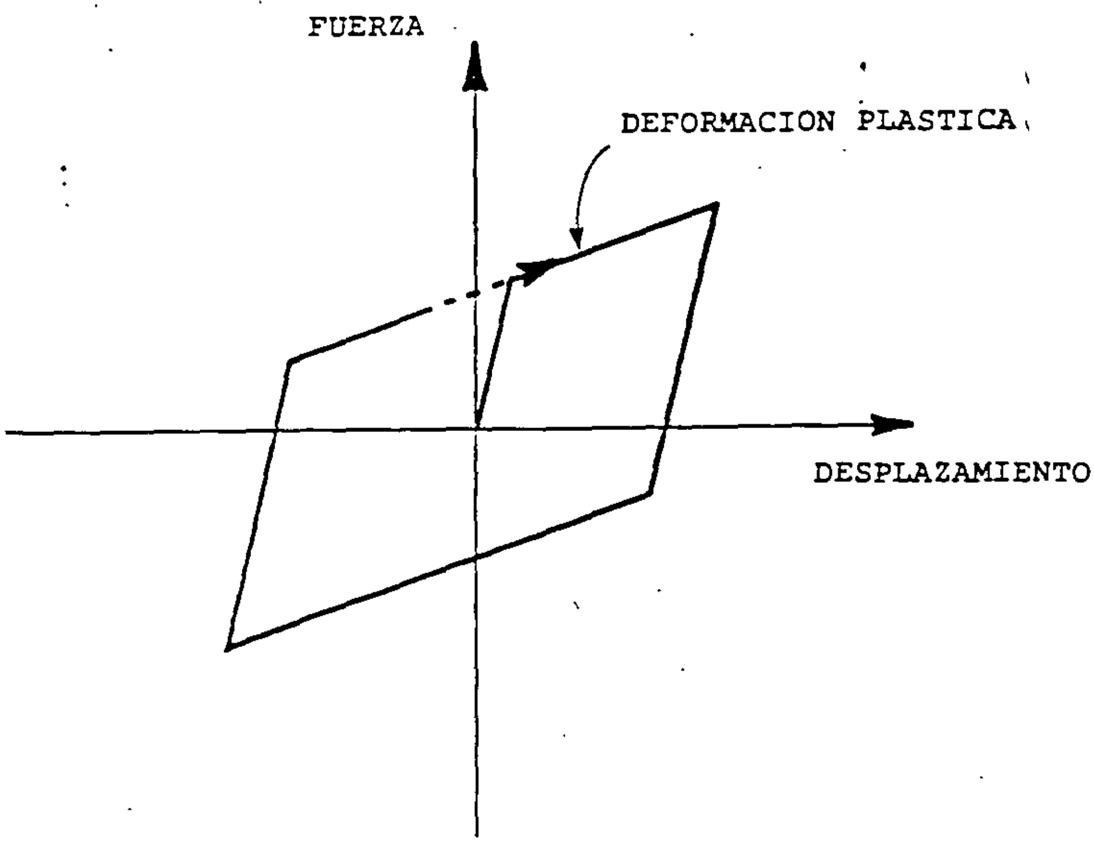

CICLO HISTERETICO IDEALIZADO

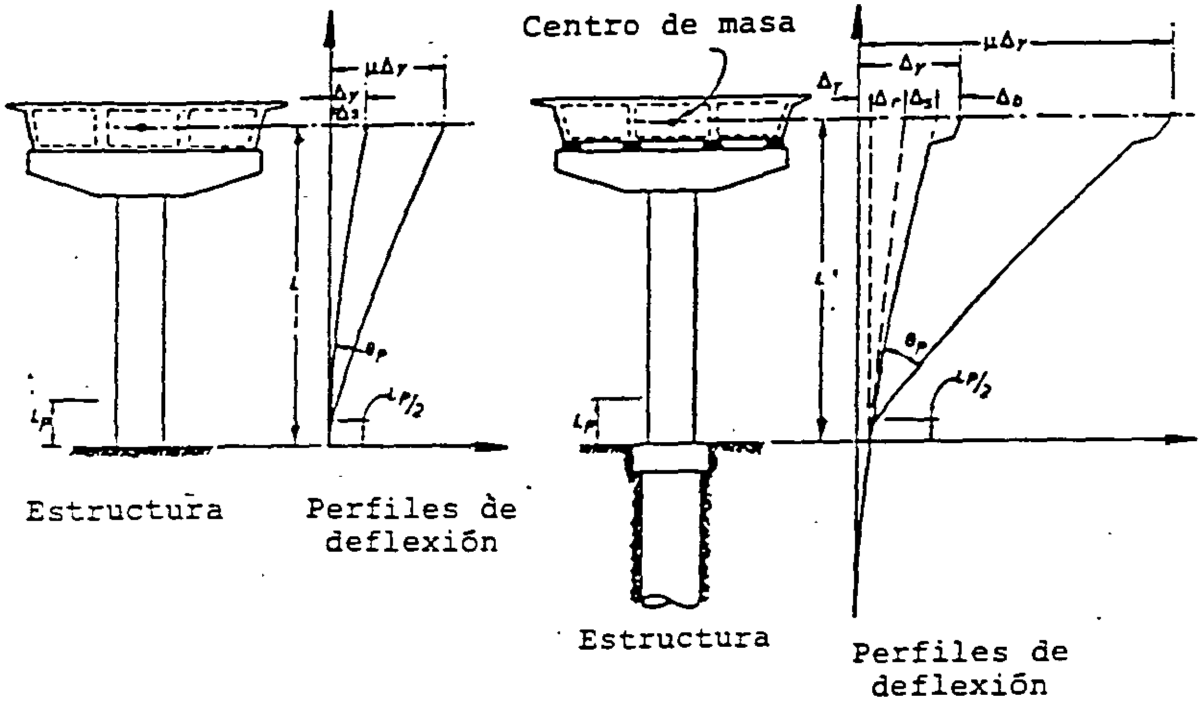

DEFORMACIONES ELASTICA E INELASTICA DE UNA COLUMNA DE UN PUENTE

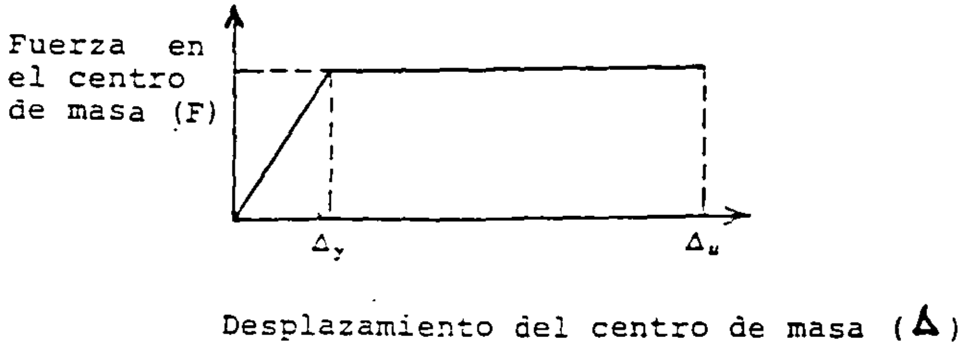

IDEALIZACION DE LA CAPACIDAD DUCTIL DE LA ESTRUCTURA

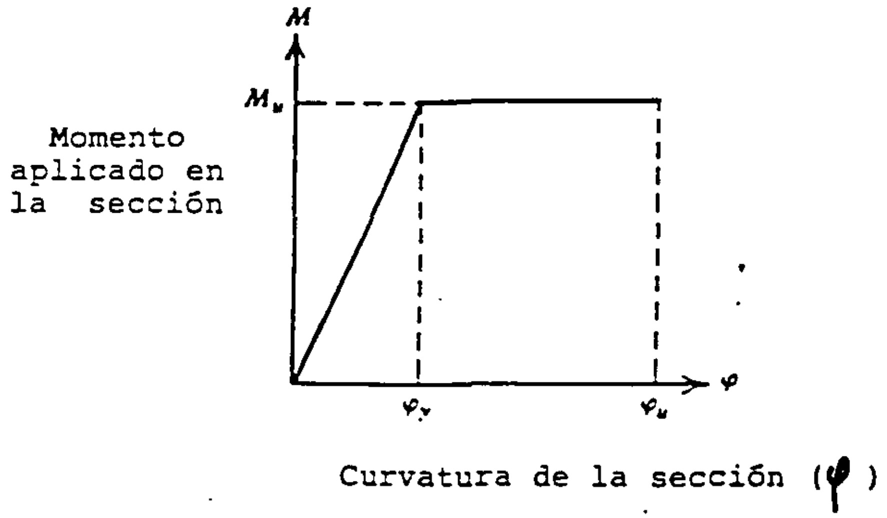

IDEALIZACION DE LA CAPACIDAD DUCTIL DE LA SECCION

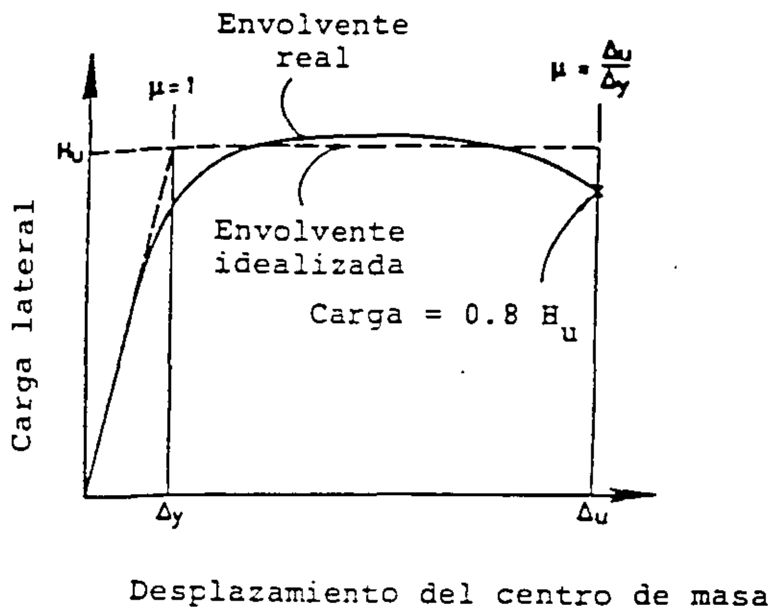

CURVA REAL CARGA-DESPLAZAMIENTO DE LA ESTRUCTURA

INTERACCION SUELO - ESTRUCTURA

- ZAPATAS
- PILOTES
- PILASTRONES
  (PILAS COLADAS EN SITIO)
- CILINDROS

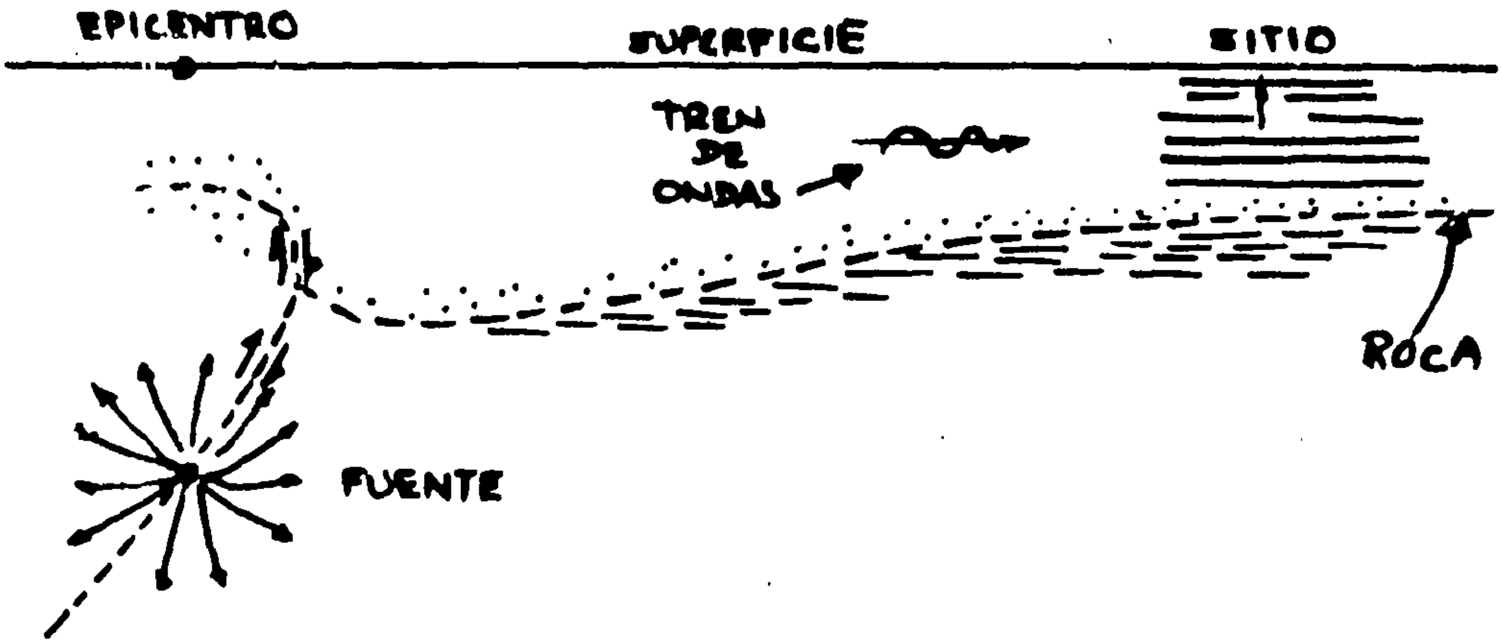
EPICENTRO
SUPERFICIE
SITIO
TREN
DE
ONDAS
ROCA
FUENTE

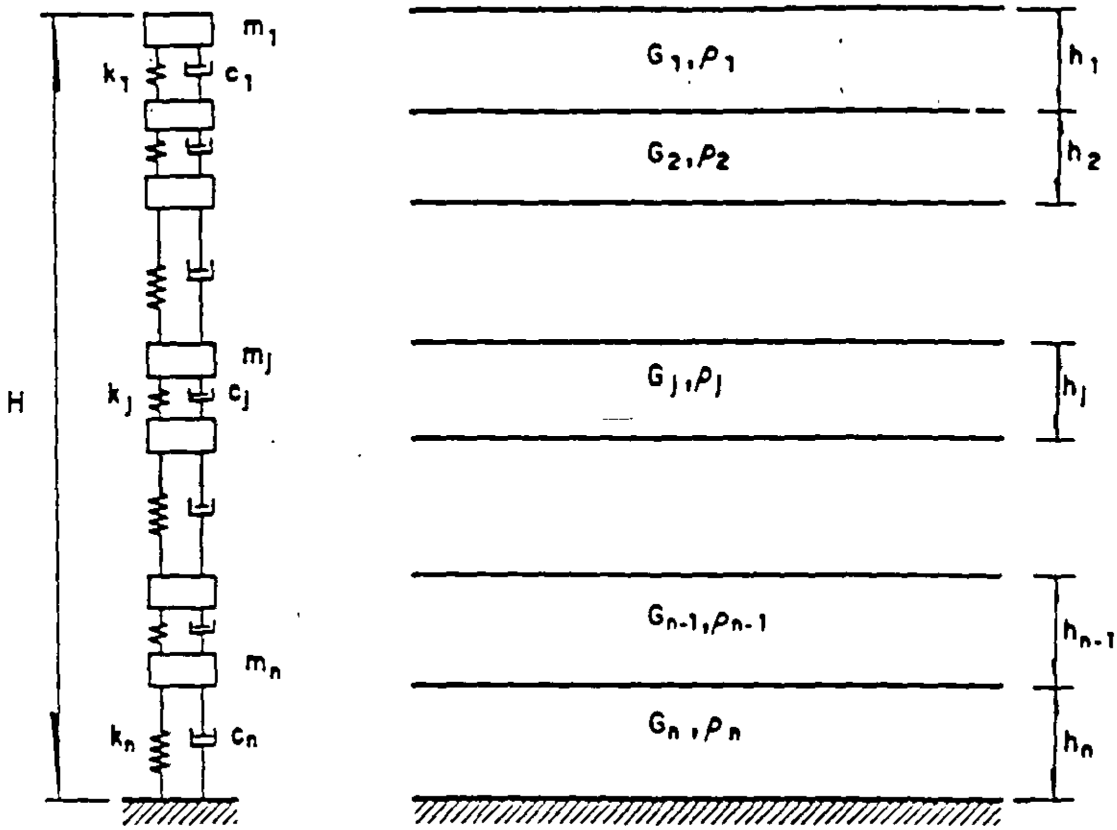

m_1
k_1
c_1
m_j
k_j
c_j
H
m_n
k_n
c_n
G_1, ρ_1
G_2, ρ_2
G_j, ρ_j
G_{n-1}, ρ_{n-1}
G_n, ρ_n
h_1
h_2
h_j
h_{n-1}
h_n

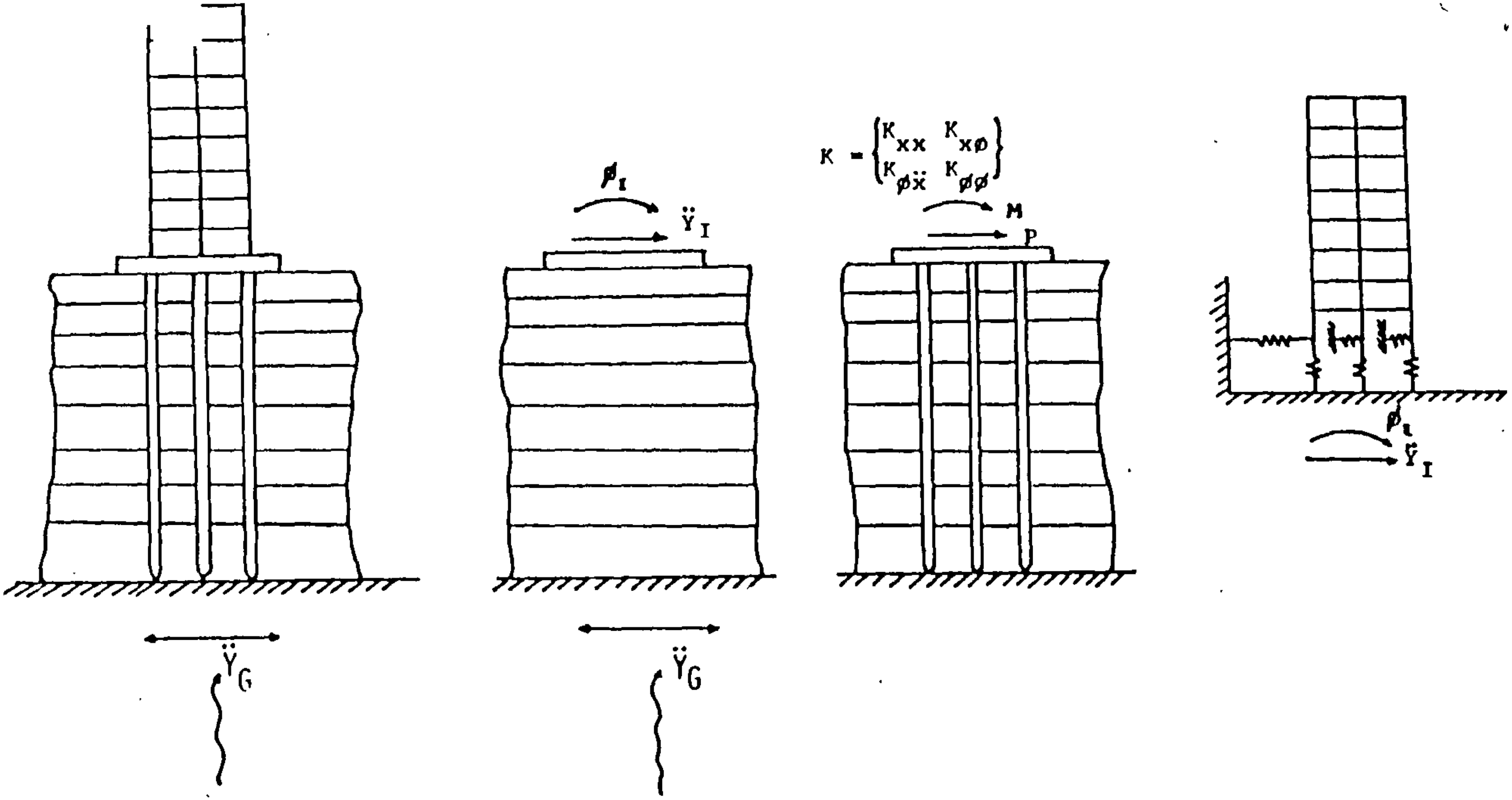

TOTAL SOLUTION   1   +   2   +   3

THE 3-STEP SOLUTION

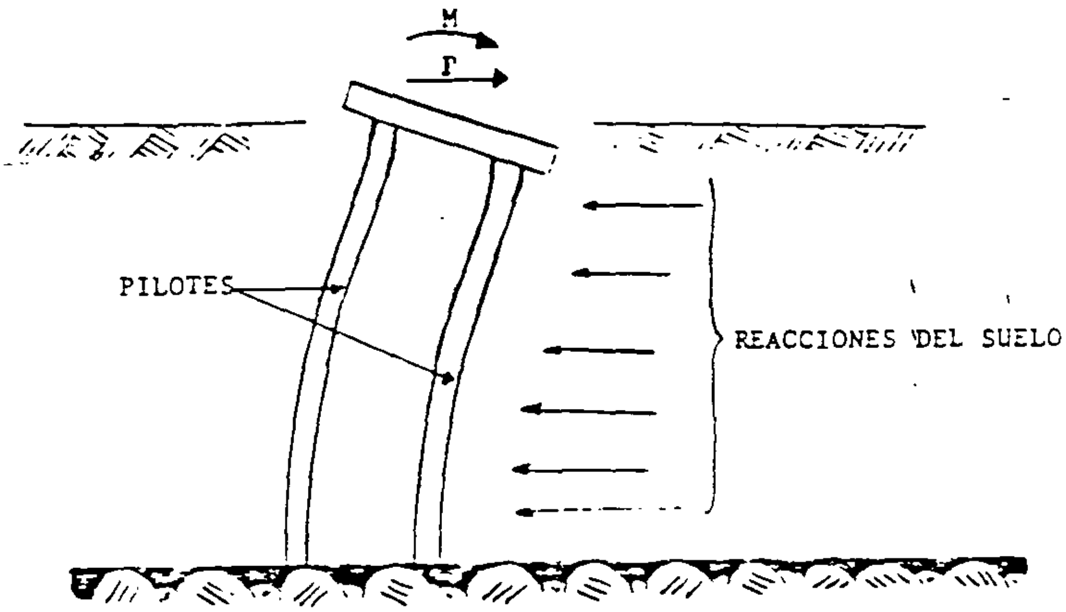

INTERACCION SUELO-PILOTES

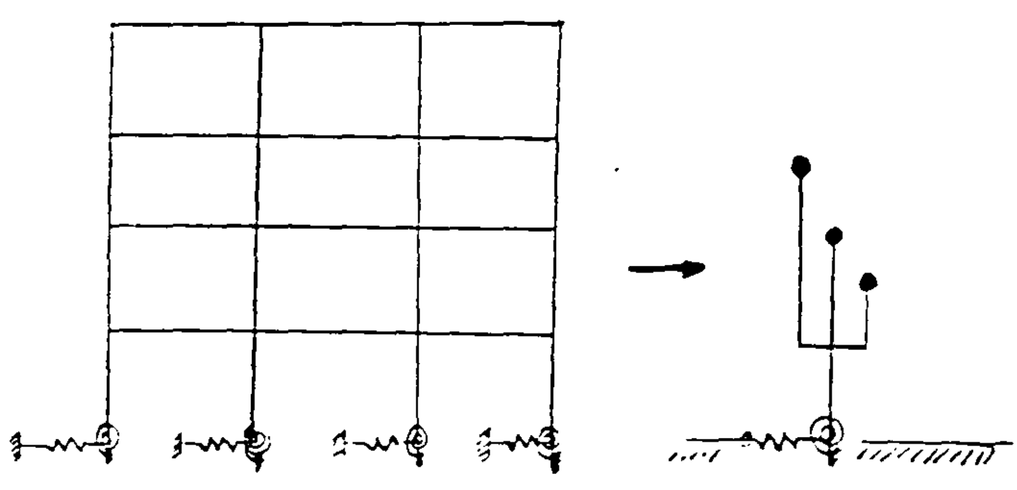

MODELOS DE ANALISIS SIMPLIFICADO

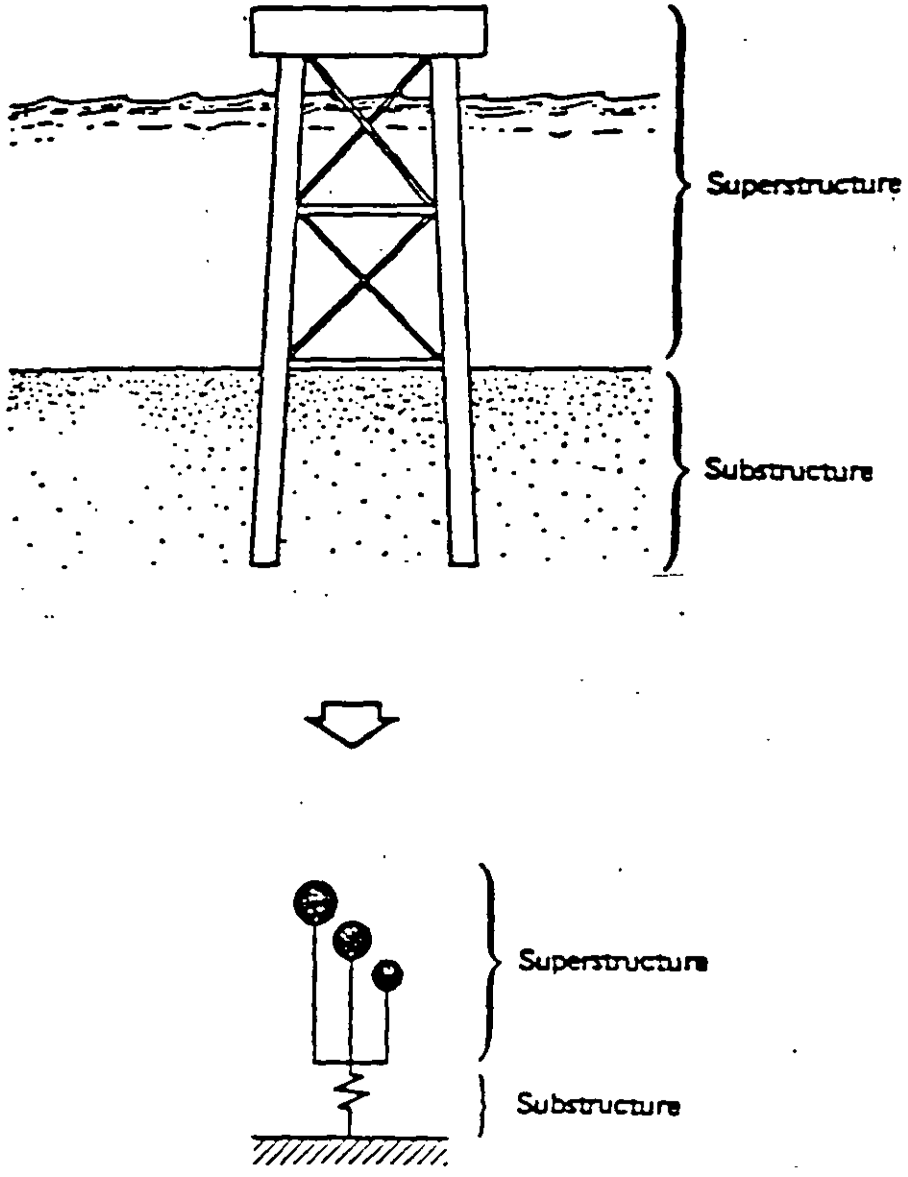

- Analytical Model of Soil-Pile-Structure System

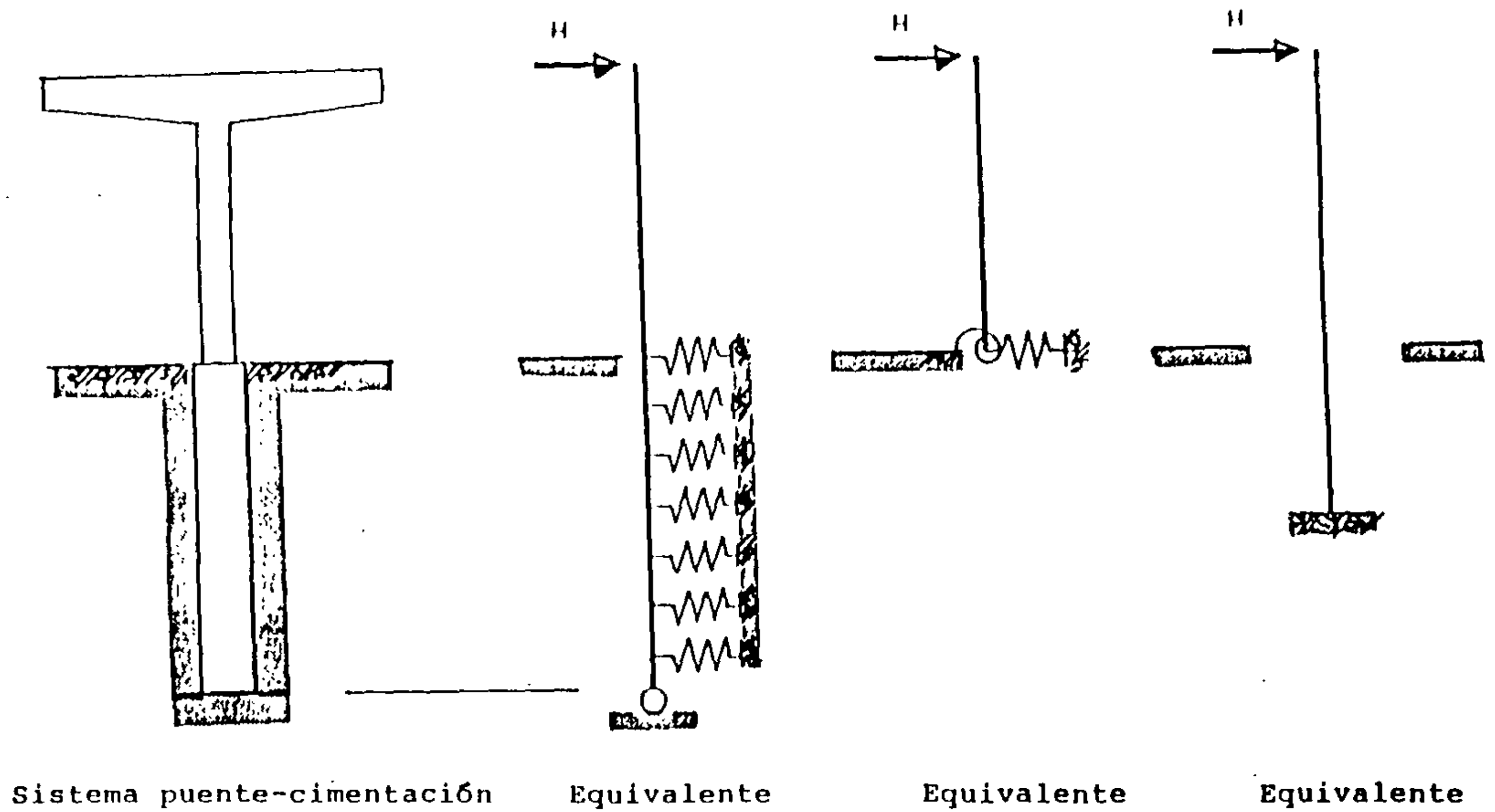

MODELOS PARA REPRESENTAR LA RIGIDEZ DE LA CIMENTACION

k_n = rigidez a compresión del relleno

k_v = rigidez axial de pilotes y suelo

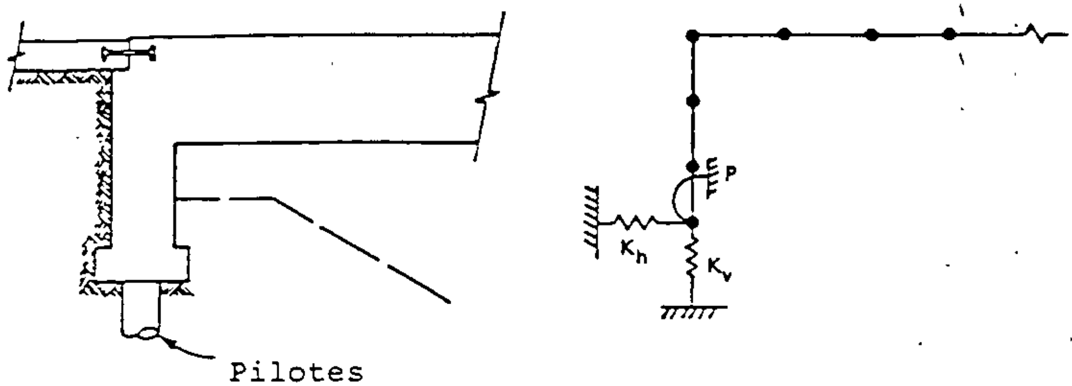

Estribo monolítico

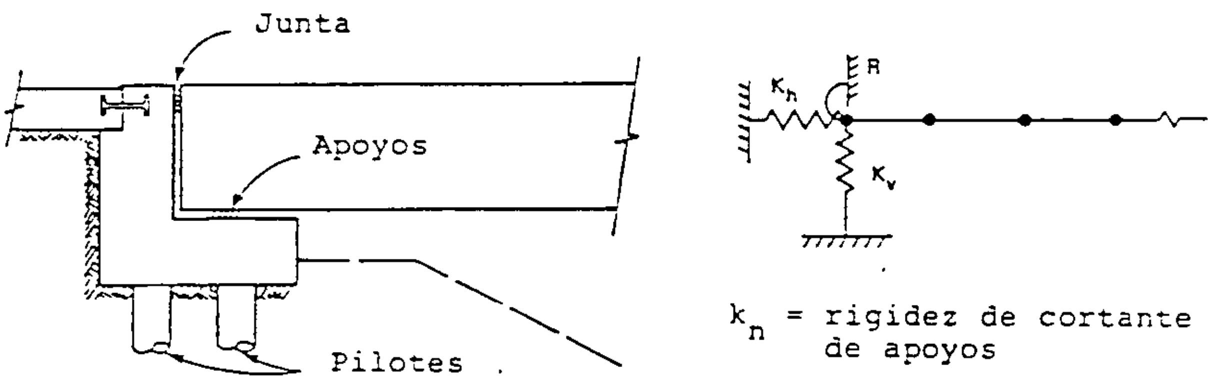

k_n = rigidez de cortante de apoyos

k_v = rigidez axial de pilotes y suelo

Estribo no monolítico

MODELOS DE ESTRIBOS

OBJETIVOS:

1) METODO DE ANALISIS DINAMICO PARA GRUPOS DE PILOTES

2) MATRIZ DE RIGIDECES EN LA CABEZA DEL GRUPO DE PILOTES (FUNCIONES DE IMPEDANCIA)

ANTECEDENTES

INTERACCION SUELO-PILOTE AISLADO

METODOS DE ANALISIS :

1) ESTATICO

1.A) DISCRETOS
1.B) CONTINUOS

2) DINAMICO

2.A) DISCRETOS
2.B) CONTINUOS

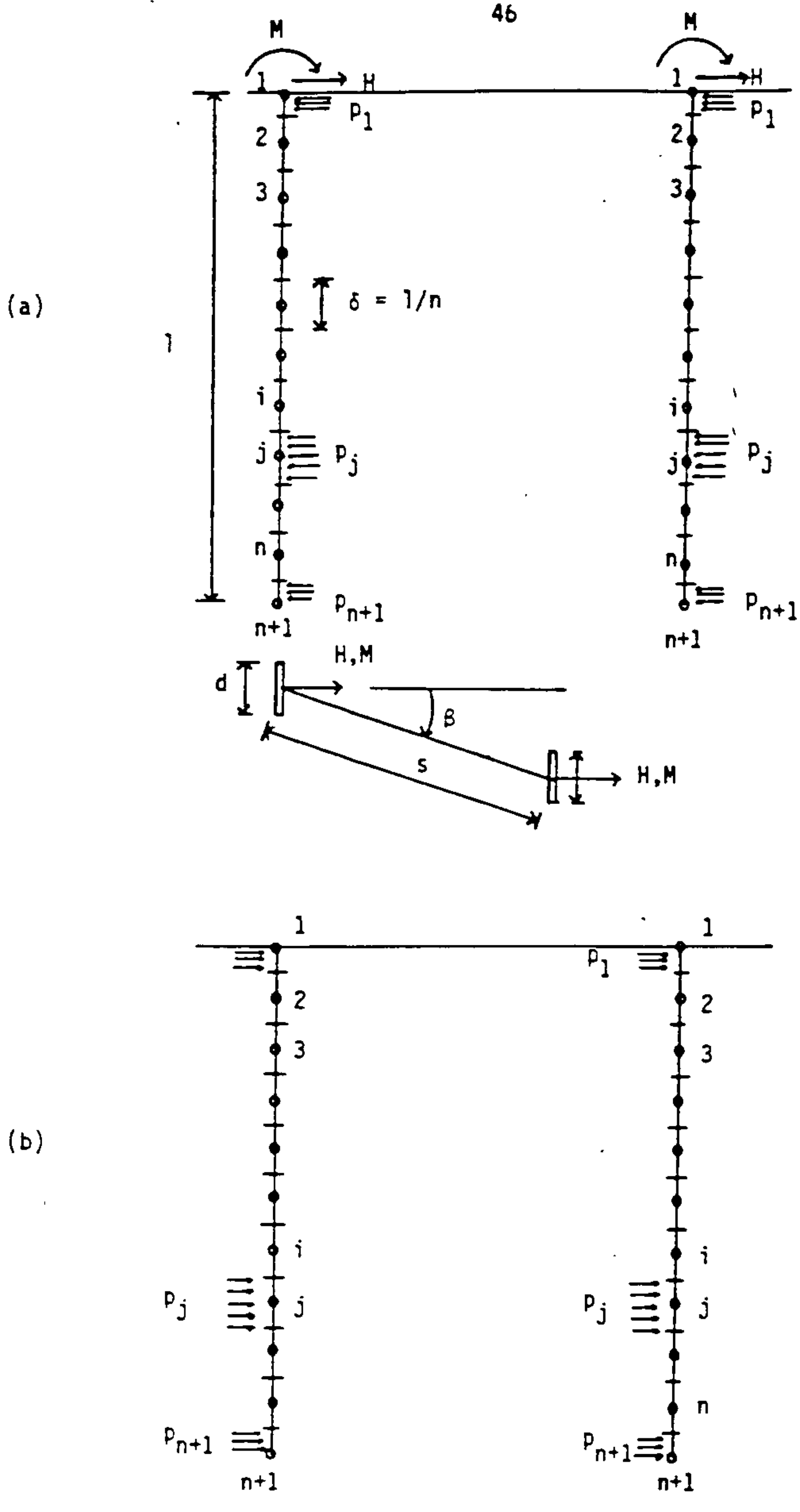

Fig 3.1 (a): Fuerzas y presiones sobre el pilote
(b): Presiones en el suelo

CIMENTACIONES CIRCULARES

TIPO DE MOVIMIENTO	K
TRASLACION VERTICAL	$4GR/(1 - \nu)$
TRASLACION HORIZONTAL	$8GR/(2 - \nu)$
GIRO DE TORSION	$16GR^3 / 3$
GIRO DE FLEXION	$8GR^3 / 3(1 - \nu)$

G = módulo de rigidez al corte del semi-espacio

ν = módulo de Poisson del semi-espacio

R = radio de la zapata

MEX/1

MEXICO

5.1 ESTRUCTURAS TIPO 7. PUENTES

5.1.1 ELECCION DEL TIPO DE ANALISIS

A) METODO SIMPLIFICADO DE ANALISIS

B) ANALISIS ESTATICO

C) ANALISIS DINAMICO

CRITERIOS DE ANALISIS SISMICO - ESTRUCTURAS TIPO 7

3.7.1 Elección del Tipo de Análisis

Para el análisis sísmico de estructuras tipo 7, se puede recurrir a tres métodos: a) método simplificado de análisis, b) método de análisis estático y c) método de análisis dinámico. El método simplificado de análisis que se describe en la sección 3.7.2 solo es aplicable a puentes regulares. Aquellos puentes que posean un cierto grado de irregularidad se analizarán con el método estático, y aquellos puentes aún más irregulares y los puentes especiales, con el método dinámico.

3.7.2 Método Simplificado de Análisis

Este método será aplicable al análisis de aquellos puentes que cumplan con los siguientes requisitos:

a) Que tengan dos o más claros o tramos
b) Que sean rectos y que la longitud de sus tramos sea muy parecida.
c) Que se pueda suponer que los marcos del puente trabajan de manera independiente , tanto en sentido longitudinal como transversal.
d) Que sus claros sean menores de 40 m y el ancho de la calzada sea menor de 30 m.

El método consta esencialmente de los siguientes pasos:

1. Se elige el marco a diseñar.

2. Se obtiene la masa tributaria correspondiente.
3. Se calcula la rigidez lineal del marco en el sentido de análisis.
4. Se obtiene el período fundamental de vibración.
5. Se calcula el valor de c correspondiente al período fundamental de vibración y se define el factor de ductilidad Q del marco.
6. La fuerza lateral equivalente E se obtiene con

$$E = \frac{c}{Q} W \qquad 7.1$$

donde W es el peso de la masa tributaria.

3.7.3 Método de Análisis Estático

Este método será aplicable al análisis de aquellos puentes que cumplan con los siguientes requisitos:

a) Que tengan dos o más claros o tramos
b) Que sean rectos o alojados horizontalmente en curvas de poco grado
c) Que la longitud de sus tramos sea muy parecida.
d) Que la fuerza sísmica se distribuya en todos los marcos resistentes.
e) Que la relación de la rigidez lineal de toda la superestructura y la rigidez transversal de la superestructura sea menor que 2.
f) Que sus claros sean menores de 120 m y el ancho de la calzada no supere los 30 m.

La aplicación de este método se lleva a cabo de la siguiente manera:

1. Se aplica una carga uniforme horizontal de magnitud unitaria, en dirección perpendicular a la superestructura.
2. Se obtienen los desplazamientos y elementos mecánicos resultantes de la aplicación de la carga uniforme.
3. Con base en los desplazamientos calculados en el paso anterior se escala el valor de la carga uniforme para que produzca un

desplazamiento horizontal máximo de 1 cm en la estructura.

4. Se calcula la rigidez lineal total de la estructura multiplicando la longitud por el nuevo valor de la carga uniforme.
5. Se calcula la carga muerta total de la estructura.
6. Se determina el período natural de vibración.
7. Se calcula el valor de c correspondiente al período fundamental de vibración y se define el factor de ductilidad Q de la estructura.
8. La fuerza lateral equivalente (E) se obtiene con

$$E = \frac{c}{Q} W \qquad 7.2$$

donde W es el peso de la carga muerta total.

9. La fuerza E se transforma en una carga uniforme equivalente.

Efectos bidireccionales

Los efectos de ambas componentes horizontales del movimiento del terreno se combinarán tomando, en cada dirección que se analice el puente, el 100% de los efectos de la componente que obra en esa dirección y el 30% de los efectos de la que obra perpendicularmente a ella, con los signos que para cada concepto resulten más desfavorables.

3.7.4 Métodos de Analisis Dinámico

Cuando no se satisfagan los requisitos para aplicar cualquiera de los métodos de análisis estático se emplearán como métodos de análisis dinámico los siguientes:

a) Análisis modal
b) Análisis por integración paso a paso

a) Análisis modal

La participación de cada modo natural de vibración en las fuerzas que actúan sobre la estructura se definirá con base en las aceleraciones espectrales de diseño reducidas de acuerdo como se indica en el capítulo 3.

Las respuestas modales S_i (donde S_i puede ser fuerza cortante, fuerza axial, desplazamiento lateral, momento flexionante, etc.), se combinarán para calcular las respuestas totales S de acuerdo con la expresión

$$S = (\Sigma S_i^2)^{1/2} \qquad 7.3$$

b) Análisis paso a paso

Si se emplea este método, podrá acudirse a acelerogramas de temblores reales o de movimientos simulados, o combinaciones de estos siempre y cuando sus intensidades y duraciones sean compatibles con lo especificado en el capítulo 3.

Efectos bidireccionales

Cualquiera que sea el método de análisis dinámico que se emplee, los efectos de movimientos horizontales del terreno en direcciones ortogonales, se combinarán como se especifica en relación con el método de análisis estático.

3.7.5 Estados Limite de Servicio

Además del cálculo de las longitudes de apoyo y holguras para tener en cuenta los efectos por cambios de temperatura, fluencia y contracción del concreto, se deben calcular las longitudes de apoyo para tomar en cuenta los efectos del sismo.

Longitud de apoyo

La longitud mínima de apoyo D (en mm), de las trabes o tableros sobre la subestructura se calculará como sigue

$$D = 254 + 2.08L + 8.35H \qquad 7.4$$

donde L es : a) la longitud, en metros, entre dos apoyos adyacentes; b) la longitud entre el apoyo y la junta de expansión más cercana; o, c) la suma de las longitudes a los lados de una articulación dentro de un claro; H es : a) la altura de la pila, en metros, cuando está formada por una o varias columnas; b) la altura promedio de las columnas o pilas más cercanas, si se trata de una junta de expansión; o, c) la altura promedio de las columnas entre el estribo y la junta de expansión más cercana que soporta la superestructura, si se trata de un estribo; H=0 para puentes de un solo tramo.

Movimientos relativos

Además de los efectos anteriores, los puentes deben ser diseñados para soportar los efectos de movimientos relativos ocasionados por los mismos movimientos sísmicos o por fallas del terreno.

3.7.6 Interaccion Suelo-Estructura

Como una aproximación a los efectos de la interacción suelo-estructura será valido incrementar el período fundamental de vibración y los desplazamientos calculados en el puente bajo la hipótesis de que éste se apoya rígidamente en su base, de acuerdo con las expresiones reportadas en el capítulo 6.

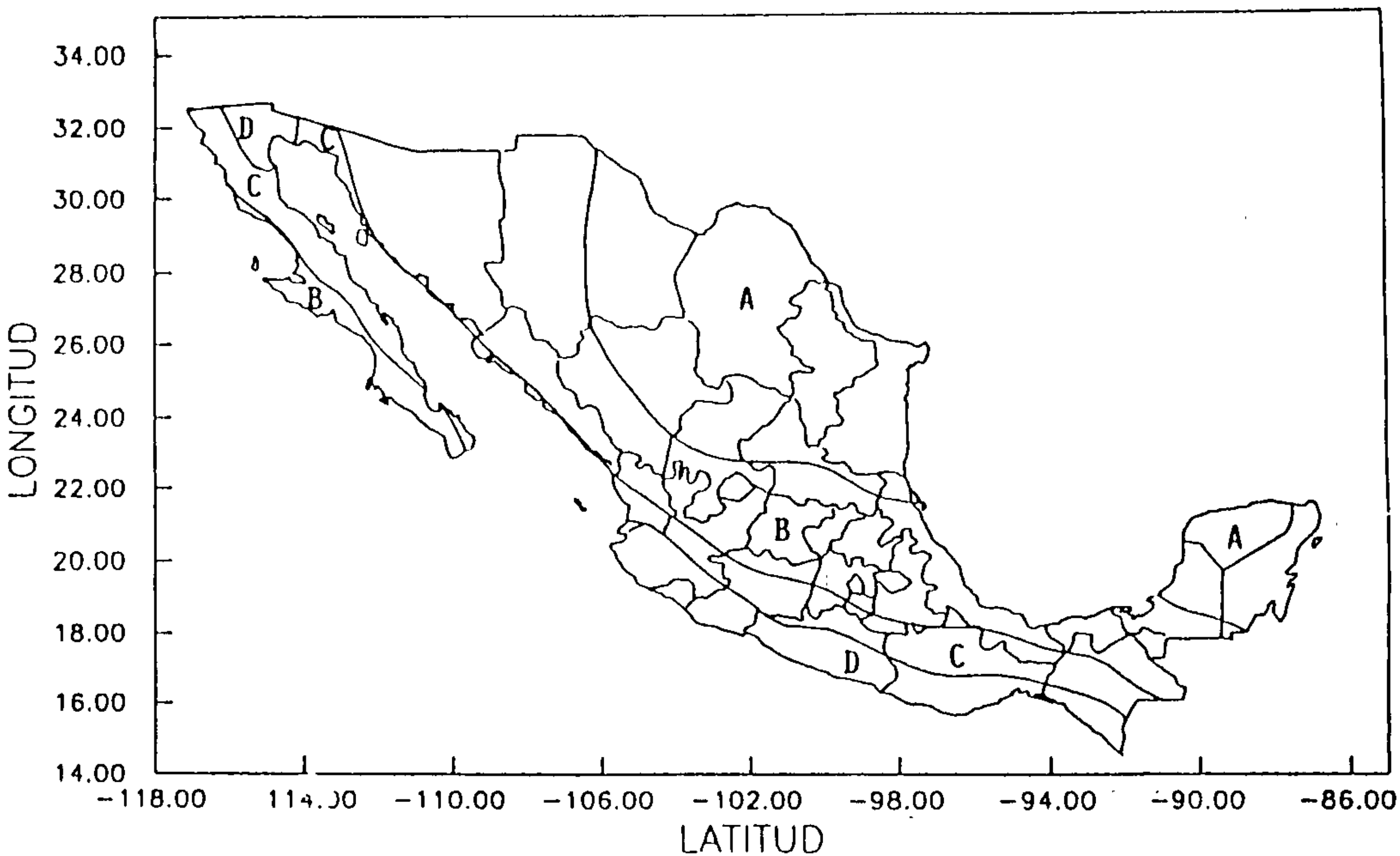

Regionalización sísmica de la República Mexicana

Tabla 3.1 Espectros de diseño para estructuras del grupo B

Zona sísmica	Tipo de suelo	a_0	c	T_a(s)	T_b(s)	r
A	I II III	0.02 0.04 0.05	0.08 0.16 0.20	0.2 0.3 0.6	0.6 1.5 2.9	1/2 2/3 1
B	I II III	0.04 0.08 0.10	0.14 0.30 0.36	0.2 0.3 0.6	0.6 1.5 2.9	1/2 2/3 1
C	I II III	0.36 0.64 0.64	0.36 0.64 0.64	0.0 0.0 0.0	0.6 1.4 1.9	1/2 2/3 1
D	I II III	0.50 0.86 0.86	0.50 0.86 0.86	0.0 0.0 0.0	0.6 1.2 1.7	1/2 2/3 1

$$a = a_0 + \left(c - a_0 \right) \frac{T}{T_a}; \quad \text{si } T < T_a \tag{3.1}$$

$$a = c; \quad \text{si } T_a \leq T \leq T_b \tag{3.2}$$

$$a = c \left[\frac{T_b}{T} \right]^r; \quad \text{si } T > T_b \tag{3.3}$$

a_0 = coeficiente de aceleración del terreno

T = periodo natural de interés

r = exponente

c = coeficiente sísmico

MEX/2

A) METODO SIMPLIFICADO DE ANALISIS

HIPOTESIS: LOS MARCOS DEL PUENTE TRABAJAN DE MANERA INDEPENDIENTE

LA FUERZA SE CALCULA CON BASE EN UN CRITERIO DE AREAS TRIBUTARIAS

i) SE CALCULA LA RIGIDEZ TRANSVERSAL DEL MARCO EN EL SENTIDO DE ANALISIS

(K)

ii) SE OBTIENE LA CARGA MUERTA TRIBUTARIA

(W)

iii) SE OBTIENE EL PERIODO NATURAL DE VIBRACION

$$T = 2\pi \sqrt{\frac{W}{gK}} = 2\pi \sqrt{\frac{M}{K}}$$

MEX/2-a

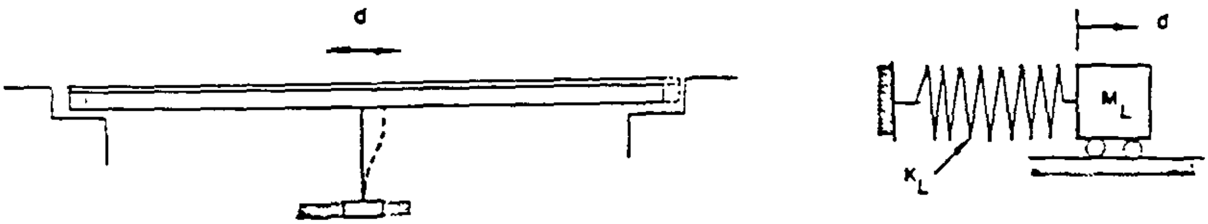

K_L = rigidez en la dirección longitudinal

M_L = masa total de la superestructura

MODELO EQUIVALENTE PARA ANALISIS LONGITUDINAL

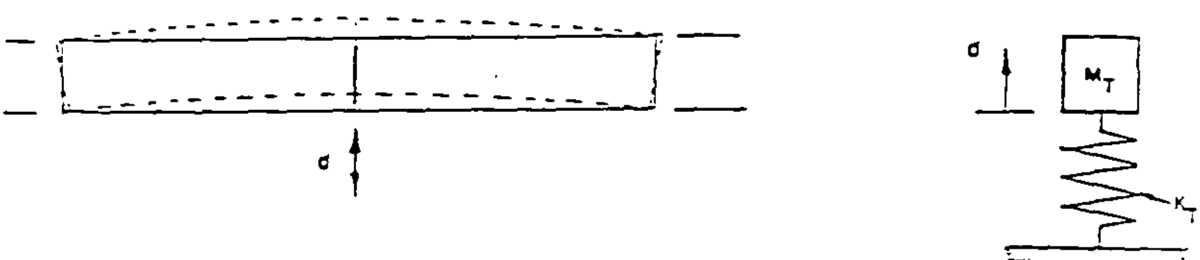

K_T = rigidez equivalente en la dirección transversal

M_T = masa equivalente en la dirección transversal

MODELO EQUIVALENTE PARA ANALISIS TRANSVERSAL

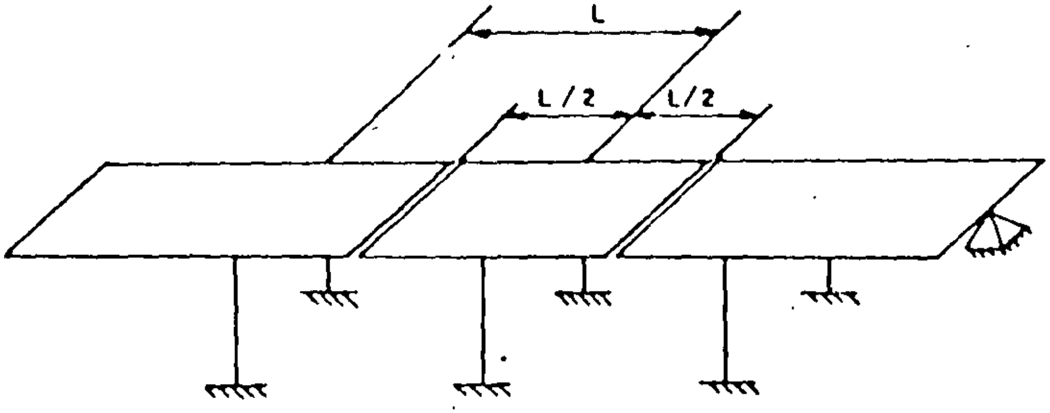

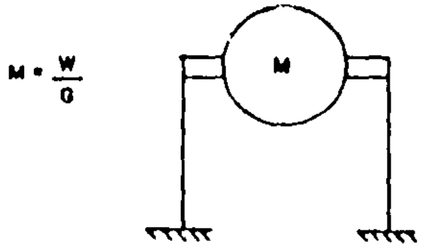

IDEALIZACION DE LA ESTRUCTURA

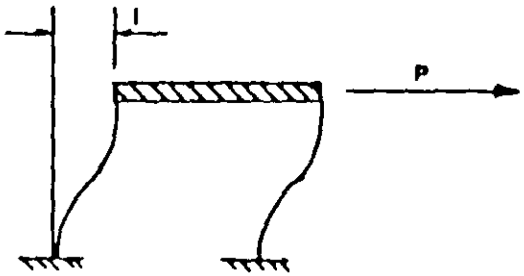

RIGIDEZ DE LA ESTRUCTURA

METODO SIMPLIFICADO DE ANALISIS

B) ANALISIS ESTATICO. METODO DE LA CARGA UNIFORME

- SE TOMA EN CUENTA LA CONTINUIDAD DE LA ESTRUCTURA
- LA FUERZA SISMICA SE DISTRIBUYE ENTRE TODOS LOS ELEMENTOS DEL PUENTE

i) SE APLICA UNA CARGA UNIFORMEMENTE DISTRIBUIDA (Q) EN EL SENTIDO DE ANALISIS

ii) SE DETERMINAN LOS DESPLAZAMIENTOS Y ELEMENTOS MECANICOS ORIGINADOS POR LA CARGA

iii) SE DETERMINA UN FACTOR DE AJUSTE DE TAL MANERA QUE EL MAXIMO DESPLAZAMIENTO PROVOCADO POR Q SEA 1 (K)

iv) SE MULTIPLICA LA CARGA Q (YA AFECTADA POR EL FACTOR DE AJUSTE) POR LA LONGITUD DE LA ESTRUCTURA (K)

v) SE DETERMINA EL PESO TOTAL DE LA SUPERESTRUCTURA (W)

vi) SE OBTIENE EL PERIODO NATURAL DE VIBRACION

$$T = 2\Pi \sqrt{\frac{W}{gK}}$$

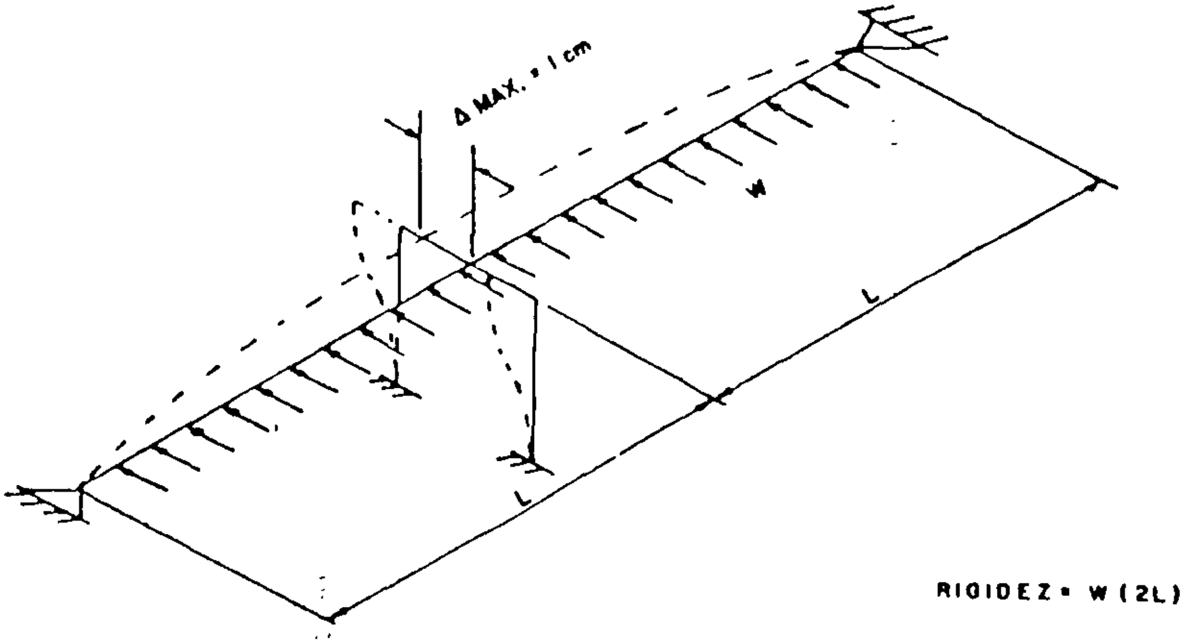

METODO DE LA CARGA UNIFORME

III x/5

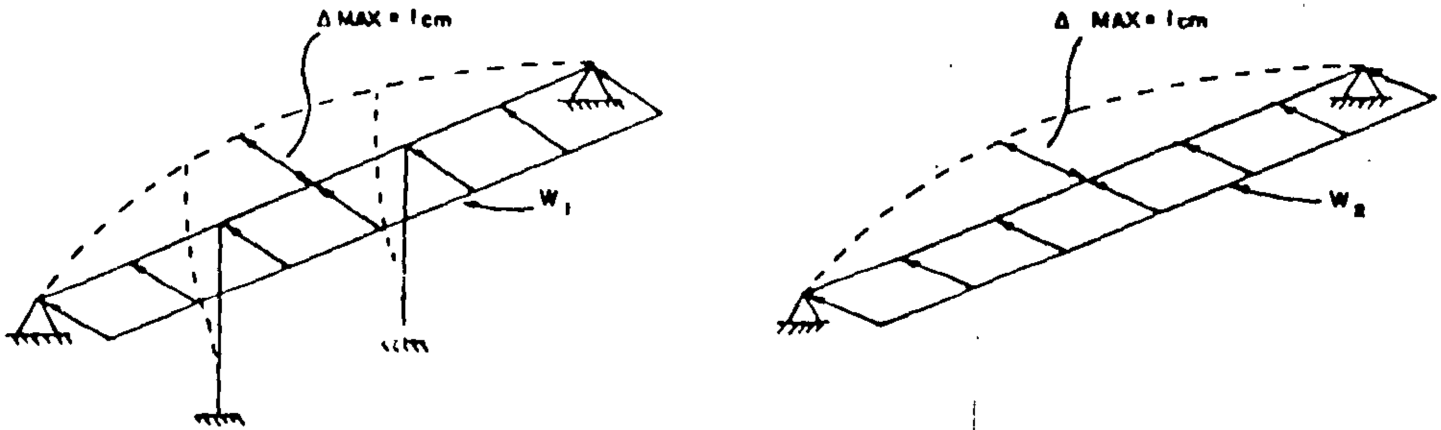

$$\text{INDICE DE RIGIDEZ} = \frac{W_1}{W_2}$$

MEX/7

B) ANALISIS ESTATICO. METODO DE LA COORDENADA GENERALIZADA

i) SE SUPONE EL MODO FUNDAMENTAL DE VIBRACION (LONGITUDINAL Y TRANSVERSAL)

ii) SE EXPRESA EL MODO FUNDAMENTAL EN FUNCION DE UN DESPLAZAMIENTO GENERALIZADO.

iii) SE DEFINE LA PARTE DE LA SUPERESTRUCTURA QUE SE CONSIDERARA EN EL ANALISIS

iv) SE CALCULA EL PESO DE LA PARTE ELEGIDA DE LA SUPERESTRUCTURA (W)

v) SE DETERMINA LA RIGIDEZ DE LOS MIEMBROS VERTICALES QUE SOPORTAN LA PARTE ELEGIDA DE LA SUPERESTRUCTURA (K)

vi) SE OBTIENE EL PERIODO NATURAL DE VIBRACION

$$T = 2\pi \sqrt{\frac{W}{gK}}$$

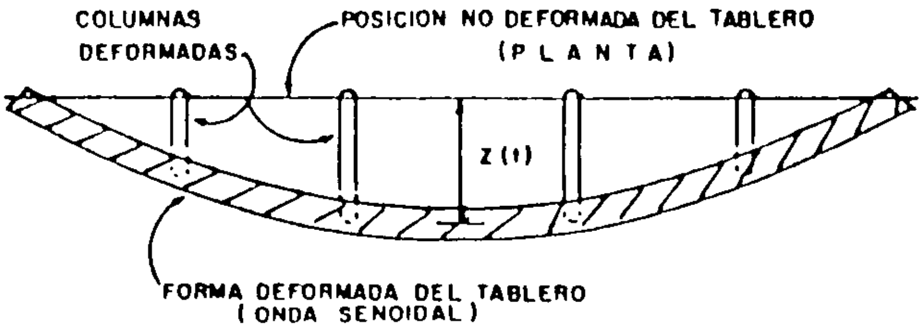

FORMA MODAL SUPUESTA

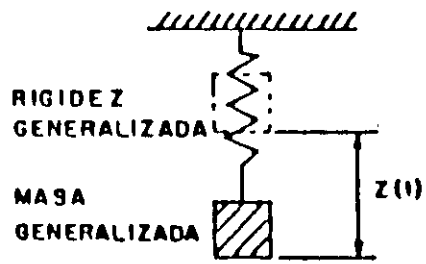

SISTEMA GENERALIZADO DE UN GRADO DE LIBERTAD

METODO DE LA COORDENADA GENERALIZADA
(TRANSVERSAL)

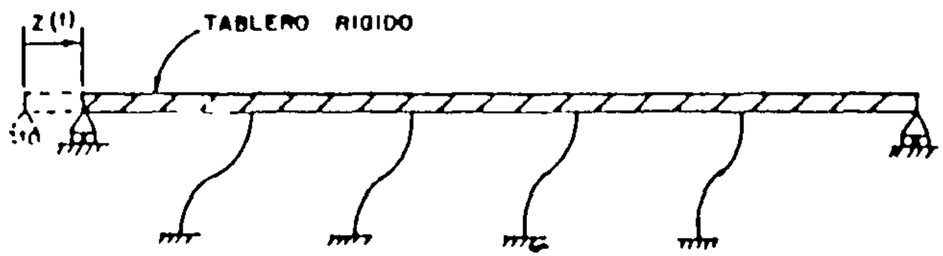

FORMA MODAL SUPUESTA

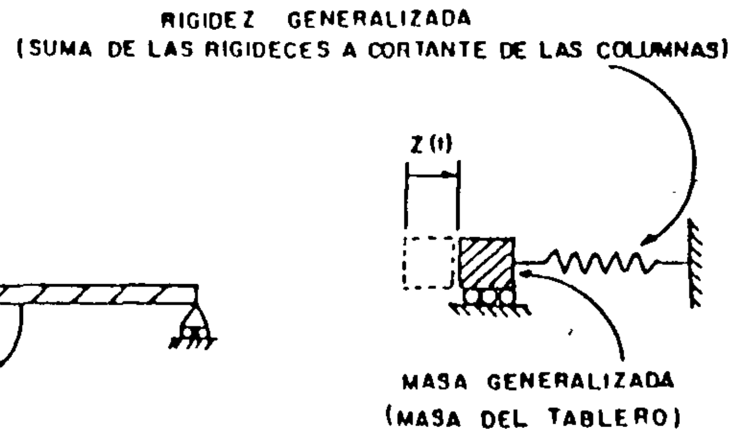

SISTEMA GENERALIZADO
DE UN GRADO DE LIBERTAD

METODO DE LA COORDENADA GENERALIZADA
(LONGITUDINAL)

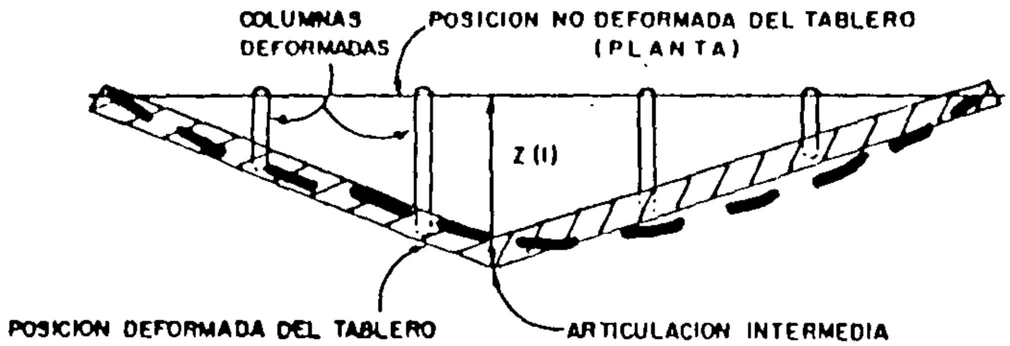

FORMA MODAL SUPUESTA

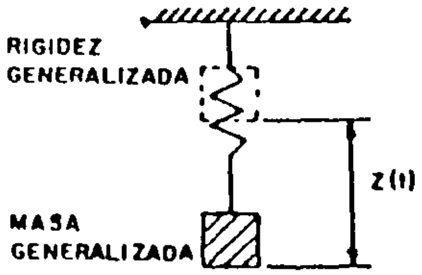

SISTEMA GENERALIZADO DE UN GRADO DE LIBERTAD

c) ANALISIS DINAMICO

- ANALISIS MODAL ESPECTRAL
- ANALISIS PASO A PASO

DISEÑO SISMICO DE PUENTES

TEMA 6 COMPORTAMIENTO SISMICO DE PUENTES CON ELEMENTOS DISIPADORES DE ENERGIA

Profesor : Ing. Marcos García Kong
Instituto de Ingeniería, UNAM

MEXICO, 1998

periodo de vibración aumenta, se reduce el cortante basal. Sin embargo, como se puede notar, la flexibilidad proporcional adicional que se necesitó para incrementar el periodo da origen a mayores desplazamientos (fig. 1.3).

1.2 Disipación de energía

Los desplazamientos relativos generados pueden ser controlados si se introduce un amortiguamiento adicional a la estructura. Esto puede verse en la figura 1 4, así como el efecto de suavización de la curva para un mayor amortiguamiento.

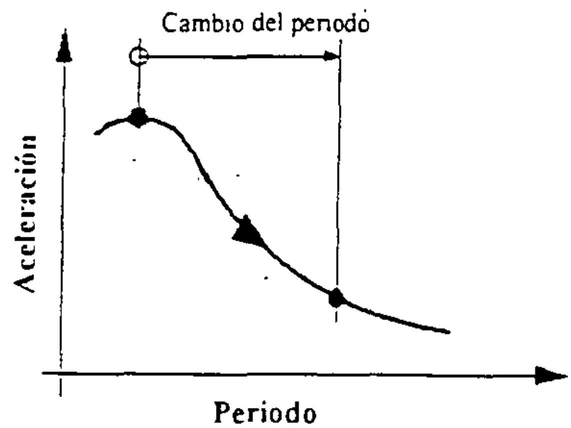

Figura 1 2 Curva idealizada del espectro de respuesta de aceleraciones

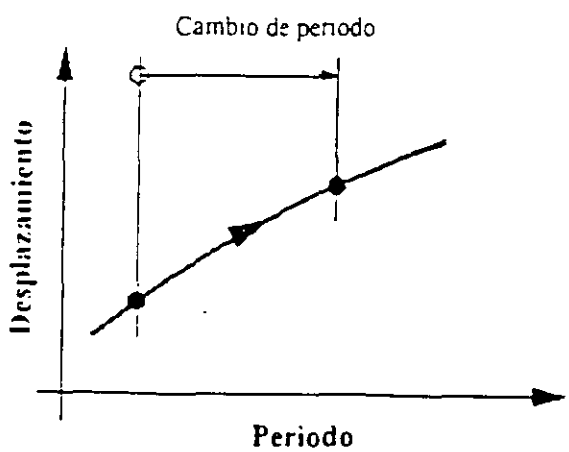

Figura 1 3 Curva idealizada del espectro de respuesta de desplazamientos

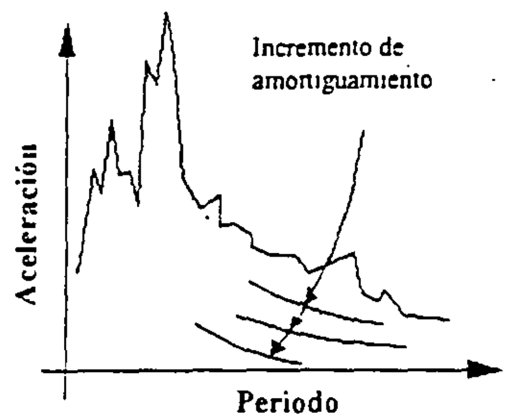

Figura 1 4 Espectro de respuesta para diferentes niveles de amortiguamiento

Uno de los medios más efectivos de proveer un sustancial nivel de amortiguamiento es la disipación de energia por histéresis [ref 1]. En la figura 1.5 se muestra una curva idealizada fuerza desplazamiento, donde el área encerrada es una medida de la energía disipada durante un ciclo de movimiento Para puentes se han desarrollado varios dispositivos mecánicos, de acero suave o plomo, los cuales pueden lograr este tipo de comportamiento.

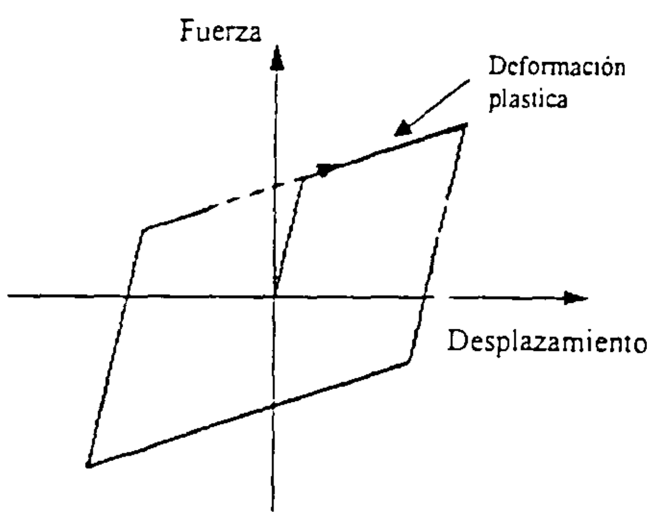

Figura 1 5 Curva de histéresis idealizada

1.3 Rigidez bajo cargas laterales pequeñas

Mientras que una flexibilidad lateral es altamente deseable para cargas sísmicas, es claro que no es recomendable tener un sistema estructural que vibre perceptiblemente bajo cargas que ocurren frecuentemente tales como las producidas por sismos pequeños o cargas de viento. Los mecanismos disipadores de energía proveen de una rigidez y amortiguamiento aceptables deseada para resistir estas cargas (de servicio), en virtud de la alta rigidez elástica que poseen y de su capacidad para disipar energía (Fig 1.5). De este modo las deflexiones son minimizadas.

2. MECANISMOS DE DISIPACIÓN DE ENERGÍA PARA PUENTES

2.1 Introducción.

A partir de 1970 se diseñaron varios tipos de dispositivos disipadores de energia, a los cuales se les han hecho un gran número de pruebas en laboratorio para conocer sus propiedades físicas [ref. 2]. Con base en el material empleado para la deformación plástica estos dispositivos pueden dividirse en dos categorías: disipadores histeréticos de acero y disipadores histeréticos de plomo.

2.2 Disipadores histeréticos de acero.

El acero fue el primer material utilizado para construir mecanismos disipadores de energia. Su elección se basó ya que era un material utilizado comúnmente en las estructuras y por lo tanto no presentaban problemas inusuales de diseño, construcción o mantenimiento, aparte de las posibles fallas en las soldaduras y concentraciones de esfuerzos. Principalmente, se ha utilizado el acero suave, ya sea el estándar británico 4360/43A o el estándar australiano CS 10308 ó CS 10208 [ref. 3], los cuales tienen esencialmente la misma composición química. Entre los mecanismos de esta categoria se encuentran los siguientes:

2.2.1 Viga torsional (fig. 2.1)

La sección rectangular sólida es de acero suave y generalmente tiene una longitud variable de 500 mm a 1 m. Estos dispositivos se anclan en sus extremos sujetándolos a una base fija del puente mediante tornillos a cortante y sus brazos cargadores se unen a la superestructura, de modo que se generan momentos flexionantes relativos entre los brazos cargadores en cada extremo de la viga en una direccion y el centro de la viga en la otra dirección, los cuales inducen torsión en la viga. La energia es disipada por los ciclos de deformación plástica torsional [ref. 3].

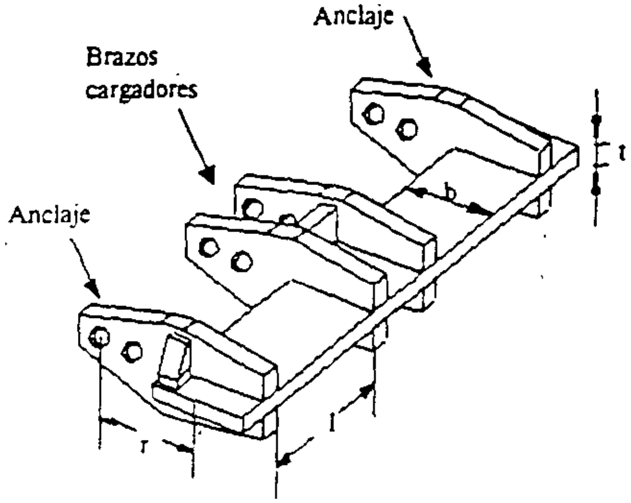

Figura 2.1 Viga torsional.

2.2.2 Viga a flexión (fig. 2.2)

Se compone de una viga corta vertical en cantiliver, de sección cuadrada o circular, la cual es plásticamente deformada primariamente a flexión y que opera para movimientos relativos en cualquier dirección horizontal. [ref 4] Esta viga se coloca debajo de la superestructura en los estribos, como se muestra en la figura 2.3

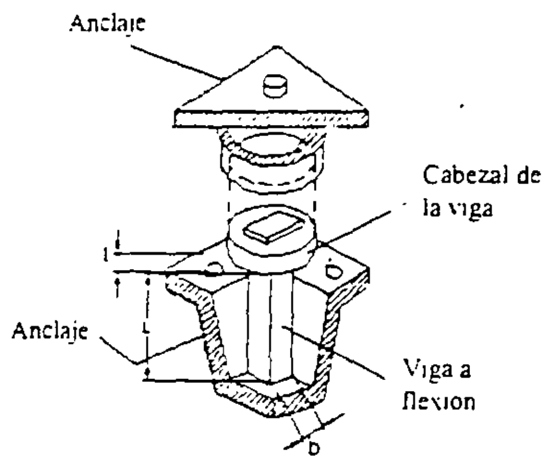

Figura 2.2 Viga a flexión

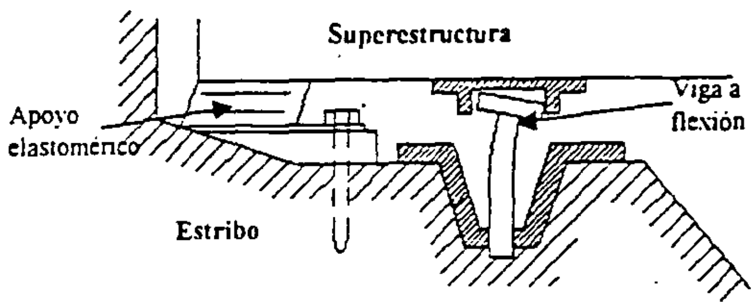

Figura 2.3 Colocación de la viga a flexión

A pesar de las propiedades de disipación de estos dos mecanismos, se tienen grandes desventajas, como su relativa dificultad de colocación, además de que estos mecanismos requieren de un amortiguador que disminuya los desplazamientos inducidos por estos 3

2.3 Disipadores histeréticos de plomo.

La investigación en el uso de la capacidad de deformación plástica del plomo para disipadores histeréticos comenzó en 1971 con la invención del mecanismo de extrusión. Las razones de la elección del plomo son fluye a esfuerzos relativamente pequeños, cercanos a 10 Mpa., y su comportamiento se aproxima a un sólido plástico lineal. Por otro lado, la deformación plástica del plomo a 20° centigrados es equivalente a la deformación plástica del acero a una temperatura mayor que 400° centigrados; por lo tanto, el plomo se comporta adecuadamente bajo condiciones de fatiga durante los ciclos de deformaciones plásticas

2.3.1 Mecanismos de extrusión de plomo (fig. 2.4)

Los momentos relativos entre el pistón y el cilindro, expulsan el plomo encerrado a través de un orificio en el cilindro La energia es disipada durante ciclos de deformación por extrusión del plomo a través del orificio hacia atrás y adelante Cuando el plomo es extruido, éste se recristaliza inmediatamente, restaurándose sus propiedades mecánicas originales

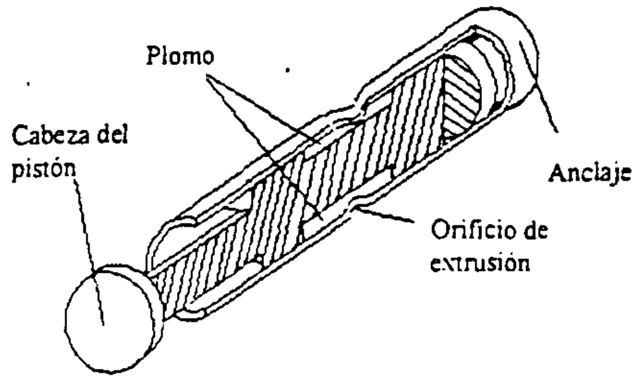

Figura 2 4 Mecanismo de extrusión de plomo

2.3.2 Apoyo elastomérico con centro de plomo (fig. 2.5)

Este mecanismo se compone de un apoyo elastomérico reforzado (placas de acero intercaladas) con un centro de plomo cilíndrico insertado a presión. Cuando el mecanismo es deformado en cortante bajo una carga sísmica, el plomo tiene una deformación plástica, de modo que la energia es disipada.

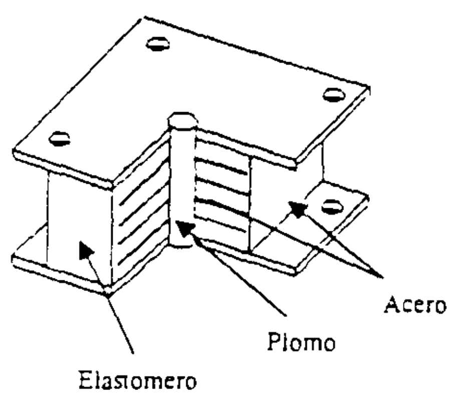

Figura 2 5 Apoyo elastomérico con centro de plomo

Los apoyos elastoméricos son muy utilizados en estructuras de puentes, ya que resultan ser un mecanismo muy practico· pueden acomodar los movimientos provocados por flujo plástico del concreto, asi como la expansión térmica del mismo, además absorben impactos de los automóviles y permiten giros por carga viva; además de que resultan muy económicos, en comparación con cualquier otro sistema de apoyo y requieren de poco mantenimiento.

El hule natural o sintético (neopreno), tiene insertadas varias placas de acero las que tienen para 3 funciones principales:

a) soportar el peso de la estructura
b) proveer de elasticidad que puede sobrepasar el punto de fluencia y
c) dar confinamiento al núcleo de plomo.

Si a estos apoyos se les incorpora un centro de plomo, este permite disipar energia durante la acción de un sismo, además de que aumenta la rigidez para soportar los efectos de cargas estáticas. El resultado es un sistema disipador de energia compacto.

El centro de plomo se deforma plásticamente y disipa energia. Este tiene dos efectos en la respuesta de un puente: el primero, es que cambia la rigidez de la estructura, resultando generalmente en un incremento del periodo natural, y el segundo, es que incrementa el amortiguamiento debido a las propiedades histeréticas de la deformación inelástica.

Este apoyo es diseñado para resistir en el rango elástico niveles bajos de cortante (como los producidos por cargas de viento) con una rigidez inicial alta (Ku) hasta que se alcanza un nivel defluencia determinado por la resistencia caracteristica (Q), la cual depende del diámetro del centro de plomo. La rigidez en la post-fluencia (Kd) es mantenida en un minimo para asegurar una buena disipación de energia y una rigidez baja de la estructura durante una carga sismica más severa. La curva de histéresis bilineal formada por estas dos rigideces (fig 2.6) tiene una forma estable y un área encerrada grande, demostrando las propiedades de disipación de energia

Dependiendo de la magnitud y orientación de las cargas aplicadas, estos apoyos pueden tener varios grados de rigidez

1) Una alta rigidez vertical que permite soportar cargas estáticas con una deflexión vertical mínima. Esta rigidez la proporcionan las placas laminadas, ya que estas disminuyen el pandeo de las caras laterales de los apoyos por la adherencia entre los dos materiales.

2) Una baja rigidez horizontal ante cargas sismicas. Esto hace que el apoyo funcione como disipador sismico; su rigidez lateral depende de las propiedades del elastómero

3) Una alta rigidez horizontal para controlar cargas laterales pequeñas debidas a viento o para evitar deflexiones laterales grandes bajo condiciones de servicio.

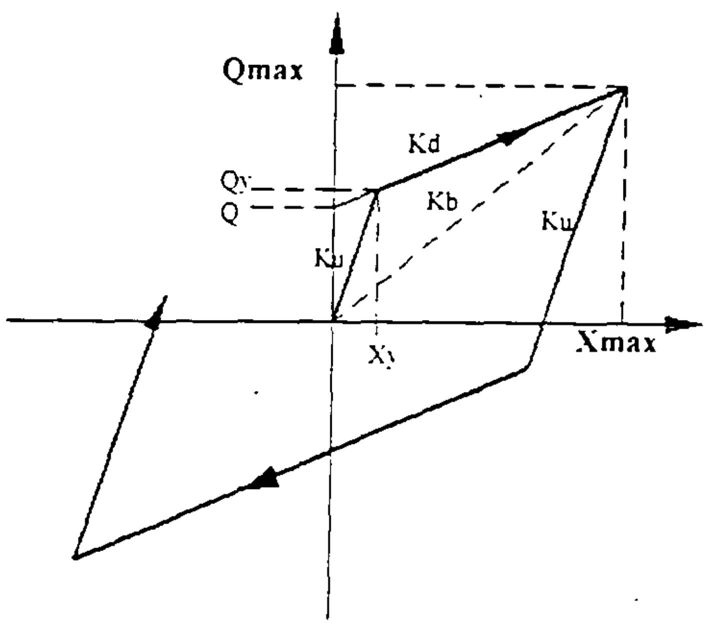

Figura 2.6 Modelo bilineal de histéresis

Donde

Q = Resistencia caracteristica

Qy = Fuerza cortante de fluencia

Qmax = Fuerza máxima

Kd = Rigidez en la postfluencia

Ku = Rigidez elástica (carga y descarga)

Kb = Rigidez secante del aislador = $Qmax / Xmax$

Xy = Desplazamiento en la fluencia

$Xmax$ = Máximo desplazamiento

La determinación de la curva carga – deformación de estos dispositivos es de primordial importancia para definir modelos elásticos e inelásticos de estructuras provistas con este tipo de elementos.

De pruebas experimentales para medir los ciclos de carga – deflexión del apoyo elastomérico con centro de plomo [ref. 5], se encontró que una descripción razonable del ciclo de histeresis es un sólido bilineal con las siguientes caracteristicas:

$$Ku = 10\ Kb(r) \qquad \text{ec.2.1}$$

$$Kd = Kb(r) \qquad \text{ec. 2.2}$$

$$Kb(r) = G\ A / h \qquad \text{ec 2.3}$$

$$Qy = \tau(Pb)\ A' \qquad \text{ec. 2.4}$$

$$Xy = \tau(Pb)\ A(Pb) / Kb(r) \qquad \text{ec 2.5}$$

En estas ecuaciones, G es el módulo de cortante del elastómero, A es el área del apoyo elastomérico, h es la altura total del apoyo elastomérico, $\tau(Pb)$ representa el esfuerzo cortante de fluencia del plomo (aproximadamente 10 Mpa), A´ denota el área a cortante del centro de plomo, Ab es el área transversal del centro de plomo y Kb(r) es la rigidez del elastómero en un plano horizontal

Se encontró además que la fuerza horizontal F, requerida para deformar al apoyo horizontalmente puede ser considerada como equivalente a dos fuerzas actuando en paralelo: la primera debida a la elasticidad del elastómero y la segunda debida a la plasticidad del plomo. La elasticidad del elastómero resulta en una fuerza que es proporcional al desplazamiento mientras que la plastificación requiere una fuerza que es independiente del desplazamiento. Por lo tanto, una buena aproximación resulta ser:

$$F = \tau(Pb)\, A(Pb) + Kb(r)\, X \qquad \text{ec. 2.6}$$

donde X es el desplazamiento relativo de la parte superior con la parte inferior del elastómero. De esta fórmula puede verse entonces la gran dependencia del tamaño del centro de plomo con la fuerza F, con lo que el tamaño del centro de plomo puede ser usado como una variable adicional del diseño, para obtener las características deseadas del sistema disipador.

Los efectos conceptuales de las variaciones geométricas tanto del centro de plomo como del elastómero se resumen en la figura 2 7. El tamaño del centro de plomo es proporcional a la fuerza de fluencia del aislador, mientras que la rigidez en la post-fluencia es proporcional a la rigidez del elastómero, por lo tanto, incrementa cuando el tamaño en planta del apoyo elastomérico incrementa y cuando su altura decrece.

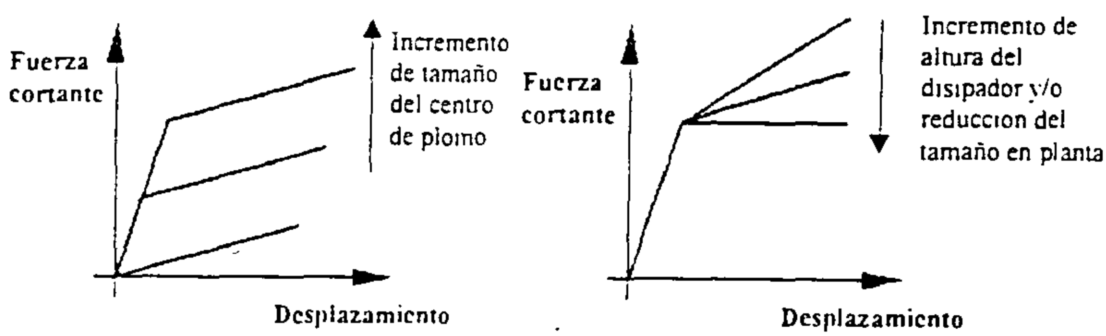

Figura 2 7 Efecto de variaciones geometricas del centro de plomo y del elastómero en la respuesta total

2.4 Selección del tipo de disipador.

La selección de un mecanismo disipador en particular, depende de varios parámetros. el costo, el mérito técnico y su adaptabilidad a la aplicación requerida

Es opinión general, que el apoyo elastomérico con centro de plomo es la mejor selección para puentes en general, ya que incorpora en una sola unidad dos funciones: servir de apoyo para los puentes y a su vez como mecanismo disipador, además de que ofrece simplicidad en su instalación. En virtud de lo anterior se seleccionó este mecanismo en los modelos de puente estudiados.

3. FILOSOFÍA DE DISEÑO

3.1 Antecedentes

De acuerdo con Turkington et. al. [ref. 6], dos de los procedimientos más comunes para diseñar puentes con apoyos de centro de plomo son:

1) La guia de diseño del Ministerio de trabajo y desarrollo de Nueva Zelanda (MWD, 1983),
2) El procedimiento de sistemas de aislamiento dinámico de California (DIS, 1984).

El procedimiento MWD supone que la superestructura es infinitamente rigida y que la rigidez del sistema equivalente de un grado de libertad es la suma de las rigideces de todas las pilas y los estribos; y supone además que la masa del sistema equivalente es igual a la masa total del tablero de la superestructura. Con este método la respuesta se puede obtener de dos formas: determinando la respuesta directamente de unas tablas ó ayudas de diseño, aunque son muy pocas las que se presentan no se puede apreciar qué parámetros se consideraron, o la forma en que éstos se consideraron, además son para un peso asumido de la pila La otra forma es determinar la respuesta directamente del espectro inelástico Pudiera parecer que es éste el método mas confiable. No lo es asi, ya que el periodo real no se calcula directamente y la respuesta debe estimarse utilizando el procedimiento de prueba y error.

En el procedimiento DIS, los apoyos en las pilas y estribos se consideran independientes y la respuesta se basa en el esfuerzo de compresión o la carga vertical en los estribos o pilas individuales, en éste metodo se hacen suposiciones que limitan la aplicación de éste, como por ejemplo, solamente se considera un tipo de disipador con una resistencia caracteristica caracteristica de 5% el peso de la superestructura

En ninguno de los dos procedimientos descritos se toman en cuenta los efectos de la inercia rotacional de la masa de la superestructura Por esto Turkington et al [ref 7] proponen un procedimiento de diseño de acuerdo con los resultados obtenidos anteriormente por ellos mismos [ref. 6] Con su procedimiento, la respuesta sismica inelástica de las superestructuras de puentes sobre apoyos elastoméricos con centro de plomo se representa por una estructura elástica de un solo grado de libertad. La respuesta se estima directamente del espectro de respuesta elástico utilizando un periodo y un amortiguamiento efectivo calculado con el procedimiento propuesto [ref. 6]. El periodo efectivo es el periodo inicial fundamental de la estructura mas un cambio de periodo, resultado de la deformación inelástica de los apoyos con centro de plomo. El amortiguamiento efectivo es un amortiguamiento asumido de 5% asociado con el modo fundamental, más un amortiguamiento adicional histerético debido a la deformación inelástica de los apoyos con centro de plomo; estos dos parámetros se determinan directamente de gráficas de diseño ya realizadas.

En el trabajo [ref. 7] se muestra que los resultados obtenidos utilizando el procedimiento propuesto concuerdan bien con los resultados obtenidos de un análisis por computadora en el dominio del tiempo, además éste procedimiento provee un método para evaluar la respuesta sismica de puentes y es apropiado para diseño, ya que el espectro de diseño elástico puede ser usado directamente y el cambio de parámetros se puede realizar fácilmente. Se muestran también varios ejemplos numéricos para mostrar el procedimiento, que es bastante sencillo, sin embargo se pudo apreciar que el método presenta errores en la determinación de la fuerza cortante en la base de las pilas y el momento flexionante, que son uno de los puntos más importantes en el diseño. Entonces volvemos a lo mismo, necesita desarrollarse un procedimiento de diseño o mejorar el presentado anteriormente de modo que se puedan eliminar esas fallas.

3.2 Aspectos generales a considerar

3.2.1 Aplicación

Los mecanismos de disipación de energia pueden ser aplicados al diseño de estructuras de puentes nuevos o para rehabilitacion de estructuras existentes Para puentes existentes, la disipación de energia representa una solucion efectiva para las 3 deficiencias más comunes en puentes construidos a mediados de los 70's.

a) Vulnerabilidad de los apoyos existentes y sus conexiones
b) Insuficiente resistencia y ductilidad de columnas
c) Longitud de soporte inadecuada de las vigas.

Para puentes nuevos, la aplicación de los disipadores de energía resulta ser más efectiva en los siguientes casos:

a) en regiones de alta sismicidad
b) cuando se tiene una subestructura rígida

3.2.2 Costo

Los factores a considerar son los siguientes:

a) Costo total del mecanismo (fabricación, instalación y mantenimiento)
b) Ahorro en el sistema estructural
c) Ahorro en el tiempo de construccion
d) Reducción del costo en reparaciones estructurales después de un sismo
e) Beneficios indirectos tales como accidentes, muertes y demandas como resultado del daño de un sismo.
f) Importancia de la continuidad de operación después de un sismo
g) Dispositivos adicionales necesarios.

3.2.3 Ventajas y desventajas

El uso de mecanismos disipadores de energia ofrece un número de ventajas potenciales para el diseño sismo resistente de puentes

a) <u>Simplicidad conceptual</u> - esto es, el atractivo de concentrar la disipación de energia de un sismo en componentes especialmente diseñados para este propósito y detallados para un facil reemplazo si es necesario.

b) Eliminación de grandes demandas de ductilidad y por lo tanto el daño a las pilas.

c) Reducción en las fuerzas sismicas en columnas y cimentación.

Las posibles desventajas que se pueden presentar son debidas a requerimientos de mantenimiento y el costo que esto pueda presentar.

REFERENCIAS:

1. Mayes, R. L., Buckle, I. G., Kelly, T. E. y Jones, L R., *AASHTO Seismic isolation design requirements for highway bridges.* Journal of structural engineering, ASCE, Vol. 118, No. 1, enero 1992.

2. Skinner, R. I., Tyler, R. G., Heine, A. J. y Robinson, W. H., *Hysteretic dampers for the protection of structures from earthquakes.* Bulletin of the new zealand national society for earthquake engineering, Vol. 13, No. 1, marzo 1980.

3. Skinner, R I., Kelly, J M. y Heine, A. J., *Hysteretic dampers for earthquake resistant structues.* Earthquake engineering and structural dynamics, Vol. 3, 287-296, 1975.

4. Skinner, R. I., Beck, J L. y Bycroft G. N., *A practical system for isolating structures from earthquake attack,* Earthquake engineering and structural dynamics, Vol. 3, 297-309, 1975.

5. Robinson, W. H., *Lead rubber hysteretic bearings suitable for protecting structures during earthqueakes,* Earthquake engineering and structural dynamics Vol 10, 593-604, 1982

6. Turkington, D H., Carr, A. J., Cooke, N. y Moss P. J., *Seismic design of bridges on lead – rubber bearings.* Journal of structural Engineering, ASCE. Vol 115, No 12, diciembre, 1989.

7. Turkington, D. H., Carr, A J., Cooke, N y Moss, P. J., *Design method for bridges on lead – rubber bearings.* Journal of structural engineering, ASCE. Vol 115, No 12, diciembre, 1989

FACULTAD DE INGENIERIA U.N.A.M.
DIVISION DE EDUCACION CONTINUA

CURSOS ABIERTOS

XXV CURSO INTERNACIONAL DE INGENIERÍA SÍSMICA

MÓDULO III:

DISEÑO SÍSMICO DE PUENTES

TEMA

REFUERZO SÍSMICO DE PUENTES

DR. ROBERTO GÓMEZ MARTÍNEZ
PALACIO DE MINERÍA
AGOSTO DE 1999

REFUERZO SÍSMICO DE PUENTES

Roberto Gómez Martínez
Instituto de Ingeniería, UNAM

EI REFUERZO NO EVITA QUE LA ESTRUCTURA DE UN PUENTE FALLE O SUFRA UN CIERTO NIVEL DE DAÑO

- SUPERESTRUCTURA
- SUBESTRUCTURA
- CIMENTACIÓN

❖ EL REFUERZO DE UN PUENTE AUMENTA SU NIVEL DE RESISTENCIA ANTE UN EVENTO SÍSMICO MAYOR

Restricciones:

a) CARACTERÍSTICAS DE LA ESTRUCTURA

b) VIABILIDAD DE LA REPARACIÓN

c) COSTO

METODOLOGÍA DEL REFUERZO

- CLASIFICACIÓN PRELIMINAR
- EVALUACIÓN
- ALTERNATIVAS DE REFUERZO

CLASIFICACIÓN PRELIMINAR

ATC

- VULNERABILIDAD SÍSMICA
- SISMICIDAD DEL SITIO
- IMPORTANCIA DEL PUENTE

CALIFORNIA

- SISMICIDAD DEL SITIO
- IMPORTANCIA DEL PUENTE
- ESTRUCTURA
- TIPO DE SUELO

JAPÓN

- ESTRUCTURA
- TIPO DE SUELO

COMBINACIÓN DE FACTORES

$$\sum_i \text{(FACTORES)} * \text{(PESOS)} = \text{CALIFICACIÓN}$$

$$\sum_i f_i \, W_i = \text{CALIFICACIÓN}$$

o

$$\sum_i \text{(FACTORES)} = \text{CALIFICACIÓN}$$

$$\sum_i f_i = \text{CALIFICACIÓN}$$

* información
* juicio ingenieril
* experiencia en el diseño de puentes

REFUERZO

- INSPECCION SOMERA

  - Identificación
  - Aspectos sociales
  - Aspectos económicos
  - Aspectos prácticos

- EVALUACION DETALLADA

$$r = C/D$$

  - Elementos
  - Todo el puente

- ALTERNATIVAS

  - Falla local
  - Falla global

BECO = Relación beneficio/costo
PEAR = Pérdidas antes de reforzar
PEDR = Pérdidas después de reforzar
CR = Costo del refuerzo

$$BECO = \frac{PEAR - PEDR}{CR}$$

❖ EVALUACION DETALLADA

- Inspección detallada

  - Ampliaciones
  - Espesor de la carpeta asfáltica
  - Apoyos
  - Juntas
  - Desplomes de pilas
  - Cambios del proyecto original
  - Socavación o erosión

- Evaluación cuantitativa (elementos)

  - Juntas
  - Apoyos
  - Pilas
  - Estribos
  - Licuación

❖ EVALUACION DETALLADA

- Inspección detallada

  - Ampliaciones
  - Espesor de la carpeta asfáltica
  - Apoyos
  - Juntas
  - Desplomes de pilas
  - Cambios del proyecto original
  - Socavación o erosión

- Evaluación cuantitativa (elementos)

  - Juntas
  - Apoyos
  - Pilas
  - Estribos
  - Licuación

1. DISPOSITIVOS PARA ACOMODAR DESPLAZAMIENTOS EXCESIVOS	1.1 CAIDA DE LA SUPERESTRUCTURA	- CONEXIONES ENTRE SUPERESTRUCTURA Y SUBESTRUCTURA
2. REFUERZO DE CIMENTACION	2.1 TIPO DE CIMENTACION 2.2 LICUACION 2.3 SOCAVACION	- NUMERO DE PILOTES - ENSANCHAMIENTO DE ZAPATAS
3. REFUERZO DE SUBESTRUCTURA	3.1 TIPO DE SUBESTRUCTURA 3.2 MATERIAL DE LA SUBESTRUCTURA 3.3 ACERO PRINCIPAL DE REFUERZO	- NUMERO DE COLUMNAS - ENCAMISADOS - MUROS - ANCLAJE (ESTRIBOS) - DISMINUCION DE EMPUJES DE TIERRA
4. REDUCCION DE FUERZAS SISMICAS	4.1 INTENSIDAD DE LOS MOVIMIENTOS SISMICOS	- DISIPACION - AISLAMIENTO

ALTERNATIVAS DE REFUERZO CONTRA SISMO PARA PUENTES

❖ EVALUACION DETALLADA

- Desplazamiento de juntas

$$r = \frac{N(C)}{N(D)}$$

N = longitud de apoyo

$$r = \frac{\Delta_a(C) - \Delta_i(D)}{\Delta_{eq}(D)}$$

Δ_a = desplazamiento permisible

Δ_i = desplazamiento máximo inducido por efectos de temperatura (acortamiento y fluencia)

Δ_{eq} = desplazamiento relativo máximo producido durante un temblor

<u>REDUCTORES DE MOVIMIENTOS</u>

Diseño Conceptual

- FUERZA DE DISEÑO
- MÍNIMO DE 2
- ORIENTACIÓN
- PERMITIR MOVIMIENTO
- NIVEL DE CARGA PARA QUE FUNCIONEN

REDUCTORES DE MOVIMIENTO

Criterios de diseño

- **EUA**
- **JAPÓN**

Opciones:

- **Cables**
- **Barras**

Método de análisis

- **Estático**

1. CALCULAR EL ALARGAMIENTO MÁXIMO PERMISIBLE EN EL REDUCTOR DE MOVIMIENTO

* $D_r = D_y + D_g$

donde:

D_r = deflexión máxima permisible del dispositivo de restricción

D_y = deflexión de fluencia del dispositivo de restricción

D_g = holgura de la junta o articulación

* $D_y = \sigma_y L/E$

donde:

σ_y = esfuerzo de fluencia del dispositivo de restricción

L = longitud del dispositivo de restricción

E = módulo de elásticidad del dispositivo de restricción

Si D_r > longitud de apoyo disponible, entonces

a) reducir la longitud del dispositivo de restricción

b) reducir la holgura

c) reducir el esfuerzo en el dispositivo de restricción

2. CALCULE LA SEPARACIÓN LONGITUDINAL MÁXIMA PRODUCIDA POR EL SISMO EN AMBOS LADOS DE LA JUNTA

* $D_\ell = \dfrac{C_s W}{K_u}$

donde:

K_u = rigidez del claro o segmento de la superestructura entre dos juntas o artículaciones

W = peso del claro o segmento

Nota: Se deben incluir los efectos de la componente transversal del sismo (D_t)

Con los valores anteriores se calcula el valor máximo de:

* $D_{eq} = D_\ell + 0.3\ D_t$

* $D_{eq} = 0.3\ D_\ell + D_t$

donde:

D_{eq} = separación máxima producida por el sismo

3. COMPARAR RESULTADOS DE LOS PASOS 1 y 2

Si $D_{eq} < D_r \Rightarrow$ no dispositivos de restricción $\rightarrow$ (mínimo de 2)

Si $D_{eq} > D_r \Rightarrow$ calcular el número de constrictores de movimiento

4. DETERMINAR EL NÚMERO DE CONSTRICTORES DE MOVIMIENTO

* $N_r = K_u\ (D_{eq} - D_r)/F_y A_r$

donde:

N_r = número de constrictores

A_r = área de la sección transversal de un constrictor

5. REVISIÓN

* $D_{ref} = C_sW/K_t + 0.3\ D_t$

* $D_{ref} = 0.3\ C_sW/K_t + D_t$

donde:

D_{ref} = separación de la junta o articulación, pero con el dispositivo de restricciones ya instalado

Si $D_{ref} \neq D_r \Rightarrow$ ajustar N_r

Si $D_r > D_{ref} \Rightarrow$ reducir N_r

Si $D_r < D_{ref} \Rightarrow$ aumentar N_r

CONSTRICTORES DE MOVIMIENTO

Aspectos constructivos

- ACCESO
- TRÁNSITO
- MUERTOS/DESVIADORES DE CONCRETO
- PERFORACIONES

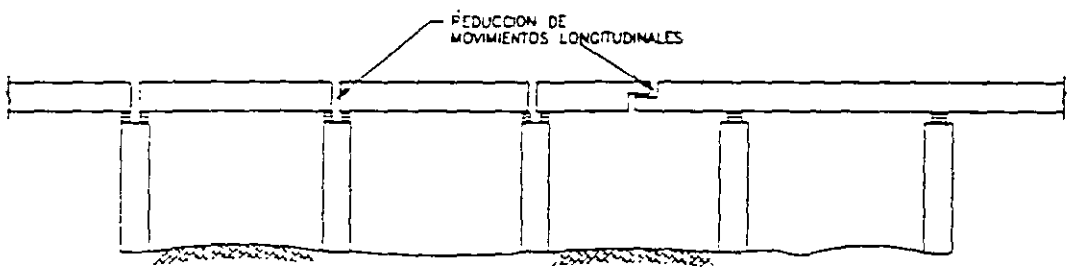

COLOCACION DE REDUCTORES
O CONSTRICTORES DE MOVIMIENTO

REFUERZO SÍSMICO DE SUBESTRUCTURAS

COLUMNAS

- CONCRETO
- ACERO

REFUERZO SÍSMICO DE SUBESTRUCTURAS

- ENCAMISADO DE PLACAS DE ACERO
- ACERO ADICIONAL
- ACERO DE PRESFUERZO
- AUMENTOS DE SECCIÓN
- OTROS MATERIALES

EVALUACIÓN PRELIMINAR DE LA RESISTENCIA DE ELEMENTOS DE SUBESTRUCTURAS DE PUENTES

Para tomar decisiones en cuanto al tipo y nivel de refuerzo sísmico de la subestructura de un puente, es necesario realizar una evaluación sísmica de la misma. El refuerzo se provee con el objeto de minimizar la probabilidad de colapso total y/o daño estructural del puente.

En empalmes en regiones críticas, o por el desgaste prematuro del refuerzo longitudinal, las columnas de concreto son generalmente deficientes en ductilidad a la flexión, resistencia al cortante y resistencia a la flexión.

METODOLOGÍA

1. EVALUACIÓN DE LA PILA POR CARGA MUERTA

2. ESTIMACIÓN DE LAS PROPIEDADES DE LOS MATERIALES

3. ANÁLISIS LATERAL BAJO CARGA SISMICA

4. IDENTIFICACIÓN DE PROBABLES MODOS DE FALLA

5. ESTIMACIÓN DE LA RESISTENCIA A FLEXIÓN

   a) empalmes
   b) articulaciones plásticas

6. ESTIMACIÓN DE LA RESISTENCIA BAJO FUERZAS CORTANTES

7. REVISIÓN DE UNIONES VIGA-COLUMNA

8. REVISIÓN DE ZAPATAS

RESISTENCIA ESTIMADA DE LOS MATERIALES

Es necesario conocer la resistencia y las características de deformación de los miembros de la subestructura. Así se obtiene una mejor estimación del comportamiento esperado. Se recurre a pruebas no destructivas en sitio, incluyendo pruebas de compresión en corazones de concreto tomados de elementos del puente.

Cuando sea posible, la resistencia del acero de refuerzo debe ser determinada con base en pruebas representativas y confiables o con muestras adecuadas tomadas de la estructura del puente. Cuando las pruebas no sean factibles de realizar, se sugiere utilizar los siguientes valores de resistencia :

$$f'_{ca} = 1.5\ f'_c$$

$$f_{ya} = 1.1\ f_y$$

donde: f'_{ca} y f_{ya} son los valores estimados de la resistencia a la compresión del concreto y la resistencia a la fluencia del acero, respectivamente ; f'_c y f_y son las resistencias del material (concreto y acero) especificadas en el proyecto ejecutivo del puente.

MODO DE FALLA DE LOS ELEMENTOS

Se debe identificar el mecanismo de deformación inelástica que puede ocurrir :

- flexión : $\varphi_f M_n \geq M_{req}$
- cortante : $\varphi_s V_n \geq V_{req}$

donde :

φ_f = factor de reducción por flexión
φ_s = factor de reducción por cortante
M_n = resistencia a flexión, estimada
V_n = resistencia a cortante, estimada
M_{req} = resistencia a flexión, requerida
V_{req} = resistencia a cortante, requerida

Según AASHTO :

$$0.9 \geq (\varphi_f = 0.9 - 2P/f'_c A_g) \geq 0.5$$

Otros reglamentos :

$\varphi_f = 1.0$ CALTRANS
$\varphi_f = 1.0$ NUEVA ZELANDA
$\varphi_f = 1.0$ JAPON

RIGIDEZ ELÁSTICA

Con este parámetro se estiman los desplazamientos últimos y los desplazamientos de fluencia de los elementos dúctiles. Cuando sea el caso, se debe tener en cuenta la rigidez de las secciones agrietadas.

Miembros con articulaciones plásticas deben ser modelados con propiedades de rigidez elástica apropiadas para el nivel de fluencia correspondiente. De resultados de un análisis momento curvatura:

$$I_{eff} = \frac{M_{cm}}{\phi_{cm} E}$$

donde M_{cm} y ϕ_{cm} son el momento y curvatura a la fluencia, respectivamente.

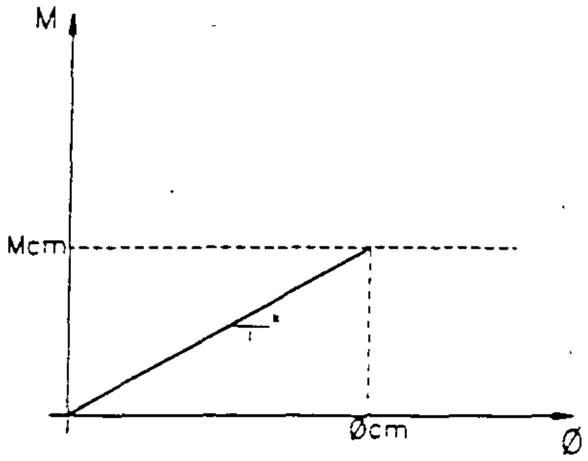

M
Mcm
Øcm
Ø

RESISTENCIA A LA FLEXIÓN

Se debe emplear un análisis momento-curvatura considerando los efectos de confinamiento del núcleo de concreto por refuerzo transversal y el endurecimiento por deformación del refuerzo longitudinal.

La resistencia a flexión es el momento correspondiente a :

a) la deformación por compresión de la fibra extrema de concreto $\varepsilon_c = 0.004$
b) la deformación por tensión de la barra extrema del acero de refuerzo $\varepsilon_s = 0.005$

Concreto : Del análisis momento-curvatura:

$$\phi = \frac{\varepsilon_c}{c}$$

donde: ϕ es la curvatura, ε_c es la deformación por compresión de la fibra extrema y c es la profundidad del bloque de compresión.

Acero : Cuantía de refuerzo en columnas :

$1\% \leq \rho_l \leq 8\%$	USA
$0.8\% \leq \rho_l \leq 8\%$	NZ
$0.5\% \leq \rho_l \leq 8\%$	JAPON

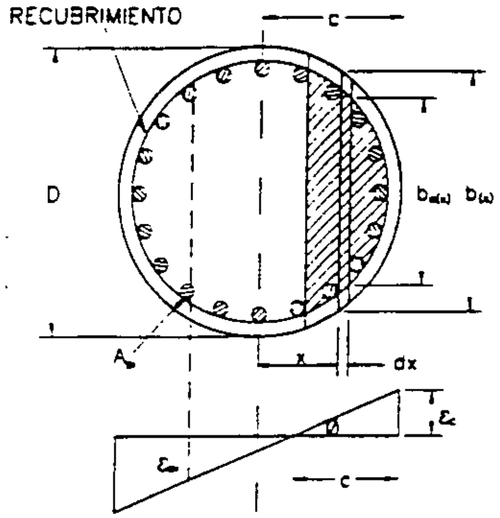

columna circular

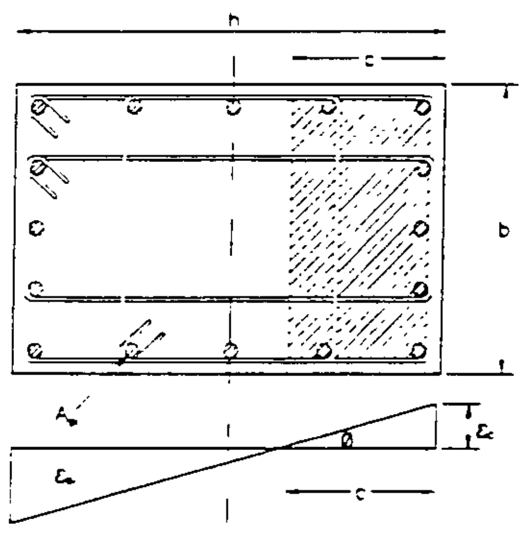

columna rectangular

RESISTENCIA LATERAL DE LAS COLUMNAS CON EMPALMES DE REFUERZO LONGITUDINAL

Cuando se diseña para baja ductilidad, es probable que ocurra falla en los empalmes, excepto cuando las cantidades de refuerzo transversal provistas son muy grandes.

La resistencia a flexión de columnas con empalmes en la base se degrada de la resistencia inicial (correspondiente a la fuerza de tensión máxima) a la resistencia residual M_{res}.

Para columnas con confinamiento transversal no efectivo, la capacidad de momento residual puede ser llevado por la fuerza de compresión axial (P) en la columna, sin que contribuya el refuerzo longitudinal.

Para una sección rectangular, la capacidad del momento residual (M_{res}), basada en la fuerza axial es:

$$M_{res} = P\left(\frac{h'-a}{2}\right)$$

donde $a = P/0.85f'_{ca}b'$; b' y h' son las dimensiones del núcleo residual de la sección, es decir el núcleo de concreto confinado por el estribo.

Para una columna circular, la resistencia residual correspondiente es:

$$M_{res} = P\left(\frac{D'}{2-x}\right)$$

donde x define el centroide de la curva de zona de compresión y D' es la dimensión del núcleo, de centro a centro del estribo alrededor de la columna.

Si el empalme es efectivamente confinado con refuerzo transversal la resistencia residual de la sección se incrementará. Una columna circular con refuerzo debidamente confinado será capaz de desarrollar la resistencia total a la flexión.

El refuerzo confinado puede detallarse con aros soldados o espirales continuos soldados cada vuelta, o con aros o espirales doblados con ganchos estándar de 135°.

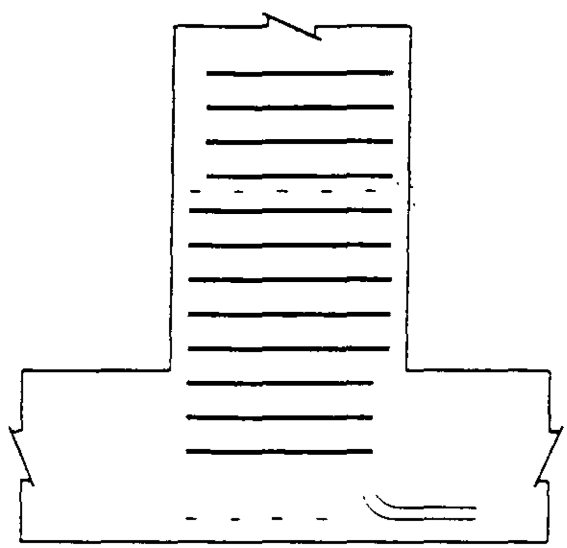

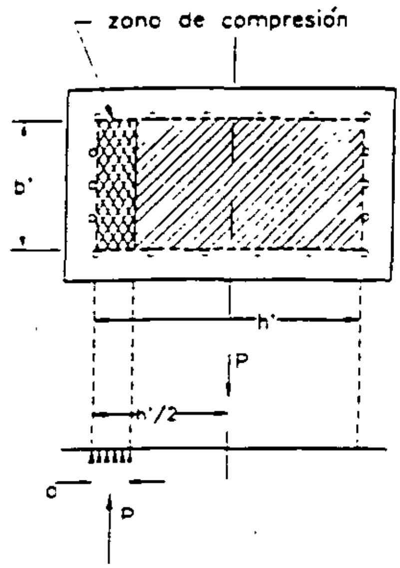

columna rectangular

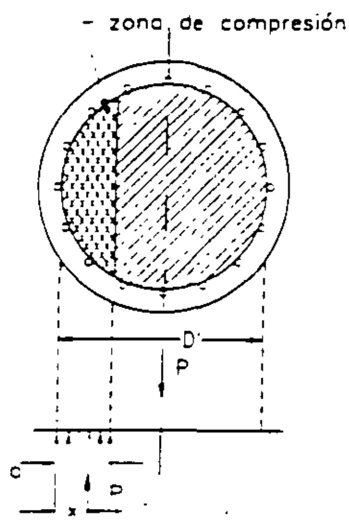

columna circular

CAPACIDAD DE DEFORMACION DE ARTICULACIONES PLÁSTICAS

Secciones sin empalmes del acero de refuerzo. En lugar del valor dado por :

$$\varepsilon_{cu} = 0.004 + (1.4\, \rho_s\, f_{yh}\, \varepsilon_{su} / f'_{cc})$$

donde :

ρ_s = cuantía
f_{yh} = esfuerzo de fluencia del acero de los estribos
ε_{su} = deformación máxima a tensión en el acero
f'_{cc} = resistencia del concreto confinado

se recomienda emplear un valor de 0.005 para la deformación última por compresión ε_{cu}.

No se debe confiar en los efectos benéficos del confinamiento, a menos que este sea propiamente anclado con soldadura o con ganchos en el núcleo, dado que los empalmes de aros (estribos) en el núcleo de concreto pierden su integridad una vez que la cubierta del concreto se astilla o deteriora.

En columnas, los elementos críticos son las articulaciones plásticas. El análisis momento-curvatura debe ser desarrollado para determinar la respuesta inelástica apropiada para incorporarse en el análisis de colapso plástico.

Para secciones pobremente confinadas con ε_{cu} = 0.005, el momento último (M_u) es aproximadamente igual al momento nominal (M_n).

Durante el análisis de colapso plástico, la rigidez elástica del miembro se calcula con la rigidez efectiva $EI_{eff} = M_n/\phi_y$. Cuando se forma la articulación plástica en el elemento, se utiliza la siguiente rigidez efectiva reducida:

$$EI_p = \frac{M_u - M_n}{\phi_u - \phi_y}$$

La curvatura de fluencia es independiente de las relaciones de carga axial y de refuerzo, y su magnitud se obtiene con :

$$\phi_y D = 2.45\varepsilon_y \pm 15\%$$

$$\phi_y h = 2.14\varepsilon_y \pm 10\%$$

para secciones circulares y rectangulares, respectivamente; ε_y es la deformación de fluencia del refuerzo longitudinal, D es el diámetro y h el peralte de la sección transversal.

Secciones con empalmes de acero de refuerzo. Para secciones donde el empalme falla antes que la resistencia nominal a flexión sea alcanzada es necesario una ductilidad de curvatura $\mu_\phi \approx 8$ para alcanzar la capacidad residual M_{res}. Donde la falla de empalmes ocurre después que la capacidad nominal M_n es alcanzada, la capacidad residual es desarrollada para una ductilidad de curvatura alta.

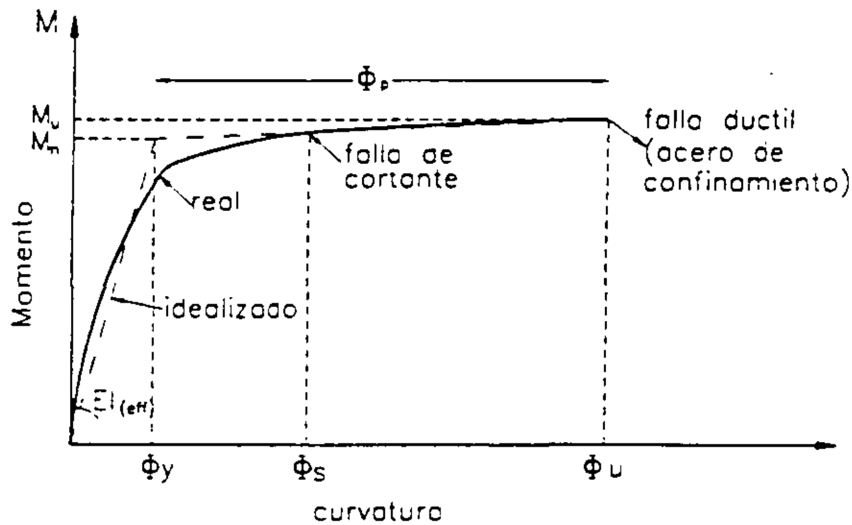

M
Φ_p
M_u
M_n
falla ductil
(acero de
confinamiento)
falla de
cortante
real
Momento
idealizado
$EI_{(eff)}$
Φy
Φs
Φu
curvatura

RESISTENCIA AL CORTANTE

La resistencia al cortante de miembros puede ser estimada usando las siguientes ecuaciones:

$$V_n = V_c + V_s + V_p$$

donde:

V_c es la resistencia al cortante del concreto
V_s es la resistencia al cortainte del acero
V_p es la resistencia la cortante resultado de la compresión del puntal diagonal

$$V_c = k\sqrt{f'_c}\,A_e$$

$$V_s = \begin{cases} \dfrac{\pi}{2}\dfrac{A_h f_{yh} D' \cot\theta}{s} & \text{columa circular} \\[2ex] \dfrac{A_v f_y D' \cot\theta}{s} & \text{columna rectangular} \end{cases}$$

$$V_p = P\tan\alpha$$

donde:

$A_e = 0.8\ A_g$
θ = ángulo de inclinación de la grieta de flexión con respecto al eje de la columna (30°)

A_h = área de la sección transversal de uno de los estribos
A_v = área total de una capa de refuerzo transversal en la dirección de la fuerza cortante
D' = dimensión del núcleo de centro a centro del estribo periférico para columna circular y rectangular
k = factor que puede ser expresado en términos del factor de ductilidad de curvatura μ_ϕ.
s = distancia o separación entre estribos, a lo largo del elemento
P = fuerza axial
α = ángulo formado entre el eje de la columna y el punto donde se aplica la carga

Fuera de las zonas extremas de las articulaciones plásticas (extensión de distancia de 2D o 2h), el valor de k aplicable para μ_ϕ = 1 puede ser adoptado.

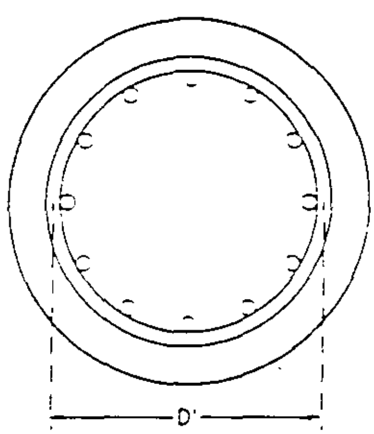
D'

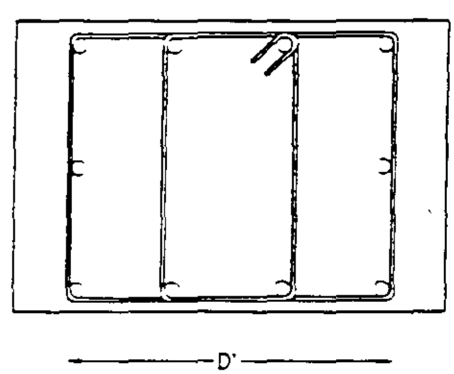
D'

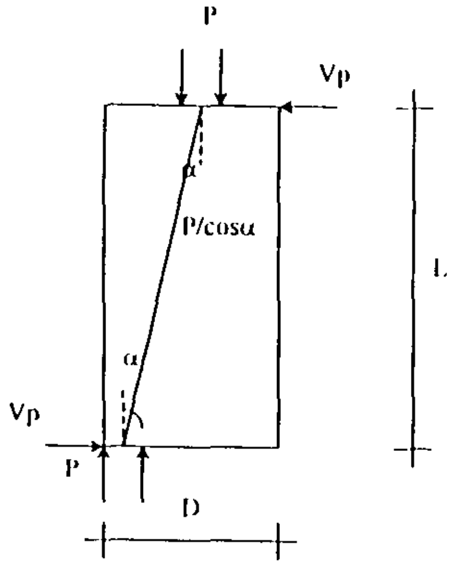
P
Vp
α
P/cosα
L
α
Vp
P
D

CARACTERISTICAS DE DEFORMACIÓN Y RESISTENCIA DE UNIONES VIGA-COLUMNA

Sea p_t el esfuerzo principal de tensión en la unión, el cual se calcula con

$$p_t = \frac{f_v + f_h}{2} \pm \sqrt{\left(\frac{f_v - f_h}{2}\right)^2 + v_j^2}$$

donde:

f_v = esfuerzo promedio en la dirección vertical
f_h = esfuerzo promedio en la dirección horizontal
v_j = esfuerzo cortante en la junta

Si $p_t \geq 3.5\sqrt{f'c}$ (psi) se inicia el agrietamiento de la junta

Si $p_t \geq 5\sqrt{f'c}$ (psi) se desarrolla un patrón completo de grietas

Si la articulación plástica se desarrolla para esfuerzos en el rango de $3.5\sqrt{f'c} \leq p_t \leq 5\sqrt{f'c}$ (psi), la fuerza de fluencia en la unión incrementa con la ductilidad, y la falla de la unión ocurre eventualmente.

Si el esfuerzo principal de tensión permanece debajo de la envolvente de resistencia, la unión no limitará la capacidad de ductilidad de miembros adyacentes. Sin embargo, si este esfuerzo principal alcanza la resistencia, la resistencia en la unión se degradará.

Con la degradación de la unión es poco probable que ocurra una falla por colapso. Ya que puede ocurrir que la falla de la unión ocasione un mecanismo de colapso lateral de resistencia muy reducida.

CARACTERISTICAS DE DEFORMACIÓN Y RESISTENCIA DE ZAPATAS

Estabilidad. En primer término se debe revisar el siguiente requisito de estabilidad :

$\varphi\,(P + W_f)(L_f - a)/2 \geq M'' + V''\,h_f$

donde :

φ = factor de resistencia = 1.0
P = carga axial
M" = momento flexionante
V" = fuerza cortante
W_f = peso total de la zapata
L_f = loongitud de la zapata
a = $(P + W_f) / p_u B_f$
h_f = peralte de la zapata
p_u = presión del suelo
B_f = ancho de la zapata

Si la cimentación es claramente inestable, las condiciones de balanceo deben ser cuidadosamente consideradas.

Resistencia a la flexión. Para revisar esta resistencia es necesario incrementar el ancho efectivo b_{eff}. Cuando se provee acero de refuerzo superior e inferior, se recomienda que el ancho efectivo se incremente a:

$$b_{eff} = \begin{cases} D_c + 3d_f \\ B_c + 3d_f \end{cases}$$

donde :

D_c = diametro de la columna
B_c = ancho de la columna
d_f = peralte efectivo de la zapata

La ductilidad de curvatura máxima, y la capacidad de rotación de una articulación plástica en la zapata, pueden ser estimadas basada en la deformación de compresión máxima de $\varepsilon_c = 0.005$ o en la deformación de tensión máxima de $\varepsilon_s = 0.04$.

Resistencia al cortante. Se recomienda utilizar el mismo ancho efectivo b_{eff} que para la revisión por flexión.

Uniones zapata-columna. Se utilizarán los procedimientos descritos anteriormente para uniones viga-columna pero utilizando el siguiente ancho efectivo :

$b_{jef} = \sqrt{2}\, D$ para columnas circulares

$b_{jef} = h_c + b_c$ para columnas rectangulares

por lo que el esfuerzo cortante promedio v_{jv} en la junta se calcula con :

$v_{jv} = V_{jv} / b_{jel}\, h_f$

donde :

V_{jv} = fuerza cortante en la unión zapata-columna

Falla del cimiento como un mecanismo de respuesta aceptado. En todos los casos la zapata debe ser capaz de soportar la carga gravitacional de la columna durante y después del sismo. Cuando ocurre un daño severo de la zapata asociado con la formación de una articulación plástica, la región central debe ser capaz de soportar la carga total transferida de la columna.

Cuando se asegura el soporte de la carga gravitacional, el diseñador puede escoger deliberadamente tener daño considerable en algunas o todas las columnas y considerarlas articuladas durante el análisis de colapso plástico global.

Capacidad de los pilotes. Cuando se estima la resistencia lateral de cimentaciones con pilotes o cilindros, la resistencia lateral provista por estos elementos debe ser considerada en la estimación de la capacidad de carga de la zapata.

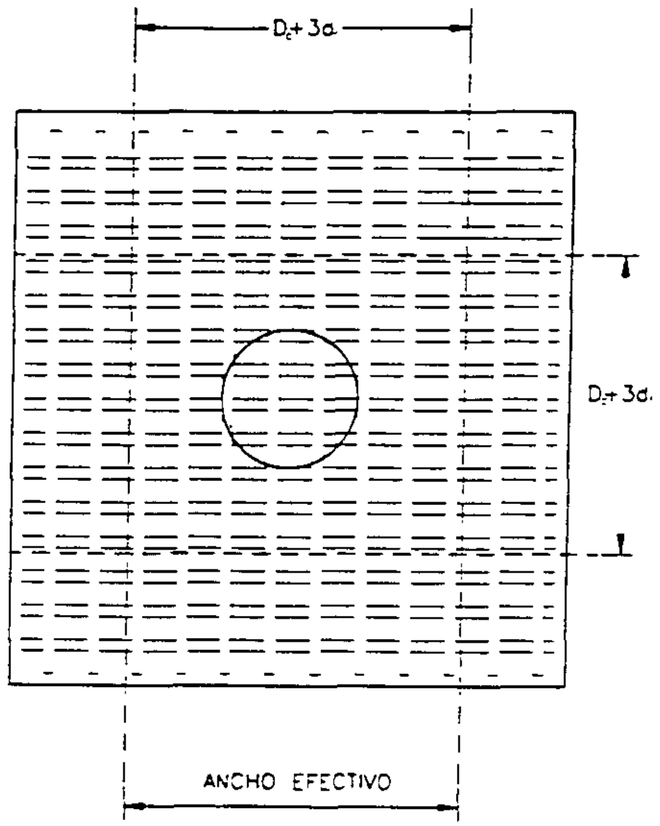
Dc+ 3a
Dc+ 3a.
ANCHO EFECTIVO

❖ EVALUACIÓN DETALLADA

- Fuerza en los apoyos

$$r = \frac{V(C)}{V(D)}$$

V = Cortante

- PILAS

  - Formación de articulaciones plásticas
  - Modos de falla
  - Momentos elásticos
  - Momentos últimos

a) revisar r = M(C) / M(D) para el momento

b) revisar $r = \frac{la(C)}{la\,(D)} * r'$ para el anclaje

c) revisar $r = \frac{A_{tr}(C)}{A_{TR}(D)} * r'$ para los empalmes

d) revisar r para confinamiento transversal

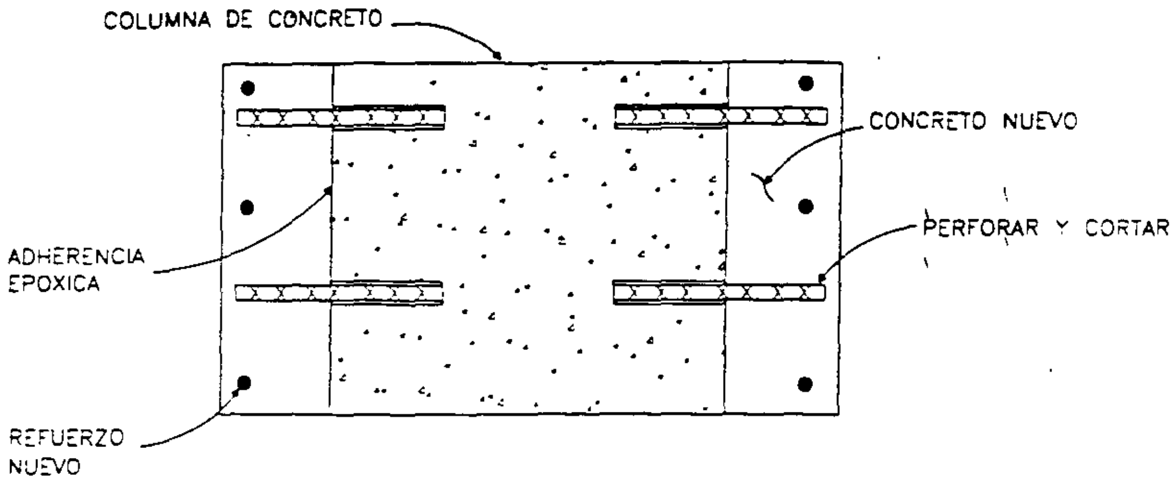

SECCION TRANSVERSAL

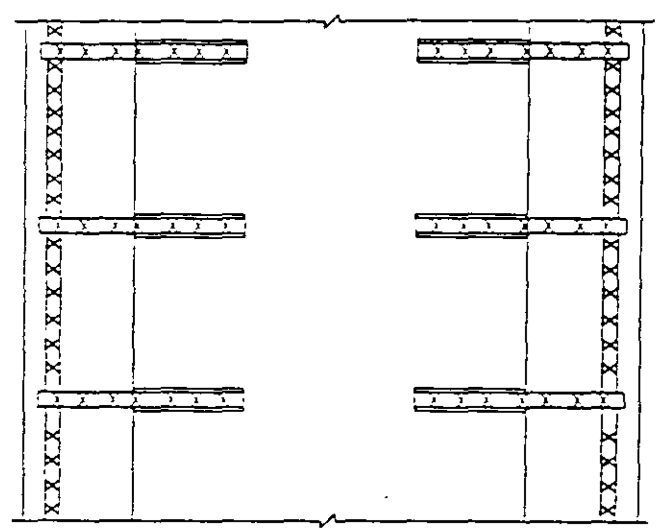

ELEVACION

REFUERZO DE COLUMNA CON SOBRECAPAS DE CONCRETO

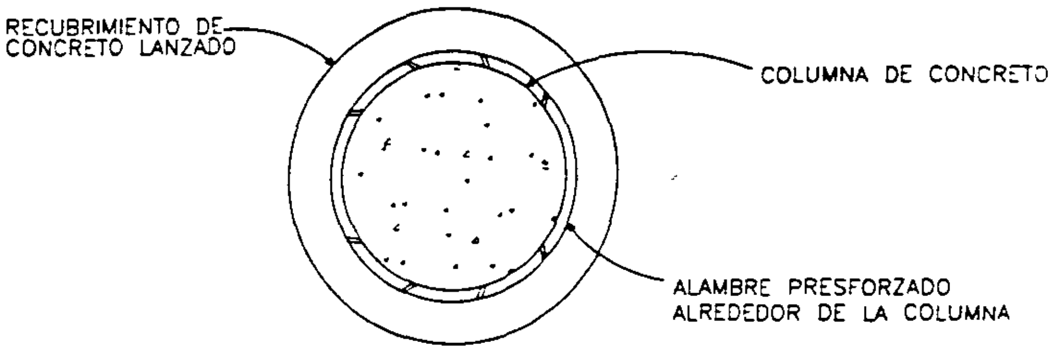

SECCION TRANSVERSAL

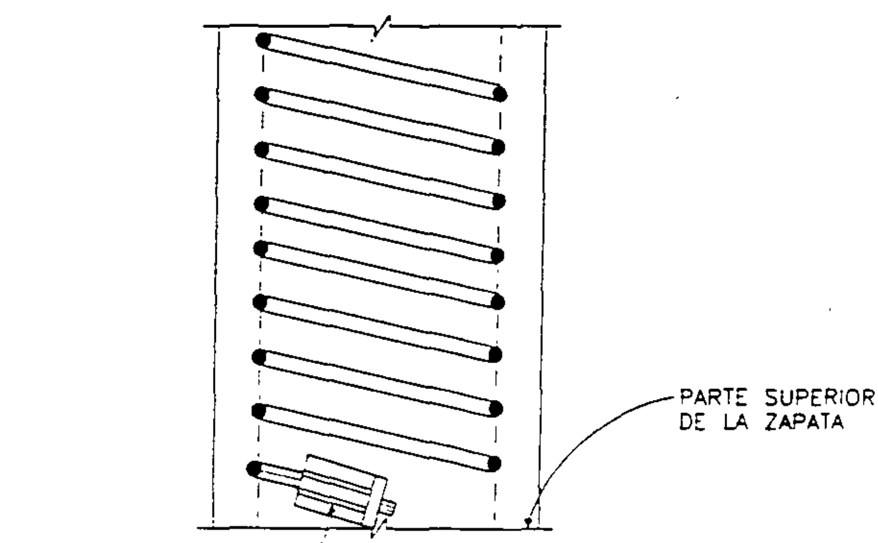

ELEVACION

REFUERZO DE COLUMNA

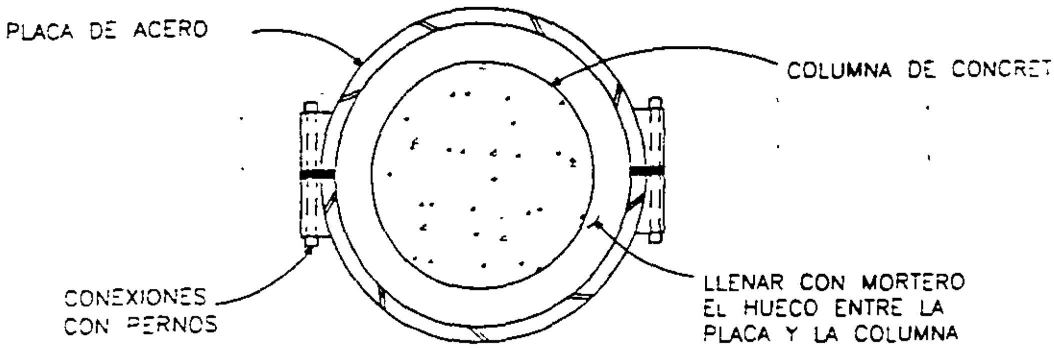

SECCION TRANSVERSAL

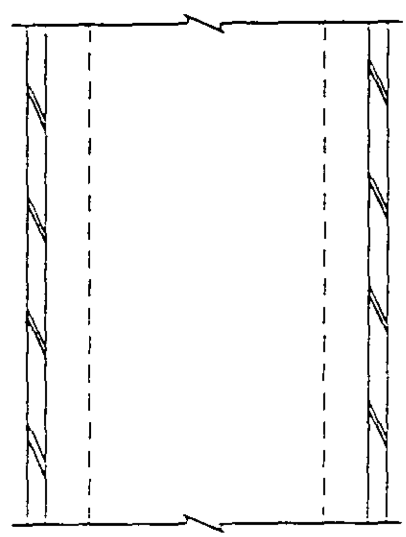

ELEVACION

REFUERZO DE COLUMNA CON PLACA DE ACERO

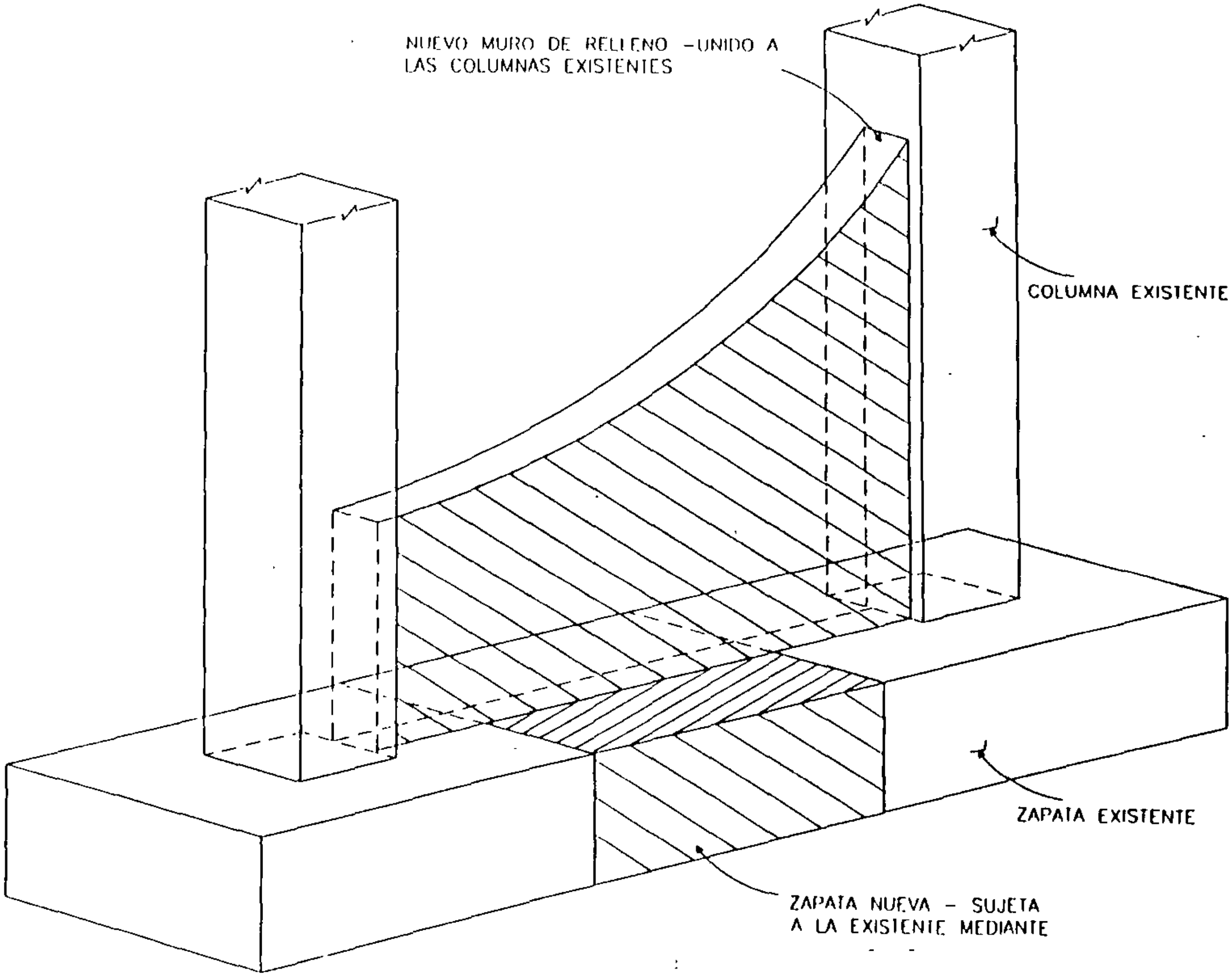

REFUERZO CON MUROS DE CORTANTE

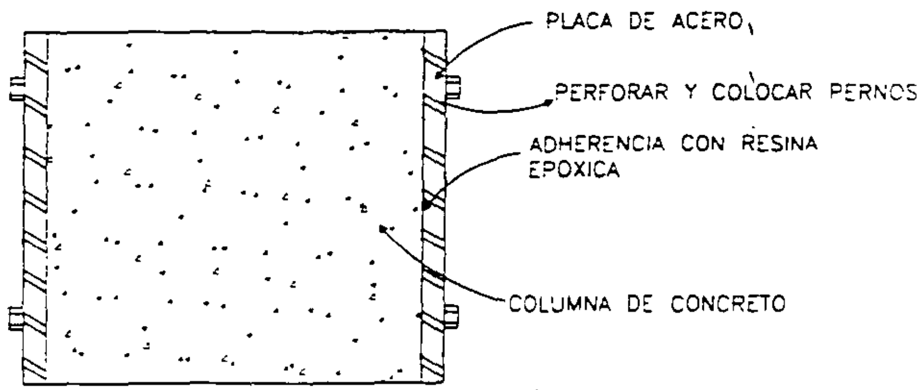

SECCION TRANSVERSAL

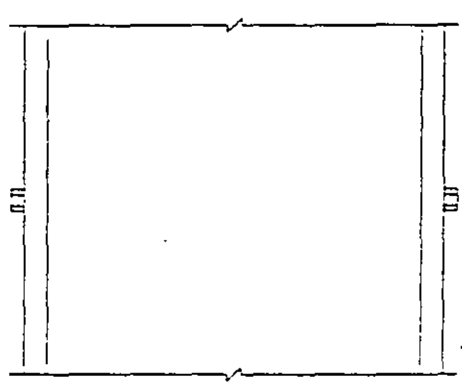

ELEVACION

REFUERZO DE COLUMNA CON PLACAS DE ACERO

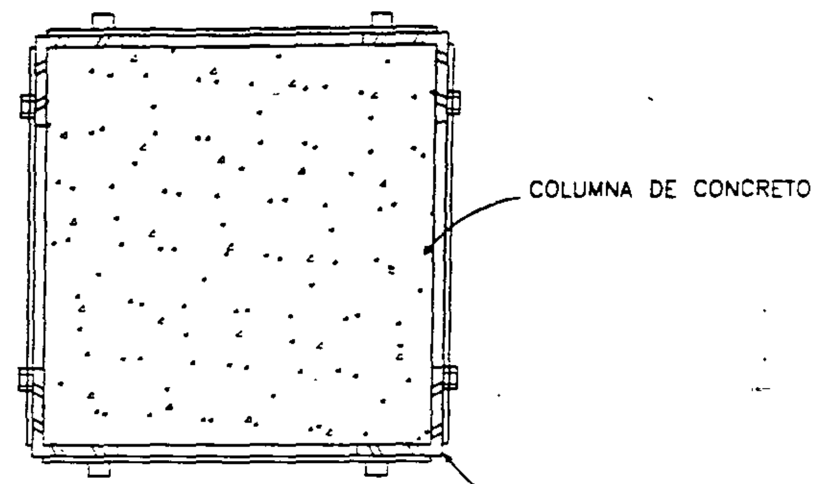

SECCION TRANSVERSAL

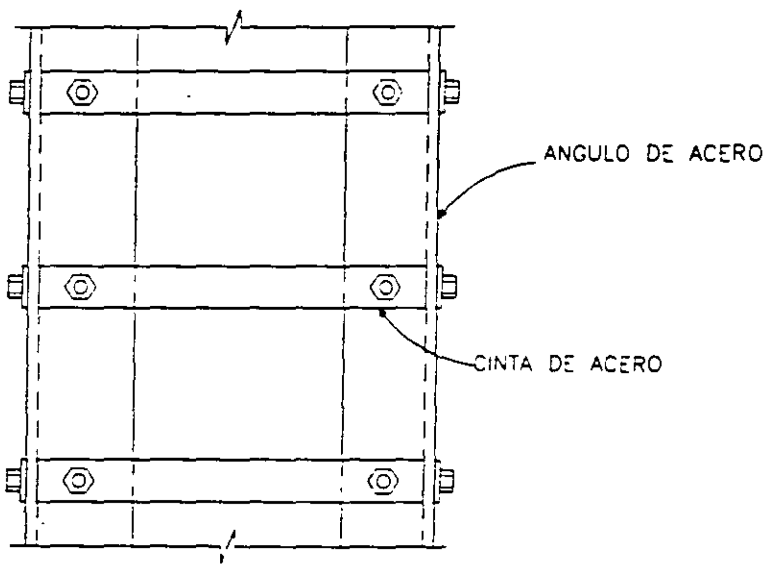

ELEVACION

REFUERZO DE COLUMNA CON ANGULOS DE ACERO

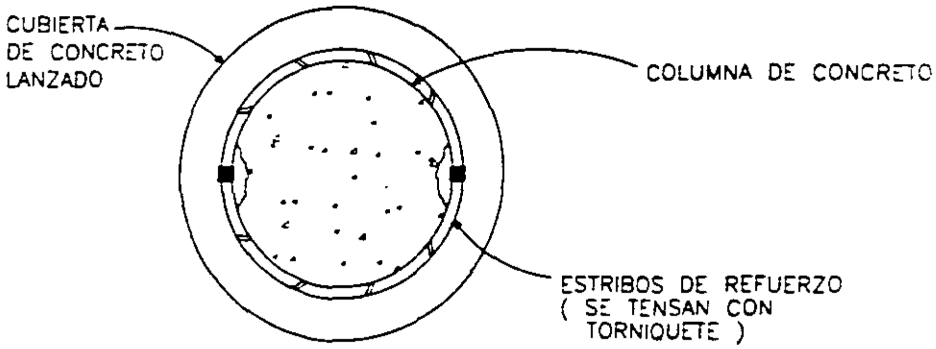

SECCION TRANSVERSAL

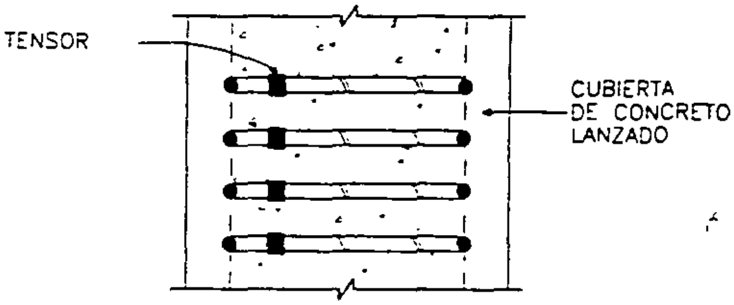

ELEVACION

DETALLE DEL TENSOR

REFUERZO DE COLUMNA

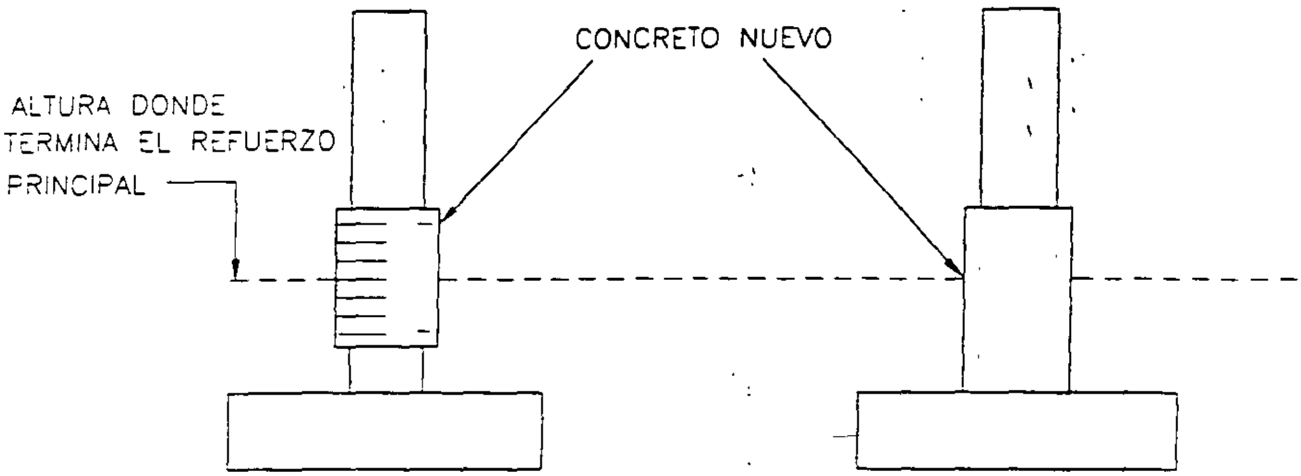

(A) SECCION NUEVA DE CONCRETO

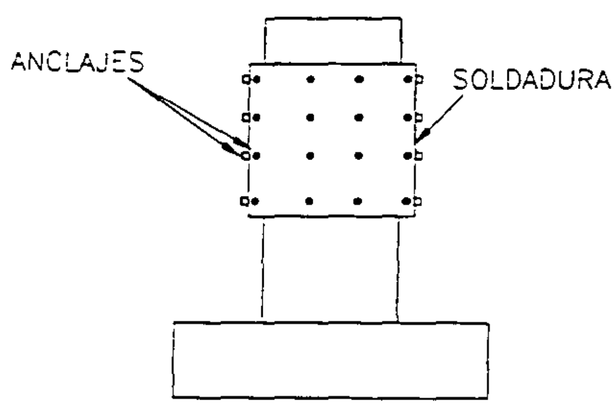

(B) CAMISA DE ACERO

REFUERZO DE PILAS DE CONCRETO CON TERMINACION
DEL REFUERZO PRINCIPAL A LA MITAD DE LA ALTURA

FACULTAD DE INGENIERIA U.N.A.M.
DIVISION DE EDUCACION CONTINUA

CURSOS ABIERTOS

XXV CURSO INTERNACIONAL INGENIERÍA DE SÍSMICA

MÓDULO III:

DISEÑO SÍSMICO DE PUENTES

TEMA :

ESTRUCTURAS DE CONCRETO REFORZADO

DR. OSCAR LÓPEZ BÁTIZ
PALACIO DE MINERÍA
AGOSTO - SEPTIEMBRE 1999

Basic Design Concepts

U.S.A.
[J. Gates, I. G. Buckle]

Present Criteria [J Gates]

INTRODUCTION

The following discussion presents US seismic design view from two primary perspectives The AASHTO code viewpoint, which refers to the current version of the AASHTO seismic code (1) which was previously known as the Seismic Design Guideline and earlier known as ATC-6, hereafter referred to as AASHTO The second viewpoint, the current CALTRANS code(2), (used by the State of California), is very similar to AASHTO in many respects and hereafter will be referred to as CALTRANS. It is the intent of this paper to discuss primarily the above two criteria but there are currently several bridge designs and retrofits underway in the US which apply a modified code which departs somewhat from either of the two above major codes. These departures will also be discussed in this paper

1. DESIGN PHILOSOPHY

The basic design philosophy of both major US codes is to prevent collapse under a major seismic event. The AASHTO code indicates that:

> "Bridges and their components that are designed to resist these forces and that are constructed in a[ccordan]ce with the design details contained in the provisions may suffer damage, but should have low probability of collapse due to seismically induced ground shaking"

The CALTRANS code, while not specifying this directly in their code, does use similar wording in Memos and commentary material.

A secondary philosophy is also spelled out in the AASHTO code:

> "Small to moderate earthquakes should be resisted within the elastic range of the structural components without significant damage".

Although implicit in the current CALTRANS code, this secondary philosophy is not spelled out directly.

1.1 Evaluation of importance of the bridge

The AASHTO code currently defines two importance categories as follows:

1. Essential Bridges
2. Other Bridges

AASHTO only requires the application of the importance classification to bridges located with a seismic coefficient greater than 0 29 Classification of Essential Bridges (IC Classification 1) is based on social/survival and security/defense requirements:

> "An Importance Classification (IC) shall be assigned for all bridges with an Acceleration Coefficient greater than 0.29 for the purpose of determining the Seismic Performance Category (SPC) in Sec 3 4 as follows
>
> 1 Essential bridges - IC = I
>
> 2 Other bridges - IC - II
>
> Bridges shall be classified on the basis of Social/Survival and Security/Defense requirements, guidelines for which are given in the Commentary."

The current CALTRANS code does not specifically address importance in the criteria. The assumption made at the time of the development of the current code (in 1973) was that all bridges were important. Recommendations by the Loma Prieta Investigation Board (3) require CALTRANS to address this issue. Future codes at CALTRANS will specify importance in terms of emergency and economic need to the community.

Currently CALTRANS is developing guidelines for evaluation of bridges for seismic retrofit and are proposing a three level importance classification as follows:

Category 1 -- Essential structures for emergency response
Category 2 -- Structures necessary for recovery (determined by cost-benefit evaluation)
Category 3 -- Structures needed for normal operations (others)

1.2 Definition of limit states and their probability of occurrence

Both the AASHTO and CALTRANS codes do not specifically address this issue. Implicit in both codes is the fact that a yield limit state will occur in column members. AASHTO assumes the probability of the elastic design force levels not being exceeded in 50 years is in the range of 80 to 95%. However, AASHTO states that;

> " the design earthquake force level by itself does not determine risk; the risk is also affected by the design rules and analysis procedures used in connection with the design ground motion"

AASHTO provides additional material on this in the commentary to the criteria.

CALTRANS does not make any probabilistic assumptions, their code is based on deterministic methods defining a maximum credible event where return periods vary from hundreds to many thousands of years, depending on the particular fault adjacent to the site. Additional discussion is provided in their commentary material to their specification.

This particular consideration in the various US criteria is currently undergoing change. For example the Transportation Corridor Agency in Orange County is building a new privately owned toll facility in Orange County(4). Their design return period about 2500 years which compares favorably with the CALTRANS values for the region under consideration. Various groups evaluating the current AASHTO criteria are also investigating the possibility of increasing the return period of the design motion.

The recently issued recommendations by the Loma Prieta Investigation Board (3) requires CALTRANS to perform a comprehensive seismic safety assessment of each major toll crossing. The first step recommended in this process is to perform a seismic hazard analysis to establish the annual probability of exceedance relation for peak free-field ground acceleration on firm soil and/or bedrock at the bridge sites.

1.3 Basic design choices: structural systems, bridge types, isolation or dissipation devices

Bridge designs in the US fall into two general categories:

1. Monolithic systems
2. Girder/bearing systems.

The monolithic systems are generally concrete girder systems with columns constructed monolithic with the superstructure. Girder/bearing systems utilize some form of bearing assembly installed at the superstructure soffit level, separating it from the column and/or cap beam substructure.

In new facilities, the Eastern portion of the US the girder/bearing system predominates, while in the western US, the monolithic configuration is more common. Both systems appear to be approximately equally seismically resistant, however in either case it is generally accepted that superstructures must be continuous as much as possible in order to minimize joint pull apart and subsequent collapse

The use of base isolation has presently somewhat limited use in the US, with about 4 installations in California as a retrofit measure and a few installations in other parts of the country. AASHTO recently adopted a Guide Specification for base isolation which will be available as an option on a Nationwide basis(5)

2. SEISMIC ACTION

2.1 Definition of ground motion (ground acceleration and frequency content)

Both US codes utilize 5% damped acceleration response spectra to define elastic (unreduced) design forces over a period range of about 0 to 5 seconds. The AASHTO code spectra are based on basic spectra defined for buildings (6).

Smooth elastic spectra for 5% damping were developed to be used with regional maps. An example set of response spectra for a maximum ground acceleration of 0.4g is shown in Figure 1. This represents the maximum level of shaking specified by the criteria.

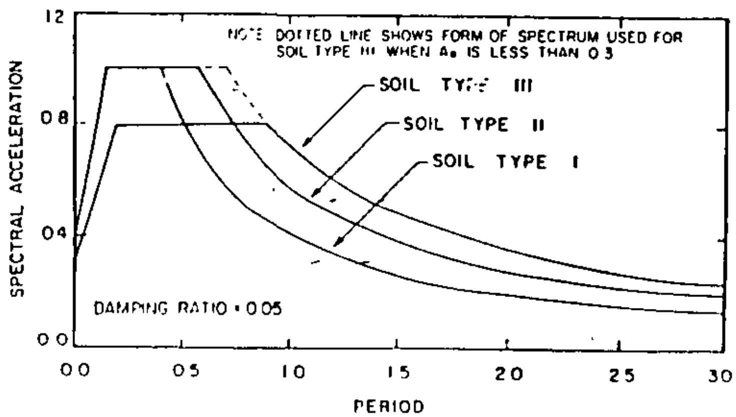

Fig. 1 AASHTO Ground Motion Spectra for A = 0 4

The CALTRANS spectra were developed in 1973 and are based on elastic rock spectra derived from several California earthquakes recorded on rock. Rock acceleration levels vary from 0.1 to 0.7g. The CALTRANS rock spectra (0' to 10' Alluvium) is shown in Figure 2.

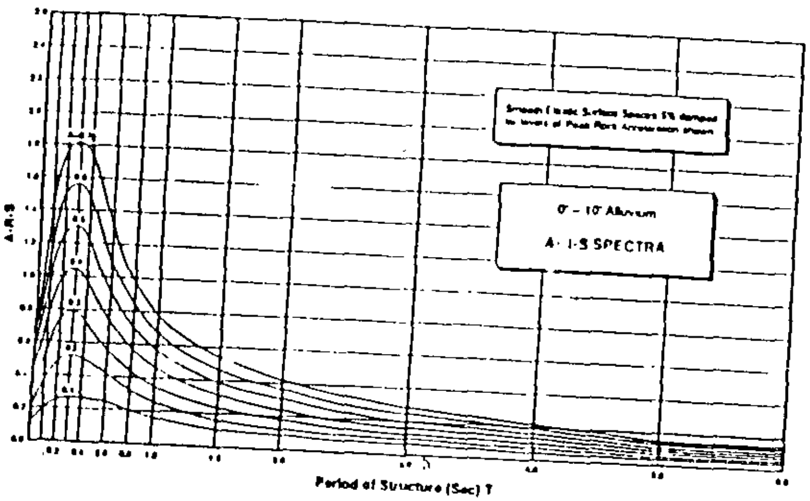

Fig. 2 CALTRANS Rock Spectra

2.2 Effects of soil conditions

Three soil types are used to differentiate site conditions in the AASHTO code:
Soil Profile Type I - Rock or Stiff Soils
Soil Profile Type II - Stiff Clay or Cohesionless Soils
Soil Profile Type III - Soft to Medium-Stiff Clays and Sands. This Characterization is based on ATC-3 soil types (6).

CALTRANS utilizes 4 categories to describe various depths of alluvium over rock-like material: 0 to 10 feet, 10 to 80 feet, 80 to 150 feet, and greater than 150 feet in depth.

Both criteria recognize the need to permit the development of 'site- specific spectra for special sites. The CALTRANS criteria permits the development of special spectra when site conditions and structure importance warrants:

> "Sites adjacent to active faults, sites with unusual geologic conditions, unusual structure types, and structures with a fundamental period greater than 3.0 seconds will be considered special cases. In such cases, structures shall be evaluated for seismic loads by utilization of approved soil response and dynamic analysis techniques."

2.3 Assumptions on the ground motion at the base of different piers.

All current US design specifications assume equal motions at each support.

Several of the larger California Toll bridges are currently being evaluated using state-of-the-art techniques including the consideration of variation of support motions (or coherence) along the length of the structure. Hopefully the results of these studies will better define the practical limits where such refinement in analysis is required.

2.4 Treatment of vertical acceleration

Vertical acceleration is currently not directly specified in the two major criteria in use in the US. Both codes specify hold down requirements for resultant uplift forces obtained from the horizontal loads as follows:

> "Hold-down devices shall be provided at all supports and intermediate hinges where the vertical seismic force (from a horizontal seismic load) exceeds 50% of the dead load reaction. The hold-down device (when required) shall be designed for the greater of 10% of the dead load reaction or 1.2 times the net upward force."

CALTRANS standard superstructure expansion hinge details provide for uplift.

The retrofit of portions of the San Francisco Viaducts are being performed using a vertical spectra of 0.67 times the horizontal. It is expected that future criteria in California will contain vertical load considerations.

3. PROCEDURES OF ANALYSIS

3.1 Linear static

Both AASHTO and CALTRANS permit the use of a linear static analysis.

AASHTO specifies a more complex procedure based on a generalized coordinate approach.

CALTRANS specifies a simple uniform load approach. CALTRANS also requires that the static load approach always be used to determine forces in longitudinal restrainer systems.

Both codes restrict the use of the static load approach to simple framed structures where a single mode of vibration in the direction under consideration can accurately replicate the results of a simple modal analysis.

3.2 Linear dynamic (Modal Analysis)

Both AASHTO and CALTRANS permit the use of linear dynamic analysis. AASHTO specifies in greater detail the number of nodes to be used in the model. CALTRANS uses the same numbers in their models, however they have no written specification. Nationally, there is a very small percentage of bridges being designed using linear dynamic analysis procedures, however usage is slowly growing as a result of the complexity of the AASHTO simplified model, the availability of a simple and easy to use dynamic analysis too[illegible] SEISAB), and the recent adoption of the AASHTO Guide Specificati[illegible] equired specification for Nationwide use.

CALTRANS has automated the linear dynamic procedure to the point where it is being used on virtually every bridge The program STRUDL is being used in conjunction with an efficient pre-processor call BAG to generate a lateral specific model which can be utilized for all horizontal loads including wind, temperature, and centrifugal forces as well as seismic

Uncracked section properties are utilized in the space frame model

3 3 Nonlinear

Neither US code currently specifies a non-linear analysis. Both codes allude to this as a method, but no specific guidelines are presented

CALTRANS is currently evaluating several large toll bridges utilizing both linear and non-linear analysis Hopefully the results of these studies will enable a better definition of what structure configurations, sizes and force-levels will justify this refinement of analysis

3.4 Foundations (abutments) and soil structure interaction

Both AASHTO and CALTRANS recognize the need to consider the abutment stiffness in the analytical model CALTRANS assumes a linear spring equivalent to 200 k/in per linear foot of abutment with a maximum force limitation of 7.7 KSF on mobilized abutment structural members

Pier footings, whether located on rock or piles are usually considered fixed unless founded on very soft materials Large diameter shaft foundations are analyzed assuming soil springs as a lateral support

4. DUCTILITY LEVELS

4.1 Bridge types

Both AASHTO and CALTRANS define ductility levels (or reductions) in terms of specific components and substructure configurations AASHTO limits vary from 0 8 to 5. CALTRANS reduction values can be as high as 8. CALTRANS specifically states in their commentary that a basic ductility of 4 is assumed for their column members and then a risk of up to 2 is applied depending on the substructure configuration and size AASHTO uses a single value over the entire period range

Retrofit and replacement analysis of the San Francisco Viaducts utilizes an overall ductility reduction of 4

4.2 Curvature ductility

Curvature ductility is not specified in either US criteria It has been utilized in special cases on several important California retrofit projects including those where peer reviews are utilized to better define the ductility demand on existing columns to verify the decision to not retrofit the member.

4.3 Displacement ductility

Displacement ductility is not normally computed. It is assummed that it is approximately equal to the force reduction factor. Effort is currently underway at CALTRANS to implement displacement ductility calculations on a routine basis

4.4 Force reduction factors

The force reduction factors used by AASHTO are shown in Figure 3.

Substructure[1]	R	Connections	R
Wall-Type Pier[2]	2	Superstructure to Abutment	0 8
Reinforced Concrete Pile Bents		Expansion Joints within	
a Vertical Piles Only	3	a Span of the Superstructure	0 8
b One or more Batter Piles	2	Columns, Piers or Pile Bents	
Single Columns	3	to Cap Beam or Superstructure[3]	1 0
Steel or Composite Steel		Columns or Piers to Foundations[3]	1 0
and Concrete Pile Bents			
a Vertical Piles Only	5		
b One or more Batter Piles	3		
Multiple Column Bent	5		

[1] The R Factor is to be used for both orthogonal axes of the substructure

[2] A wall type pier may be designed as a column in the weak direction of the pier provided all the provisions for columns in Chapter 8 are followed The R Factor for a single column can then be used.

[3] For bridges classified as SPC C and D it is recommended that the connections be designed for the maximum forces capable of being developed by plastic hinging of the column or column bent as specified in Sec 4 8 5 These forces will often be significantly less than those obtained using an R Factor of 1

Fig 3 AASHTO Response Modification Factors (R)

The Force reduction factors used by CALTRANS are shown in Figure 4.

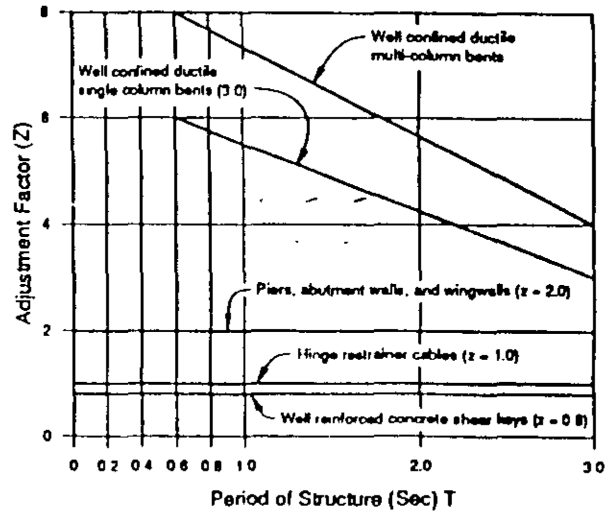

Fig. 4 CALTRANS Adjustment for Ductility and Risk Assessment Factors (7)

In both criteria, the adjustment is applied by dividing into the elastic seismic moments to obtain design moments.

Both criteria define two load cases which utilize a transverse and longitudinal earthquake. Load Case 1 - Combines 100% of the forces from one earthquake to 30% of the forces from the other direction. Load Case 2 is the opposite of Load Case 1. This combination accounts for the directional uncertainty of the earthquake motions.

4.5 Maximum displacements

Neither US criteria specify any maximum displacements or drift limitations. Drift limitations of about 1% were used for evaluation of portions of the viaducts in San Francisco as part of their retrofit evaluation.

The AASHTO specification indirectly considers differential motions by specifying seat widths to assure span support after some longitudinal movements have occurred. Figure 5 shows the AASHTO seat width dimensions. These dimensions apply to both low seismic zones (Category A and B) and for high seismic zones (Category C and D).

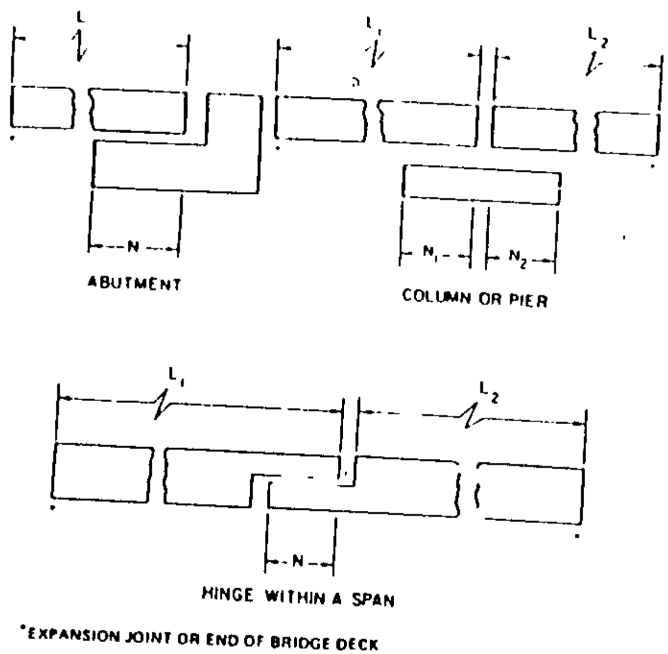

Fig 5 AASHTO Seat width dimensions

Seat width (N) is specified as follows:

In Categories A and B zones (Low seismic):
$N = 8 + 0.02L + 0.08H$ (inches)

In Categories C and D zones (High seismic):
$N = 12 + 0.03L + 0.12H$ (inches)

Where:
L = Length in Feet between expansion joints and,
H = Height in Feet of the column or pier

CALTRANS does not specify seat width in their specification, however the AASHTO seat width specification is mentioned in commentary and support material for abutments. This specification is also applied to larger structures. CALTRANS uses a 24 inch minimum seat on all bridges. Also at CALTRANS, additional seat width is recommended at abutments on high skew.

4.6 Second order effects (pi delta)

AASHTO requires that moment magnification and slenderness effects be considered as part of the seismic loading case. CALTRANS does not include this refinement in their calculations. Neither code specifically requires the consideration of other second order effects, however CALTRANS recommends maintaining a KL/R ratio of less than 100 on all column members.

REFERENCES

1 Bridge Design Specifications Manual, American Association of State Highway and Transportation Officials, Washington, D.C., 1990.

2 Bridge Design Specifications, California Department of Transportation, Division of Structures, Sacramento, California, 1990.

3 Competing Against Time, Report to Governor George Deukmejian from the Governor's Board of Inquiry on the 1989 Loma Prieta Earthquake, George W. Housner, Chairman, State of California Office of Planning and Research, May, 1990

4 Development of Project-Specific Seismic Design Criteria, for Corridor Design Management Group, Costa Mesa, CA, By Computech Engineering Services and Imbsen & Assoc, July, 1990.

5 Guide Specifications for Base Isolation of Bridges, American Association of State Highway and Transportation Officials, Washington, D C , 1990.

6 Tentative Provisions for the Development of Seismic Regulations for Buildings, Applied Technology Council, (ATC-3), Palo Alto, California, 1978. Also available as Special Publication 510, National Institute of Standards and Technology, Washington, D.C and National Science Foundation Publication 78-8, Washington, D C

Design Details

U.S.A.

[S. A. Mahin, I. G. Buckle, R. Mayes]

Design Details [S. A. Mahin]

1. PRELIMINARY REMARKS

Achievement of satisfactory structural performance in the event of rare and unusually severe earthquake ground motions depends on a wide variety of parameters. Possibly none of these parameters is more important than the selection and implementation of details to achieve ductile response.

This paper reviews the basic detailing, proportioning and related design principles incorporated in the design of reinforced concrete bridge structures located in regions of high seismic risk in the United States, with an emphasis on specifications adopted by the California Department of Transportations (Caltrans).

The basis for the design of reinforced concrete bridges in the United States is Standard Specifications for Highway Bridges as promulgated by the American Association of State Highway and Transportation Officials (1987 edition [1]). California bridge design practice is governed by Bridge Design Specifications (1990 edition [2]). The California specifications are in large measure based on Ref. 1, with various sections, especially those related to earthquake resistant design, modified to reflect California design conditions and practices. In addition, a series of memos to designers [3-7] have been developed by Caltrans to deal with specialized design details and standards, such as restrainers at hinges and bearings, abutments, earthquake retrofit of single column bridges, and so on.

Some of these details and guidelines are summarized herein as applicable to California. Where appropriate, comparisons are also made to code recommendations for reinforced concrete buildings [8].

2. MEMBER PROPORTIONING AND DETAILS

2.1 Basic Parameters and Choices for Member Proportioning

The basic U.S. and Caltrans design practice is to design structures capable of resisting small to moderate earthquakes with little or no damage and maximum credible events with no serious damage or collapse [9]. Thus, while essentially elastic behavior is expected for moderate level excitations, damage associated with inelastic response is anticipated in the event of a large earthquake. It is the intent of current Caltrans design practices to limit damage to repairable levels and to have important interchanges remain operable following a major earthquake.

To achieve these performance goals Caltrans usually adopts a moment resisting frame system for resisting earthquake induced loads. Ductile details are implemented in the frame to impart the desired degree of member ductility. Caltrans also adopts capacity design principles to insure an overall ductile system response. As currently stipulated, design provisions tend to concentrate damage (flexural plastic hinging) in columns, and to minimize i astic behavior in the bridge decks, bent caps, joints and foundations. Localized damage in abutments is anticipated by current Caltrans provisions.

Monolithic structures have become the standard of practice in California. Special details are required at all expansion joints, hinges and abutments to prevent unseating during earthquakes.

To provide a more rational means of assessing member ultimate capacities and the distribution of forces in the structure during earthquakes, Caltrans stipulates that the earthquake design of concrete structures and members be performed using strength methods. The design forces are determined for critical members, typically the columns, using results of elastic dynamic analyses based on response spectrum for the site corresponding to the maximum credible earthquake. These elastic forces are reduced by a response modification (ductility/importance) factor, Z, accounting for the inelastic deformations permitted in the columns and other elements. The value of Z depends on the importance of the structure and member as well as on the period and perceived ductility capacity of the structure.

Within these general guidelines a wide variety of structural forms are utilized. In California, aesthetic considerations have an important role in the selection of member shapes and proportions. For example, drain pipes and utilities may not be exposed, necessitating the positioning of these items within structural members. Similarly, rectangular columns are only infrequently employed, with more complex and aesthetically appealing shapes being preferred. Typically, columns are flared, rather than being prismatic, and octagonal or circular cross-sectional shapes are favored (Fig. 1). Hexagonal columns and rectangular columns (with beveled corners) are used in some special cases (10). Simple prismatic columns are only recommended by Caltrans for "multi-column bents, bridges with low public exposure and highly industialized areas." Architectural treatments in the form of texturing, insets and fillets on the column surfaces are frequently used where pedestrian and vehicular densities are significant. In spite of these complexities, use of standardized column sizes and shapes is encouraged by Caltrans for aesthetic, economic and practical reasons.

Pier walls are also utilized in some situations. These are defined as vertical elements with heights less than 2.5 times the width. Again, tapered or flared geometries are most commonly used (Fig. 1). Although ductile details are stipulate for these elements, their relatively poor behavior under seismic loading conditions has led Caltrans to utilize forces 2 to 4 times greater (i.e., a lower Z factor is utilized) than for ductile columns.

Bridge decks are monolithic. Generally, box girders with either vertical and inclined edge girders are utilized. The depth of a continuous box girder section is typically equal to the span divided by 18. Vertical deflections due to live load plus impact are limited to the span length divided by 800.

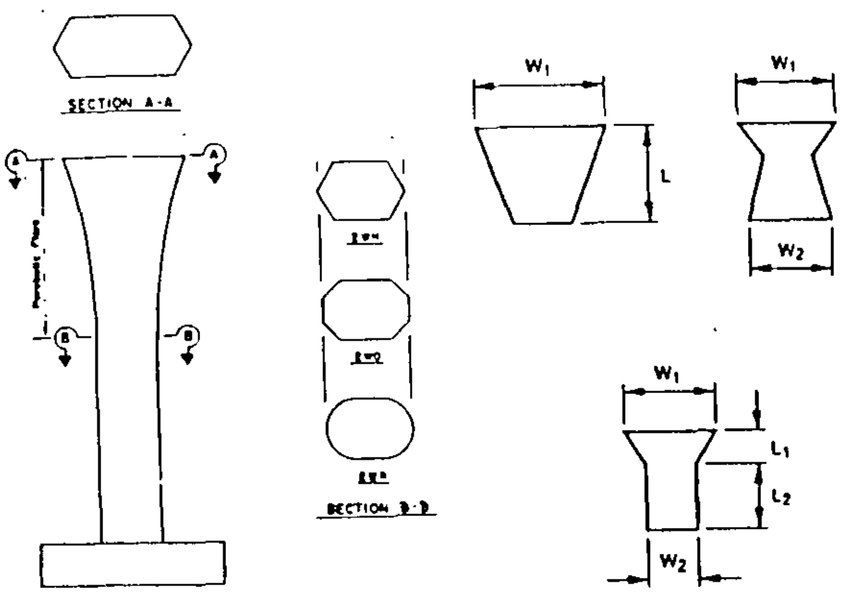

(a) Column Geometries

(b) Pier Geometries

Fig. 1 Typical Column and Pier Geometries

2.2 Foundations

Foundations are either of the spread or pile type. Piles are constructed from timber, concrete, steel or cast-in-drilled-hole (CIDH) concrete. Friction and point bearing may be considered as the load resisting mechanism for pile foundations. Piles may be spaced no closer on center than twice the largest sectional dimension of the pile or 3 ft. (910 mm). Friction piles may be considered able to resist an intermittent seismic uplift equivalent to 50% of the pile's ultimate compressive load capacity (providing proper provision is made to anchor the pile to the footing and sufficient skin friction can be developed). The Commentary to Caltrans' Bridge Design Specifications stipulates against the allowance of uplift forces for saturated cohesionless soils, because of the possible loss of frictional resistance due to the buildup of pore-water pressures during earthquakes.

Standard details are utilized for piles. With the exception of cast-in-place piles, details for confinement and shear reinforcement do not conform to ductile detailing requirements imposed for columns above ground. However, special analysis is required for moment, shear, axial load and stability when piles are embedded in soils with measured standard penetration resistance values of 10 or less.

Footings are typically reinforced top and bottom in both directions and minimum reinforcement is stipulated for shear. A typical detail is shown in Fig. 2. Design loads for footings are based on capacity design principles, i.e., the moment and shear induced by the supported column is taken as the lessor of the forces resulting from plastic hinging in the column, or from the elastic response spectrum analysis of the structure plus dead load. The plastic hinge capacity of the column is taken as 1.3 times the nominal capacity of the critical section. The capacity reduction factor for footings (and piles) is taken as unity. Thus, yielding is expected to initiate in the column and the footing is designed to be able to develop the full plastic capacity of the column.

A top layer of reinforcement is provided both ways in all footings to resist uplift and bending effects. This layer of reinforcement is often controlled by the minimum flexural reinforcement requirements for concrete sections, rather than by computed internal forces.

The need for shear reinforcement in footings is computed as for flexural elements. However, no distinction is made in the capacity reduction factors applied to flexure and shear. Thus, no apparent preference is made regarding the possible eventual failure (flexural vs. shear) mode of the footing. None the less, a minimum amount of shear reinforcement is stipulated for all footings in a band located near the column. Vertical hooked ties (No. 5) are required at 12 in. (305 mm) spacing in each direction in a band extending from 6 in. (152 mm) away from the column face to a distance away from the column face equal to the effective depth of the footing (see Fig. 2). These ties must be hooked around the top and bottom layers of flexural reinforcement in the footing. This steel is intended to prevent delamination of the footing due to tensile yielding of the column longitudinal reinforcement. It undoubtedly plays an important role in resisting the anchorage forces developed by the hooked column bars terminating in the footing.

The connection of the column reinforcement to footing is called out for special attention by the Caltrans' Bridge Design Specification. When a moment connection is provided, the column longitudinal bars must be anchored by hooking them at the bottom of the footing (Fig. 2). Typical design practices have the hooks turned outward. The commentary to the Caltrans' specifications indicates that it is preferable from a performance perspective to turn the hooks inward, but that outwardly turned hooks are used in practice in order to provide a more stable base for supporting the column reinforcement cage during construction. The adequacy of this detail remains to be evaluated.

In many cases columns are intended to be pin connected to the footings (see Fig. 2). In these cases, a minimum of four bars are used with a combined area of not less than 0.5% of the gross area of the supported column. The required shear capacity of the pin is based on the plastic shear demand provided by the column or the force resulting from the elastic (unreduced) earthquake response

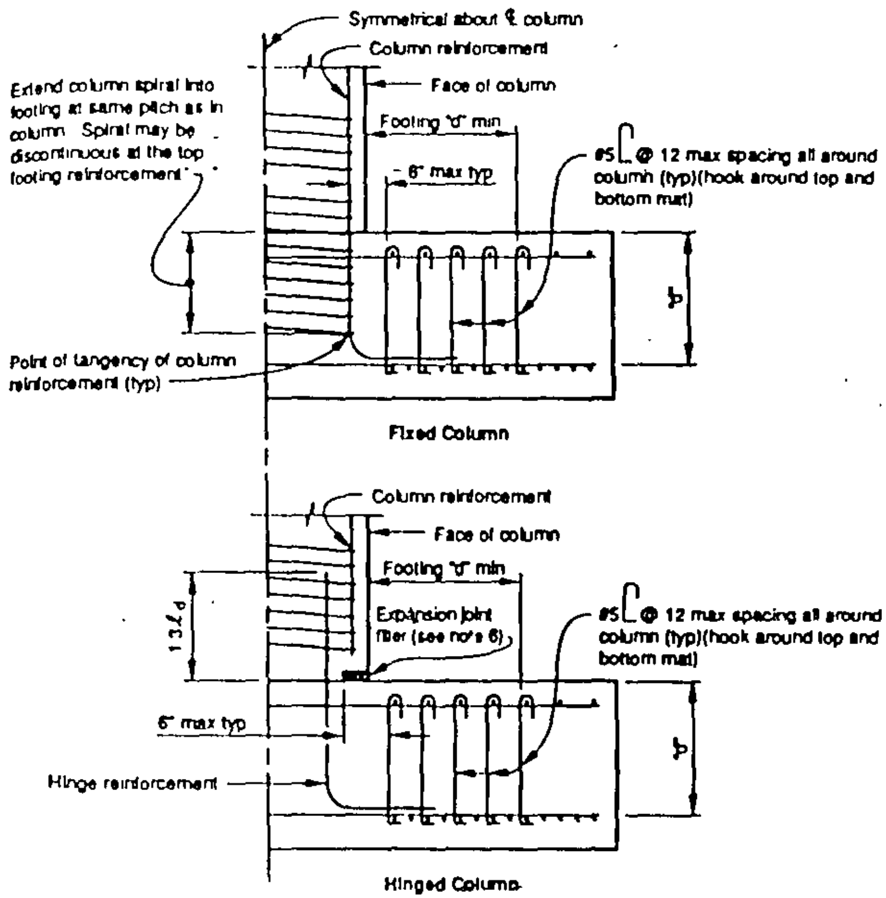

Footing Reinforcement

Notes to Designer:

1 #5 @ 12 is the minimum equivalent required, see BDS Article 4.4.7.3.
2 For minimum top of footing reinforcement requirements, see BDS Article 4.4.6.3.3
3 For design requirements for column hinge, see BDS Article 8.16.4.5.
4 When hinge is used for oblong columns having overlapping spirals, hinge reinforcement must be detailed to clear the spirals
5 Locations for permissible discontinuities in spiral reinforcing must be shown on the plans
6 The thickness of the expansion joint filler should allow maximum column deflection without crushing the edge of the column concrete against the footing and should have a minimum thickness of ½"

Fig. 3 Typical Footing Details

spectrum analysis (which ever is less). The shear capacity of dowels passing through the center portion of the connection is estimated as:

$$V_n = A_{vf} f_y \mu \qquad (1)$$

where A_{vf} is the area of steel provided in excess of that needed for compression loading and μ is the friction coefficient (μ equals 1.4 for monolithic concrete and 1.0 concrete cast against a roughened, but hardened concrete surface. If uplift is developed in a pinned connection, an additional area of steel must be provided to resist the full applied tensile force with a capacity reduction factor of unity for seismic loading. The tensile design force is computed based on equilibrium considerations for the case where plastic hinges occur in all of the columns (plus dead load). The large shear and axial forces associated with plastic hinging in the column frequently necessitates the use of clusters of rebar bound in a spiral cage, or steel H-beam or tube sections, instead of the traditional grouping of a few unconfined, large diameter, rebars near the center of the column.

2.3 Abutments

The selection of abutment type depends on the needs for structural support, structure movement, drainage, structure approach and earthquake effects. Six principal types of abutments are utilized, but two are the most common: diaphragm abutments, and short seat abutments (Fig. 3). Both of these types of abutment are usually placed at the top of the approach embankment in order to provide the structure with a relatively open appearance. Support for the abutments is provided by spread footings or piles, depending on loading and soil conditions. The main difference between the two types of abutments is that the seat abutment permits relative movement between the superstructure and the embankment, and the diaphragm abutment does not.

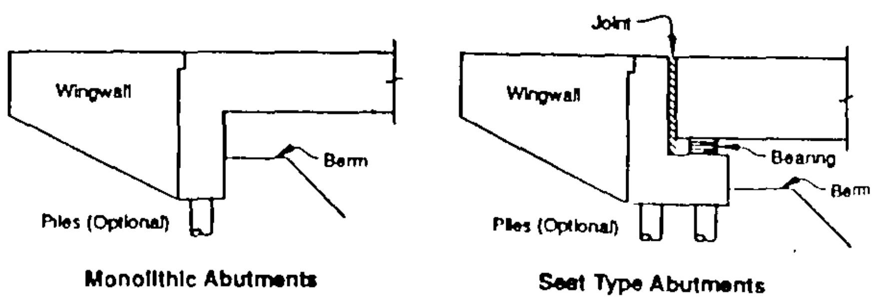

Fig. 3 Common Types of Abutments

Diaphragm abutments monolithically connect the superstructure to the supporting piles or footing. This integral behavior facilities resistance of large seismic loads. While this type of abutment is economical, it often requires substantial long term maintenance due to settlement of the approach roadway relative to the abutment and due to potential erosion of the embankment resulting from water intruding in the joint between the diaphragm abutment and the approach roadway. Special details can be employed to alleviate these problems. None the less, this approach is most commonly utilized in relatively short structures (spans less than 400 ft. (123 m).

The short seat abutment permits the superstructure to move independent of the abutment. As such, the abutment is designed as an independent structural element for relatively low forces. The road surface usually rests on top of the abutment, eliminating problems associated with settlement and water intrusion in diaphragm abutments.

Caltrans design procedures anticipate earthquake damage to the abutment. Design forces and detailing provisions are intended to limit damage (a Z factor of 2 is employed (see Fig. 4)) and prevent loss of support for the superstructure. Typically, the design is done such that the damage is localized in key ways or in the abutment backwall so as to minimize damage below grade.

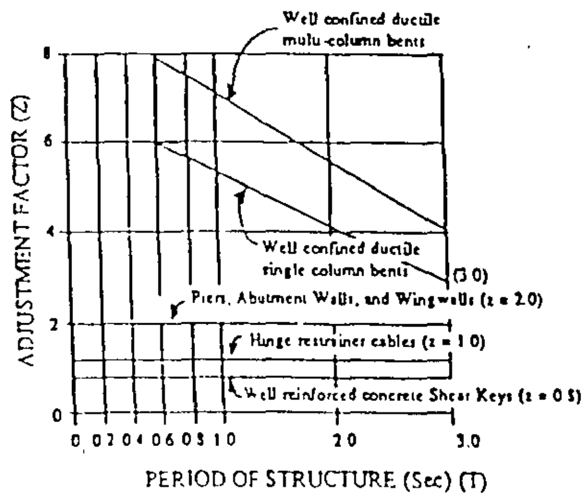

Fig. 4 Response Modification Factors for Importance and Ductility

2.4 Provisions for Deck Joint Seismic Movement

A positive restraint mechanism is required at all deck hinges and expansion joints in order to limit relative displacements and minimize the possibility of unseating. In the transverse direction keys are generally utilized. Restraint in the longitudinal direction is generally provided by flexible, unidirectional devices which can limit superstructure displacement. Longitudinal restraint at the abutments is optional depending on site conditions, abutment type and the need to limit overall displacements of the structure.

Often multiple post-tension strands are utilized by Caltrans for the longitudinal restrainers. A minimum of two restraining units are required at an expansion joint, one near each side of the deck. A minimum of four and a maximum of seven cables per restraining unit are recommended on the basis of practical considerations, the likely strength of the deck and [illegible] results.

The design criterion for restrainers and keys at intermediate hinges requires them to remain elastic. Keys at abutments are permitted to yield to limit damage in the abutment and foundation.

3. REINFORCEMENT DETAILS

3.1 Typical Material Properties and Reinforcement Ratios

Bridge structures are designed using Grade 60 deformed bars. Plain bars and smooth wire may be used for column spirals and ties. Prestressing steel is permitted, but not as a part of the critical earthquake load resisting system that is allowed to yield.

The ACI code [8] contains requirements for the minimum and maximum ultimate strength of the bars, as well as for the minimum yield strength of the reinforcement. The omission of such requirements from the Caltrans' Bridge Design Specifications may not be generally significant in view of manufacturing practices in the U.S.

Concrete with a minimum strength of 3250 psi (230 kg/cm2) is stipulated by Caltrans. Special quality assurance measures are required for strengths equal to or greater than 6000psi (420 kg/m2). Normal weight and light weight concrete may be used. No limit is apparently placed on the strength of light weight concrete, unlike the ACI which stipulates a maximum strength of 4000 psi (280kg/cm2) for lightweight concrete.

3.1.1 Flexural Members

The maximum reinforcement ratio permitted in flexural elements is limited to 75% of the balance ratio considering the beneficial effects of any compression steel. Since it is not expected that flexural members will significantly yield for bridge structures, requirements for flexural elements are far less stringent in References 1 and 2 than in the ACI code [8]. For example, the Bridge Design Specifications do not mandate minimum ratios for compression reinforcement, minimum ratios of positive to negative moment capacities at critical moment locations and so on.

Moreover, bridge seismic detailing requirements are far less

demanding than the ACI code with regards to the need for and amount of continuous reinforcement in flexural members. However, requirements for side face crack control reinforcement require that a minimum of one No. 8 bar be placed in the top corners of all girders with a depth greater than 2 feet (610 mm). Additionally, 10% of the tensile steel provided at any section along the length of the member must be distributed across the sides of the member. (The 1989 ACI Code has been revised with regard to the amount of side steel required.)

A minimum amount of tensile longitudinal reinforcement is required at locations in flexural members where tensile stresses are computed. Reinforcement able to resist the lessor of 1.2 times the cracking moment or 1.33 times the computed design load is required.

For continuous flexural members a minimum of 25% of the maximum amount of flexural reinforcement must be continued into the support. This reinforcement must be anchored to develop the full yield capacity of the bars.

A minimum amount of shear reinforcement is required in all members (except slabs and footings) where the computed shear force exceeds 43% of the nominal shear capacity of the concrete. Where this value is exceeded, stirrups should be provided to contribute 50 psi (3.5 kg/cm2) to the ultimate average shear stress over the section. The maximum spacing of shear reinforcement is half of the effective depth of the member or 24 inches (610 mm) which ever is less. In the lateral load resisting system, shears are computed considering equilibrium for plastic hinging in the columns.

3.1.2 Columns

In columns the reinforcement ratio (total area of longitudinal steel to effective area of the column) is limited to a range between 1 and 8 percent. The ACI Code limits the maximum reinforcement ratio to 6%. Where architectural treatments increase the cover the Bridge Design Specifications permit the effective area may be arbitrarily reduced to satisfy the 1% requirement (provided the design load can still be carried).

For spiral columns a minimum of six bars are to be used. Four bars can be used in the case where rectangular hoops are used for transverse reinforcement. Rectangular columns are usually reinforced with overlapping spiral cages (see Fig. 5). A minimum overlap of between adjacent spiral cages shall not be less than 0.75 cage diameters. At least 4 longitudinal bars shall be located in the overlapped region.

The shear capacity in columns is estimated identically by the ACI and Caltrans' specifications. Shear capacity of the concrete is increased with axial compression and decreased for axial tension. At the plastic hinge regions Caltrans stipulates that the concrete shear strength should be be varied linearly from zero to $2\sqrt{f'c}$ as the axial load increases from zero to $0.1f'cAg$, where Ag is the

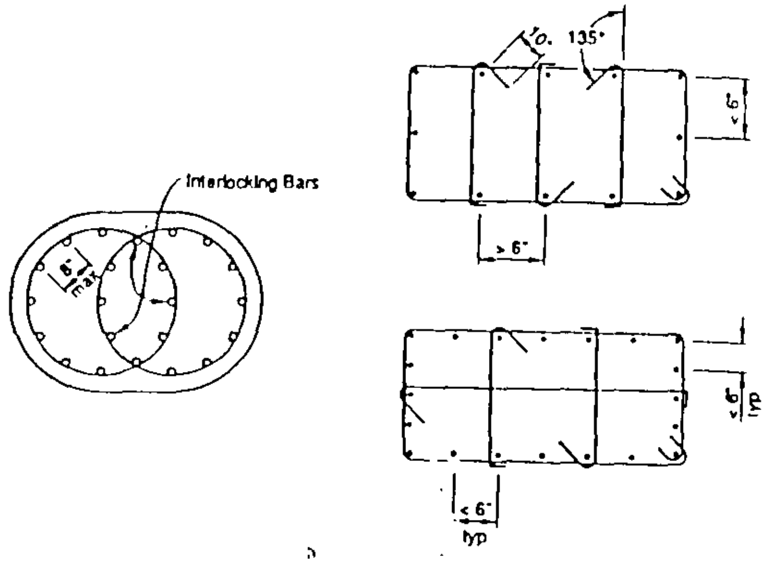

(a) Interlocking Spirals (b) Tied Columns

Fig. 5 Ductile Column Details

gross area of the section. Where the axial stress intensity is greater than 0.1f'cAg the normal shear relation is used for concrete. The contribution of the steel is based on only the transverse steel in the core and the effective depth of the member is taken to be 80% of the dimension of the column in the direction of the applied shear. The Caltrans specifications do not say what should be done in the event of tensile loads. Current ACI requirements stipulate that the contribution of the concrete be taken to be zero for axial loads less than 0.05f'cAg. This results in the ACI being more conservative for loads less that 0.05f'cAg and less so for larger loads. However, given the limited amount of experimental data on this range of behavior, greater refinement may be unwarranted at this time.

In pier walls the minimum reinforcement ratio is 0.25 percent. Spacing of bars on each face shall is limited to 12 in (300mm). More stringent requirements are placed on the plastic hinge region.

3.2 Critical Regions

3.2.1 Flexural Members

As indicated previously, bridge design philosophies in the U.S. envision yielding to take place primarily in the columns. As such, few special earthquake provisions are stipulated for ductile detailing of flexural members. The Bridge Design Specifications indicate that transverse reinforcement must be provided for compression reinforcement used to increase the flexural strength of members (No. 4 stirrups for No. 10 and larger bars, spaced no more than 16 bar diameters on center).

However, the maximum spacing of lateral reinforcement for compression members is stipulated to be the smaller of 1/5 the least dimension of the cross-section, 6 times the nominal diameter of the longitudinal reinforcement or 8 inches (200 mm). The maximum spacing between longitudinal reinforcement in compression members is limited to 8 inches (200 mm). The application of these requirements to bent caps and other flexural members that develop axial compression forces as a result of seismic loading is uncertain. There is no formal definition of the axial load necessary in an element to qualify it as a compression member in the Caltrans' specifications.

The Bridge Design Specifications [2] indicate that "in seismic areas, where an earthquake that could cause major damage to construction has a high probability of occurrence, lateral reinforcement shall be designed and detailed to provide adequate strength and ductility to resist expected seismic movements." However, no guidance is provided regarding the application of this provision.

Closed ties are required where computed torsional forces indicate the need for torsional reinforcement. The stipulated detailing for these elements do not anticipate, consistent with the design criteria, that torsion would develop in a critical region.

3.2.2 Compression Members

Special lateral reinforcement is required in columns in order to develop the required ductility during seismic events. This consists generally of spiral reinforcement, but circular hoops and a combination of perimeter and cross ties may be used where spirals are not feasible.

Lateral reinforcement is continued over the full height of the column and continues into the footing and bent cap connection. In the footing it must continue to the beginning of the hook. In a bent cap connection it must continue into the cap for a distance equal to the lessor of: (a) one-half of the maximum horizontal dimension of the column's confined core; (b) the development length of the longitudinal column reinforcement, if the bars are straight; and (c) the straight portion of the column reinforcement, if the bars are hooked (see Fig. 6). This later provision may have significantly adverse effects with regard to joint confinement and shear, if the lateral reinforcement is actually terminated within the joint. Practical considerations normally dictate that the reinforcement continue over the full extent of the joint.

As indicated previously the maximum spacing allowed for the lateral

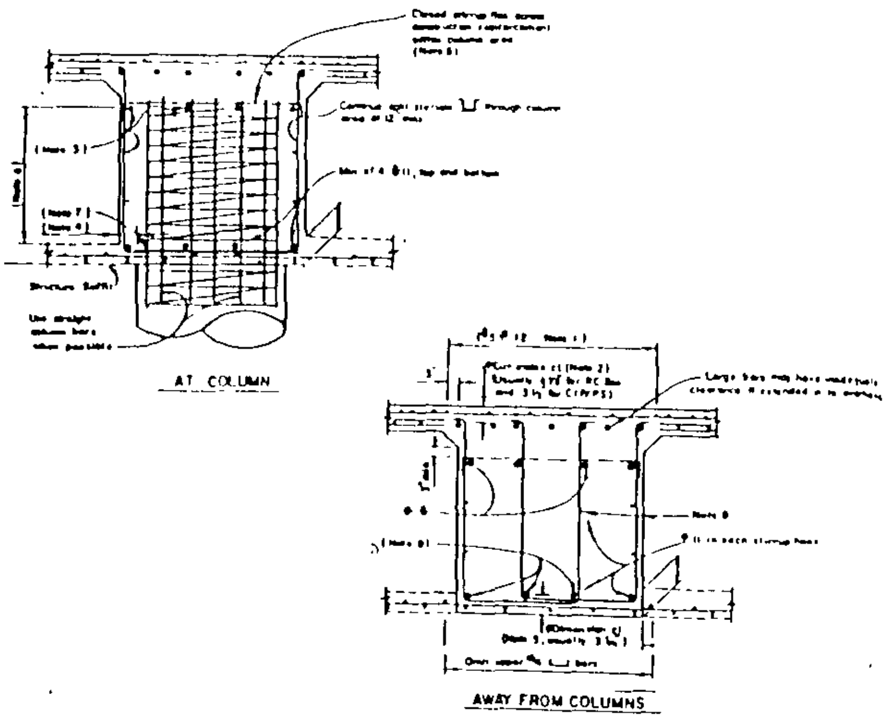

Fig. 6 Bent Cap and Joint Details

reinforcement is the lessor of 1/5th of the least dimension of the column, 6 times the diameter of the longitudinal bar or 8 inches (200 mm). This is in excess of spacing requirements in the ACI Code which limits spirals to a 3 inch (76 mm) clear spacing and a center to center spacing in tied columns to 1/4th the minimum column dimension or 4 inches (100 mm)(or he lessor of six bar diameters or 6 inches (150 mm) away from the plastic hinge region).

For spirally reinforced columns the ratio of spiral reinforcement is given by:

$$P_s = 0.45(Ag/Ac - 1)f'c/fy \qquad (2)$$

where Ag is the gross area of the section, Ac is the area of the confined core, f'c is the specified strength of the concrete and fy is the yield strength of the spiral. Where architectural or other features result in large covers, the value of Ag may be based on an assumed 2 inch (50 mm) cover over the spirals.

In the plastic hinge region it may be necessary to increase the amount of lateral reinforcement. The length of the plastic hinge is specified to be not less than the maximum horizontal dimension of the column, 1/6th the length of the column, or 24 inches (610 mm). In these regions, the ratio of spiral reinforcement may not be taken less than specified by the previous expression or the greater of:

(a) for columns 3 feet (910 mm) or less in diameter:

$$P_s = 0.45(Ag/Ac - 1)f'c/fy\,[0.5 + 1.25Pe/f'cAg] \qquad (3)$$

and (b) for columns 3 feet (910 mm) or more in diameter:

$$P_s = 0.12f'c/fy\,[0.5 + 1.25Pe/f'cAg] \qquad (4)$$

These later provisions, based on research in New Zealand, require larger amounts of confinement than stipulated by the ACI Code for columns when Pe/f'cAg exceeds 40%. Current practices do not normally result in such large axial load intensities.

Where longitudinal bars are provided outside of the special transverse reinforcement, they shall be supported laterally by cross ties (see Fig 7). The cross tie must be hooked around the longitudinal bar at one end and fully developed in the confined core of the column at the other. The Caltrans' specifications are not specific regarding the design of these cross ties. Use of a single cross tie designed to nominal minimum specifications for tie diameter (No. 4 ties for No. 10 longitudinal bars or greater) and spacing (the lessor of 1/5th of the least dimension of the column, 6 times the diameter of the longitudinal bar or 8 inches (200 mm)) would not be expected to allow these longitudinal bars to contribute to the capacity of the plastic hinge and would likely result in significant spalling of the cover.

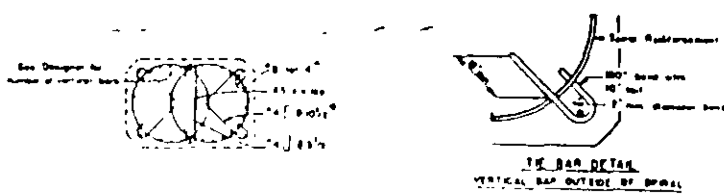

Fig. 7 Cross Tie Detail for Bars Outside of Confined Core

Piers are often designed as walls about the strong axis and as columns about the weak axis. Overlapping spirals or closely spaced ties and cross ties are used as lateral reinforcement when a z

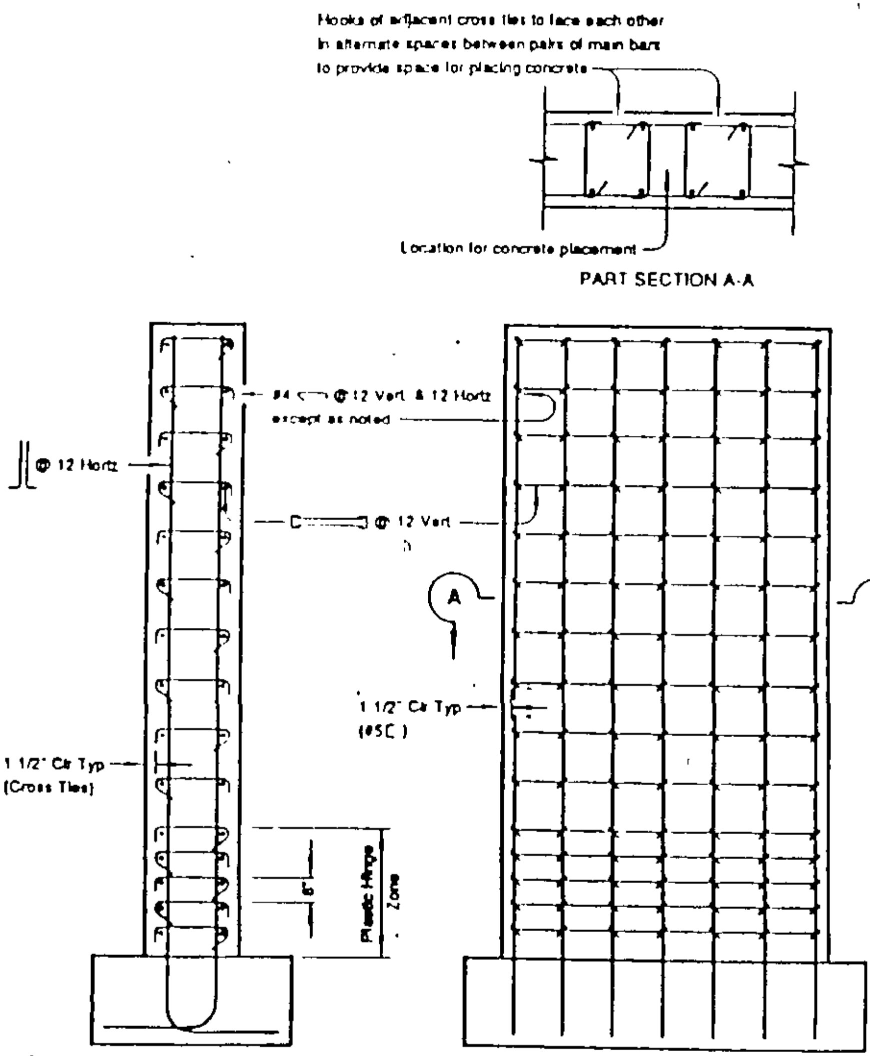

PIER WALL EXAMPLE REINFORCEMENT FOR LIGHTLY LOADED WALLS
DESIGNED FOR DUCTILITY/RISK FACTOR EQUAL TO 2
FOOTING REINFORCEMENT NOT SHOWN

Fig 8 Pier Wall Details

factor corresponding to column design is employed n the weak axis direction. However, Memo to Designers 6-5 [5] indicates that, if the axial load in the pier is less than 40% of the balanced load and a Z factor of 2 or less is used, less stringent criteria may be employed (see Fig. 8) In this case, vertical spacing of horizontal ties shall not exceed the smaller cross-sectional dimension or 12 inches (300 mm) whichever is less. In a possible plastic hinge zone, the maximum spacing is reduced to 6 inches (150 mm). Special requirements are stipulated for bundled bars. Cross ties, with 135 degree hooks on one end and 90 degree hooks on the other end, are used at each intersection of longitudinal and transverse reinforcement.

3.3 Anchorages

Development length requirements in the Caltrans' Bridge Design Specifications are essentially the same as in the 1983 ACI Code for gravity load. Revisions to these provisions in the 1989 ACI Code are not reflected in the Bridge Design Specifications. The main difference is that the basic development length of No. 18 bars is increased in the new ACI specifications by about 14%. The ACI has more definitive descriptions for cases where bar spacing and transverse reinforcement modify the basic development length. Relatively severe penalties are imposed by the new ACI code for close bar spacing. These new ACI modification factors could give substantially different development length requirements than computed using the Caltrans' Bridge Design Specifications, depending on the particular situation. Requirements for bundled bars and hooked bars are virtually identical for the ACI Code and the Bridge Design Specification. As a practical matter the Caltrans' Division of Structures is using the 1989 ACI Code development length provisions in design.

The ACI stipulates special anchorage length requirements for hooked and straight bars in joints. These lengths take advantage of reductions in the basic development length provided by mandated confinement for joints and include increased due to the expected deterioration of anchorage due to cyclic load reversals. The Caltrans' Bridge Design Specifications contain no such special anchorage requirements for seismic loading conditions.

3.4 Joints

Column to bent cap joints are designed through a combination of nominal detailing and limitations on ultimate shear stresses at the joint. Lateral reinforcement in the columns is continued into the joint (at least partially) and column and bent cap steel are (with exceptions) to be fully developed into the joint region (see Fig. 6). The shear stress for the joint may not exceed 12 f'c for normal weight concrete and 75% of this value for lightweight concrete. These values are the same as provided by the ACI Code for a joint with members framing into fewer than two of its transverse sides.

However, it should be noted that the design philosophy adopted by the ACI Code tends to force plastic hinging into the beams. Since the column reinforcement is expected to remain elastic and additional lateral reinforcement (spirals or ties) is provided in joints, a joint is confined horizontally and vertically by closely spaced reinforcement that remains essentially elastic. In the case where column longitudinal steel is expected to yield significantly, as is the case with bridges designed in accordance with Refs. 1 and 2, it is doubtful that the column flexural reinforcement can contribute effectively to the required confinement and shear resistance. Consequently, the adequacy of these types of joint details remains unclear. Elementary calculations can be carried out to demonstrate that vertically oriented stirrups may be required in typical cases on the basis of joint equilibrium. Furthermore, vertical ties may be needed to help confine the joint when the column steel is yielding. Additional investigations are required to assess this situation.

4. CAPACITY DESIGN PRINCIPLES

4.1 General

Capacity design is a intrinsic part of U.S. bridge design procedures. As adopted by Caltrans [2] this consists of postulating plastic hinges in the columns,[3] making a realistic assessment of the maximum likely flexural capacity of the critical plastic hinges, and distributing the effects of these plastic capacities to other elements in the structure on the basis of equilibrium. In addition, variations in capacity reduction factors further promote the development of flexural failures in all elements over those associated with shear and axial load. As indicated previously, smaller amounts of yielding are anticipated in some regions of the structure. Notably, abutments are expected to yield, and where keys exist in abutments they are typically designed as fuses that protect subgrade elements.

The results of the elastic dynamic analysis is used to select the capacity of the plastic hinge regions. The elastically computed moments may be used directly (without reduction) or may be reduced by the ductility and importance factor, Z. The column plastic hinge is then designed for 83% of this moment, as a moment capacity reduction factor of 1.2 is specified for earthquake loading. The probable plastic moment capacity of the plastic hinge is then taken as 1.3 times the nominal moment capacity of the actual section selected. The 1.3 factor is used to account approximately for increases in strength due to overstrength material properties resulting from as-built conditions, age strengthening of concrete, confinement effects on concrete and strain hardening in the reinforcement, and an anticipated ultimate concrete compressive strain in excess of 0.003 at failure. The code stipulates that more refined analyses are warranted to determine probable capacity in some cases, such as when axial loads exceed the balanced load.

The column axial load specified for seismic design consists of the

dead load plus or minus the axial forces resulting from an analysis of the distribution of forces due to plastic hinging in the bent. The dependence of flexural capacity on axial load makes design of the column an iterative process. In addition, it is interesting to note that the capacity reduction factor for axial loads in columns is 1.0. The difference between this value and 1.2, utilized for flexure, tends to promote a flexural, over an axial, failure mode.

Column shear forces are based on statics considering the probable plastic moment capacity of the column and the distance between hinges (Fig. 9). When columns are flared, plastic hinges are conservatively assumed (for shear) to occur outside of the flared regions. The length of the plastic hinge is estimated as the greater of: (a) the maximum horizontal dimension of the prismatic portion of the column; (b) 1/6th of the length of the column; or (c) 24 inches (61 cm). Special provisions are stipulated for shear design of the flared portions of the column as well as for cases where the column is the extension of a CIDH concrete pile. The capacity reduction factor utilized for shear design is 0.85, which further mitigates against a shear failure in the columns.

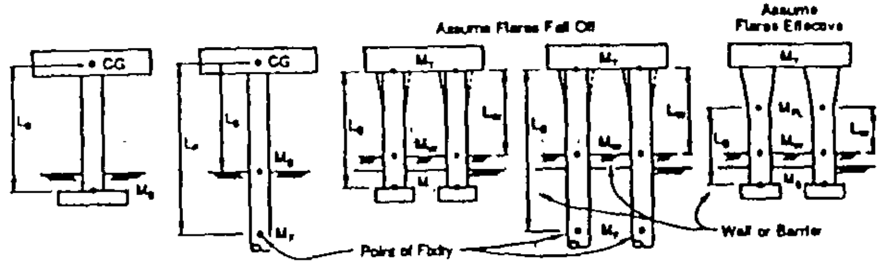

$$V = \frac{M_B}{L_B} \qquad V = \frac{M_B}{L_B} \text{ or } V = \frac{M_F}{L_F} \qquad V = \frac{M_T + M_W}{L_W} \text{ or } V = \frac{M_T + M_B}{L_B} \qquad V = \frac{M_T + M_W}{L_W} \text{ or } V = \frac{M_T + M_F}{L_F} \qquad V = \frac{M_{FL} + M_W}{L_W} \text{ or } V = \frac{M_{FL} + M_B}{L_B}$$

Fig. 9 Potential Plastic Hinge Locations and Column Shears

The design of other elements of the lateral load resisting system is stipulated in terms of developing the forces obtained from the elastic dynamic analysis of the structure (unreduced) or the forces consistent with plastic hinging in the columns. The intent of these provisions is clear, though their location in the specifications and the manner in which they are written may confuse the inexperienced designer.

The Caltrans' Bridge Design Specification stipulates lateral load conditions combining 100% of the design load in one direction with 30% of the load associated with the orthogonal direction. This criterion is applied about both principal axes of the structure. An implication of this criterion is that whenever Z values greater than 1/0.3 = 3.3 are employed in design, bidirectional yielding must be anticipated in columns. This can be easily accounted for in circular or other types of columns. It may necessitate, however, special considerations when applying capacity design methods to the design of bent caps and, especially, outriggers.

4.2 Columns

As indicated above capacity design principles are clearly elucidated by Caltrans for columns. Procedures for computing maximum forces in columns are well developed on a practical basis. Potential problems that may develop due to difficulties in estimating axial loading in the column due to bidirectional loading and vertical ground and structural accelerations are treated on a case by case basis.

4.3 Soil-Foundation System

Typically, common practice is to avoid yielding and damage to subgrade elements. However, local yielding and distress may be anticipated in footings due to the use of a capacity reduction factor of unity for both shear and flexure. The adequacy of pin connection details where the plastic shear capacity of the column must be transferred by shear friction may be questioned. However, so long as the column is adequately confined, slippage at the pin connection would not be expected to be a life safety issue.

In areas supported on soft soil, special ductile detailing provisions should be incorporated in pile foundations. Detailing these elements on the basis of strength and pile driving considerations may not be sufficient considering the uncertainties in predicting pile response.

4.4 Connections between Deck and Columns

Joint provisions in the Bridge Design Specifications are not highly developed. The performance of joints in even relatively new bridges during the Loma Prieta earthquake suggests that these provisions need re-evaluation.

4.5 Abutments

The lateral load resisting elements of the abutment system are designed using the strength method consistent with the assumptions utilized in seismic analysis. The response modification factor utilized in the design of seismic elements is 2, less than half of that used for column bents. Thus, damage in the abutments is expected, but the damage should be less than that in the column bents. The design of the abutments is directed towards prevention of collapse, control deformations at the support and realistic

assessment of displacements at the column bents.

In diaphragm abutments it is assumed that the abutment engages the backfill immediately. As such, it is impracticable to proportion the diaphragm just below the level of the roadway to be stronger than the capacity of the backfill. Damage to the diaphragm would be expected. The analytical model utilized is modified (softened) when this overstress is detected.

Seat abutments are designed for less force than diaphragm abutments, but measures must be taken to prevent the superstructure from being unseated during the earthquake. Positive longitudinal and transverse restraints are required. Typically, this is provided by shear keys in the transverse direction and by passive soil resistance of one abutment backwall for the longitudinal direction. Because of the high capacity of the backfill the back wall adjacent to superstructure is expected to be critical and designed accordingly. Th stiffness of the analytical modeling is reduced to reflect overstressed conditions when they occur..

The bearing support width for seat abutments is based on the maximum displacement predicted by the elastic seismic analysis or the following expression which ever is greater:

$$N = (12 + 0.03L + 0.12\,H)(S^2/8000 + 1) \qquad (5)$$

where L is the length of the bridge deck in feet from the abutment to the first expansion joint, H is the average height in feet of the columns supporting the deck, S is the skew of the abutment in degrees. The bearing support width should not be less than 2 ft. - 6 in. (762 mm). These provisions of the Caltrans specifications are adapted from AASHTO guideline to account for skew.

4.6 Deck

The deck is not usually considered part of the lateral load resisting system. However, consistent with the objective of maintaining the operability of the structure following a major earthquake, it is desired to maintain elastic behavior in the deck.

Provisions are not specified for cases where the deck is to actively participate in the lateral load resisting system, as might b the case for the longitudinal direction of the roadway. Detailing requirements and load transfer mechanisms are developed on a case by case basis.

4.7 Deck Joint Restraining Devices

Longitudinal restraining devices at expansion joints and hinges are intended to remain elastic under the earthquake induced loading in order to prevent unseating of adjacent sections of the deck. The equivalent static method of analysis is recommended for determining the longitudinal forces in the restrainers. This procedure is believed to be conservative and avoids problems in estimating seat openings that occur with dynamic analysis methods as a result of trying to superimpose the deflections of incompatible modes. Friction forces developed on the seat surface may not be considered as contributing to the required restraining force.

The static method of design isolates a small segment of the structure located between expansion joints. Lateral displacements at the expansion joint in question are initially estimated by applying unreduced static earthquake loads to a deck segment on one side of the joint. Two separate analyses are required. One analysis for each segment adjacent to the joint. Any restraining effect of the restrainers is ignored in these initial calculations. The contribution of one additional adjacent segment may be considered in the direction of deck motion, if the computed displacements are sufficient to close the gap separating the two segments. If the computed displacements exceed the seat width provided (minus a 4 in. (10 cm) safety margin), restrainers are provided to reduce the displacements. The displacement of the restrained system is then checked (assuming the restrainers are fixed at the end away from the direction of motion). Because the weaker of the two segments will be forced to move along with the stronger segment by the restrainers, the smaller number of restrainers computed for each segment is used at the joint. Clearly, this process is complex and iterative involving modifications in number, size and length (i.e., stiffness) of restrainers, initial slack in the restrainer system, the gap width between segments, seat width and segment (column) stiffness.

When vertical seismic forces are computed at a hinge that exceed 50% of the dead load reaction, hold down devices are required. These devices are intended to minimize the potential effects of vertical motions.

When rigid restraining devices, like keys, are used, they are designed for amplified loadings relative to the elastic response spectrum analysis results (i.e., a Z factor of 0.8 is employed). However, keys at abutments are most often intentionally designed to have a smaller capacity than than the piles, footings and soil in order to limit damage to these subgrade elements.

5. CONCLUDING REMARKS

The earthquake resistant design provisions utilized in the U.S. for areas of high seismic risk are based on absorbing a significant amount of the energy imparted by the earthquake through ductile yielding. Satisfactory performance is regulated though the used of ductility/importance factors which control the degree of yielding, capacity design concepts that control the distribution of damage (plastic hinging), and local details that insure adequate ductility capacity at the critical plastic hinges.

Due to the limited research that has been carried out on the seismic

performance of bridge structures, bridge design specifications are not as refined as those promulgated for buildings. While the overall earthquake design procedures stipulated by Caltrans for bridges is conceptually sound, the format makes its implementation by inexperienced designers problematic. In addition, significant areas exist which need additional research upon which improved code provisions might be based. These areas include joint shear and confinement, foundation design, built-in pins, hinge restrainers, abutment design details, and so on. Similarly, a whole spectrum of unresolved problems exist related to the three dimensional response and behavior of elements and bridges.

Problems associated with precast and other types of non-monolithic bridge construction also need to be addressed. Such structural types are common in the U.S. in areas of lessor seismic hazard. The relationship of seismic hazard, required details and expected performance needs to be carefully assessed for areas of moderate seismic risk.

6. REFERENCES

1. Standard Specifications for Highway Bridges, American Association of State Highway and Transportation Officials, 444 N. Capitol Street, N.W., Suite 225, Washington DC 20001, 1987.

2. Bridge Design Specifications Manual, State of California, Department of Transportation, Office of Structure Design, Sacramento, June 1990.

3. Warriner, P. and Mancarti, G., "Abutments," Memos to Designers (5-1), State of California, Department of Transportation, Office of Structure Design, Sacramento, Sept. 1988.

4. Mellon, F. and Mancarti, G., "Column Analysis Considerations," Memos to Designers (6-1), State of California, Department of Transportation, Office of Structure Design, Sacramento, June 1990.

5. Warriner, P. and Mancarti, G., "Reinforced Concrete Pier Walls," Memos to Designers (6-5), State of California, Department of Transportation, Office of Structure Design, Sacramento, Oct. 1988.

6. Mellon, F. and Mancarti, G., "Restrainers at Hinges and Bearings," Memos to Designers (20-3), State of California, Department of Transportation, Office of Structure Design, Sacramento, Nov. 1989.

7. Mellon, F. and Mancarti, G., "Earthquake Retrofit Analysis of Single Column Bridges," Memos to Designers (20-3), State of California, Department of Transportation, Office of Structure Design, Sacramento, Jan. 1990.

8. Committee 318, Building Code Requirements for Reinforced

Concrete and Commentary, American Concrete Institute, Detroit, MI, 1989.

9. Roberts, J. and Maroney, B., "Theory of California Seismic Bridge Design and Analysis for the Beginner," Training Material, State of California, Department of Transportation, Office of Structure Design, Sacramento, 1990.

10. Bridge Design Details Manual, State of California, Department of Transportation, Office of Structure Design, Sacramento, June 1989.

Basic Design Concepts

Japan
[K. Kawashima, H. Ichimasu, J. Kodera]

1.1 INTRODUCTION

Highways in Japan consist of Expressways (3,721 km), National Highways (46,661 km), Prefectural Roads (128,202 km), and Municipal Roads (925,138 km). Along the highways and roads, excluding the Municipal Roads, there are about 60,000 bridges with span lengths (deck length between two adjacent substructures) of 15 m or longer.

Although the number of bridges constructed per year depends on the year and span length, it is about 6000 for concrete bridges and 2000 for steel bridges with a length of 15 m or longer.

Design of highway bridges with span lengths less than 200 m is made in accordance with the "Design Specifications of Highway Bridges" issued by the Ministry of Construction. The Design Specifications of Highway Bridges consist of "Part I Common Part", "Part II Steel Bridges", "Part III Concrete Bridges", "Part IV Foundations" and "Part V Seismic Design". The explanation for the main body of the specifications are provided and published by the Japan Road Association [1-1] .

Design of highway bridges with span length larger than 200 m, such as the Honshu-Shikoku Bridge Project, is made in accordance with the specifications which are stipulated exclusively for the bridges However the basic concepts of seismic design for such long bridges are essentially the same as those in the Design Specifications of Highway Bridges

This paper summarizes the current seismic design philosophy of highway bridges with span lengths less than 200 m in Japan.

1 2 DAMAGES OF HIGHWAY BRIDGES IN THE PAST EARTHQUAKES

Located along the Pacific Seismic Belt, Japan is one of the most seismically disastrous countries in the world and has often suffered significant damage from large earthquakes. Fig. 1.1 shows the largest magnitude of the earthquakes which occurred in the past [1-2] . It is recognized that the earthquakes with magnitude over 8 have occurred with rather short recurrent period in and around Japan in the past It should be noted that seismicity is especially high along the Pacific coast. Cities large in population and industrial products such as Tokyo, Osaka and Nagoya are located in this region.

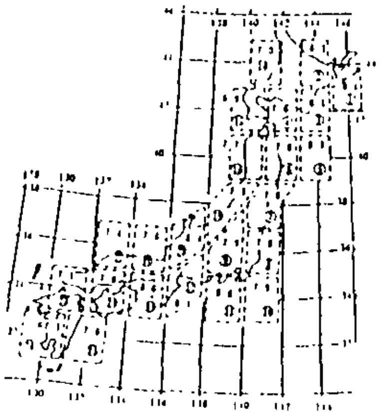

Fig 1-1 Largest Magnitude of Earthquakes in the Past

Table 1 1 shows the highway bridges which suffered damage in the past earthquakes since the Kanto Earthquake of 1923 It should be noted that although there were many bridges which suffered damage due to earthquakes, the number of bridges which fell down was only 15

Based on surveys of the damaged bridges, it is pointed out that the three major factors which contributed to the damage of bridges are [1 3] :

a) weakness of substructure,
b) weakness of bearing supports, and
c) weakness of surrounding subsoils.

From such factors, the following types of damages were most often developed in the past :

a) substructure tilting, settlement, sliding, cracks, and overturning
b) superstructure : movement, buckling and cracks near the supports, and falling of girder
c) bearing supports · failure of supports, and pull out or rupture of anchor bolts

Table 1-1 Damage of Highway Bridges in the Past since Kanto Earthquake of 1923

DATE	EARTHQUAKE	MAGNITUDE	NUMBER OF BRIDGES DAMAGED	NUMBER OF BRIDGES WHICH FELL DOWN
1923 9 1	KANTO	7.9	1785	6
1946 12 21	NANKAI	8.1	346	1
1948 6 28	FUKUI	7.3	243	4
1949 12 26	IMAICHI	6.4	1	0
1952 3 4	TOKACHI OKI	8.1	128	0
1962 4 30	MIYAGI KEN HOKUBU	6.5	187	0
1964 6 16	NIIGATA	7.5	98	3
1968 2 21	EBINO	6.1	10	0
1968 5 16	TOKACHI OKI	7.9	101	0
1978 1 14	IZU OHSHIMA	7.0	7	0
1978 6 12	MIYAGI KEN OKI	7.4	95	1
1982 3 21	URAKAWA OKI	7.1	5	0
1983 5 26	NIHON KAI CHUBU	7.7	176	0
1984 9 14	NAGANO KEN SEIBU	6.8	14	0
TOTAL			3191	15

Although these kinds of damage are the ones commonly observed in past earthquakes, the damage types have been changing in accordance with the progress of seismic design methods and improvements in construction practice. Seismic damage since the 1923 Kanto Earthquake may be classified into three stages from their significance [1-4] (refer to Table 1-2).

(1) Damage due to Inadequate Strength of Foundations - Stage I -

After experiencing the destructive damage of the 1923 Kanto Earthquake, the first requirements for seismic design of highway bridges were included in the "Details of Road Structures (Draft)" issued by the Ministry of Internal Affairs in 1926. No seismic effects were considered for design of highway bridges prior to the Kanto Earthquake. Even after the first stipulations issued in 1926, seismic design was not adequate because the stipulations only described design force levels without providing a detailed design method or design details. Therefore, seismic safety of bridge substructures was inadequate until the 1950's when seismic design for foundations and substructures came to be widely adopted

In those days, when seismic effects were either disregarded or inadequately considered, seismic damage was characterized by failure of foundations and substructures as shown in Photos 1-1 and 1-2. In most cases, foundations

Table 1-2 Change of Damage Types

Year	Major Earthquakes	Change of Major Seismic Damage	Seismic Design Method	Seismic Inspection and Strengthening
1920	1923 Kanto Earthquake (M7.9)	Failure of Superstructure due to Tilting/Movement of Foundation	1926 Initiation of Seismic Design (Details of Road Structures)	
1930				
1940	1946 Nankai Earthquake (M8.1) 1948 Fukui Earthquake (M7.3)	Failure of Concrete around Fixed Bearing Damage due to Liquefaction	1939 Introduction of Standard Seismic Coefficient (Design Specifications of Steel Highway Bridges)	
1950	1952 Tokachi-oki Earthquake (M8.1)	Failure of RC Piers, and Bearing	1956 Seismic Coefficient depending on Zone and Ground Condition (Design Specifications of Steel Highway Bridges)	
1960	1964 Niigata Earthquake (M7.5)			
1970	1978 Miyagi-ken-oki Earthquake (M7.4)		1971 • Seismic Coefficient depending on Zone, Ground Conditions, Importance and Structural Response • Introduction of Evaluation Method for Liquefaction (Specifications for Seismic Design)	1971 Seismic Inspection 1976 Seismic Inspection 1979 Seismic Inspection
1980	1982 Urakawa-oki Earthquake (M7.1) 1983 Nihon-kai-chubu Earthquake (M7.7)		1980 • Part V Seismic Design, Specifications for Design of Highway Bridges • Introduction of New Evaluation Method for Liquefactions	1986 Seismic Inspection
1990			1990 Part V Seismic Design, Specifications for Design of Highway Bridges	

tilted, moved or even overturned due to inadequate strength of the foundations and the surrounding subsoils. This led to falling-off of the superstructures.

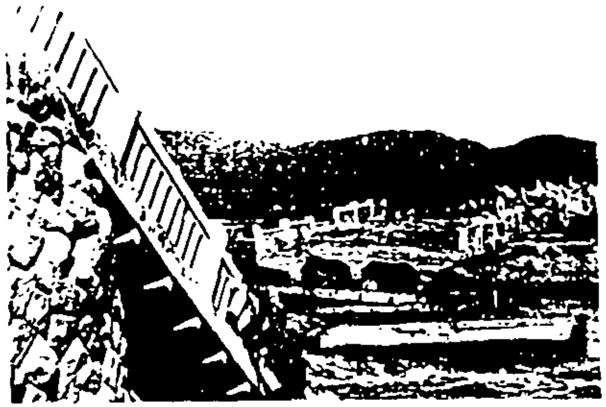

Photo 1-1 Damage of Sakawa-gawa Bridge on National Highway No. 1 by the Kanto Earthquake of 1923

Photo 1-2 Damage of Nakazuno Bridge by the Fukui Earthquake of 1948

(2) Damage due to Soil Liquefaction - Stage 2 -

Although the damage due to inadequate strength of foundations became less frequent in accordance with the improvement of seismic design and construction methods, the next stage of damage encountered was soil failure during the 1964

Niigata Earthquake. Soil liquefaction, which took place extensively around sites, caused destructive damage to bridges. Photos 1-3 and 1-4 shows the falling off of the decks of the Showa Bridge and th Higashi Overcrossing. Extensive soil movement associated with liquefact. . [1-5] caused large lateral movements of bent pile foundations, which caused the deck to fall. Fig 1-2 shows the damage of Yachiyo Bridge due to such liquefaction induced lateral movement of soils.

Photo 1-3 Damage of Showa Bridge by the Niigata Earthquake of 1964

Photo 1-4 Damage of Higashi-Kosen Bridge by the Niigata Earthquake of 1964

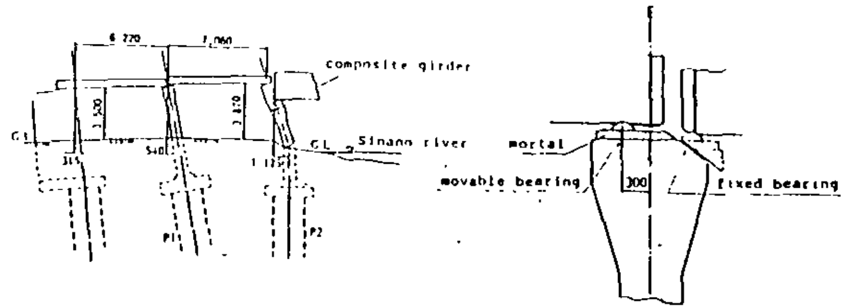

(a) Residual Displacement of piers (b) Damage of Bearing Seat

Fig. 1-2 Damage of Yachiyo Bridge due to Liquefaction Induced Soil Movement during Niigata Earthquake of 1964

Through the damage, it was learned that it is important to take account of liquefaction in design of bridges, and various studies for assessing and evaluating the effects of liquefaction were initiated. Through such studies, the first stipulations for assessment of liquefaction were introduced in the "Seismic Design Specifications of Highway Bridges" in 1971 [1-6].

One more important lesson gained from the Niigata Earthquake was that devices for preventing superstructures from falling from the crest of substructures are required. It was considered that even if large relative movements between the deck and substructures occurred due to either failure of substructures or failures of soils such as soil liquefaction, critical failure causing the deck to fall could be prevented if such devices were provided. Various devices were then developed, and design recommendations were included in the Seismic Design Specifications of Highway Bridges issued in 1971.

(3) Damage to Piers and Bearing Supports - Stage 3 -

In recent earthquakes including the Miyagi-ken-oki Earthquake (M7.4) of 1978 and the Nihon-kai-chubu Earthquake (M7.7) of 1983, substantial damage due to inadequate strength of foundations and effects of soil liquefaction did not develop in those bridges designed and constructed in accordance with the recent design specifications. However, damage to reinforced concrete piers and bearing supports did develop extensively as shown in Photos 1-5, 1-6 and 1-7. This is due to the fact that other modes of failures such as tilting or movement of the foundations, soil liquefaction, and falling-off of superstructures were prevented by the new design recommendations.

The new strengthening and earthquake resistant countermeasures brought damage at the next weak points such as the reinforced concrete piers and the bearing supports. This obviously shows that countermeasures aiming only at minimizing the damage observed in past earthquakes do not necessarily contribute to avoiding new types of damage in future earthquake . now required to take account of the total seismic safety of highway . , and this was the main scope of the latest revision of the seismic design specifications in 1990.

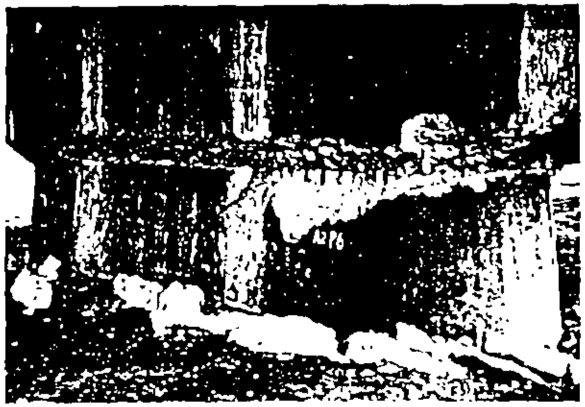

Photo 1-5 Damage to Reinforced Concrete Piers of Sendai Bridge by the Miyagi-ken-oki Earthquake of 1978

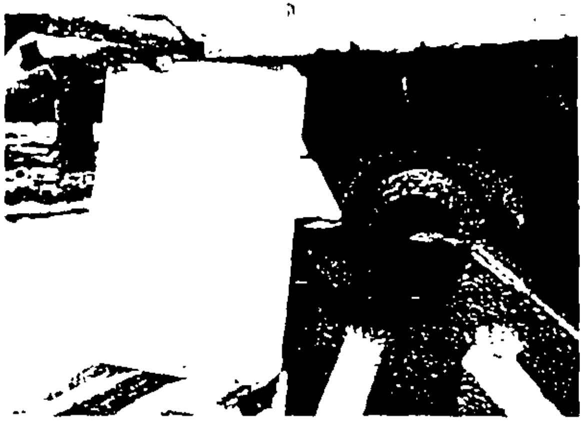

Photo 1-6 Damage to Bearing Supports of Date Bridge by the Miyagi-ken-oki Earthquake of 1978

It should be noted here that the damage shown in Photo 1-7 was developed by shear at the mid-height of the reinforced concrete piers where main reinforcement was terminated. In the design specifications issued prior to 1980, the main reinforcement was terminated with the bond length of 20 times the diameter of the main reinforcement. Through the damage, such as that shown in Photo 1-7, the bond length was revised in the 1980 specifications to 20 times the diameter of the main reinforcement plus the effective depth of the pier.

Photo 1-7 Damage to Reinforced Concrete Piers of Shizunai Bridge by the Urakawa-oki Earthquake of 1982

1.3 HISTORY OF SEISMIC DESIGN OF HIGHWAY BRIDGES

Seismic design was initiated for highway bridges in 1926 after the experience of the Kanto Earthquake in 1923. The importance of considering seismic effects in design of highway bridges was recognized from the extensive damage resulting from the Kanto Earthquake. The first stipulations requiring seismic effects for highway bridges were included in "Details of Road Structures (Draft)" issued by the Ministry of Internal Affairs in 1926. It was stipulated in the draft details that the maximum lateral force expected to develop at the site shall be considered in seismic design. It was also recommended in the draft details that the 30 % of gravity force shall be adopted for the reconstruction of the bridges damaged by the Kanto Earthquake at Tokyo and Yokohama.

After experiencing significant damage during strong earthquakes seismic regulations were reviewed and amended several times as shown in Table 1-3. "Design Specifications of Steel Highway Bridges (Draft)" were issued in 1939, and "Design Specifications of Steel Highway Bridges" and the revised version were issued in 1956 and 1964, respectively. A seismic lateral force of 20 % of the gravity force was stipulated in these specifications. The 20 % gravity force was considered for a long time as a basic design force for highway bridges.

The first comprehensive seismic design stipulations were issued by the Ministry of Construction in 1971 in a separate volume exclusively for seismic design as "Specifications for Seismic Design of Highway Bridges". It was described in the specifications that lateral force shall be determined depending on zone, importance and ground condition in the static lateral force method (seismic coefficient method) and structural response shall be further considered in the modified static lateral force method (modified seismic coefficient method). Evaluation of soil liquefaction was firstly incorporated in view of the damage caused in the 1964 Niigata Earthquake. Design details to increase the seismic safety such as devices to prevent the superstructure falling from substructures were newly introduced. Design methods for substructures were also issued between 1964 and 1971 in the form of "Design Specifications of Substructures". Therefore, it is considered that considerable increases in seismic safety were made for those bridges designed and constructed in accordance with the 1971 Specifications.

Table 1.3 History of Design Seismic Loads for Highway Bridges in Japan

Year	Name of Regulations	Seismic Design Methods	Other Stipulations for Seismic Effects	Major Earthquakes
1886	Order No. 13, Ministry of Internal Affairs	Not Considered	Not Considered	1891 Nohbi (M8.4) 1923 Kanto (M7.9)
1926	Details of Road Structures (Draft), Road Law, MIA	Seismic Coefficient Method k_h=0.15~0.4 ($k_h \geq$0.3 advised in Tokyo and Yokohama)	Not Considered	
1939	Design Specifications of Steel Highway Bridges (Draft), MIA	Seismic Coefficient Method (k_h=0.2, k_v=0.1)	Not Considered	1946 Nankai (M8.1) 1948 Fukui (M7.3)
1956 (and 1964)	Design Specifications of Steel Highway Bridges, Ministry of Construction	Seismic Coefficient Method (k_h=0.1~0.35)	Not Considered	1952 Tokachi-oki (M8.2) 1964 Niigata (M7.5)
1971	Specifications for Seismic Design of Highway Bridges, MOC	• Seismic Coefficient Method (k_h=0.1~0.24) • Modified Seismic Coefficient Method (k_h=0.05~0.3)	• Evaluation of Sandy Layers Vulnerable to Liquefaction • Device for Preventing Falling-off of Superstructure	1978 Miyagi-ken-oki (M7.4)
1980	Part V Seismic Design of Design Specifications of Highway Bridges, MOC	• Seismic Coefficient Method (k_h=0.1~0.24) • Modified Seismic Coefficient Method (k_h=0.05~0.3) • Check of Deformation Capability of RC Piers • Dynamic Response Analysis	• F_L Method for Evaluation of Liquefaction • Device for Preventing Falling-off of Superstructure	1982 Urakawa-oki (M7.1) 1983 Nihon-kai-chubu (M7.7)
1990	Part V Seismic Design of Design Specifications of Highway Bridges, MOC	• Seismic Coefficient Method (k_h=0.1~0.3) • Check of Bearing Capacity of RC Piers for Lateral Force • Dynamic Response Analysis	• F_L Method for Evaluation of Liquefaction • Device for Preventing Falling-off of Superstructure	

The 1971 specifications were revised by the Ministry of Construction in the form of "Part V Seismic Design" of the "Design Specifications of Highway Bridges" in 1980. Although the Part V was essentially the same as the 1971 Specifications, a rational evaluation method for predicting soil liquefaction as well as practical design methods at the time when liquefaction is judged to occur (1-6) were included in the Part V Seismic Design.

The latest specifications were issued by the Ministry of Construction in February 1990 in the form of "Part V Seismic Design " for the " Design Specifications of Highway Bridges" (1-1,1-8) . Major revisions introduced in the 1990 Specifications were unification of static lateral force method (seismic coefficient method) and the modified static lateral force method (modified seismic coefficient method) including the revision of the seismic design force, a new method for computing inertia force for multi-span continuous bridges, a new ductility check for reinforced concrete piers, and detailed stipulations for dynamic response analysis. These revisions were incorporated based on the recent studies for predicting earthquake ground motions and strength of reinforced concrete piers (1-9~1-27)

The "Part V Seismic Design" of the "Design Specifications of Highway Bridges" has the following contents :

1.4 SEISMIC DESIGN PHILOSOPHY OF HIGHWAY BRIDGES

Fig. 1-3 shows the flow of seismic design of highway bridges. Basic concepts for seismic design are as

a) Seismic design shall be made to provide highway bridges with sufficient stability against earthquake disturbance, using the seismic design method

specified in the "Part V Seismic Design" of the "Design Specifications of Highway Bridges". Structural characteristics, topographical, geological and soil conditions at the site, past experience of seismic damage and importance of

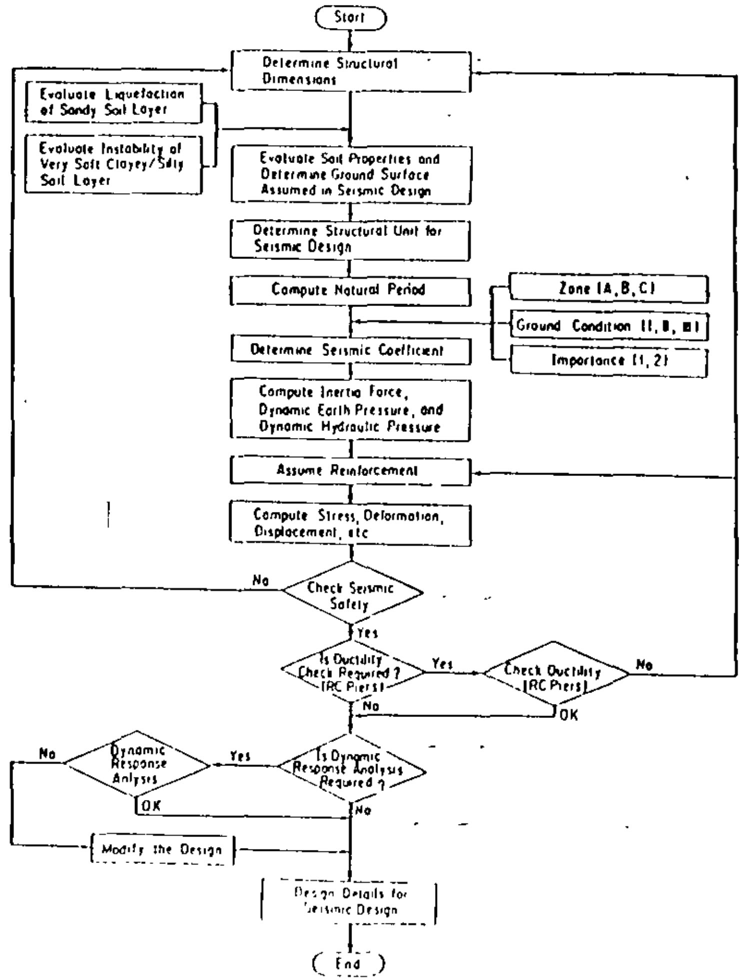

Fig. 1-3 Flow of Seismic Design of Highway Bridge

the bridge have to be taken into account in seismic design. Highway bridges shall not suffer structural damage to avoid suspension of traffic against small to moderate earthquakes which have a high possibility of occuring at the site, and shall be designed not to cause catastrophic damage such as falling off of superstructure from the substructure even for large earthquakes such as the Kanto Earthquake in 1923.

b) Design shall be made based on the allowable stress design method. The load combination for seismic design is of the principal load (P) + seismic effects (EQ). The principal load (P) includes dead weight (D), prestressing force (PS), effects of creep (CR), effects of shrinkage (SH), earth pressure (E), hydropressure (HP) and uplift force (U). The seismic effects include inertia force, increase of earth pressure during earthquakes and hydrodynamic pressure. Effects of unstability of subsoils such as failure of weak cohesive soils and liquefaction of saturated sandy soils has to be considered in seismic design. Allowable stress can be increased 50 % for load combination of P + EQ.

c) Lateral force shall be computed by the static lateral force method, in which the lateral force is determined by multiplying the weight W of the structure with the lateral force coefficient k. Lateral force in vertical direction may be generally neglected in design calculation except for design at bearing supports, where the vertical force coefficient of 0.1 is considered.

d) Seismic lateral force shall be applied to structures, soils and water above the "ground surface assumed in seismic design". Seismic lateral force for structural members, soils and water below the ground surface assumed in seismic design shall be considered as zero. The ground surface assumed in seismic design is taken at the upper level of stable soils, and is generally assumed as the base of footing for pile foundations. When the surface soils are vulnerable to liquefaction or unstability of weak cohesive soils, the ground surface assumed in seismic design has to be assumed below such unstable soils.

e) Lateral force coefficient k_h shall be determined in accordance with region, ground condition, importance and natural period. The lateral force coefficient k_h shall not be less than 0.1.

f) A Check of the bearing capacity is recommended for reinforced concrete piers to avoiding brittle failure. Check of bearing capacity of reinforced concrete piers shall be made based on the lateral force coefficient k_{hc} which is exclusively specified in the specifications for this purpose.

g) Dynamic response analysis is recommended for new types of bridges and those which have complex structural response characteristics.

h) devices for preventing the superstructure from falling must be installed.

1.5 SEISMIC LATERAL FORCE FOR STATIC LATERAL FORCE METHOD

1.5.1 Seismic Lateral Force Coefficient

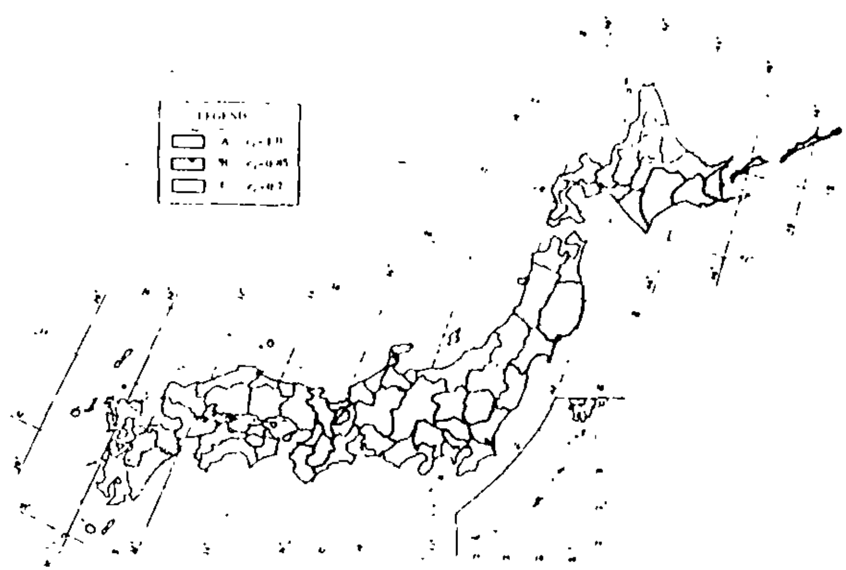

Fig. 1-4 Seismic Zoning Map and Modification Coefficient c_z

Table 1-4 Ground Condition Factor c_G

Ground Group	I	II	III
c_G	0.8	1.0	1.2

Table 1-5 Importance Factor c_I

Group	c_I	Definition
1st class	1.0	Bridges on expressway (limited access highways), general national road and principal prefectural road. Important bridges on general prefectural road and municipal road.
2nd class	0.8	Other than the above

Table 1-6 Structural Response Factor c_T

Ground - Group	Structural Response Coefficient c_T		
Group I	$T < 0.1$ $c_T = 2.69T^{1/3} \geqq 1.00$	$0.1 \leqq T \leqq 1.1$ $c_T = 1.25$	$1.1 < T$ $c_T = 1.33T^{-2/3}$
Group II	$T < 0.2$ $c_T = 2.15T^{1/3} \geqq 1.00$	$0.2 \leqq T \leqq 1.3$ $c_T = 1.25$	$1.3 < T$ $c_T = 1.49T^{-2/3}$
Group III	$T < 0.34$ $c_T = 1.80T^{1/3} \geqq 1.00$	$0.34 \leqq T \leqq 1.5$ $c_T = 1.25$	$1.5 < T$ $c_T = 1.64T^{-2/3}$

In the static lateral force method (seismic coefficient method), the design seismic lateral force coefficient shall be determined by Eq (1-1), but no less than 0.1

$$k_h = c_z \cdot c_G \cdot c_I \cdot c_T \cdot k_{h0} \qquad (1\text{-}1)$$

where

- k_h : design seismic lateral force coefficient,
- k_{h0} : standard design seismic lateral force coefficient (0.2),
- c_z : modification factor for zone (refer to Fig 1.4),
- c_G : modification factor for ground condition (refer to Table 1-4),
- c_I : modification factor for importance (refer to Table 1-5), and
- c_T : modification factor for structural response (refer to Table 1-6). For computing inertia force associated with weight of soils and dynamic earth pressure, c_T shall be 1.0

Eq (1-1) was determined based on the statistical analyses of 394 components of strong motion records obtained on ground surface in Japan [1-9]. Effects of composition of two horizontal components were studied. It should be noted in Eq (1-1) that although k_h was derived from the acceleration response spectra, considerable modifications were incorporated into k_h based on the past experience of seismic damage and bridge response characteristics. Special attention was paid to determine the seismic lateral force level at the natural period over 1 second

Fig. 1-5 shows the seismic lateral force coefficient k_h assuming c_z = c_I = 1.0

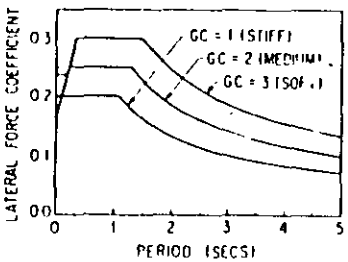

Fig 1.5 Seismic Lateral Force Coefficient k_h for Static Lateral Force Method (c_z = c_I = 1.0)

1.5.2 Classification of Ground Condition

Ground conditions are classified into three groups according to Table 1-7, in which characteristic value T_G shall be evaluated as

$$T_G = \sum_i \frac{4h_i}{V_{si}} \qquad (1\text{-}2)$$

Table 1-7 Classification of Ground Condition

GROUND CONDITION	DEFINITION	APPROXIMATE ESTIMATION
GROUP I	$T_G < 0.2$ SEC	TERTIALY OR OLDER
GROUP II	$0.2 \le T_G < 0.6$ SEC	ALLUVIUM AND DILUVIUM
GROUP III	$0.6 \le T_G$	SOFT ALLUVIUM

where

- T_G : characteristic value (sec)
- H_i : thickness of i-th subsoil layer (m)
- V_{si} : shear wave velocity of i-th sublayer (m/sec)
- i : sublayer's number counted from ground surface

1.5.3 Earth Pressure During Earthquakes

Earth pressure during earthquakes, which shall be applied to structures below the ground surface, is specified based on the Mononobe-Okabe formulae as a distributed load as

(1) Active earth pressure

$$\left.\begin{aligned} P_{EA} &= \gamma \cdot x \cdot K_{EA} - 2c \cdot \sqrt{K_{EA}} + q' \cdot K_{EA} \\ K_{EA} &= \frac{\cos^2(\phi-\theta_0-\theta)}{\cos\theta_0 \cdot \cos^2\theta \cdot \cos(\theta+\theta_0+\delta_E)\left[1+\sqrt{\dfrac{\sin(\phi+\delta_E)\sin(\phi+\alpha-\theta_0)}{\cos(\theta+\theta_0+\delta_E)\cos(\theta-\alpha)}}\right]^2} \end{aligned}\right\} \qquad (1\text{-}3)$$

(2) Passive earth pressure

$$\left.\begin{aligned} P_{EP} &= \gamma \cdot x \cdot K_{EP} + 2c \cdot \sqrt{K_{EP}} + q' \cdot K_{EP} \\ K_{EP} &= \frac{\cos^2(\phi-\theta_0-\theta)}{\cos\theta_0 \cdot \cos^2\theta \cdot \cos(\theta-\theta_0+\delta_E)\left[1-\sqrt{\dfrac{\sin(\phi-\delta_E)\sin(\phi+\alpha-\theta_0)}{\cos(\theta-\theta_0+\delta_E)\cos(\theta-\alpha)}}\right]^2} \end{aligned}\right\} \qquad (1\text{-}4)$$

If $\phi+\alpha-\theta_0 < 0$, $\sin(\phi+\alpha-\theta)$ shall be zero

where

- P_{EA} and P_{EP}: active and passive earth pressure at depth x (m) from the ground surface (tf/m²)
- K_{EA} and K_{EP}: coefficient of active and passive earth pressure
- γ : unit weight of soils (tf/m³)
- C. cohesion of soils (tf/m²)
- q' : surcharge on the ground surface (tf/m²)

θ angle between the back wall and vertical plane
δ : angle of friction between the back wall and back soils
$\theta_0 = \tan^{-1} k_h$
k_h: seismic lateral force coefficient

1.5.4 Hydrodynamic Pressure

(1) Hydrodynamic pressure on walls

Hydrodynamic pressure P (tf) acting on one side of a wall-type structures and the height h_g (m) of the pressure P from the bottom of the water shall be determined from

$$P = \frac{7}{12} \cdot k_h w_0 b h^2 \qquad (1\text{-}5)$$

$$h_g = 0.5\,h \qquad (1\text{-}6)$$

where, k_h = lateral force coefficient, w_0 = unit weight of water (tf/m³), h = depth of water (m) and b = width of wall (m).

(2) Hydrodynamic pressure on columns

Hydrodynamic pressure P (tf) acting on column type structures surrounded by water and the height h_g (m) of the pressure P from the bottom of the water shall be determined as

$$P = \begin{cases} \frac{3}{4}\, k_h w_0 A_0 h\, \frac{b}{a}\left(1 - \frac{b}{4h}\right) & \frac{b}{h} \le 2.0 \\ \frac{3}{4}\, k_h w_0 A_0 h\, \frac{b}{a}\left(0.7 - \frac{b}{10\,h}\right) & 2.0 < \frac{b}{h} \le 4.0 \\ \frac{9}{40}\, k_h w_0 A_0 h\, \frac{b}{a} & 4.0 < \frac{b}{h} \end{cases} \qquad (1\text{-}7)$$

$$h_g = 0.5\,h \qquad (1\text{-}8)$$

where, k_h = lateral force coefficient, w_0 = unit weight of water (tf/m³), h = depth of water (m), a = depth of column (m), b = width of column (m) and A_0 = sectional area of column (m²)

1.6 TREATMENT OF VERY LOOSE COHESIVE SOILS AND LIQUEFACTION

1.6.1 Sandy Soil Layers Vulnerable to Liquefaction

(1) Sandy Soil Layers to be Checked for Liquefaction

Saturated alluvial sandy layers which have the water table within 10 m from the ground surface and have D_{50}-values on the grain size accumulation curve

Saturated alluvial sandy layers which have the water table within 10 m from the ground surface and have D_{50}-values on the grain size accumulation curve between 0.02 and 20. mm are vulnerable to liquefaction up to a depth of 20 m below the ground surface, and liquefaction potential of these layers shall be estimated according to item (2).

(2) Estimation of Liquefaction

For those soil layers which are judged to be vulnerable to liquefaction, liquefaction potential shall be checked based on the liquefaction resistance factor F_L defined as

$$F_L = R / L \qquad (1\text{-}9)$$

where

F_L : liquefaction resistance factor

R : resistance of soil elements against dynamic load defined as

$$R = R_1 + R_2 + R_3$$

$$R_1 = 0.0882 \sqrt{\frac{N}{\sigma_v' + 0.7}}$$

$$R_2 = \begin{cases} 0.19 & (0.02\text{ mm} \le D_{50} \le 0.05\text{ mm}) \\ 0.225\log_{10}(0.35/D_{50}) & (0.05\text{ mm} < D_{50} \le 0.6\text{ mm}) \\ -0.05 & (0.6\text{ mm} < D_{50} \le 2.0\text{ mm}) \end{cases}$$

$$R_3 = \begin{cases} 0.0 & (0\,\% \le F_c \le 40\,\%) \\ 0.004F_c - 0.16 & (40\,\% < F_c \le 100\,\%) \end{cases}$$

N : N-value of standard penetration test

D_{50} : averaged grain size on grain size accumulation curve

F_c : fine sand (grain size less than 74 μm) content

L : dynamic load induced in soil elements during an earthquake defined as

$$L = r_d \cdot k_s \cdot \frac{\sigma_v}{\sigma_v'}$$

$$r_d = 1.0 - 0.015x$$

x : depth from the ground surface (m)

k_s : seismic coefficient for evaluating liquefaction, and shall be determined as

$$k_s = c_z \cdot c_G \cdot c_I \cdot k_{s0}$$

c_z, c_G and c_I : modification factors for zone, ground condition, and importance (refer to Fig. 1-4, Table 1-4 and Table 1-5)

k_{s0} : standard design horizontal seismic coefficient for check of liquefaction (= 0.15)

σ_v : total overburden pressure (kgf/cm²), and

$$\sigma_v = \{\gamma_{t1} h_w + \gamma_{t2}(x - h_w)\} / 10$$

σ_v' : effective overburden pressure (kgf/cm²), and

$$\sigma_v' = \{\gamma_{t1} h_w + \gamma_{t2}(x - h_w)\} / 10$$

Soil layers having liquefaction resistance factors, F_L, smaller than 1.0 shall be judged to liquefy during earthquakes, and treatment of these soils shall be made in accordance with 1.6.3.

1 6.2 Very Soft Cohesive Soils and Silty Soils

Cohesive soil layers and silty soil layers which are within 3 meters of the ground surface, and have a compression strength estimated by unconfined compression tests or field tests, less than 0 2 kgf/cm^2, shall be defined as very soft soils in seismic design. Treatment of these soils in seismic design shall be made in accordance with 1 6 3

1 6.3 Soils Whose Soil Constants are Reduced in Seismic Design

(1) For those soil layers which were judged to liquefy in the above estimation and which are within 20 m from the ground surface, the spring stiffness and other soil constants shall be either neglected or reduced in seismic design as shown in Fig 1-6, by multiplying the original spring stiffness and other soil constants by the reduction factor D_E which is determined in accordance with F_L-value and tabulated in Table 1 9

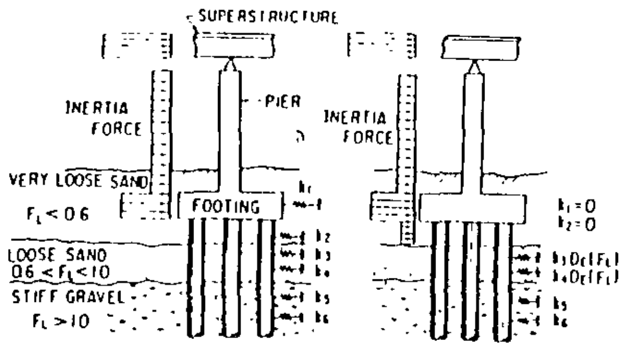

Fig 1-6 Treatment of Soil Layers Vulnerable to Liquefaction

Table 1-9 Decreasing Rate D_E of Soil Constants Depending on F_L Value

F_L VALUE	DEPTH FROM GROUND SURFACE	D_E
$F_L \leq 0.6$	$0m \leq x \leq 10m$	0
	$10m < x \leq 20m$	1/3
$0.6 < F_L \leq 0.8$	$0m \leq x \leq 10m$	1/3
	$10m < x \leq 20m$	2/3
$0.8 < F_L \leq 1.0$	$0m \leq x \leq 10m$	2/3
	$10m < x \leq 20m$	1

(2) Spring stiffness and other soil constants shall be zero for those soil layers which were defined as "very soft cohesive soils".

(3) For those soil layers whose spring stiffness and other soil constants are assumed zero in seismic design, the "ground surface assumed in seismic design" shall be assumed to be at the bottom of these layers. It should be noted that because the inertia force is to be applied to the structures, soils and water above the ground surface assumed in seismic design, larger lateral forces in addition to the zero stiffness of soil spring and other soil constants have to be considered when the ground surface assumed in seismic design is taken lower.

(4) The surcharge effect of the weight of soil layers where soil springs and other soil constants are assumed to be either reduced or zero must be considered on the lower soil layers.

1.7 EVALUATION OF INERTIA FORCE

Inertia forces in the static lateral force method shall be applied to bridges in two ways depending on the seismic design structural unit. The seismic design structural unit shall be selected in accordance with Table 1-8.

Natural period and the inertia force shall be determined from:

(1)Seismic design structural unit consisting of a substructure and the part of superstructure supported vertically by the substructure

Natural period and inertia force shall be determined from

$$F_{si} = k_{hi} R_i \qquad (1\text{-}10)$$

$$T = 2.01 \sqrt{\delta} \qquad (1\text{-}11)$$

where

- F_{si} : inertia force associated with ~~dead~~ weight of superstructure for design of i-th substructure
- k_{hi} seismic coefficient considered for i-th structural segment
- R_i : reaction force developed at i-th substructure due to dead weight of the part of superstructure supported by the i-th substructure
- T natural period, in second, of the seismic design structural unit
- δ lateral displacement, in meter, of the substructure subjected to a lateral force equivalent to 80 % of the dead weight of a substructure above the ground surface assumed in seismic design and the dead weight of a part of the superstructure supported by the substructure.

Because soil-structure interaction is important for evaluating the seismic

Table 1-8 Seismic Design Structural Unit

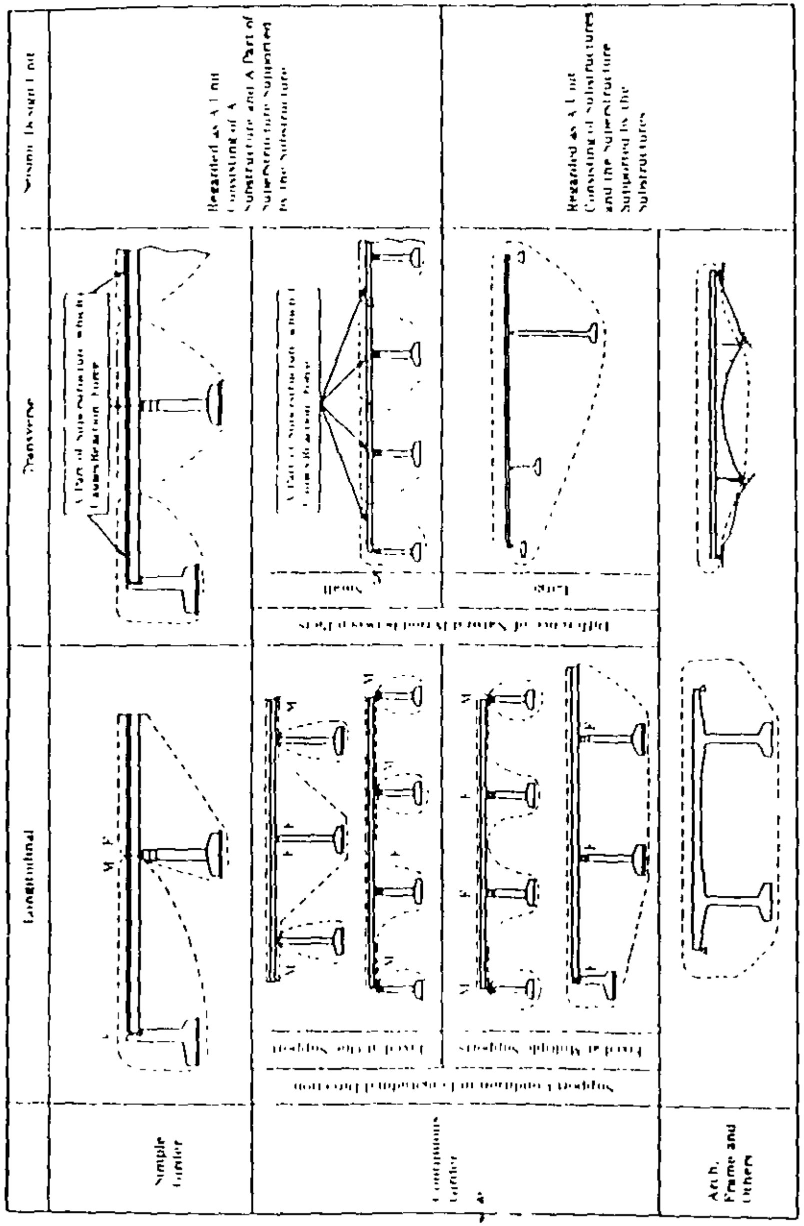

lateral force, it is generally idealized by a set of soil springs. The stiffnesses of soil springs are dietermined based on k-values, which represents the spring stiffness per unit area, as follow

$$k = \frac{1}{30} E_D \qquad (1\text{-}12)$$

$$E_D = 2(1+\nu_D)G_D \qquad (1\text{-}13)$$

$$G_D = \frac{\gamma_t}{10g} V_s^2 \qquad (1\text{-}14)$$

$$V_S = \begin{cases} 0.8 \times V_{SD} & V_{SD} < 300 \text{ m/sec} \\ V_s & V_{SD} \geq 300 \text{ m/sec} \end{cases} \qquad (1\text{-}15)$$

where

k : stiffness of soil spring per unit area (kgf/cm³)

G_D and E_D : shear modulus and elastic modulus of soils depending on shear strain induced during earthquakes

ν_D: poisson's ratio

V_s : shear wave velocity assumed in seismic design (m/sec)

V_{SD} : shear wave velocity measured at the site (m/sec)

(2)Seismic design structural unit consisting of several substructures and the part of superstructure supported vertically by the substructures.

Inertia force shall be evaluated in accordance with Fig. 1-7, i.e.,

i)idealize the bridge by a linear elastic frame model. Soil-structure interaction effects are idealized by the same way with (1).

ii)apply a lateral force equivalent with the dead weight of superstructure and substructures above the ground surface assumed in seismic design, and compute the natural period as

$$T = 2.01\sqrt{\delta} \qquad (1\text{-}16)$$

$$\delta = \frac{\int w(s)u(s)^2 ds}{\int w(s)u(s) ds} \qquad (1\text{-}17)$$

where

w(s) : dead weight of the seismic design structural unit (superstructure and substructure above the ground surface assumed in seismic design) at point "s" (tf/m)

u(s) : lateral displacement developed in the seismic design structural unit at point "s" (m) when subjected to w(s) in the direction considered in design.

iii)determine the seismic coefficient k_h depending on the natural period T.

iv)compute inertia force as

$$F_s = k_h \times F \qquad (1\text{-}18)$$

where

F_a : shear force (tf) or bending moment (tfm) due to inertia force

k_h : seismic coefficient

F : force developed in the seismic design structural unit when subjected to a lateral force equivalent to the dead weight of the seismic desiginstructural unit above the ground surface assumed in seismic design (tf/tfm)

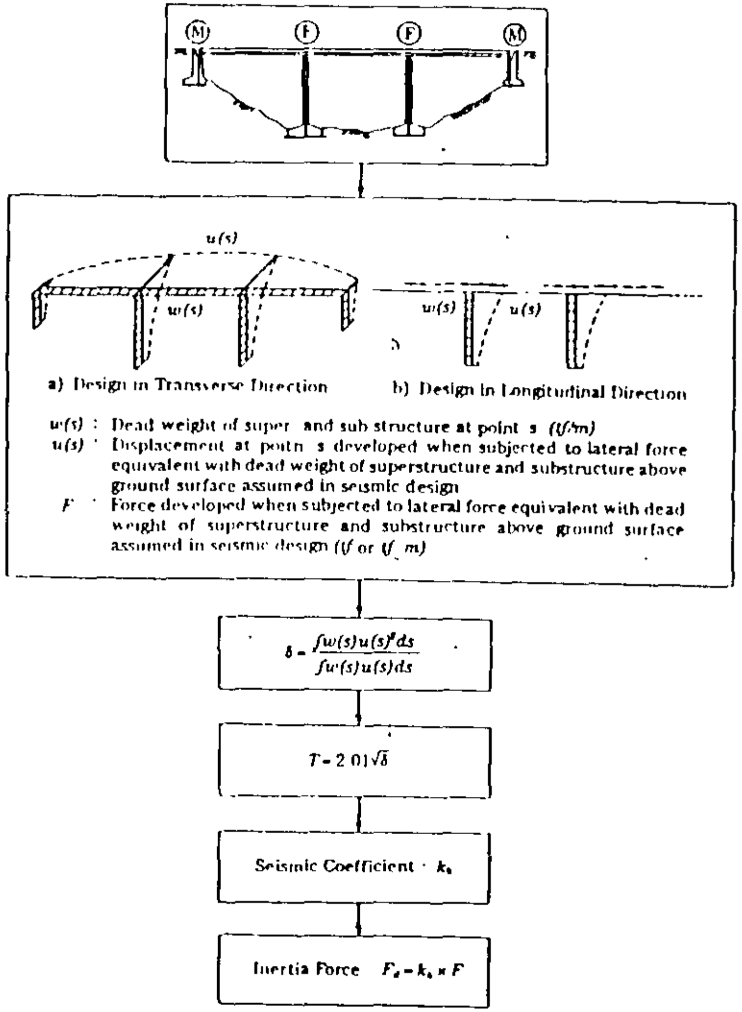

Fig. 1-7 Calculation of Inertia Force

For substructures supporting girder bridges, the shear force developed at the center of gravity of the superstructure shall be regarded as the lateral force for seismic design of substructures. However, when the inertia force computed by Eq.(1-18) is smaller than the inertia force computed by Eq.(1-10), the latter shall be adopted for design. This needs some explanation. The inertia force computed by Eq.(1-18) is approximately proportional to the stiffness of each substructure. This implies that the majority of the inertia force tends to be carried by the substructures with higher stiffness. Depending on the stiffness distribution of substructures, the inertia force carried by piers with lower stiffness takes even negative values. However, if failure of the structure, such as at a bearing support, occurs, the contribution of load carried by each substructure will be changed from the distribution computed by Eq.(1-18). Based on such considerations, a lower limit for the inertia force evaluated by Eq.(1-18) is included.

For substructures which support the superstructure with movable bearings, friction force developed by relative movement between the superstructure and substructure is applied in longitudinal direction in stead of inertia force. The friction force is determined by multiplying the coefficient of friction with the dead weight at the bearing supports. The coefficient of friction depends on the type of bearing supports, and the value of 0.05 ~ 0.15 is generally adopted.

1.8 CHECK OF BEARING CAPACITY OF REINFORCED CONCRETE PIERS FOR LATERAL FORCE

1.8.1 Judgement of Bearing Capacity of Reinforced Concrete Piers for Lateral Force

To prevent reinforced concrete piers from failing in a brittle manner, it is recommended that the bearing capacity of the reinforced concrete piers be checked in accordance with the flow-chart presented in Fig. 1-8.

Bearing capacity of reinforced concrete piers for lateral force shall be checked using

$$P_a > k_{he} W \tag{1-19}$$

where

P_a : bearing capacity of the reinforced concrete piers for lateral force(tf)

k_{he} : equivalent horizontal seismic coefficient for check of bearing capacity of the reinforced concrete piers for lateral load

W : equivalent dead weight (tf), and shall be determined as

$$W = W_u + c_p W_p \tag{1-20}$$

$$c_p = \begin{cases} 0.5 & P_u \le P_s \\ 1.0 & P_u > P_s \end{cases} \tag{1-21}$$

W_u: dead weight of a part of superstructure supported by the reinforced concrete piers (tf)
W_p: dead weight of the reinforced concrete piers (tf)
P_u: bearing capacity of reinforced concrete piers for flexural failure (tf)
P_s: bearing capacity of reinforced concrete piers for shear failure (tf)

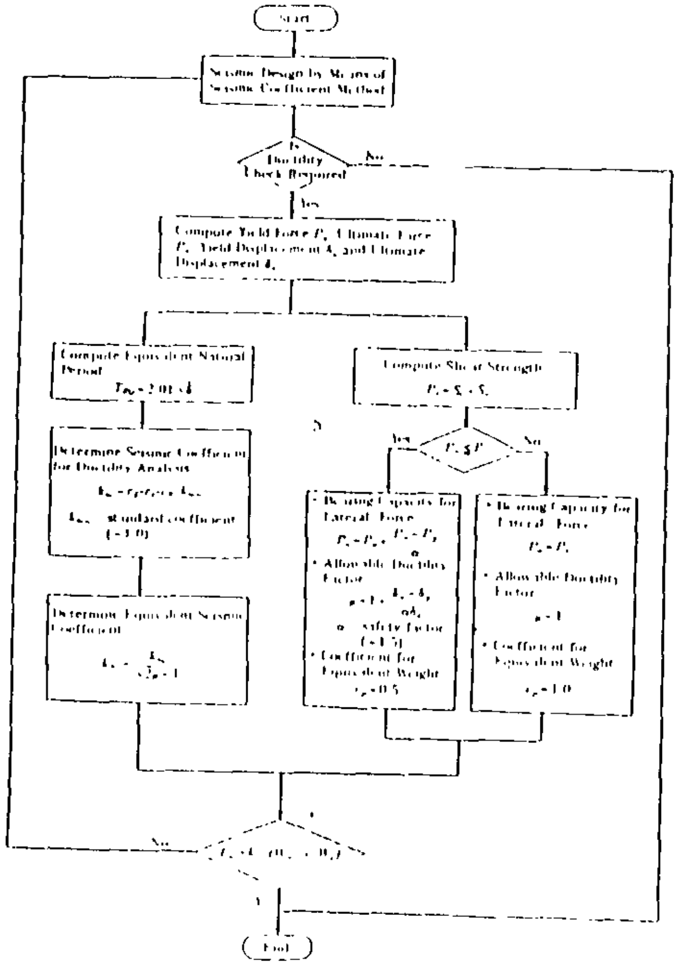

Fig 1-8 Check of Bearing Capacity of Reinforced Concrete Pier For Lateral Force

1.8.2 Equivalent Seismic Lateral Force Coefficient for Check of Bearing Capacity of Reinforced Concrete Piers for Lateral Force

Equivalent seismic lateral force coefficient for check of bearing capacity of reinforced concrete piers for lateral force shall be determined according to the equal energy assumption as

$$k_{he} = \frac{k_{ho}}{\sqrt{2\mu - 1}} \quad (1\text{-}22)$$

$$k_{ho} = c_Z \cdot c_I \cdot c_R \cdot k_{hoo} \geq 0.3 \quad (1\text{-}23)$$

where

k_{he} : equivalent seismic lateral force coefficient for check of bearing capacity of reinforced concrete piers for lateral force
k_{ho} : seismic lateral force coefficient for check of bearing capacity of reinforced concrete piers for lateral force
μ : allowable ductility factor
c_Z : modification factor for zone (refer to Fig. 1-4)
c_I : modification factor for importance (refer to Table 1-5)
c_R : modification factor for structural response (refer to Table 1-10)
k_{hoo}: standard seismic lateral force coefficient for check of bearing capacity of reinforced concrete piers for lateral force

Table 1-10 Structual Response Factor c_R

Ground Group	Structural Response Coefficient c_R		
Group I	$T_{EQ} \leq 1.4$ $c_R = 0.7$		$1.4 < T_{EQ}$ $c_R = 0.876 T_{EQ}^{-2/3}$
Group II	$T_{EQ} < 0.18$ $c_R = 1.51 T_{EQ}^{1/3} \geq 0.7$	$0.18 \leq T_{EQ} \leq 1.6$ $c_R = 0.85$	$1.6 < T_{EQ}$ $c_R = 1.16 T_{EQ}^{-2/3}$
Group III	$T_{EQ} < 0.29$ $c_R = 1.51 T_{EQ}^{1/3} \geq 0.7$	$0.29 \leq T_{EQ} \leq 2.0$ $c_R = 1.0$	$2.0 < T_{EQ}$ $c_R = 1.59 T_{EQ}^{-2/3}$

The standard seismic lateral force coefficient k_{hoo} was determined based on the statistical analysis of 394 components of strong motion records [1-9] to represent a realistic ground motion developed during significant earthquakes with magnitude as large as 8. Similar modification to the seismic lateral force coefficient k_h given by Eq.(1-1) was incorporated in determining the design force level over 1 second. It should be noted that the natural period where the coefficient k_{hoo} decreases with increasing natural period is assumed larger than that for the seismic lateral force coefficient k_h given by Eq.(1-1) due to considerations for long period ground motions [1-12].

Fig 1-9 shows the seismic lateral force coefficient k_{ho} for the check of bearing capacity of reinforced concrete piers for lateral force when $c_z = c_I = 1.0$.

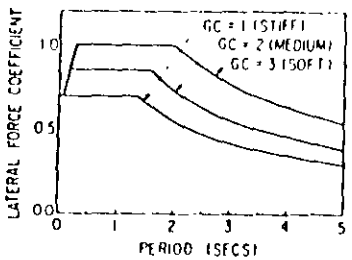

Fig 1-9 Seismic Lateral Force Coefficient k_{ho} for Check of Bearing Capacity of Reinforced Concrete Piers for Lateral Force ($C_z = c_I = 1.0$)

1.8.3 Bearing Capacity of Reinforced Concrete Piers for Lateral Force and Allowable Ductility Factor

Bearing capacity of reinforced concrete piers for lateral force P_a and the allowable ductility factor μ shall be determined based on the failure mode as :

(1)Flexural failure

$$P_a = P_y + \frac{P_u - P_y}{\alpha} \qquad (1\text{-}24)$$

$$\mu = 1 + \frac{\delta_u - \delta_y}{\alpha\, \delta_y} \qquad (1\text{-}25)$$

where

P_u, δ_u : bearing capacity (tf) and ultimate displacement (m) for flexural failure

P_y, δ_y : yielding force (tf) and yielding displacement (m) for flexural failure

α : safety factor (= 1.5)

In seismic design, Pu, Py, δ_u and δ_y are computed for each reinforced concrete pier assuming the stress vs. strain relation presented in Fig. 1-10. The "yield" and "ultimate" is defined as the deformation of pier when the strain of main reinforcement yields at the bottom and when the strain of concrete at the extreme compression fiber reaches 0.0035, respectively.

It was confirmed from the comparison with the dynamic loading tests of model specimens that the ultimate displacement δ_u approximately corresponds to the point on hysteresis loops where rupture of main reinforcements was initiated to be developed at the bottom. The seismic safety factor α of 1.5 was determined so that the allowable ductility factor given by Eq.(1-25) corresponds to the point on hysteresis loops where decrease of the load was initiated due to falling-off of cover concrete [1-14,1-15] .

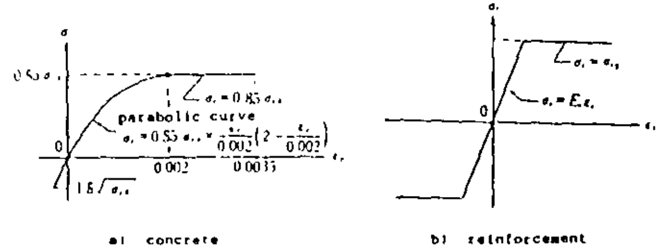

σ_{ck} : Standard design strength of concrete
σ_{sy} : Yield strength of reinforcement
σ_c : Stress of concrete
σ_s : Stress of reinforcement
ε_c : Strain of concrete
ε_s : Strain of reinforcement
E_s : Coefficient of elastic modulus

Fig. 1-10 Stress vs. Strain Relation of Reinforcement and Concrete Assumed to Compute δ_y, δ_u, P_y and P_u of Reinforced Concrete Piers

This may lead to a conservative estimation associated closely with the loading procedure adopted for the model tests. Although various loading procedures are proposed [1-19 ~ 1-24] , the number of alternative loading cycle per each loading step (loading displacement) in the displacement controlled loading tests, as shown in Photo 1-8, was assumed as 10 in the Public Works Research Institute. Rupture of main reinforcement depends on the number of loading cycles, and it was found from the shaking table test, as shown in Photo 1-9, that the failure at a specific ductility factor developed during the earthquake excitation tests is much smaller than that developed during the loading test under displacement control with loading cycle of 10 [1-15] . It was however pointed out that piers subjected to larger ground acceleration tend to cause larger residual deformation. Such effects may be significant for those piers which are subjected to eccentric bending moment due to dead weight of the superstructure. Although such residual deformation of reinforced concrete piers subjected to significant earthquake ground motions is still being studied, it seems important to keep enough safety in determining the allowable ductility factor.

(2)Shear failure

$$P_a = P_s \qquad (1\text{-}26)$$

$$\mu = 1 \qquad (1\text{-}27)$$

where

P_s : bearing capacity (tf) for shear failure, and shall be deterimned as

$$P_s = S_c + S_s \qquad (1\text{-}28)$$

$$S_c = \tau_c \, bd \tag{1-29}$$

$$S_s = \frac{A_w \sigma_{sy} d}{1.15 a} \tag{1-30}$$

where
- S_c shear force supported by concrete (tf)
- S_s shear force supported by tie reinforcement (tf)
- τ_c: averaged shear stress of concrete (tf/m)
- A_w: sectional area of tie reinforcement (m²)
- σ_{sy} yiels stress of tie reinforcement (tf/m²)
- a interval of tie reinforcement (m)
- d effective width of pier (m)

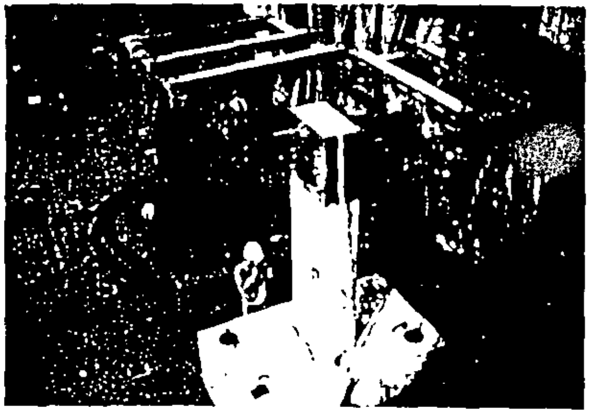

Photo 1.8 Dynamic Loading Tests of Reinforced Concrete Pier Models

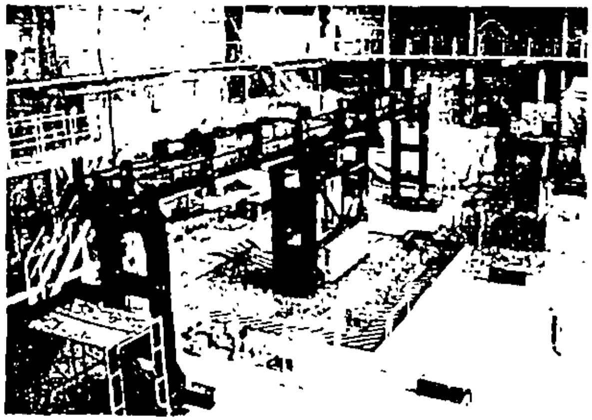

Photo 1.9 Shaking Table Tests of Reinforced Concrete Pier Supporting Two Span Simply Supported Girders (Weight = 40 tf)

1.9 DYNAMIC RESPONSE ANALYSIS

For bridges with complicated dynamic response and for new types of bridges, dynamic response analysis is recommended to check seismic safety of the design made by means of the static lateral force method

In principle, dynamic response analysis shall be made by means of modal response spectral analysis with use of an analytical model which simulates dynamic characteristics of the bridge. Acceleration response spectrum for the modal response spectrum analysis shall be determined as

$$S = c_z \cdot c_I \cdot c_D \cdot S_0 \tag{1-31}$$

where
- S : response spectrum for modal response spectrum analysis (gal(=cm/sec²))
- c_z : modification factor for zone (refer to Fig. 1-4)
- c_I : modification factor for importance (refer to Table 1-5)
- c_D: modification factor for damping, and shall be determined based on model damping ratio h_i as

$$c_D = \frac{1.5}{40h_i + 1} + 0.5 \tag{1-32}$$

S_0: standard response spectrum for modal response analysis method (gal) (refer to Table 1-11)

Table 1-11 Standard Response Spectral Value S_0 for Modal Dynamic Response Analysis

Ground Condition	S_0 (gal)		
Group I	$T_i < 0.1$ $S_0 = 431T_i^{1/3} \geq 160$	$0.1 \leq T_i \leq 1.1$ $S_0 = 200$	$1.1 < T_i$ $S_0 = 220/T_i$
Group II	$T_i < 0.2$ $S_0 = 427T_i^{1/3} \geq 200$	$0.2 \leq T_i \leq 1.3$ $S_0 = 250$	$1.3 < T_i$ $S_0 = 325/T_i$
Group III	$T_i < 0.34$ $S_0 = 430T_i^{1/3} \geq 240$	$0.34 \leq T_i \leq 1.5$ $S_0 = 300$	$1.5 < T_i$ $S_0 = 450/T_i$

Fig. 1-11 shows the design response spectra assuming $c_z = c_I = 1.0$ and $c_D = 1.0$ ($h_i = 5\%$) Fig. 1-12 shows the modification factor c_D

When a time history analysis is required, strong motion records which have the similar characteristics with S by Eq.(1-31) shall be used with the consideration on site condition and structural response of the bridge. Three ground acceleration records, as shown in Fig 1-13, which were modified in frequency domain so that their response characteristics match with S_0 in Eq.(1-31) are provided in the Specifications.

Design Details

Japan

[H. Ichimasu, J. Kodera, K. Kawashima]

2.1. Total Bridge System and Connections

2.1.1 Seismic capacity of total bridge structure

(1) Seismic damages to bridge structure

In order to examine seismic capacity of a system, it is necessary to consider a bridge as a total structural system composed of superstructure, ground and substructure. Although deformation or displacement due to a large earthquake is inevitable to a certain extent, it is essential to maintain the bridge function.

Past seismic experiences indicate that loss of the basic bridge function generally resulted from:

1) Falling down of girders
2) Movement of footings caused by flow of soft ground and slope
3) Horizontal movement of abutments

As mentioned in Section 1, a large earthquake may cause ground failure. Especially when ground layer near ground surface collapses, it would damage foundations located in the layer, and finally lead to the damage of the whole bridge structures.

There is a prominent correlation between bridge damages by earthquakes and ground conditions where the damage has developed in longitudinal direction, especially when the bridge spans over valleys, or is built on soft ground near embankments. Damages to the substructures were sometimes caused by falling of girders.

Photo 2-1 Earthquake Damage to a Bridge over a Balley

Photo 2-2 Falling off of Girders due to 1948 Fukui Earthquake

Photo 2-2 shows the damage to Nakazuno Bridge due to Fukui Earthquake in 1948. Inadequate strength of foundation and connection between footings and piers are considered main reason of such destructive damage. Seismic design at those days was inadequate.

In Niigata Earthquake in 1964, abutments and pier foundations of Yachiyo Bridge were displaced toward the river center caused by soil movement due to liquefaction. As shown in Fig. 2-1 the pier P2 closer to the left bank inclined. On pier P4, the girders were pushed by the displaced piers, slipping beyond the normal limits of the movable support, thereby pushing the adjacent girder. As a result, edge of the pier close to the fixed support sheared off and the girders were about to fall as shown in Fig. 2-2.

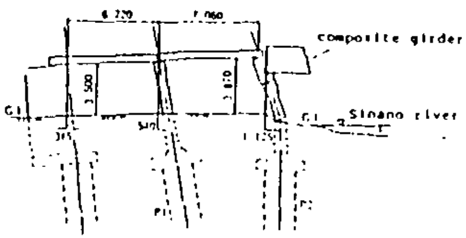

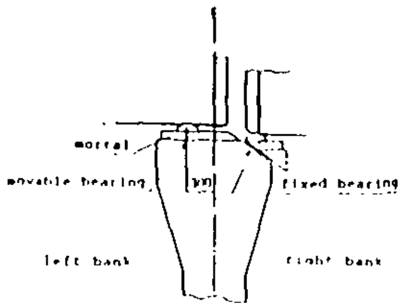

Fig. 2-1 Damage to P_1 and P_2 of Yachiyo Bridge due to 1964 Niigata Earthquake

Fig. 2-2 Damage to P_4 of Yachiyo Bridge due to 1964 Niigata Earthquake

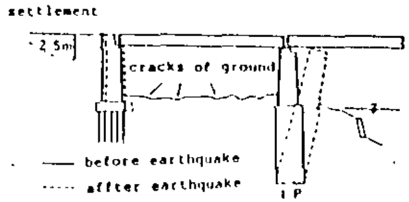

Fig. 2-3 Damage of Pier due to Liquefaction of Sandy Soil Layer due to 1964 Niigata Earthquake

Fig 2-3 shows the most severe damage to caisson foundation in Japan, which was pushed toward the river center due to effect of failure of river banks.

Settlement of foundation is one of typical damages to foundation constructed on soft cohesive soils due to an earthquake. Many damages have been experienced in the past earthquakes. A survey was made for selected railway bridge pier foundations which experienced the Great Kanto Earthquake in 1923, and the correlation between the settlement and the safety factors for their normal dead load was studied. The servey revealed that those bridge pier foundations with safety factor ranging from 1.5 to 2.4 settled several ten of centimeters, whereas those foundations with safety factor larger than 3 did not make appreciable settlements.

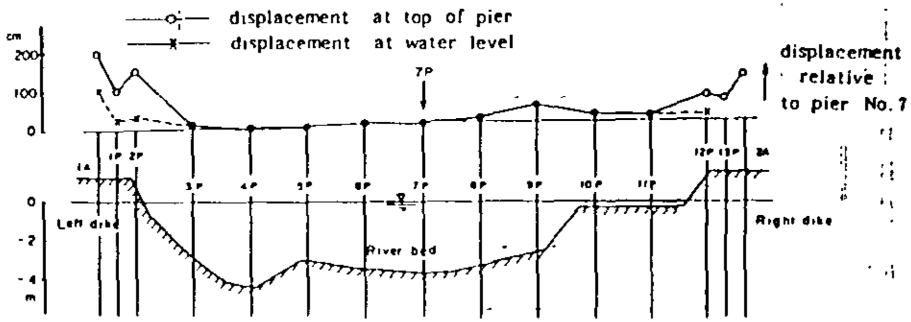

Fig 2-4 Residual Displacements of Piers of Sinano-gawa Bridge due to 1964 Niigata Earthquake

(2) Seismic countermeasures of total bridge system

It is not easy to design footings, located in layers vulnerable to collapse and lateral movement, so as not to develop lateral displacement. It is appropriate to adopt longer spans instead of constructing footings on those layers. Reinforcement or improvement of the soil layers vulnerable to lateral movement are to be considered as alternate. Arch bridges are stronger for the soil movement due to liquefaction or instability of very weak cohesive soil. For example, Bandai Bridge, which consists of 6 span continuous rigid arches with caisson foundations and is located at 300m down stream from Yachiyo Bridge, suffered only slight damage during the Niigata Earthquake in 1964. Although some settlements of the foundation occurred, no remarkable lateral movement of the bridge was developed.

When there is embankment between adjoining piers, it may be effective to tie the two foundations together to prevent outward displacement.

Embankment on soft soil deposit tends to cause failure during a destructive earthquake. In the case of a flyover on soft soil deposit, it is recommended to keep the length of the embankment as short as possible.

Photo 2.3 shows the damage to an abutment caused by failure of embankment constructed on very soft cohesive soils with N value of 2 to 5. Because seismic design was not made at those days, only wooden piles were used to support the abutment.

For those bridges with short to medium span length constructed in an embankment of soft ground, a box-type framed bridge is preferable from the view point of seismic design.

Photo 2-3 Earthquake Damege to Abutment on Soft Ground due to the Great Kanto Earthquake in 1923

2.1.2 Devices for preventing superstructures from falling, and bearings

(1) Devices for Preventing Superstructure from Falling

Since connections between superstructure and substructure or between two adjacent superstructures are quite susceptible to earthquake damage, special structural considerations are required to prevent the superstructure from falling-off due to damage of those sections. For such a purpose, the following measures are adopted as shown in Fig. 2-5.

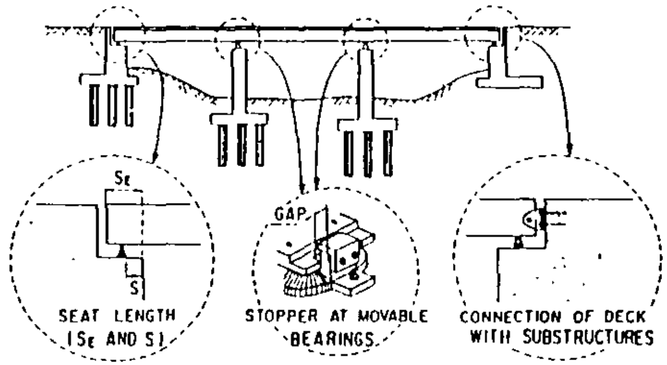

Fig. 2-5 Devices for Preventing Superstructure from Falling

i) At movable bearings, devices to prevent dislodgement of upper-bearings from the lower-bearings (stopper) are provided.

ii) At both ends of the superstructure, either of the following measures are used to prevent the superstructure from dislodging from the support of the substructures:

a) The distance from the edge of superstructure to the edge of substructure (Seat Length) should be longer than the value as

$$S_E = \begin{cases} 70 + 0.5 \times l & \text{for } l \le 100 \text{ m} \\ 80 + 0.4 \times l & \text{for } l > 100 \text{ m} \end{cases}$$

in which S_E and l represent the seat length in cm and the span length in m, respectively.

b) Installation of devices for preventing the superstructure from falling off substructures.

The design horizontal seismic coefficient for the devices should be equal to more than double the value specified in Section 1.5.

(2) Bearings

Bearings shall be designed to support lateral inertial force of the superstructure. Design of supports should consider, in addition to lateral forces, uplift force equivalent to vertical reaction force due to dead load multiplied by the design vertical seismic coefficient of 0.1. However, lateral inertial force and uplift force need not be applied simultaneously. The uplift force is required for preventing separation of superstructures from substructures.

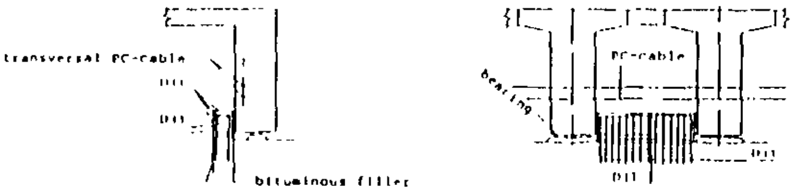

a) projection (b) front of end diaphragm

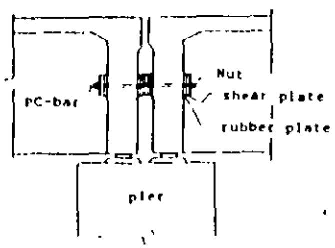

b) connection of adjacent end diaphragm with steel bar or steel wire

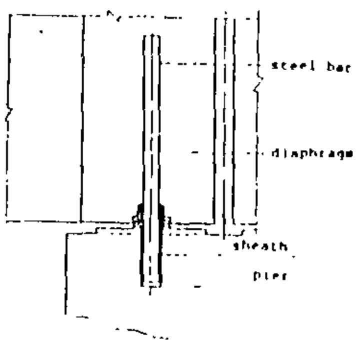

c) connection of girder with substructure

Fig 2-6 Various Types of Devices for Preventing Supestructure from Falling

2.1.3 Measures for reducing concentration of longitudinal lateral force

Various devices have been developed in Japan since the 1960's to reduce concentration of longitudinal lateral force acting at piers with fixed supports. Most of them are to distribute longitudinal force to other piers and have functioned successfully during strong earthquakes.

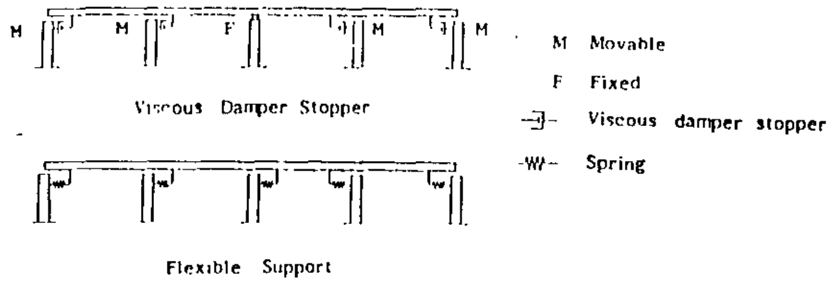

Fig 2-7 Measures to Destribute Lateral Force

Such devices can be categorized into viscous damper stopper and the flexible support as shown in Fig 2-7.

Viscous damper stopper is to behave as a fixed support during an earthquake, while it allows lateral displacement without restriction for movement with low velocity, such as those caused by temperature change. Various types of viscous damper stoppers have been developed as shown in Figs.2-8 and 2-9.

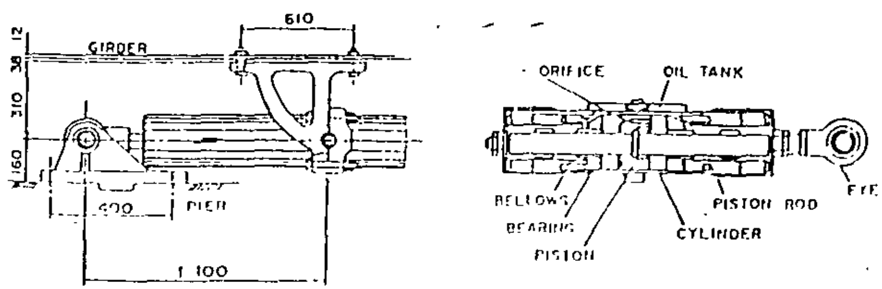

Fig. 2-8 Cylinder Type Viscous Damper Stopper

Various attempts have also been made for the flexible supports. Most common way is to support deck by rubber bearings. One of the interesting devices is the SU Damper, which consists of movable bearing and prestressed strand as shown in 2 10 By elongation of natural period of the deck as well as energy dissipation at the movable bearing, structure response of the bridge is expected to be reduced Fig 2-11 shows an example of bridge where SU-Damper was installed

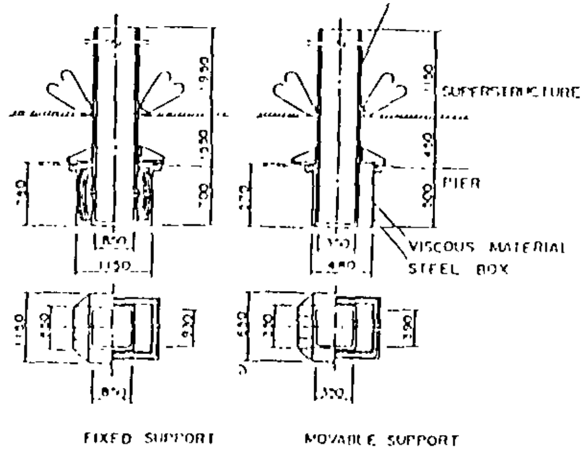

Fig 2-9(a) Rod Type Damper Stopper

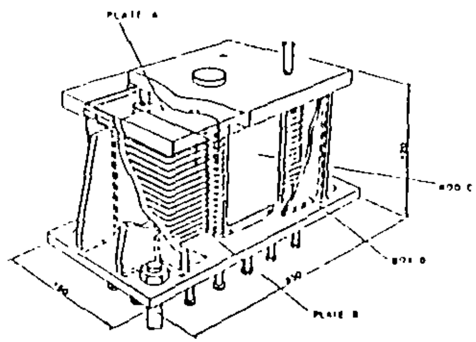

Fig 2-9(b) Plate Type Damp. r Stopper

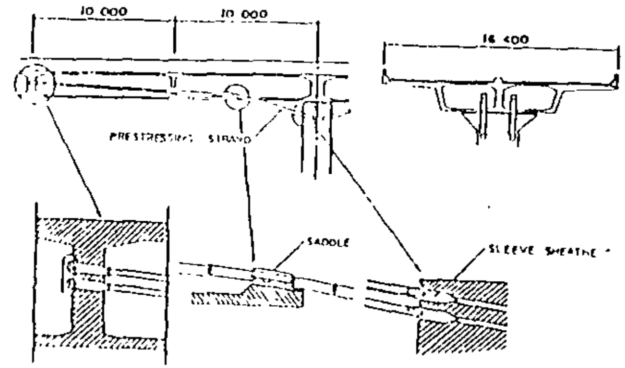

Fig 2-10 SU Damper

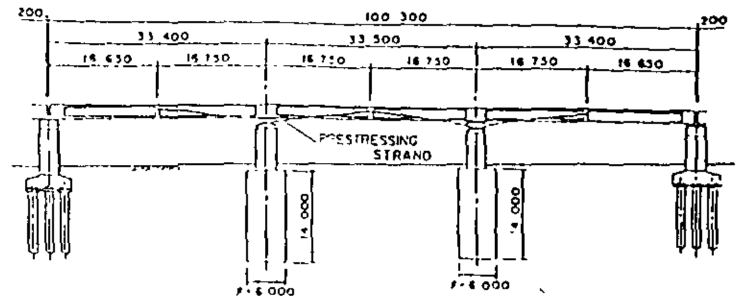

Fig 2-11 Kita-Ikebukuro Viaduct where SU Damper is installed

2.2 Piers

2.2.1 Bridge seat

To protect bridge seats from damage by seismic lateral forces, it is required to take the distance from bearing edge to the edge of substructure more than the following values

$$S = 20 + 0.5 \times l \qquad l \leq 100\text{m}$$
$$S = 30 + 0.4 \times l \qquad l > 100\text{m}$$

where

S : distance from bearing edge to the edge of substructure(cm), refer to Fig 2-5

l : bridge span (m)

For important bridges located in soils of Group III(Soft soil site), S should be more than 35cm.

The railroad bridge code makes it a principle that this portion must be reinforced with steel bars, and indicates the following details.

The shearing stress at the bridge seat shall be derived from Eq. (2-1) and shall not exceed 7kgf/cm².

$$\tau = \frac{H_s}{A_\tau} \qquad (2\text{-}1)$$
$$A_\tau = \sqrt{2} \times (2x + 2a + b)$$

where

τ : shear stress (kgf/cm²)

A_τ : area cut off by shear caused by horizontal force (cm²)

H_s : lateral force at bearing (kgf)

a : depth of stopper beneath bearing(cm)

b : width of bearing in transverse direction (cm)

x : distance from center of bearing to edge of pier crest (cm)

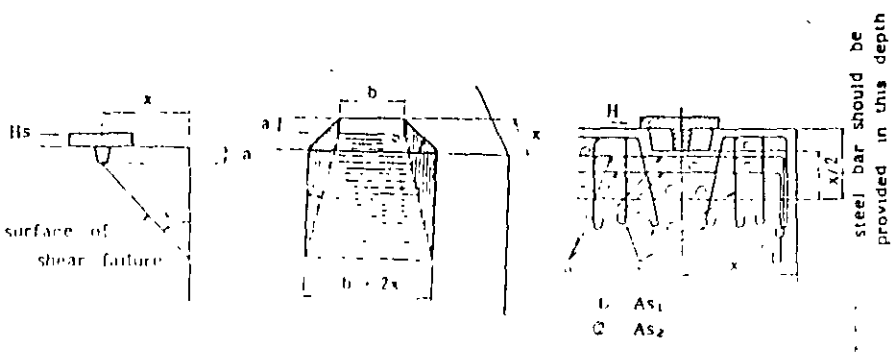

Fig 2-12 Reinforcement at Bridge Seat

At bridge seats, regardless of shear stress at the seat reinforcement shall be arranged according to Eqs. (2-2) and (2-3).

$$A_{s1} = \frac{H_s}{\sigma_{sa}} \qquad (2\text{-}2)$$

where

A_{s1} : amount of reinforcement (cm²) for lateral force

σ_{sa}: allowable tensile stress (kgf/cm²)

H_s : lateral force (kgf)

$$A_{s2} = \frac{H_s}{\tau_{sa}} \qquad (2\text{-}3)$$

where

A_{s2} : amount of reinforcement (cm²) at front of bearing ribs

τ_{sa}: allowable shear stress (kgf/cm²)

It should be noted that the allowable shear stress specified in the Standard is 1150kgf/cm².

2.2.2 Column member (pier)

(1) Bending moment

In design of single column type piers, it is generally assumed that the bending moments caused by an earthquake varies linearly in accordance with height (refer to Fig. 2-13).

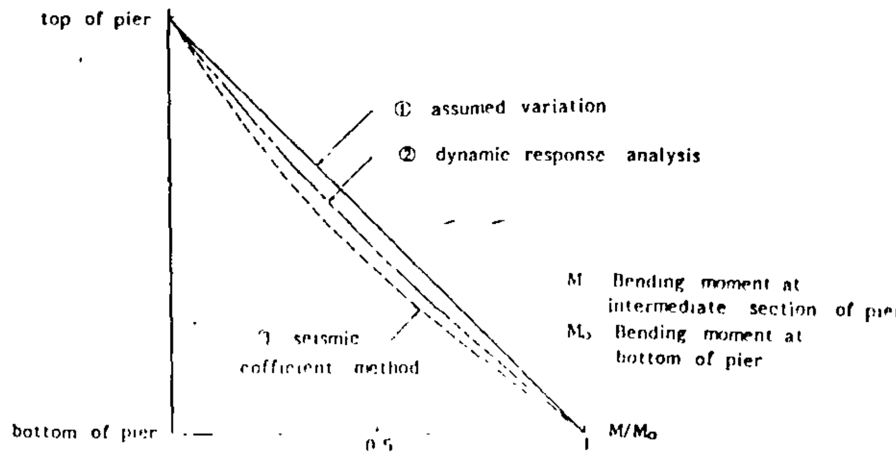

Fig 2-13 Variation of Bending Moment Assumed in Seismic Design for Single Column Piers

The allowable stress of structural members for seismic design by means of seismic coefficient method is derived multiplying σ_{ca} and σ_{sa} shown in Table 2-1 by 1.5

Table 2-1 Allowable Stresses for Concrete and Reinforcement

a) Allowable stresses of concrete (kgf/cm²)

Specified Strength	σ_{ck}	210	240	270	300
Allowable compressive stress	σ_{ca}	70	80	90	100
Allowable shear stress	τ_{a1}	3.6	3.9	4.2	4.5
	τ_{a2}	16	17	18	19

b) Allowable stresses of reinforcement (kgf/cm²)

		SR24	SD30A, SD30B	SD35
Allowable tensile stress	σ_{sa}	1400	1800	2000

(2) Shear

In the seismic coefficient method, τ_m shall be calculated as

$$\tau_m = \frac{S}{b \cdot d} \tag{2-4}$$

where

b : width of the cross section (cm)

d : effective depth of the cross section (cm)

In the case when shear force is to be resisted by only concrete

$\tau_m < \tau_{a1}$

On the other hand, where shear force is resisted by concrete and stirrups

$\tau_m < \tau_{a2}$

When $\tau_m > \tau_{a1}$, diagonal reinforcements shall be provided as

$$A_w = \frac{1.15\,(S - S_c)\,a}{\sigma_{sa} \cdot d} \tag{2-5}$$

$$S_c = \frac{\tau_{a1}\, b\, d}{2} \tag{2-6}$$

where

A_w : area of diagonal reinforcement (cm²)

σ_{sa}: allowable shear stress of reinforcement (1.5 times σ_{sa} spefcified in Table 2-1 (b))

Further, τ_{a1} can be increased by α times according to Eqs.(2-7),(2-8) and (2-9)

$$\tau_{a'1} = \alpha\, \tau_{a1} \tag{2-7}$$

$$\alpha = 1 + \frac{M_o}{2M} \leq 2.0 \tag{2-8}$$

$$M_o = \frac{N \cdot I_o}{A_c\, y} \tag{2-9}$$

where

M,N : bending moment (kgf·cm) and axial compressive force (kgf)

I_o : moment of inertia(cm⁴)

A_c : sectional area(cm²)

y : distance between center of section to the tensile edge(cm)

(3) Hoop

Hoops shall have a diameter equal to or more than 13mm, and their spacing shall be less than 1/2 of the shorter side of the cross section of the member and less than the 12 times of the diameter of longitudinal reinforcement and less than 30 cm

At the joints of column and footing, or where an amount of longitudinal reinforcement changes remarkably, hoops indicated in Table 2-2 shall be arranged within the ranges of short side of column length or diameter.

Table 2-2 Hoops Required at Joints

Pt (%)	0 < Pt ≤ 0.5	0.5 < Pt ≤ 1.0	1.0 < Pt
Pw (%)	0.15	0.20	0.25

$$P_w = \frac{A_w}{b\, a} \times 100$$

Pt : Longitudinal reinforcement ratio

P_t may be considered as 1/2 of longitudinal reinforcement ratio at column base.

(4) Intermediate Anchoring

In the Miyagi-ken-oki Earthquake in 1978 and the Urakawa-oki Earthquake in 1982, damage was developed at the intermediate anchorage of the main reinforcements of the bridge piers

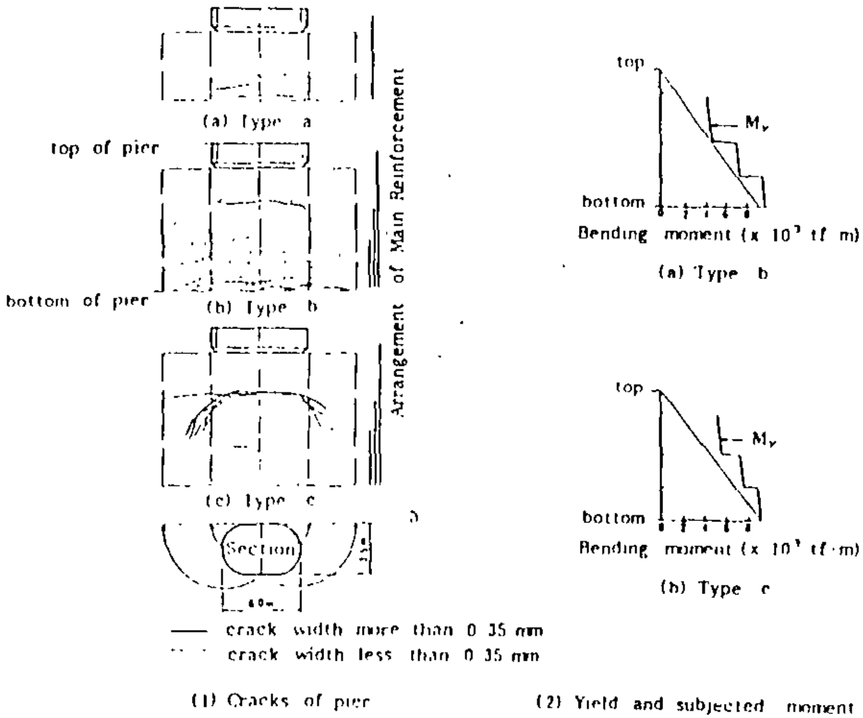

Fig 2 11 Seismic Damage of Natori Bridge due to inadequate Anchoring Length of Main Reinforcement at Mid hight(1978 Miyagi-ken-oki Earthquake)

Fig.2-14 shows an example of the damage developed at reinforced concrete piers with termination of main reinforcement at mid-height. By comparing "Type a" and "Type c" damage, it is apparent that the damage was significant where the main reinforcement was terminated at mid-height. Anchoring length specified in the specifications was inadequate at those days. It is also interesting to compare "Type b" and "Type c" damage. Redundancy of bending moment M relative to the yield bending moment My, i.e., My/M, was smaller in the "Type c". This developed more considerable damage in "Type c" than "Type b".

Based on these experiences the stipulations for the anchoring length was revised in 1980. When it is inevitable to anchor the main reinforcement in the tensile zone, the following measure must be taken.

The reinforcement to be anchored shall be extended from the section where the reinforcement is calculated to be not necessary by a length equal to the effective depth, plus a length of not less than 20 times the diameter of reinforcement and be stopped. However, in this case, the shear stress between the height where main reinforcement is calculated to be not necessary and the height of the stop shall be 2/3 or less of the value τ_{a2}.

2.2.3 Rigid-Frame

(1) Members of Rigid Frame

In the vicinity of the upper and lower ends of the rigid frame columns and both ends of beams at the junction with the columns, hoops and stirrups shall be provided at shorter spacings than in the intermediate sections of columns (Fig.2-15) to prevent brittle failure as

- I section: more than 0.002b·a and more than 1.2 times reinforcement required for lateral force
- II section: more than 0.0025b·a
- III section: more than 0.002b·a
- IV section: more than 0.0015b·a

in which b and a represent beam width (cm) and stirrup or tie spacing (cm).

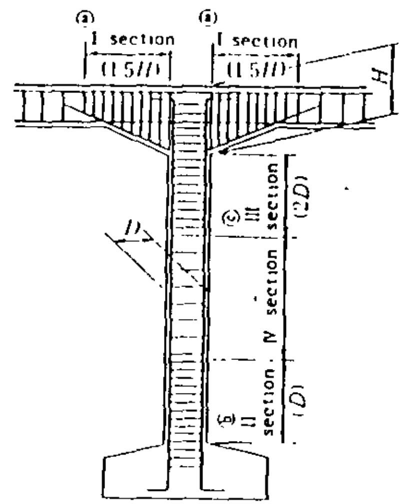

Fig 2-15 Reinforcement Arrangement at Intermediate Joint of Rigid Frame and Bridge Pier

Photo 2-1 Earthquake Damege to the Column of Railway Elevated Bridge by 1978 Miyagi-ken-oki Earthquake

5)

Photo 2-1 shows an example of damage due to inadequate amount of tie reinforcement. Special attention was not paid for the importance of the tie reinforcement in those days. This damage was caused by the 1978 Miyagi-ken-oki earthquake at columns of a rigid frame railway viaduct. It should be noted here that the damage tends to be developed at the site near the stream crossing the bridge. Although it was assumed in design that the foundation was rigidly supported by subsoils which consist of gravel layers, flexibility associated with loose gravel layers resulted in larger bending moment at the upper portion of the frame. This is considered a part of reason of the destructive damage as shown in photo 2-1. Fig 2-16 also shows the similar damage of colums due to inadequate tie reinforcement.

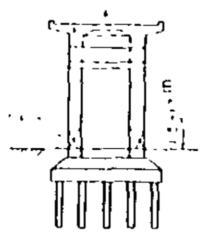

Fig 2-16 Damage to Yokoyama Railway Viaduct

(2) Joints of Rigid Frame

A haunch shall be in principls provided at the joint of a rigid frame. Reinforcement shall be arranged along the haunch as illustrated in Fig 2-17. The radius of curveture, r, of external reinforcement shall be more than 10 times of the diameter of reinforcement.

At end joints, it is advisable to place outside at least one half of the amount of the main reinforcement for the members connecting with the joints as shown in Fig 2-17.

When a bending moment acts on the end joint as shown in Fig 2-17(b), tensile stress develops in the diagonal cross section. If this tensile stress exceeds a certain values, additional reinforcement shall be placed as shown in Fig.2-17.

On the other hand, in case of Fig 2-17(b), tensile stress will act diagonally at the joint. Where the bending moment is significant, it is preferable to place additional reinforcement diagonally as shown in Fig 2-17.

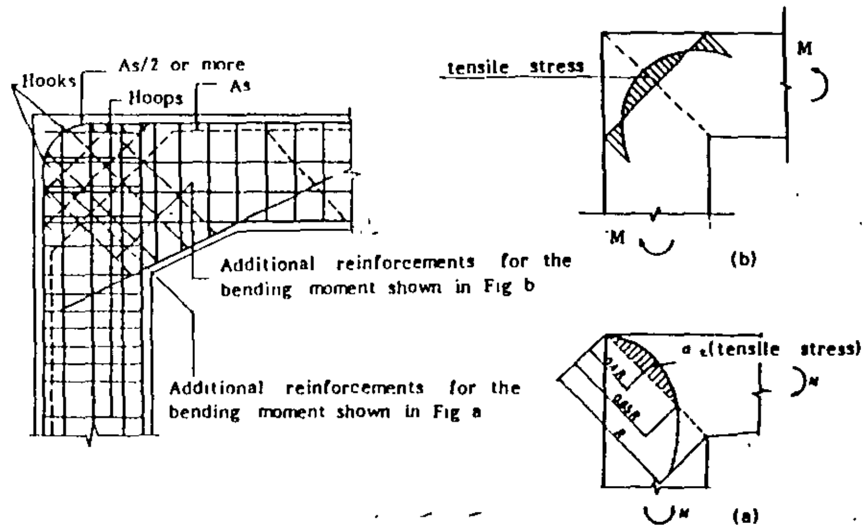

Fig. 2-17 Arrangement of Reinforcements at End Joint of Rigid Frame Members

2.2.4 Footing

Footings shall have enough thickness so that it can behave as a rigid body. Thickness shall be computed by

$$\beta\lambda \leq 1.0 \qquad (2\text{-}10)$$

$$\beta = \sqrt[4]{\frac{3k_v}{E_c h^3}} \qquad (m^{-1})$$

where

h : average thickness of footing(m)
E_c : elastic modulus of concrete(tf/m^2)
λ : equivalent projecting length of footing(m)
k_v : coefficient of subsoil reaction(tf/m^3)

Main reinforcement at the lower end of the column shall be extended into the footing over the anchorage length beyond one half of the height of the effective height of the footing or the column, whichever is less.

The amount of reinforcement to be placed on the topside of the footing shall be more than one third of the amount of the reinforcement placed on the downside.

If tensile force is generated at the piles, main reinforcement shall be arranged at the upside of the footing. In this case, the column width t_c shall in principle be taken as the effective width, but under unavoidable circumstances, the effective width may be increased to the sum of the column width t_c and the effective footing height d. The effective width to be used in stress calculations for main reinforcements at the downside of footing shall be t_c + 2d. The entire footing width shall be taken as the effective width in relation to shear force.

2.3 Foundations

2.3.1 Foundations

(1) General

Foundations shall be designed using static lateral force method (seismic coefficient method) to meet the following requirements.

1) Foundations shall be safe against bearing capacity of soils, overturning and sliding.
2) Displacement of foundations shall not exceed allowable displacement.

Table 2-3 indicates basic criteria for safety.

For elastic foundations with $\beta l > 1$, the allowable horizontal displacement is such so that the horizontal displacement shall not exceed the elastic limit of soils. The limit values are assumed as 1% of foundation width, but for foundations whose width exceed 5m the allowable displacement is limited to 5cm. For pile foundations, avoiding harmful residual displacement, the minimum allowable displacement shall be 1.5cm. For rigid foundations with $\beta l < 1$, no allowable displacement limit is prescribed because the horizontal stability is checked against the passive earth pressure.

Table 2-3 Check Items for Stability of Foundation

Foundation type \ Check item		Bearing capacity: Vertical	Bearing capacity: Horizontal	Overturn	Sliding	Horizontal displacement
Direct foundation		○	(○)	○	○	−
Caisson foundation	$\beta\ell \leq 1$	○	○	−	○	−
	$1 < \beta\ell < 2$	○	○	−	○	○
Pile	Short pile $1 < \beta\ell < 3$	○	−	−	−	○
	Long pile $\beta\ell \geq 3$	○	−	−	−	○

( ) means that the item must be checked when the penetrated part partly bears the load

ℓ : Effective penetration depth of foundation (cm)
β : Characterisitic value of foundation (cm^{-1})

For those foundations with $D_f/B < 1/2$ they should be considered as direct foundations and for those with $D_f/B > 1/2$ they should be considered as caisson foundations, in which D_f is the effective embeddment depth and B is the shorter side width of the footing. But if the passive earth pressure can not be expected, the foundation shall be assumed as a direct foundation even if $D_f/B > 1/2$.

(2) Coefficient of Subgrade Reaction

A subgrade reactions vs displacement curve is nonlinear. For design purposes, however, a certain coefficient of subgrade reaction is used on the assumption that displacement within the limits of the allowable displacement is linear as

$$k_v = k_{vo}\left(\frac{B_v}{30}\right)^{-\frac{3}{4}} \qquad (2\text{-}11)$$

$$k_{vo} = \alpha E_o / 30 \qquad (2\text{-}12)$$

$$B_v = \sqrt{A_v}$$

where

k_v : coefficient of vertical subgrade reaction (kgf/cm^3)
k_{vo} standard coefficient of vertical subgrade reaction (kgf/cm^3)
A_v loading area in vertical direction (cm^2)
E_o : equivalent linealized elastic modulus of soils (kgf/cm^2)

For obtaining E_0 from N-values in standard penetration tests, assumptions shall be made that E_0 = 28N and that the value of α is 1 for static load and 2 for seismic load.

The coefficient of horizontal subgrade reaction, k_H, shall be determined in the same way as for k_v. The equivalent loading width B_H of a rigid foundation shall be taken as $\sqrt{A_H}$ (A_H is the area of sides of foundation) and this value shall be $\sqrt{D/\beta}$ in the case of elastic foundations, in which D represents diameter of pile. Where an elastic foundation is used, a subgrade associated with horizontal resistance is assumed to be developed within the depth of $1/\beta$ below the design ground level.

2.3.2 Direct Foundation

(1) Allowable Vertical Bearing Capacity

The ultimate bearing capacity can be computed taking account of the eccentricity of bottom reaction and the gradient of the reaction.

The allowable bearing capacity of the ground shall be derived by dividing the ultimate bearing capacity by the safety factor of 2.

The eccentricity of the resultant load on the direct foundation should be within 1/3 of the bottom width from the center of foundation against seismic load.

(2) Shear Force

The allowable subgrade shear resistance shall be derived dividing the shear resistance H_u by the safety factor of 1.2. H_u shall be evaluated as

$$H_u = C_B A' + V \tan\phi_B \qquad (2\text{-}13)$$

Where

C_B : adhesion between foundation bottom and ground(kgf/cm²)

ϕ_B : angle of friction between foundation bottom and ground(degree)

A' : effective loading area(cm²)

V : effective vertical load acting on foundation bottom(kgf)

Generally, it is assumed that $\tan\phi_B$ = 0.6 or $\phi_B = \phi$ (angle of shear resistance of ground), whichever is smaller, and C_B=0.

Horizontal loads are in principle assumed to be resisted only by the subgrade shear reaction of the bottom. However, if a stable bearing stratum is found in the embedment, the latter may be allowed to carry horizontal bearing force which shall be derived by dividing the passive earth pressure by a safety factor of 1.1.

2.3.3 Caisson foundation

(1) Calculation of ground reaction

As D_f/B increases, most of lateral force tends to be suported not at the basement but at the side wall of caisson foundation. To derive apportion ratio of embedded portion and the base of the caisson, the calculation is made, assuming the caisson as a rigid body, and using the vertical ground reaction coefficient k_v at the base of the caisson, horizontal shear reaction coefficient

at the base and the horizontal ground reaction coefficient k_H at the front of footing. Considering the effect of the shear ground reaction at the embedded portion, k_H is multiplied by 1.2.

k_H values for shallow portion are decided, considering that the ground reaction can not be more than the passive earth pressure, as shown in Fig.2-18.

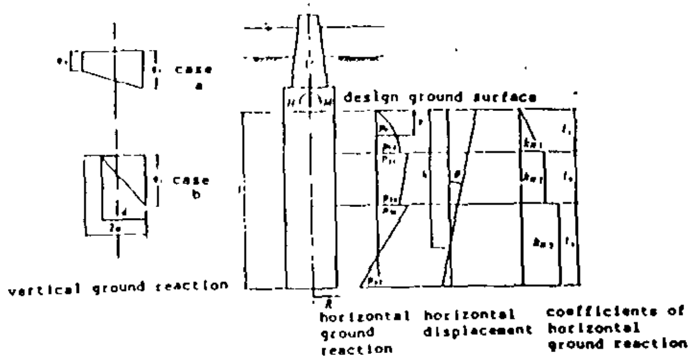

Fig 2-18 Distribution of Ground Reaction and Displacement

(2) Base of caisson

Because the lateral force and the overturning moment developed at the base is small, the ultimate bearing capacity is computed assuming that the effect of the inclination and eccentricity of the reaction force be disregarded. Allowable bearing capacity for seismic force is derived by dividing the value of ultimate bearing capacity by safety factor 2.

Allowable shear resistance of ground under the footing is derived following the same procedure of 2.3.2.

(3) Side of caisson

The allowable horizontal bearing capacity of the side of caisson is obtained by dividing the strength of passive earth pressure developed at the ground at the side of the foundation by a safety factor 1.2. In order to derive passive earth pressure during an earthquake, friction angle between caisson side and ground shall be $-\phi/6$ ($-\phi/3$ for static load), in which ϕ is shear resistant angle of the ground.

In this case, the ground reaction force for the caisson side is assumed to be derived by multiplying the ground reaction force by 0.8.

(4) Caisson

The bending moment along the axis of the caisson due to earthquake force shall be computed by the ground reaction force in Figure 2-18, then required amount of reinforcement shall be decided.

Stresses in the perpendicular direction of the caisson axis shall be calculated assuming the caisson as a rigid body supported by a side wall or partition (at outer edge for circular cross section) receiving ground reaction force from one direction. In this calculation, static earth pressure and water pressure have to be considered (refer to Fig.2-19 b)

The support for the top slab shall be examined against uplift, bearing and sliding. The reinforcement ratio required to resist the uplift shall be more than 0.2%, and bar with a diameter longer than 16mm must be used. If necessary, shear keys shall be provided against sliding (refer to Fig.2-19 a)

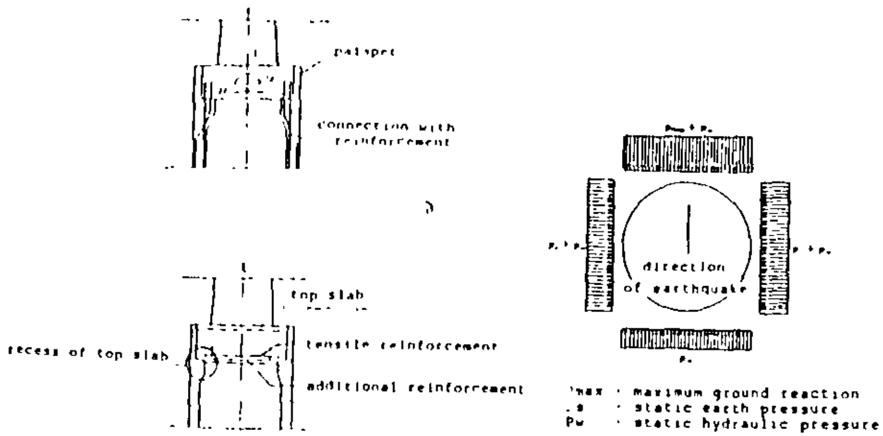

Fig 2-19 Reinforcement of Caisson Foundation and Design Earthquake Loadings

2.3.4 Pile Foundation

(1) Pile Reaction and Displacement

Calculations of the pile reaction and the displacement are made by the elastic analysis method assuming a rigid footing and displacements (vertical, horizontal and rotational) of footing.

Refer to 2.3.1 for the method of determining the coefficient of horizontal subgrade reaction of piles. Effect of group piles is important issue to be considered in design. However, taking into consideration the complexity of the actual ground conditions and insufficient test data, it is generally assumed that if the center-to-center spacing is about 2.5 times diameter of pile, the value of k_H for single piles can be used

The coefficient of pile head reaction in the vertical direction k_v (vertical spring constant of a pile) is defined based on numerous loading tests as

$$kv = a\frac{A_p E_p}{l} \qquad (2\text{-}14)$$

Where

- a : coefficients depending on type of pile (Table 2-4)
- A_p : sectional area of a pile (cm^2)
- E_p : Yang's modulus of a pile (kgf/cm^2)
- l : pile length (cm)

Table 2-4 Coefficient "a" in Eq.(2-14)

Construction methods	coefficient "a"
Steel pipe pile	$0.014(l/D)+0.78$
Prestressed Concrete pile Prestressed High strength Pile	$0.013(l/D)+0.61$
Cast-in-place Concrete pile	$0.031(l/D)-0.15$
Embedded Steel pipe pile	$0.009(l/D)+0.39$
Embedded prestressed Concrete pile	$0.011(l/D)+0.36$
Pre-boring pile	$0.009(l/D)+0.81$

(2) Allowable bearing capacity of piles

Allowable bearing capacity of pile shall be given as

$$R_a = \frac{\gamma}{n}(R_u - W_s) + W_s - W \qquad (2\text{-}15)$$

where

- R_a : allowable bearing capacity in axial direction at the pile head(kgf)
- n : safety factor (refer to Table 2-5)
- γ : modification coefficient for safety factor according to method adopted for estimating ultimate bearing capacity (refer to Table 2-6)
- R_u : ultimate bearing capacity of pile(kgf)
- W_s : effective weight of earth to be replaced by the pile(kgf)
- W : effective weight of pile and earth in pile(kgf)

Table 2-5 Safety Factor

Loading type \ Pile type	Bearing pile	Friction pile
Static Load	3	4
Seismic load	2	3

Table 2-6 Modification Coefficient γ According to Method Adopted for Estimating Ultimate Bearing Capacity

Estimation method for ultimate bearing capacity	Modification cofficient
Bearing capacity formula	1.00
Vertical loading test	1.20

The allowable pull out capacity P_a of a pile at the top of pier is given by

$$P_a = \frac{1}{n} P_u + W \qquad (2\text{-}16)$$

in which P_u represents ultimate pull out capacity

(3) Stress of the pile

An example for computing stress of piles is presented in Section 3 3. Fig 2-20 shows two examples of the connection of pile with footing

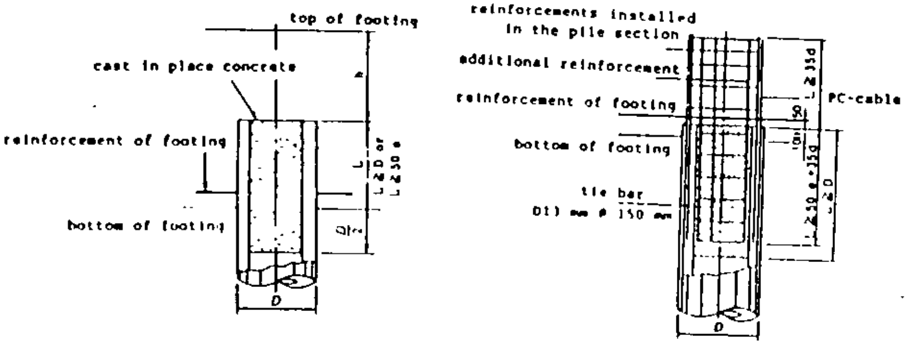

a) Method A b) Method B

Fig. 2-20 Connection with Footing and Pile

FACULTAD DE INGENIERIA U.N.A.M.
DIVISION DE EDUCACION CONTINUA

CURSOS ABIERTOS

XXV CURSO INTERNACIONAL INGENIERÍA DE SÍSMICA

MÓDULO III:

DISEÑO SÍSMICO DE PUENTES

TEMA :

ANEXO

DR. ROBERTO GÓMEZ MARTÍNEZ
PALACIO DE MINERÍA
AGOSTO - SEPTIEMBRE 1999

Palacio de Minería Calle de Tacuba 5 Primer piso Deleg. Cuauhtemoc 06000 Mexico, D F APDO Postal M-2285
Telefonos. 512-8955 512-5121 521 7335 521 1987 Fax 510-0573 521-4020 AL 26

CIMENTACIONES CIRCULARES

TIPO DE MOVIMIENTO	K
TRASLACION VERTICAL	$4GR/(1 - \nu)$
TRASLACION HORIZONTAL	$8GR/(2 - \nu)$
GIRO DE TORSION	$16GR^3 / 3$
GIRO DE FLEXION	$8GR^3 / 3(1 - \nu)$

G = módulo de rigidez al corte del semi-espacio

ν = módulo de Poisson del semi-espacio

R = radio de la zapata

CIMENTACIONES RECTANGULARES

$K_R = \alpha \beta K$

donde :

α = factor de forma
β = factor de desplante
K = coeficiente de rigidez para una cimentación circular

FACTOR DE DESPLANTE

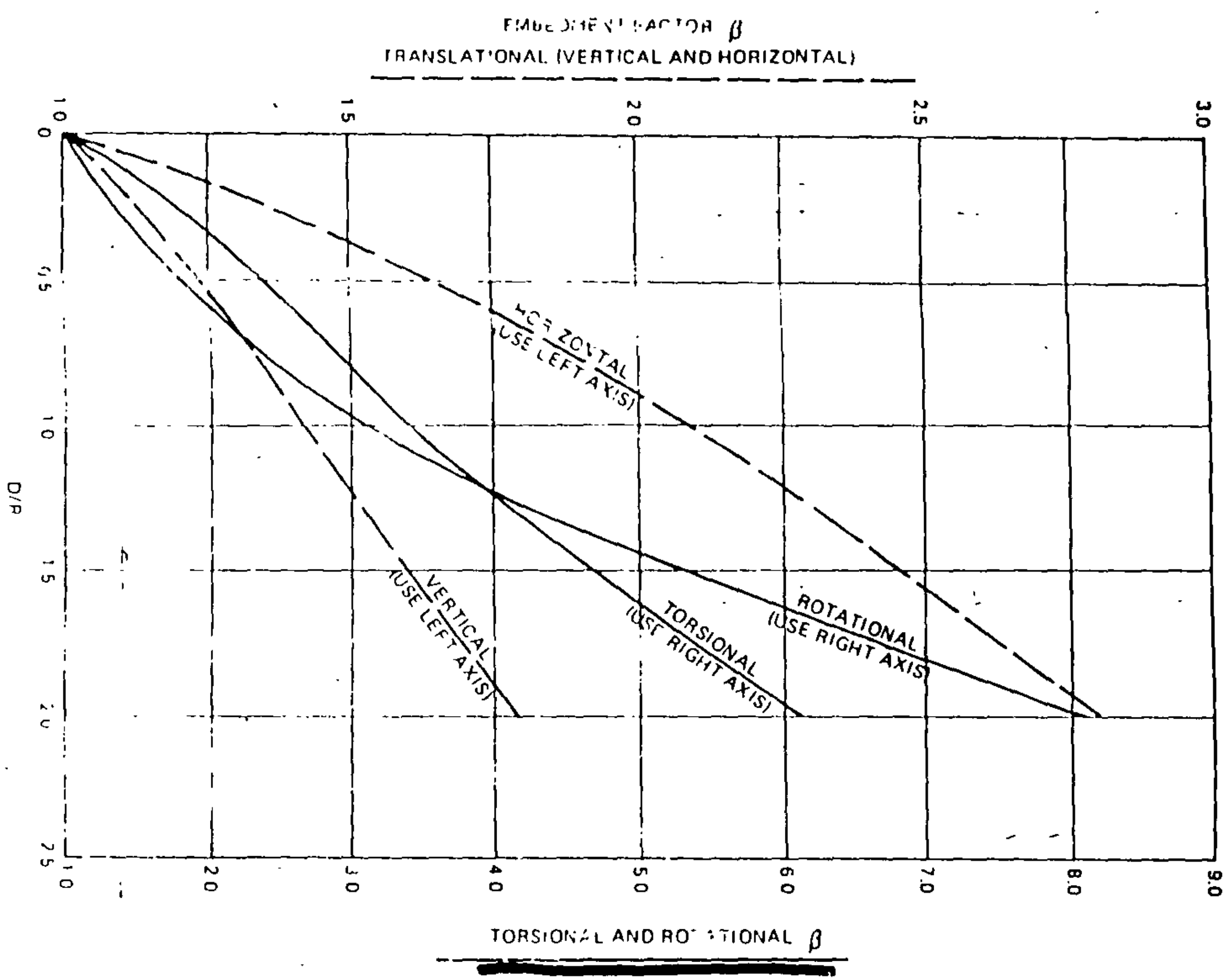

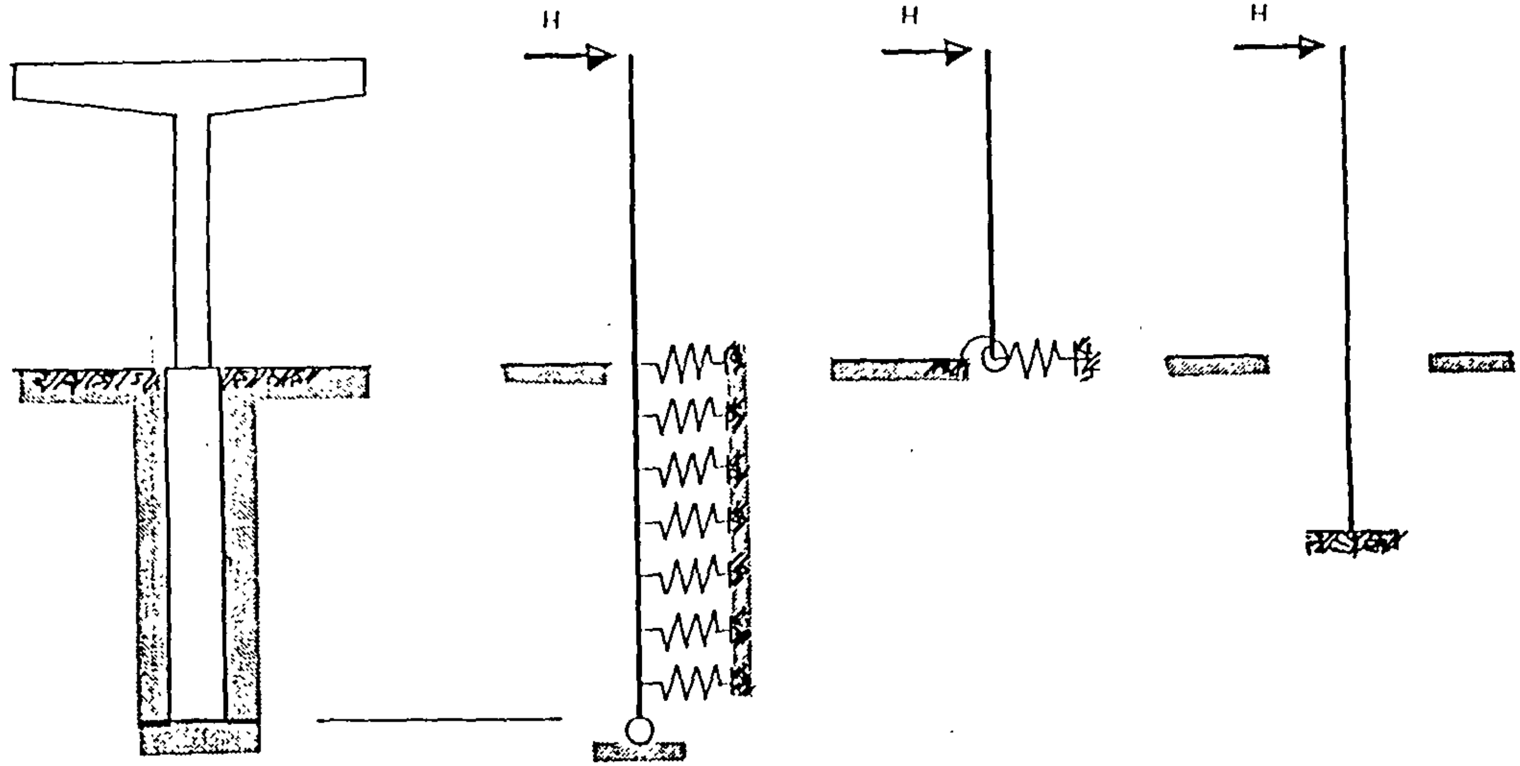

Sistema puente-cimentación | Equivalente MODELO DE RESORTES PARA EL SUELO | Equivalente MODELO DE RESORTES EN LA BASE | Equivalente MODELO DE VOLADIZO

MODELOS PARA REPRESENTAR LA RIGIDEZ DE ~~LA~~ CIMENTACIONES CON PILOTES

RADIOS EQUIVALENTES

TRASLACIÓN	$R_0 = 4BL/\pi$
ROTACIÓN (FLEXION ALREDEDOR DE X)	$R_3 = \left[\frac{4BL\,(4B^2 + 4L^2)}{6\pi}\right]^{1/4}$
ROTACIÓN (FLEXIÓN ALREDEDOR DE Y)	$R_2 = \left[\frac{(2B)^3 + (2L)}{3\pi}\right]^{1/4}$
TORSIÓN	$R_1 = \left[\frac{(2B)\,(2L)^3}{3\pi}\right]^{1/4}$

Zapata rectangular

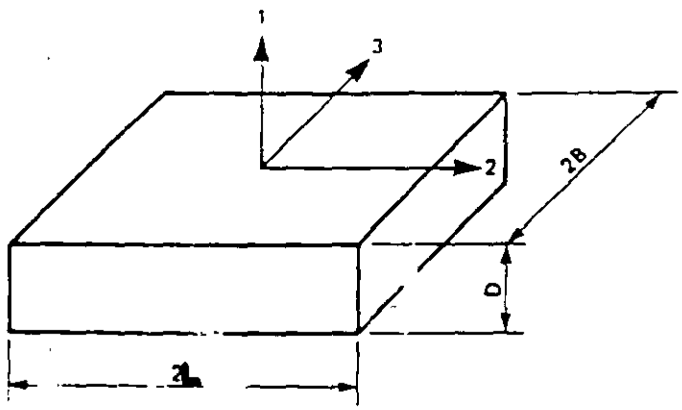

Zapata circular equivalente

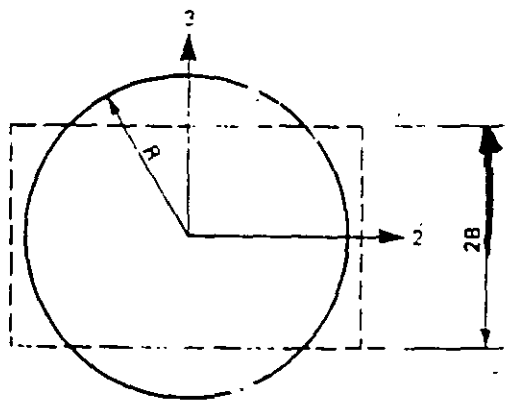

Radio equivalente

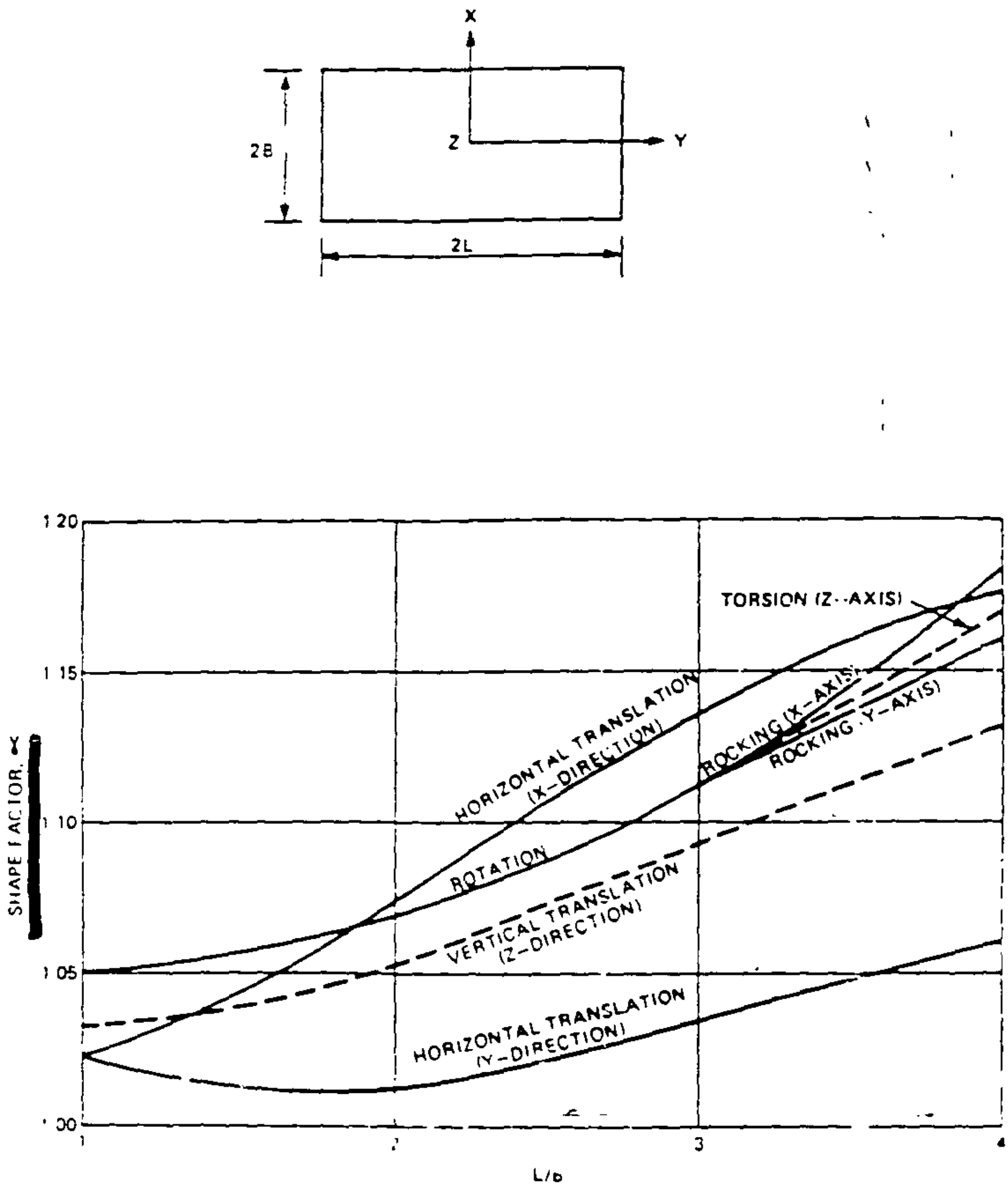

FACTOR DE FORMA

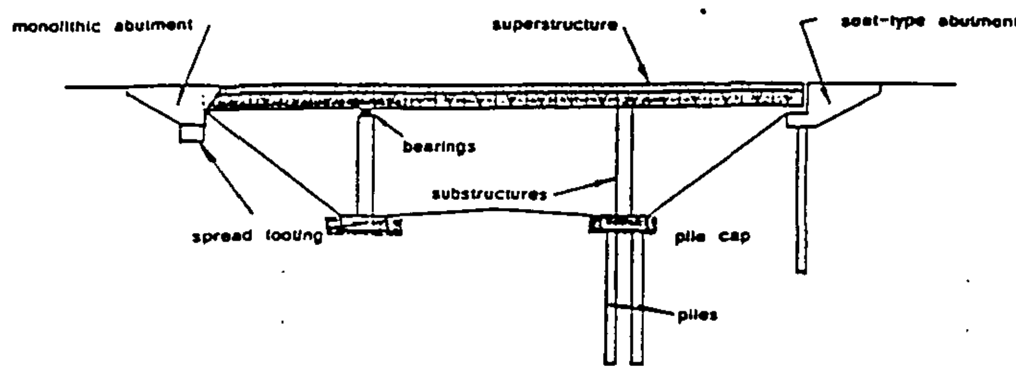

COMPONENT	FACTORS AFFECTING LATERAL STIFFNESS	RELATIVE LATERAL STIFFNESS	
		Component Type	Very Flexible — Very Stiff
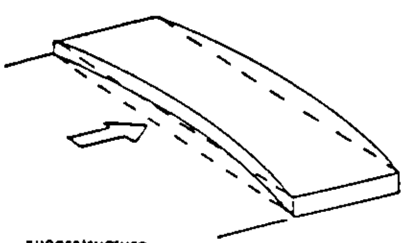 superstructure	total bridge length total bridge width structural type continuity plan geometry	• continuous box girder • continuous T-girder with diaphragms • continuous T-girder without diaphragms • simple spans T-girders with diaphragms • simple spans T-girder without diaphragms	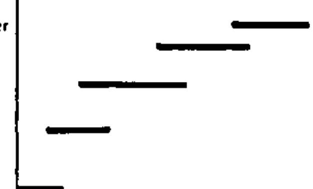
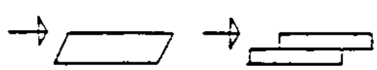 bearings	physical dimensions bearing type material properties	• sliding plates with side stops • sliding plates without side stops • elastomeric bearings • shear keys	
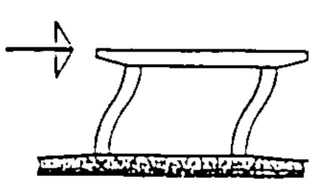 substructure	height section properties structural type end conditions	• single column • multi column • wall pier	
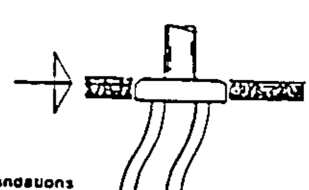 foundations	effective depth section properties structural type soil conditions	• footings on rock or dense soils • batter piles • vertical piles • spread footings on soft soils	

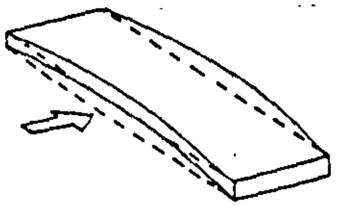

SUPERSTRUCTURE

(a)	point load at midspan	$K = 48\ EI_s/L^3(1+\alpha)$
(b)	uniform load	$K = 384\ EI_s/5L^3(1+0.8\alpha)$

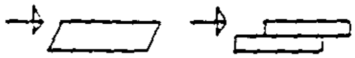

BEARINGS

(a)	elastomeric	$K = G_r A_r/T_r$
(b)	sliders	very high initially, then zero
(c)	pot bearings	very high

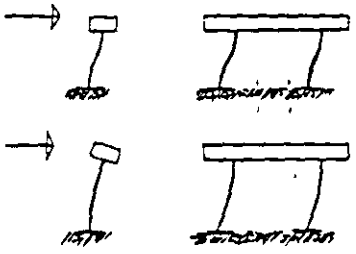

PIERS

BENTS

(a) single column[1,3]

fixed-fixed	$K = 12\ EI_c/h^3$
fixed-pinned	$K = 3\ EI_c/h^3$

(b) multi-columns[2,3]

fixed-fixed	$K = 12n\ EI_c/h^3$
fixed-pinned	$K = 3n\ EI_c/h^3$

WALLS

$K = 3\ EI_w/h^3(1+\beta)$

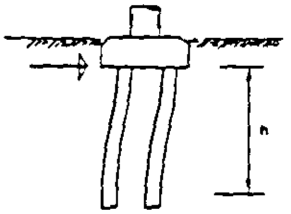

PILES

as for multicolumn bents
assume h = effective length
to point of fixity

NOTATION

E	elastic modulus
G_r	shear modulus of elastomer
I_s, I_c, I_w	moment of inertia of the superstructure, single column
L	total length of bridge
h	column or wall height
n	number of columns in each bent
A_r	bonded area of elastomer
T_r	total thickness of elastomer
α	$= 12\ EI_s/GA_sL^2$
β	$= 3\ EI_w/GA_wL^2$
A_s, A_w	effective shear areas for superstructure and wall sections, respectively

Notes

1. If torsional stiffness of superstructure is very high, use fixed-fixed result. If stiffness is very low, use fixed-pinned result. If stiffness is in between, include actual value in calculation for lateral stiffness.

2. If columns neither fixed nor pin ended but framed into bent cap use a moment distribution procedure to calculate pier stiffness.

3. If pier is piled bent or single column drilled shaft, above expression can be used provided h includes depth to fixity of pile(s)

FACULTAD DE INGENIERIA U.N.A.M.
DIVISION DE EDUCACION CONTINUA

CURSOS ABIERTOS

INSTITUTO MEXICANO DEL TRANSPORTE

XXV CURSO INTERNACIONAL DE INGENIERÍA SÍSMICA

MÓDULO III. DISEÑO SÍSMICO DE PUENTES

TEMA :

DISEÑO SÍSMICO DE PUENTES
(ACERO. PARTE I)

EXPOSITOR: DR. JOSÉ ALBERTO ESCOBAR SÁNCHEZ
PALACIO DE MINERÍA
SEPTIEMBRE 1999

DISEÑO SISMICO DE PUENTES DE ACERO

INTRODUCCION
- DISEÑO ESTRUCTURAL
- PRINCIPIOS DEL DISEÑO ESTRUCTURAL

TIPOS DE PUENTES DE ACERO
- PUENTES CORTOS
- PUENTES PARA CLAROS MEDIANOS
- PUENTES LARGOS
- PUENTES PARA GRANDES CLAROS

FILOSOFIAS DE DISEÑO DE ESTRUCTURAS DE ACERO
- CONSIDERACIONES GENERALES
- DISEÑO POR ESFUERZOS PERMISIBLES
- DISEÑO PLASTICO
- DISEÑO POR FACTORES DE CARGA Y RESISTENCIA (LRFD)

DISEÑO POR FACTORES DE CARGA Y RESISTENCIA
- CONCEPTOS BASICOS
- FACTOR DE SEGURIDAD
- INDICE DE CONFIABILIDAD
- FACTORES DE CARGA

PILAS DE ACERO
- EFECTOS NO LINEALES

DISEÑO DE ELEMENTOS A TENSION

DISEÑO DE ELEMENTOS A COMPRESION Y FLEXOCOMPRESION

DISEÑO DE SECCIONES I EN FLEXION

DISEÑO DE CONEXIONES

BIBLIOGRAFIA

DISEÑO ESTRUCTURAL

Determinación de secciones de elementos y sus uniones
para que la resistencia de la estructura sea mayor
que el efecto de las cargas ⇒ margen de seguridad.

Además, las estructuras bien diseñadas deben:

- ser seguras para sus ocupantes (sensación de robustez o fragilidad, de tranquilidad o de intranquilidad
- soportar las cargas de diseño sin sobre esforzar algunos de sus componentes
- evitar deformaciones excesivas
- ser "económicas" de construir y de operar durante su vida útil

PRINCIPIOS DEL DISEÑO ESTRUCTURAL DE PUENTES

- necesidad de un puente: salvar un obstáculo (atravezar un río, cruzar una carretera, etc.)
- evaluación económica; la vía impone sus condiciones (ancho, alturas, peraltes, trazo en planta, etc.)
- propuestas iniciales; tomar en cuenta las condiciones funcionales:
    - impuestas por el móvil que utilizarán el puente (peatones, autos y camiones, trenes etc.)
    - rigidez (control de vibraciones)
    - materialización del puente (piedra, madera, acero, concreto reforzado, etc.), (vigas, arcos, armaduras, atirantado, colgante, cimentación, problemas de socavación, etc.)
    - diseño: planos detallados y especificaciones para construcción

En resumen:

SEGURIDAD. FUNCIONALIDAD Y ECONOMIA

TIPOS DE PUENTES DE ACERO

PUENTES CORTOS

- inicialmente menos de 30 m de longitud y formados por vigas con sección I
- actualmente llegan a ser hasta de 100 m de largo y están hechos a base de trabes armadas. Lo anterior se debe a:
  - i) mejores aceros de construcción (con esfuerzos de fluencia hasta 3 veces superiores a los de los primeros aceros estructurales).
  - ii) soldaura (taller o campo)
  - iii) pernos de alta resistencia (taller o campo) conexiones resistentes a cargas cíclicas
  - iv) diseño compuesto (losa de concreto-vigas de acero)

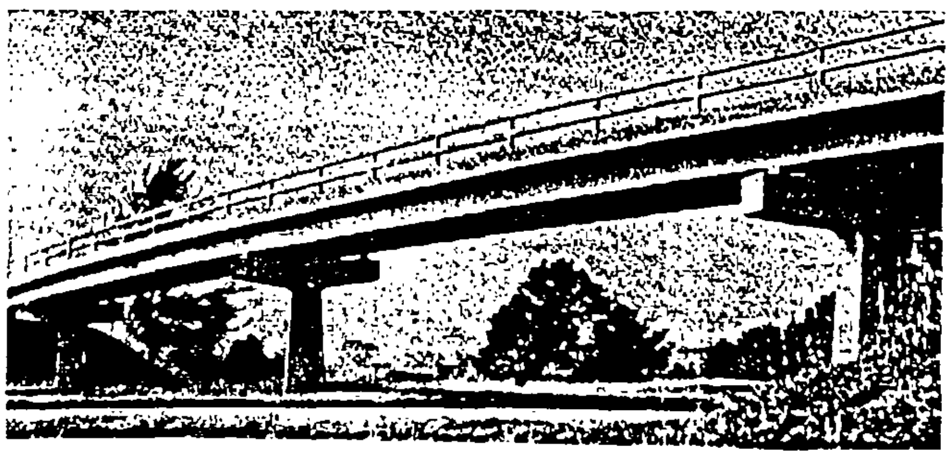

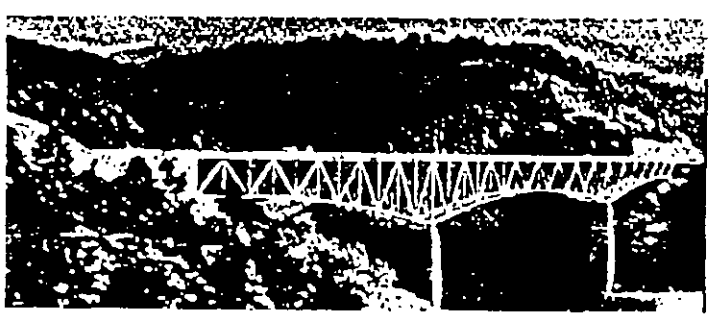

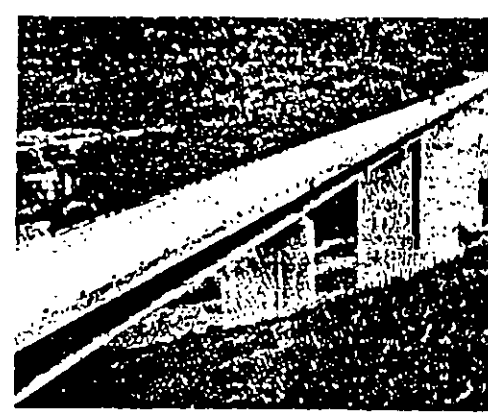

Componentes.
- vigas armadas o roladas
- vigas en cajón

PUENTES PARA CLAROS MEDIANOS

- de hasta 50 m de longitud y formados por secciones I armadas, secciones en cajón, armaduras, arcos y atirantados
- estructuras con relativo peso propio bajo
- las vigas armadas pueden construirse para verse atractivas

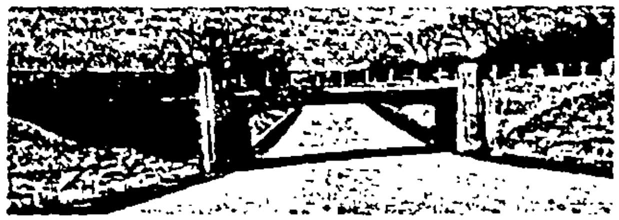

- el transporte de vigas armadas de más de 35 m de longitud puede llegar a representar un problema
- también se fabrican de vigas en cajón para resistir la torsión, en este caso se usan para claros de hasta 150 m
- pueden representar problemas debido a defectos de soldadura y en consecuencia fallas por fatiga

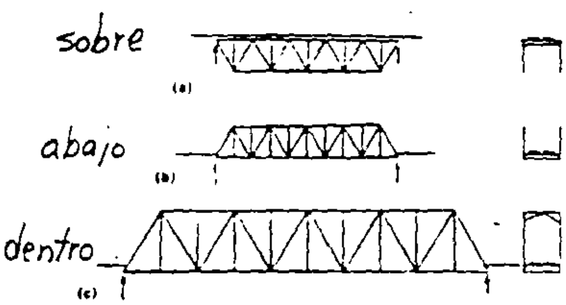

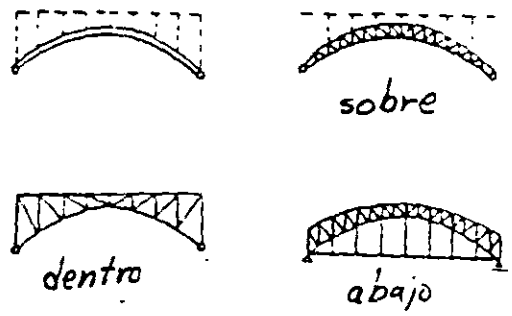

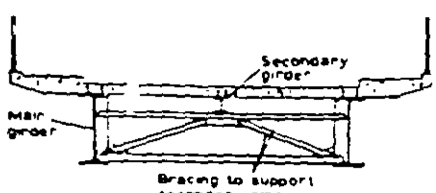

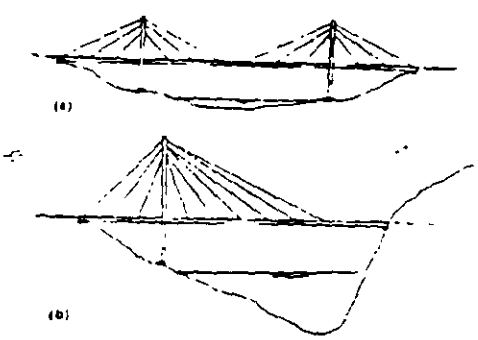

Componentes.
vigas armadas, vigas en cajón, elementos a tensión, elementos a compresión

PUENTES LARGOS

- para claros de 50 a.150 m
- pueden ser de vigas armadas, vigas en cajón, arcos, armaduras (evitan el problema de flexión en los elementos estructurales), atirantados y sus combinaciones

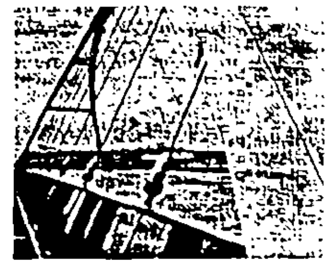

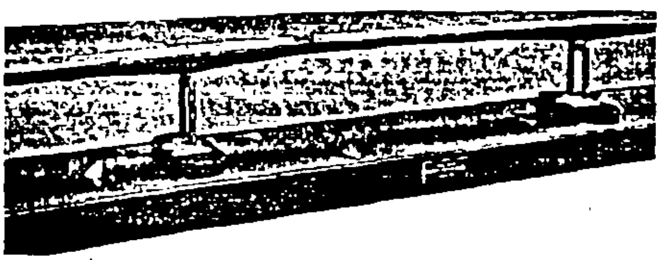

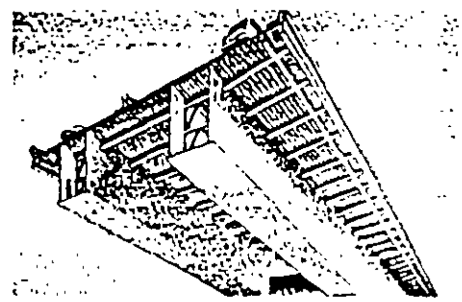

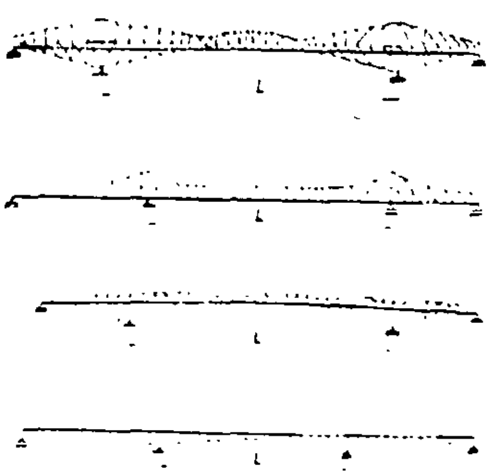

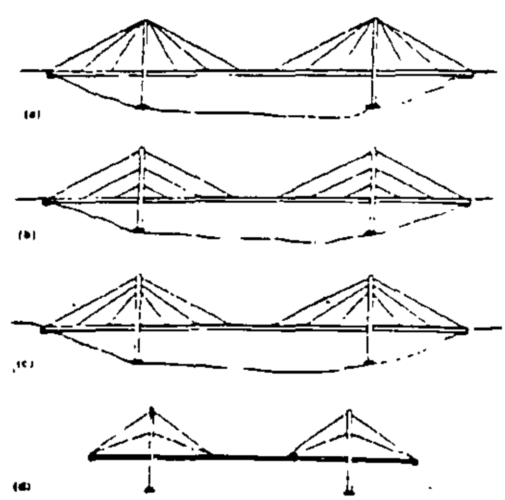

PUENTES PARA GRANDES CLAROS

- para longitudes superiores a 150 m
- puentes atirantados o colgantes (bajo peso propio)
- principal elemento de transmisión de las cargas a las torres de soporte es el cable flexible trabajando a tensión

<u>Puentes atirantados</u>

(a)

tirantes en abanico

(b)

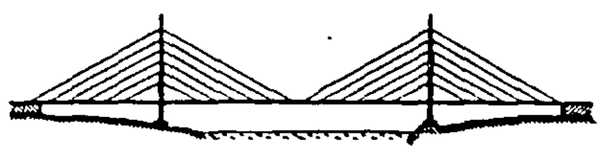

tirantes en arpa

(c)

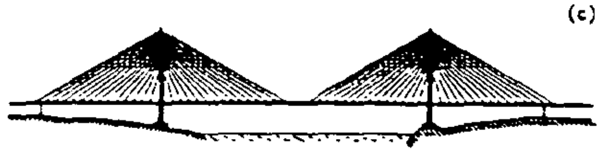

tirantes en semi-abanico

Algunas caracteristicas.

- cables rectos
- todos los cables son mas cortos que la longitud total del puente
- no se han observado problemas aerodinamicos en estas estructuras
- economicos en claros de 100 a 350 m

Puentes colgantes

Algunas características:

- cables curvos y rectos
- los anclajes de los cables pueden ser costosos si la capacidad de carga del suelo para la cimentación no es buena
- se requieren armaduras o vigas para dar rigidez vertical al soporte de cargas
- se requieren armaduras o vigas para dar rigidez lateral a la estructura y evitar problemas dinámicos
- para claros superiores a 600 m son la única alternativa, sin embargo se han construido para puentes peatonales

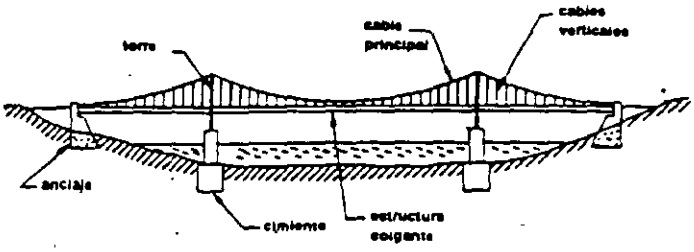

elevación

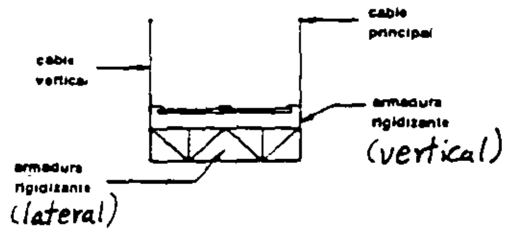

sección transversal

Componentes:
cables flexibles, torres (concreto)

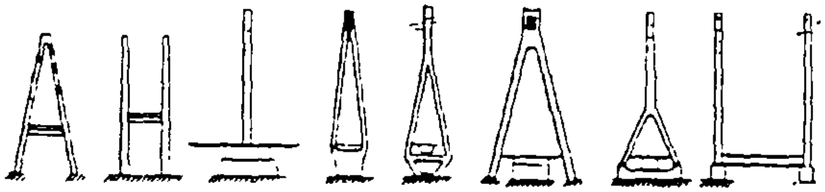

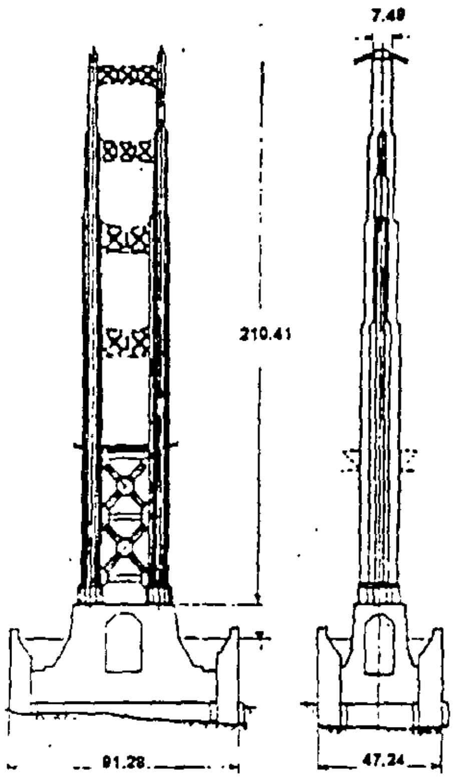

Golden Gate

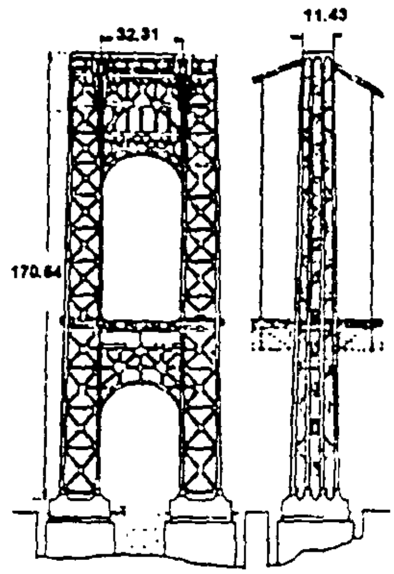

George Washington

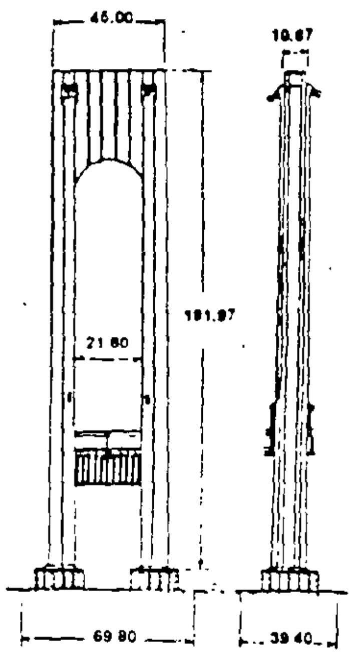

Verrazano Narrows

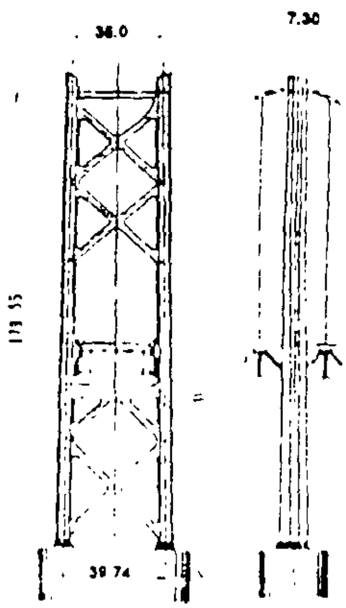

Minami Bisan Seto

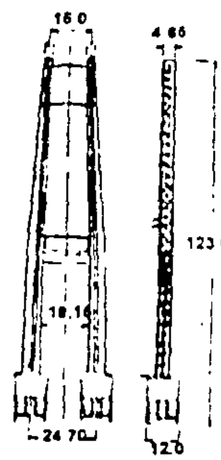

Lancarville (torre de concreto)

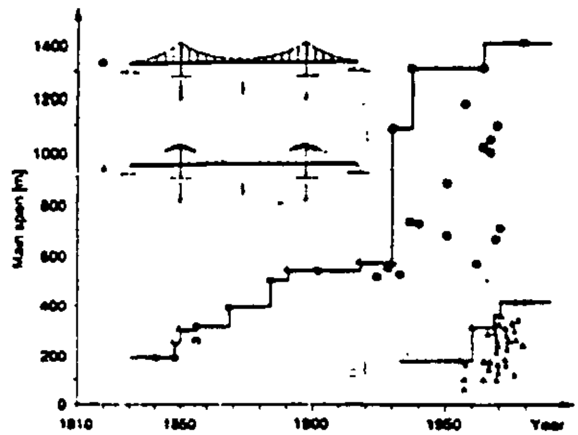
Main span [m]
1400
1200
1000
800
600
400
200
0
1810
1850
1900
1950
Year

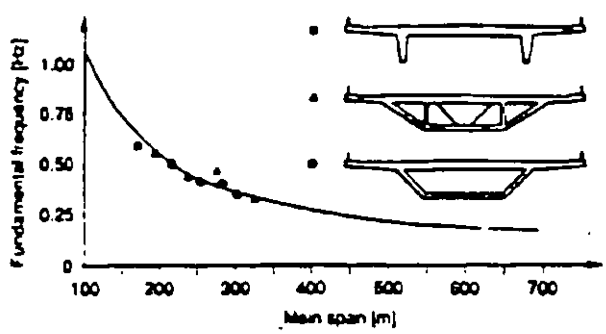
Fundamental frequency [Hz]
1.00
0.75
0.50
0.25
0
100
200
300
400
500
600
700
Main span [m]

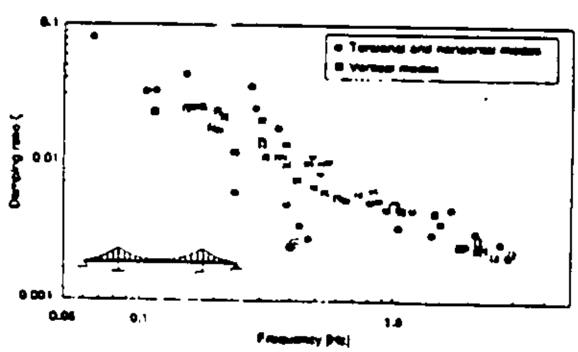
Damping ratio ζ
0.1
0.01
0.001
0.08
0.1
1.0
Frequency [Hz]
Vertical modes

RESUMEN

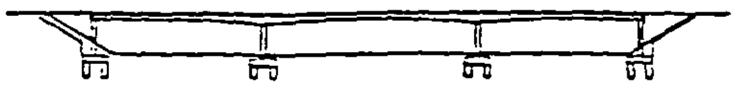

a)

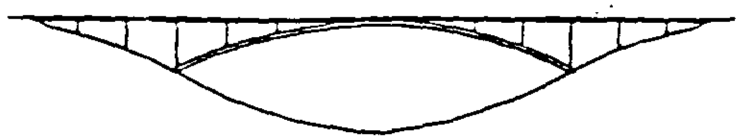

b)

c)

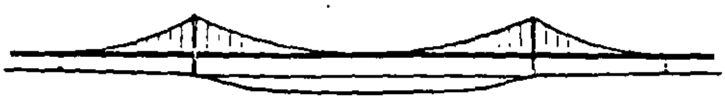

d)

TABLE 2.3 Span Lengths for Various Types of Superstructure

Structural Type	Material	Range of Spans (m)	Maximum Span in Service (m)
Slab	Concrete	0–12	
Girder	Concrete	12–250	240, Hamana-Ko Lane
	Steel	30–260	261, Sava I
Cable-stayed girder	Concrete	≤250	235, Maracaibo
	Steel	90–850	856, Normandy
Truss	Steel	90–550	550, Quebec (rail)
			480, Greater New Orleans, Nos. 1 and 2 (road)
Arch	Concrete	90–300	305, Gladesville
	Steel truss	240–500	510, New River Gorge
	Steel rib	120–360	365, Port Mann
Suspension	Steel	300–1400	1410, Humber

FILOSOFIAS DE DISEÑO DE ESTRUCTURAS DE ACERO

Cargas y resistencias inciertas $\Rightarrow$ reglamentos de diseño
$\Rightarrow$ evitar la falla estructural

CONSIDERACIONES GENERALES DEL DISEÑO ESTRUCTURAL

Condición fundamental:

resistencia $\geq$ efecto de las cargas

Si la desigualdad anterior no se cumple $\Rightarrow$ falla (estado límite)

Estado límite: condición más allá de la cual la estructura o sus componentes dejan de funcionar adecuadamente para lo que fueron diseñados

Estados límite:

- agrietamientos
- deflexiones
- fatiga
- hundimientos
- pandeo
- etc.

Objetivo importante del diseño estructural: prevenir la formación de un estado límite

Antieconómico diseñar un puente para que ninguno de sus elementos estructurales falle pero.

¿ Cuál es el riesgo aceptable ?
¿ Cómo establecerlo ?
¿ Es suficiente la experiencia individual y colectiva ?

$\Downarrow$

procedimientos de diseño

DISEÑO POR ESFUERZOS PERMISIBLES

- primeros procedimientos de diseño aplicados a estructuras de acero

$$\text{factor de seguridad} = \frac{\text{R (resistencia)}}{\text{C (efecto de cargas)}}$$

En los primeros puentes de armaduras

$$\text{área necesaria} \geq \frac{\text{efecto de carga axial}}{\text{esfuerzo permisible}}$$

Factor de seguridad = f (longitud del elemento, carga, comportamiento, etc.)

- suposiciones iniciales:
    - no existen esfuerzos antes de aplicar las cargas
    - no existen esfuerzos residuales
    - los conceptos de resistencia están basados en el comportamiento elástico no en la resistencia de los materiales
    - no existe variabilidad en las cargas ni en las resistencias

Observación

Las armaduras son estructuras estáticamente determinadas.
En sus elementos estructurales no aparecen elementos mecánicos combinados (flexion + cortante, flexion biaxial + carga axial, etc.)

DISEÑO PLASTICO

Condición límite = carga que ocasiona el colapso de la estructura
Carga de colapso plástico = carga de servicio x factor de carga

Conceptos básicos

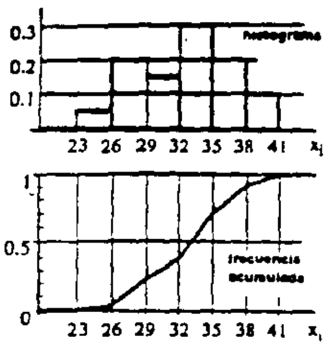

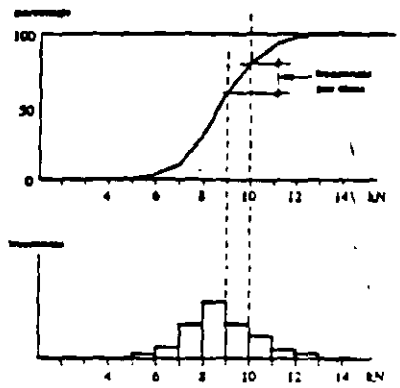

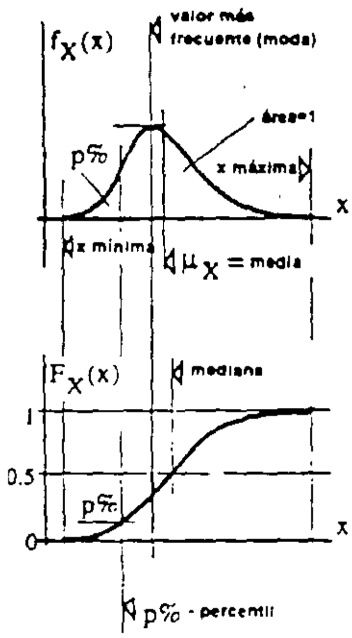

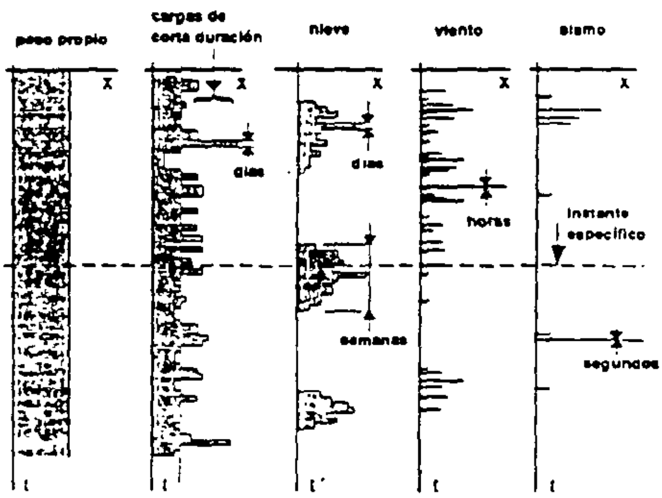

DISEÑO POR FACTORES DE CARGA Y RESISTENCIA (LRFD)

En este caso:

$$\text{resistencia } (R) \geq \text{efecto de las cargas } (C)$$

se transforma en:

$$\varnothing Rn \geq \text{ efecto } \Sigma \gamma_i C_i$$

donde $\varnothing_i$, γ_i son los factores de resistencia y de carga respectivamente

estadísticamente $\varnothing < 1.0$
$\gamma > 1.0$

El factor $\varnothing$ toma en cuenta las incertidumbres en.

- propiedades de los materiales
- ecuaciones para calcular la resistencia
- calidad de la mano de obra
- control de calidad de la obra
- consecuencias de la falla

El factor γ toma en cuenta las incertidumbres en:

- magnitud de las cargas
- variabilidad espacial de las cargas
- posibles combinaciones

FACTOR DE SEGURIDAD

Para una estructura segura se requiere que

$$C < R$$

si $C = R \Rightarrow$ se alcanza un estado límite, en este caso

$$F = R/C = 1.0$$

suponiendo ahora una sobre carga ΔC, y una disminución de la resistencia ΔR se tendrá:

$$C + \Delta C \leq R - \Delta R$$

o también:

$$\underbrace{C(1+\Delta C/C)}_{\gamma} \leq R\,\underbrace{(1-\Delta R/R)}_{\varnothing}$$

$$\gamma C \leq \varnothing R$$

el factor de carga requerido será:

$$R/C = (1+\Delta C/C)/(1-\Delta R/R) = FSR$$ (factor de seguridad requerido)

Ejemplo:
Sea una resistencia con una deficiencia del 15% ($\Delta R/R = 0.15$), y una sobrecarga del 40% en el sistema estructural ($\Delta C/C = 0.4$). Ambos estadísticamente independientes con una probabilidad de ocurrencia de 1/1000.

La probabilidad de que ocurran simultáneamente es:

$$(1/1000)\,(1/1000) = 1\times10^{-6}$$

el factor de seguridad requerido es:

$$FSR = (1+0.4)/(1-0.15) = 1.40/0.85 = 1.65 \Rightarrow R/C$$

Sea ahora $\left.\begin{array}{l}\Delta R/R = 0.25\\ \Delta C/C = 0.40\end{array}\right|$ ocurrencia de 1/1000

se tiene.

$$FSR = (1+0.4)/(1-0.25) = 1.4/0.75 = 1.87$$

Al no considerar las variaciones ΔR y ΔC, el factor de seguridad calculado por esfuerzos permisibles tendrá el mismo valor en ambos casos

Así las variaciones en la resistencia estan dadas por.

$$R = \varnothing R_n$$

donde:

R = resistencia factorizada

$\varnothing$ = factor de resistencia (toma en cuenta variaciones aleatorias)

Rn = reistencia nominal (resistencia calculada utilizando valores conservadores de las propiedades de los materiales, dimensiones de la sección, etc.)

p. ej. la resistencia nominal de una viga compacta es:

$$Rn = Mp = Z\, Fy$$

donde Mp es el mto. plástico; Z es el módulo de sección plástico (dependiendo de las dimensiones que el fabricante dice que tiene la sección y Fy esfzo. de fluencia y máximo

Los valores en las cargas están dadas por:

$$\text{Carga de diseño} = C = f\,(CM,\ CV,\ \text{sismo, etc.})\ \sum_{i=1}^{k} \gamma_i C_i$$

entonces.

$$\sum_{i=1}^{k} \gamma_i C_i \leq \varnothing\, Rn$$

INDICE DE CONFIABILIDAD

Si $C \geq R \Rightarrow$ falla

ahora

$$F = R - C \Rightarrow \text{falla si } F \leq 0$$

considerando R y C normalmente distribuidas

$$\bar{F} = \bar{R} - \bar{C} \quad ; \quad \sigma_F^2 = \sigma_R^2 + \sigma_C^2$$

entonces la probabilidad de falla es

$$Pf = Pr\,[\,F \leq \underset{\text{cero}}{0}\,] = \int_{-\infty}^{0} P\,(f)\,df$$

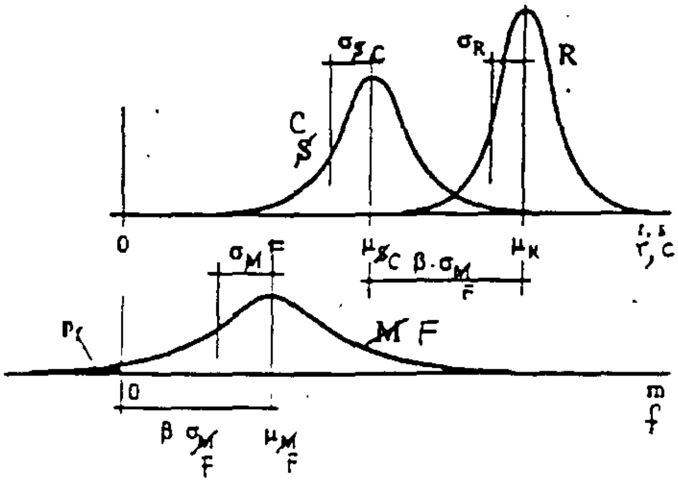

$F = \bar{F} - \beta \sigma_F = 0$ por lo tanto $\beta = \bar{F} / \sigma_F$ = índice de confiabilidad

sustituyendo:

$$\beta = (\bar{R} - \bar{C}) / \sqrt{(\sigma_R^2 + \sigma_C^2)}$$

Actualmente se considera que:

falla por resistencia $\quad P_f = 10^{-4}$; $\beta \doteq 3.5$

falla por servicio $\quad P_f = 10^{-2}$; $\beta \doteq 2.0$

Considerando ahora que R y C son lognormales:

$$\beta = \frac{\ln \bar{R} - \ln \bar{C}}{\sqrt{\sigma_R^2 + \sigma_C^2}} = \frac{\ln (\bar{R}/\bar{C})}{\sqrt{\sigma_R^2 + \sigma_C^2}}$$

de donde:

$$\ln (\bar{R}/\bar{C}) = \beta \sqrt{\sigma_R^2 + \sigma_C^2}$$

tomando exponenciales:

$$\bar{R}/\bar{C} = \exp \left(\beta \sqrt{\sigma_R^2 + \sigma_C^2} \right)$$

$$\therefore \; \bar{R} = \bar{C} \exp \left(\beta \sqrt{\sigma_R^2 + \sigma_C^2} \right)$$

de donde:

$$\bar{C}\theta \leq \bar{R}$$

para:

$$\theta = \exp \left(\beta \sqrt{\sigma_R^2 + \sigma_C^2} \right) = \exp \left(\alpha \beta (\sigma_R + \sigma_C) \right)$$

donde:

α = función de ajuste

entonces:

$$\theta = e^{\alpha\beta\sigma_R} e^{\alpha\beta\sigma_C}$$

y:

$$\bar{C}\theta = \bar{C} \left(e^{\alpha\beta\sigma_R} e^{\alpha\beta\sigma_C} \right) \leq \bar{R}$$

$$\bar{C} e^{\alpha\beta\sigma_C} \leq \bar{R} e^{-\alpha\beta\sigma_R}$$

Para las cargas de servicio:

$$C_u \underbrace{\frac{\bar{C}}{C_u} e^{\alpha\beta\sigma_C}}_{\gamma} \leq R_u \underbrace{\frac{\bar{R}}{R_u} e^{-\alpha\beta\sigma_R}}_{\phi}$$

$$C_u \gamma \leq R_u \phi$$

Ejemplo: cálculo del factor de resistencia para carga axial

Resistencia media: $\bar{R} = R_n \ \bar{M} \ \bar{A} \ \bar{P}$

donde: M es la variación de los materiales
A variación del área transversal
P factor de variación de mano de obra

estadísticamente:

$$\bar{M} = 1.08 \quad ; \quad \sigma_m = 0.10$$

$$\bar{A} = 1.0 \quad ; \quad \sigma_A = 0.05$$

$$\bar{P} = 1.02 \quad ; \quad \sigma_P = 0.05$$

entonces:

$$\sigma_R^2 = \sigma_m^2 + \sigma_A^2 + \sigma_P^2$$

$$\bar{R} = A_g F_y \ (1.08)(1.0)(1.02) = 1.10 \ R_n$$

$$\sigma_R = \sqrt{0.1^2 + 0.05^2 + 0.05^2} = 0.123$$

para $\beta \doteq 3.0$ ($P_f = 1.4 \times 10^{-3}$) y sabiendo que:

$$\phi = \frac{\bar{R}}{R_n} \exp\left(-0.55 \beta \sigma_R\right) = \frac{1.10 R_n}{R_n} \exp\left(-0.55(3)(0.123)\right) = 0.9($$

$\phi = 0.90$ ← especificación LRFD

FACTORES DE CARGA

$$\bar{C} \theta \leq \bar{R}$$

donde:

$$\theta = \exp\left(\beta \ \sqrt{\sigma_R^2 + \sigma_c^2}\right)$$

linealizando la ec. anterior:

$$\bar{C} e^{\alpha \beta \sigma_c} = \gamma_e \left(\gamma_{CM} C_M \overline{CM} + \gamma_{CV} C_{CV} \overline{CV}\right)$$

donde:

$\gamma_e = e^{-\alpha \beta \sigma_e}$ = error en el análisis estructural

$\gamma_{CM} = 1 + \alpha\beta \sqrt{\sigma_A^2 + \sigma_{CM}^2}$

$\gamma_{CV} = 1 + \alpha\beta \sqrt{\sigma_B + \sigma_{CV}^2}$

σ_A, σ_B aproximación al transformar la carga en sus efectos entonces:

$$\gamma_e \left(\underbrace{\underbrace{\gamma_{CM}\, C_M\, \overline{CM}}_{\text{tipo de carga}} + \gamma_{CV}\, C_{CV}\, \overline{CV}}_{\text{combinación de cargas}} \right) \leq \phi R_u$$

Ejemplo: para:

$\alpha = 0.55$
$\beta = 3.0$
$\sigma_e = 0.05$
$\sigma_A = 0.04$
$\sigma_B = 0.2$
$\sigma_{CV} = 0.13$

datos estadísticos

se obtiene:

$\gamma_e = 1.086$

$\gamma_{CM} = 1.093$

$\gamma_{CV} = 1.394$

CARGAS SISMICAS

Clasificación de los sismos según AASHTO: pequeños o moderados, de servicio, inte

Cargas sísmicas según AASHTO

1) coeficiente de aceleración según la zona sísmica
2) importancia del puente
3) zona de comportamiento sísmico
4) coeficiente de sitio
5) factor de modificación del comportamiento

COMBINACIONES DE CARGA

$$\gamma_{CV}\, CV + \gamma_{CM}\, CM + \gamma_S\, SISMO$$

Resistance Factors for the Strength Limit States*

Description of Mode	Resistance Factor
Flexure	$\phi_f = 1.00$
Shear	$\phi_v = 1.00$
Axial compression, steel only	$\phi_c = 0.90$
Axial compression, composite	$\phi_c = 0.90$
Tension, fracture in net section	$\phi_u = 0.80$
Tension, yielding in gross section	$\phi_y = 0.95$
Bearing on pins, in reamed, drilled or bolted holes and milled surfaces	$\phi_b = 1.00$
Bolts bearing on material	$\phi_{bb} = 0.80$
Shear connectors	$\phi_{sc} = 0.85$
A325M and A490MN bolts in tension	$\phi_t = 0.80$
A307 bolts in tension	$\phi_t = 0.67$
A325M and A490M bolts in shear	$\phi_s = 0.80$
Block shear	$\phi_{bs} = 0.80$
Weld metal in complete penetration welds:	
• Shear on effective area	$\phi_{e1} = 0.85$
• Tension or compression normal to effective area	ϕ = base metal ϕ
• Tension or compression parallel to axis of the weld	ϕ = base metal ϕ
Weld metal in partial penetration welds:	
• Shear parallel to axis of weld	$\phi_{e2} = 0.80$
• Tension or compression parallel to axis of weld	ϕ = base metal ϕ
• Tension compression normal to the effective area	ϕ = base metal ϕ
• Tension normal to the effective area	$\phi_{e1} = 0.80$
Weld metal in fillet welds:	
• Tension or compression parallel to axis of the weld	ϕ = base metal ϕ
• Shear in throat of weld metal	$\phi_{e2} = 0.80$

*In [A6.5.4.2] [From *AASHTO LRFD Bridge Design Specifications*, Copyright © 1994 by the American Association of State Highway and Transportation Officials, Washington, DC. Used by permission.]

PILAS DE ACERO

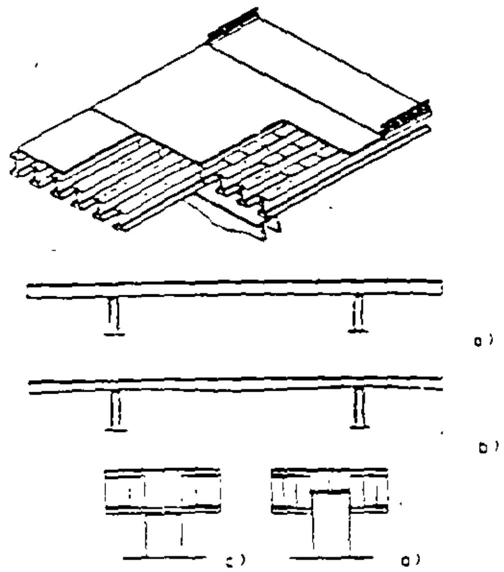

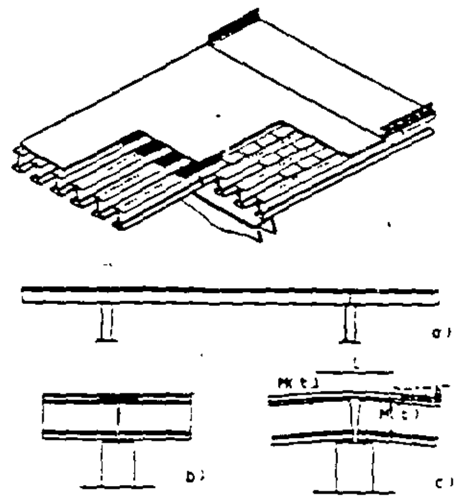

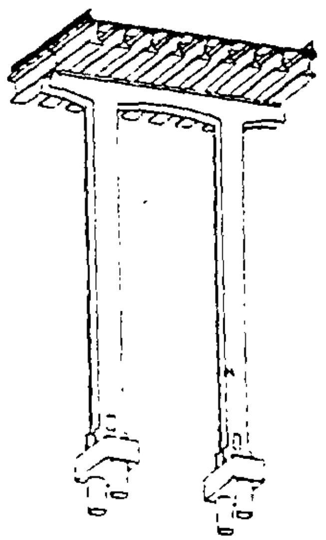

EFECTOS NO LINEALES

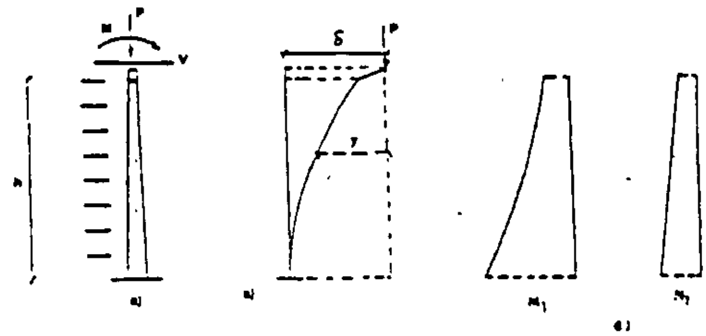

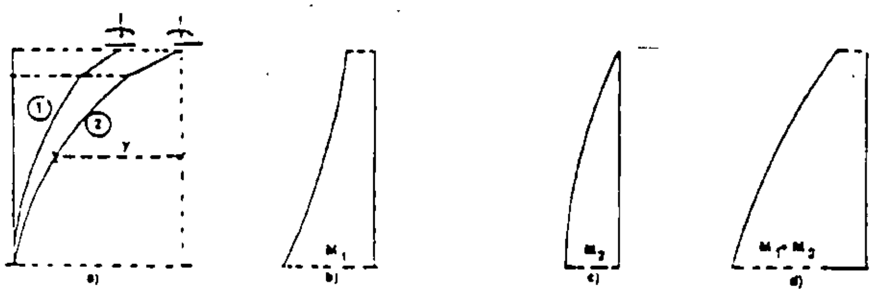

DISEÑO DE ELEMENTOS A TENSION

Sea un elemento de acero:

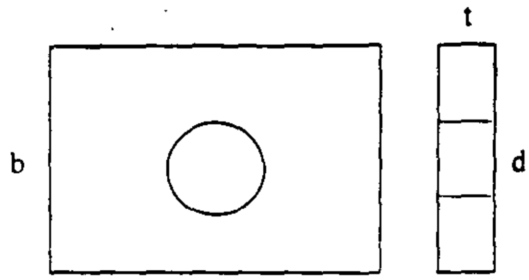

· área bruta = bt
· área neta = (b-d) t
. área efectiva

Ejemplo:
Determinar el área neta efectiva y la resistencia a tensión factorizada del ángulo mostrado en la figura. Usar acero estructural M270 grado 250 con Fu = 400 MPa (4078 kg / cm²) Fy= 250 MPa (2550 kg / cm²) (Pa = newton / mm² = (Kg/cm²)/9.807)

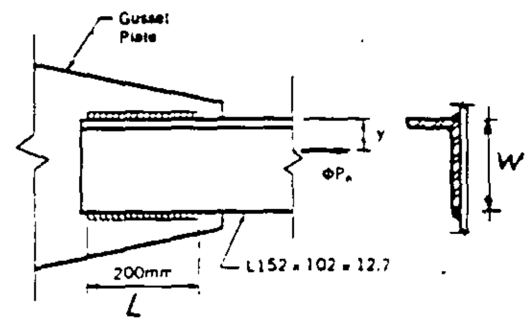

Resitencia a la tensión está definida por la menor de:

- *resistencia a fluencia de la sección transversal bruta.*
- *resistencia a ruptura de la seccion transversal reducida*

De acuerdo con AASHTO LRDF Bridge Design Specifications, 1994

Resistencia a la fluencia factorizada

$$\varnothing y\, Pny = \varnothing y\, Fy\, Ag$$

donde

$\varnothing y = 0.95$
Fy = *esfzo. de fluencia (MPa)*
Pny = *resistencia nominal a la fluencia en la sección bruta*
Ag = *area transversal bruta (mm²)*

Resistencia a la ruptura:

$$\varnothing u\, Pnu = \varnothing u\, Fu\, Ae$$

29

donde:

$\varnothing u = 0.80$
Pnu = resistencia nominal a la ruptura de la sección neta
Fu = esfuerzo a la tensión (MPa)
Ae = área de la sección transversal neta (mm^2)

Toma en cuenta la falla por factura frágil.

Para conexiones soldadas

$$Ae = UAg$$

donde:

$U = 1.0$ si $L > 2W$
$U = 0.87$ si $1.5W \leq L < 2W$
$U = 0.75$ si $W \leq L \leq 1.5W$
L = long. de la soldadura
W = separación de la soldadura

en este caso L=200 mm; W=152 mm, entonces:

$$L/W = 200/152 \;\therefore\; L = 1.3\,W \Rightarrow U = 0.75$$

Entonces, con $Ag = 3060\ mm^2$

$$Ae = U\,Ag = 0.75(3060) = 2295\ mm^2$$

La resistencia de fluencia es:

$$\varnothing y\,Pny = \varnothing y\,Fy\,Ag = 0.95(250)3060 = 727x10^3\ N \quad \underline{\textbf{RIGE}}$$

la resistencia a la ruptura es:

$$\varnothing u\,Pnu = \varnothing u\,Fu\,Ae = 0.8(400)2295 = 743x10^3\ N$$

(1 Newton= 1Kg / 9 807)

Ejemplo

Determinar el área neta y la resistencia a tensión del ángulo conectado con pernos mostrado en la figura. Los agujeros son de 22 mm de diámetro. Usar acero grado A250

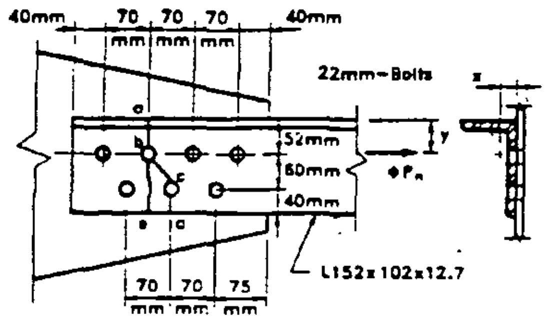

el ancho total de la sección es:

$w_g = 152 + 102 - 12.7 = 241.3$ *mm*

el diámetro efectivo de los agujeros es:

$d = \phi + 3.2 = 22 + 3.2 = 25.2$ *mm*

peralte neto para una línea de falla

$w_n = w_g - \Sigma d + \Sigma s^2/4g$

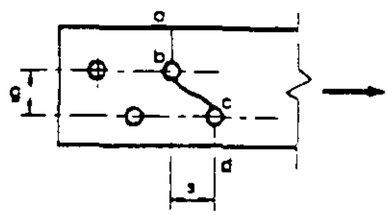

línea de falla a-b-c-d:

$w_n = 241.3 - 2(25.2) + 35^2/(4)(60) = 196.0$ *mm* <u>*RIGE*</u>

línea de falla a-b-c.

$w_n = 241.3 - 1(25.2) = 216.10$ *mm*

entonces

$A_n = t\, w_n = 12.7(196) = 2489\ mm^2$

Debido a que sólo un lado del ángulo está conectado, el área neta se debe reducir por el factor U. Para ello se usa la siguiente ecuación:

$U=1-(x/L)$

Si $x=25.2$ *mm;* $L=3x70=210$ *mm, entonces*

$A_e=U\,A_n=0.88(2489)=2910\ mm^2$

la resistencia factorizada a la fluencia es:

$\phi_y P_y=\phi_y F_y A_g=0.95(250)(3060)=725x10^3\ KN$

la resistencia factorizada a la ruptura es:

$\phi_u P_u=\phi_u F_u A_e=0.80(400)(2190)=701x10^3\ KN$ ***RIGE***

CONSIDERACIONES PARA EL DISEÑO DE CABLES

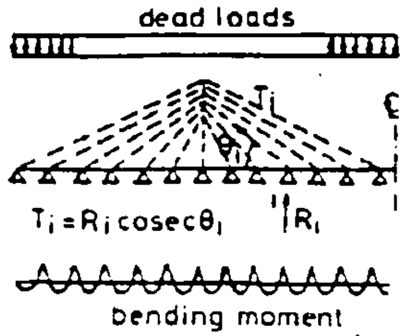

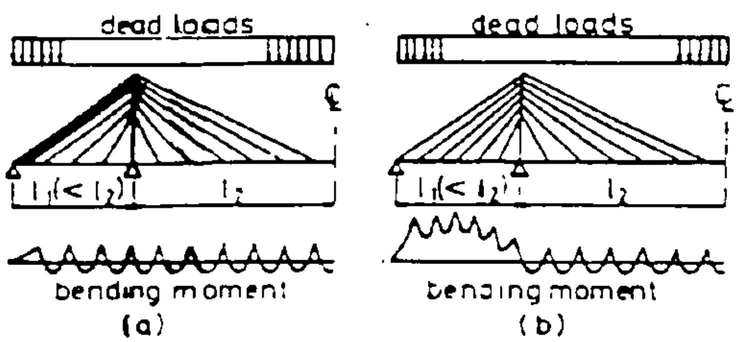

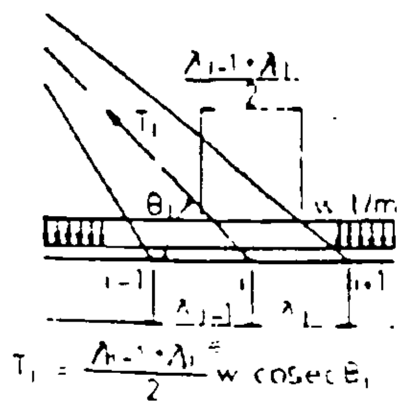

29

Tabla 2-7 Propiedades mecánicas de los torones para puentes recubiertos de zinc

Normas establecidas por la "Wire Rope Technical Board"

Diámetro nominal en plgs.	Resistencia mínima de ruptura en toneladas métricas			Area metálica aproximada en cm²	Peso aproximado en Kg/m
	Clase "A" recubrimiento completo	Clase "A" recubrimiento en los alambres interiores, Clase "B" recubrimiento en los alambres exteriores.	Clase "A" recubrimiento en los alambres interiores, Clase "C" recubrimiento en los alambres exteriores.		
1/2	13.6	13.2	12.9	0.97	0.77
9/16	17.2	16.7	16.4	1.23	0.98
5/8	21.8	21.1	20.7	1.51	1.22
11/16	26.3	25.5	24.9	1.83	1.47
3/4	30.8	29.9	29.3	2.18	1.76
13/16	36.3	35.2	34.5	2.55	2.07
7/8	41.7	40.5	39.6	2.96	2.40
15/16	50.0	47.5	46.5	3.40	2.75
1	55.3	53.7	52.5	3.87	3.13
1 1/16	62.6	60.7	59.4	4.37	3.53
1 1/8	70.8	68.7	67.2	4.90	3.96
1 3/16	78.0	75.7	74.1	5.46	4.40
1 1/4	87.1	85.4	83.6	6.05	4.88
1 5/16	96.2	94.3	92.5	6.65	5.59
1 3/8	105.2	103.4	100.7	7.29	5.91
1 7/16	114.3	111.6	109.8	8.00	6.46
1 1/2	125.2	122.5	119.8	8.71	7.04
1 9/16	136.0	133.4	130.6	9.48	7.63
1 5/8	147.0	144.2	140.6	10.28	8.26
1 11/16	159.7	156.0	153.3	11.03	8.90
1 3/4	170.6	166.9	163.3	11.87	9.57
1 13/16	183.3	179.6	176.0	12.71	10.27
1 7/8	196.0	192.3	187.8	13.61	11.00
1 15/16	208.7	205.0	200.5	14.52	11.74
2	222.3	216.6	215.9	15.48	12.50
2 1/16	236.8	233.2	229.5	16.45	13.30
2 1/8	251.3	247.7	244.0	17.48	14.52
2 3/16	265.8	262.2	257.6	18.52	14.95
2 1/4	281.2	276.7	273.1	19.61	15.83
2 3/8	312.1	322.1	303.0	21.81	17.63
2 5/16	296.7	292.1	287.6	20.71	16.73
2 7/16	326.6	322.1	316.6	23.03	18.57
2 1/2	341.1	335.7	331.1	24.20	19.54
2 9/16	355.6	350.2	344.7	25.41	20.53
2 5/8	378.3	372.9	366.4	26.65	21.53
2 11/16	391.9	385.6	380.0	27.94	22.56
2 3/4	410.1	403.7	397.3	29.29	23.63
2 7/8	448.2	440.9	434.5	32.00	25.83
3	486.1	480.6	471.5	34.84	28.12
1/8	529.8	521.6	513.4	37.81	30.52

DISEÑO DE ELEMENTOS A COMPRESION

Carga critica: $P_{cr} = \pi^2 EI / L^2$. Esfuerzo critico: $\sigma = P_{cr} / A = \pi^2 E / (KL / r)^2$
donde L / r = relación de esbeltez.

Esfuerzo de pandeo:

$$\sigma_{cr} = \frac{\pi^2 E}{(KL / r)^2}$$

pandeo inelástico (columnas cortas)

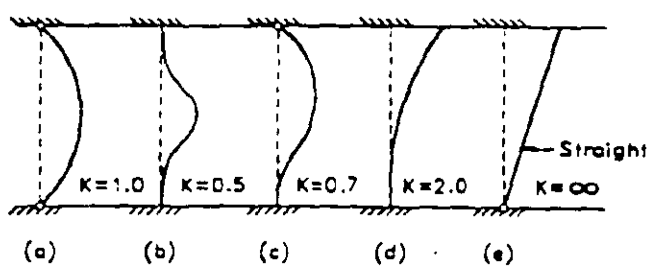

$$\sigma_T = \frac{\pi^2 E_T}{(KL / r)^2}$$

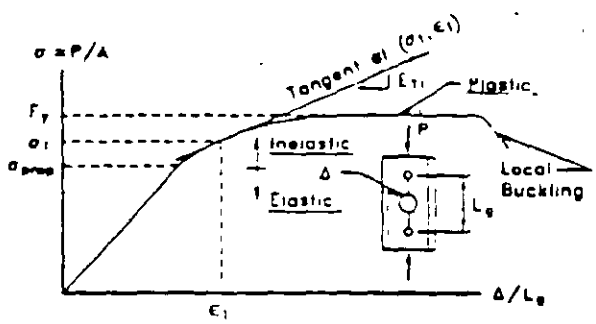

Resistencia a la compresión. Carga de fluencia Py

$$Py = As\,Fy$$

As = área total
Fy = esfuerzo de fluencia

Para columnas largas:

$$Pcr = \frac{\pi^2 EAs}{(KL/r)^2} = \sigma_{cr} As$$

$$\frac{Pcr}{Py} = \frac{1}{\lambda^2}\ ; \quad \text{donde} \quad \lambda = \left(\frac{KL}{\pi r}\right)\sqrt{\frac{Fy}{E}}$$

$$= \left(\frac{KL}{\pi r}\right)^2 \frac{Fy}{E}$$

λ = coeficiente o factor de esbeltez

<u>Resistencia nominal a la compresión</u>

Columnas largas $\lambda \geq 2.25$

$$Pn = 0.88\ Fy\ As/\lambda$$

el factor 0.88 toma en cuenta la curvatura inicial de la columna

Columnas intermedias $\lambda < 2.25$

$$Pn = 0.66^{\lambda}\ Fy\ As$$

Resistencia a la compresión

$$Pr = \varnothing c\ Pn$$

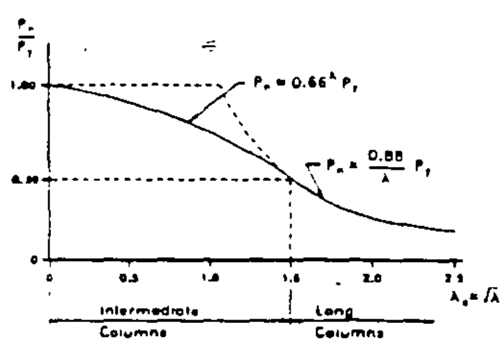

Limiting Width-Thickness Ratios*

Plates Supported Along One Edge	k	b
Flanges and projecting legs of plates	0.56	• Half-flange width of I-sections • Full-flange width of channels • Distance between free edge and first line of bolts or welds in plates • Full-width of an outstanding leg for pairs of angles in continuous contact
Stems of rolled tees	0.75	• Full-depth of tee
Other projecting elements	0.45	• Full-width of outstanding leg for single angle strut or double angle strut with separator • Full projecting width for others
Plates Supported Along Two Edges	**k**	**b**
Box flanges and cover plates	1.40	• Clear distance between webs minus inside corner radius on each side for box flanges • Distance between lines of welds or bolts for flange cover plates
Webs and other plate elements	1.49	• Clear distance between flanges minus fillet radii for webs of rolled beams • Clear distance between edge supports for all others
Perforated cover plates	1.86	• Clear distance between edge supports

*AASHTO Table 6.9.4.2-1. [From *AASHTO LRFD Bridge Design Specifications*, Copyright © 1994 by the American Association of State Highway and Transportation Officials, Washington, DC. Used by permission.]

- Relación ancho-espesor máxima para la sección transversal:

$$\frac{b}{t} \leq k\sqrt{\frac{E}{Fy}}$$

Relación de esbeltez máxima:

elementos principales $KL / r \leq 120$
elementos de contraventeo $KL / r \leq 140$

Ejemplo:

Calcular la resistencia a compresión Øc Pn de una columna con longitud de 610 mm y extremos articulados y las siguientes caracteristicas: As=14100 mm²; d=360 mm; tw=11.4 mm; bf = 256 mm; tf = 19.9mm; hc / tw = 25.3; rx = 153 mm; ry = 62.9 mm (sección I)

$$\left(\frac{KL}{r}\right)_{max} = \frac{1\,(6100)}{62.9} = 97 < 120$$

$$\frac{ancho}{espesor} = \frac{bf}{2tf} = \frac{256}{2(19.9)} = 6.4 < k\sqrt{\frac{E}{Fy}} = 0.56\sqrt{\frac{200000}{250}} = 15.8$$

$$\frac{hc}{tw} = 2.53 < k\sqrt{\frac{E}{Fy}} = 1.49\sqrt{\frac{200000}{250}} = 42.1$$

factor de esbeltez:

$$\lambda = \left(\frac{KL}{\pi r}\right)^2 \frac{Fy}{E} = \left(\frac{97}{\pi}\right)^2 \frac{250}{200000} = 1.19 < 2.25$$

columna intermedia:

$$Pn = 0.66^{\lambda}\,Fy\,As = (0.66)^{1.19}\,(250)\,(14100) = 2.15 \times 10^6\ KN$$

resistencia a compresión:

$$\underline{\varnothing c\, Pc = 0.9\,(2.15 \times 10^6)\,10^3 = 1935\ KN}$$

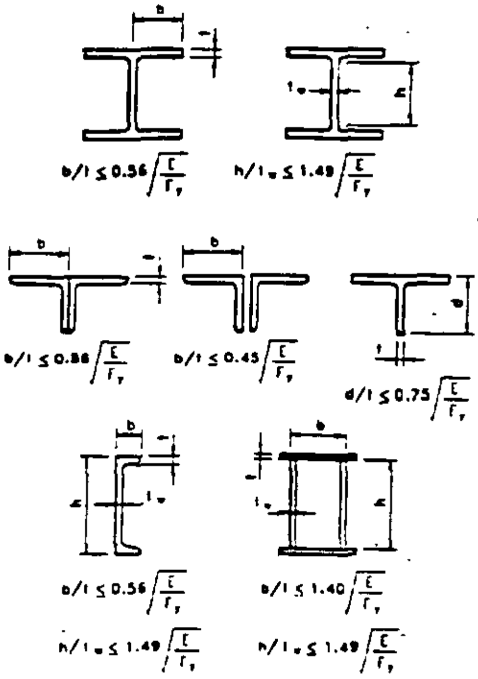

FLEXO-COMPRESION

Ecuaciones de interacción

$$\frac{P}{Pn} + \frac{Mx}{Mnx} + \frac{My}{Mny} \leq 1.0$$

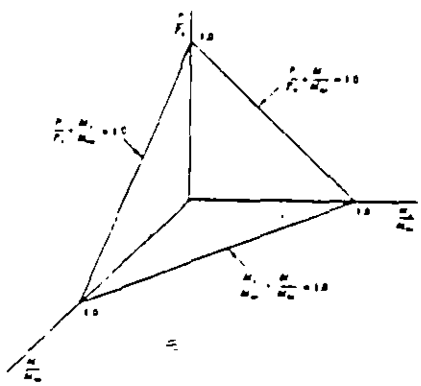

Para $Pu / \varnothing Pn \geq 0.2$

$$\frac{Pu}{\varnothing Pn} + \frac{8Mu}{9\varnothing bNm} = 1.0 \qquad (a)$$

Para $Pu / \varnothing Pn < 0.2$ (b)

$$\frac{Pu}{\varnothing Pn} + \frac{Mu}{\varnothing bNm} = 1.0$$

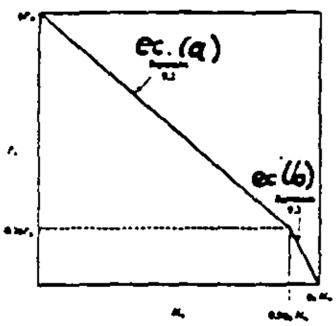

Ejemplo

Diseñar la columna de la figura. Usar una sección W8x24 con las siguientes propiedades geométricas: $A = 7.08\ in^2$; $rx/ry = 2.12$; $rx = 3.42\ in$; $Ix = 82.8\ in^4$; $KLx = KLy = 8$ pies

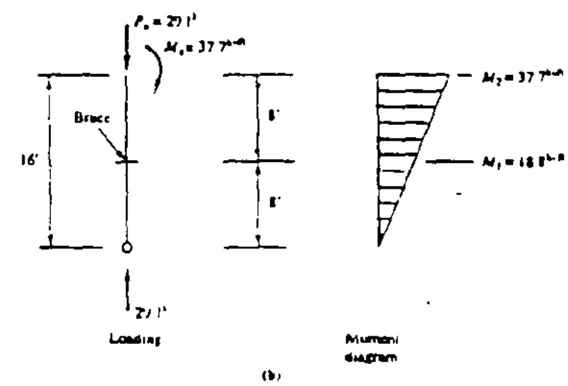

Para esta sección $\varnothing Pn = 180$ Kips > 29.1 Kips

$\varnothing My = 61.0$ Kips-pie para $Lb = 8$ pies

$$Pe = \frac{\pi^2\ EI}{KL^2} = \frac{\pi^2\,(29000)(82.8)}{[8(12)]^2} = 2571\ Kips$$

$$Cm = 0.6 - 0.4\left(\frac{M_1}{M_2}\right) = 0.6 - 0.4\,(-0.5) = 0.8$$

$$B_1 = \frac{Cm}{1 - Pu/Pe} \geq 1.0$$

$$B_1 = \frac{0.8}{1-(29.1/2571)} = 0.81 < 1.0$$

se requiere** $B_1 = 1.0$ **, entonces:

$$Mu_x = B_1 Mx = 1 \times 37.7 = 37.7$$

$$Pu / \varnothing Pn = 29.1 / 180 = 0.16 < 0.2$$

entonces:

$$\frac{Pu}{\varnothing Pn} + \frac{Mu}{\varnothing bMn} = 0.5\,(0.16) + \frac{37.7}{61.0} = 0.7 < 1.0 \quad \checkmark$$

DISEÑO DE SECCIONES I EN FLEXION

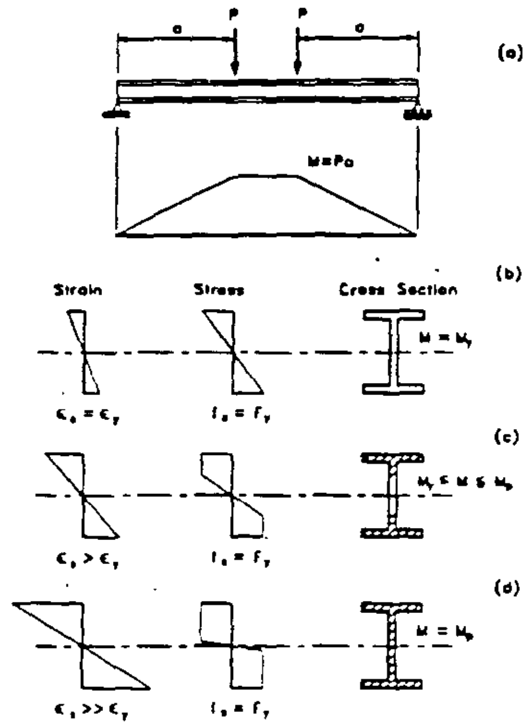

Para una sección sometida a flexión:

$$f = \frac{My}{I}$$

f = esfuerzo a flexión
M = momento flexionante
I = momento de inercia
y = distancia del eje neutro al punto de interés

$$fb = \frac{M}{S}$$

fb = esfuerzo en la fibra extrema

Al aumentar la carga:

$$Mn = Mp = ZFy$$

Z = módulo plástico de la sección
Fy = esfuerzo de fluencia

Según LRFD, el momento resistente es:

$\varnothing Mn = 0.9\ Mn$

Pandeo local

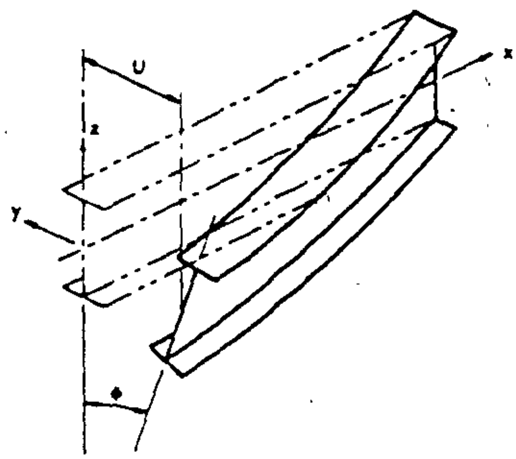

Clacificación de secciones

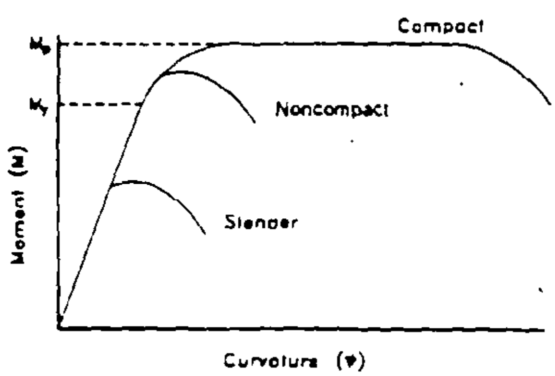

Ejemplo:

Determinar la capacidad a flexión y cortante de una viga de sección I. Suponer acero A36, longitud de 120 pies, longitud sin arriostrar 20 pies, Cb = 1.0 y suponer un espesor de 3/8 in y ¼ in en el alma y las siguientes propiedades geométricas:

a) $tw = 0.375\ in$
$A = 63.5\ in^2$
$Ix = 17039\ in^4$
$Ly = 2563\ in^4$
$Sx = 685\ in^4$
$Zx = 1328\ in^3$
$ry = 6.35\ in$

b) $tw = 0.25\ in$
$A = 57.5\ in^2$
$Ix = 15887\ in^4$
$Ly = 2563\ in^4$
$Sx = 639\ in^4$
$rt = 7.4\ in^3$
$ry = 6.35\ in$

Para la sección a)

Alma:

$$\frac{hc}{tw} = \frac{48}{0.375} = 128 > \frac{640}{\sqrt{36}} = 106.7$$

$$< \frac{970}{\sqrt{36}} = 161.7$$

por lo tanto la sección del alma es no compacta

Pandeo local de los patines:

$$\frac{bf}{2tf} = \frac{26}{2(0.785)} = 14.86 > \frac{65}{\sqrt{36}} = 10.8$$

$$< \frac{106}{\sqrt{36-16.5}} = 24.0$$

La sección de los patines es no compacta, entonces:

$$Mp = \frac{Zx\ Fy}{12} = \frac{1328 \times 36}{12} = 3984\ kip\text{-}pie$$

$$Mr = (Fy - 16.5)\ S = \frac{(36-16.5)\ 685}{12} = 113\ kip\text{-}pie$$

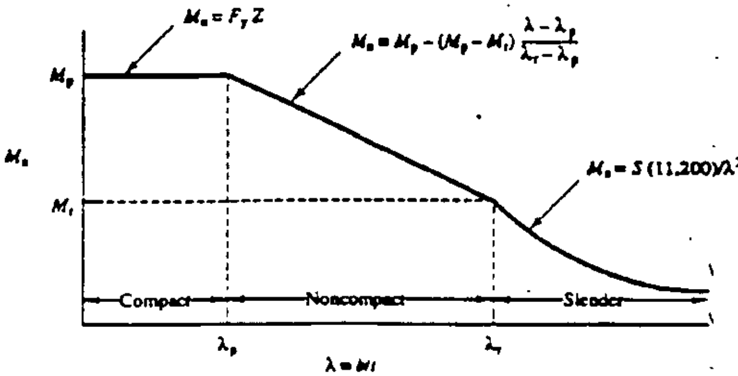

$M_r = (F_y - 16.5)\,S$

$\lambda_p = 65/\sqrt{F_y}$

$\lambda_r = 106/\sqrt{F_y - 16.5}$

Para los patines:

$$\lambda = \frac{bf}{2tf} \;;\quad \lambda p = \frac{65}{\sqrt{Fy}} \;;\quad \lambda r = \frac{106}{\sqrt{Fy}}$$

para el alma:

$$\lambda_p = 640/\sqrt{Fy} \;;\quad \lambda r = 970/\sqrt{Fy}$$

entonces:

$$Mn = 3984 - (3984 - 113)\,\frac{14.86 - 10.8}{24.0 - 10.8} = 3101 \text{ kip-pie}$$

Pandeo local del alma

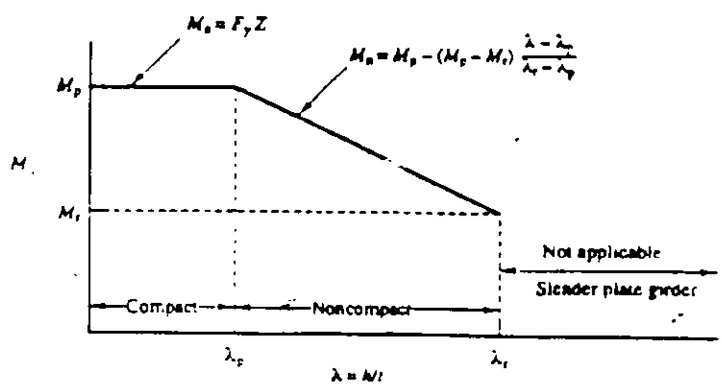

$M_r = F_y S_x$

$\lambda_p = 640/\sqrt{F_y}$

$\lambda_r = 970/\sqrt{F_y}$

$$Mr = \frac{36 \times 685}{12} = 2055 \text{ kip-pie}$$

$$Mn = 3984 - (3984 - 2055)\ \frac{128 - 106.7}{161.7 - 106.7} = 3237 \text{ kip-pie}$$

Pandeo lateral por torsión:

$$Lb / ry = \frac{20 \times 12}{6.35} = 37.8 < \frac{300}{\sqrt{36}} = 50$$

La viga está arriostrada adecuadamente. Entonces:

$$Mn = Mp = 3984 \text{ kip-pie}$$

El menor valor Mn rige, en este caso

$$\underline{Mn = 3101 \text{ kip-pie}}$$

Cortante:

$$Si\ h / tw \leq 187 \sqrt{k / Fy} \Rightarrow \varnothing Vn = \varnothing\, 0.6\, Fy\, Aw$$

$$Si\ h / tw > 187 \sqrt{k / Fy} \Rightarrow \varnothing Vn = \varnothing\, 0.6\, Fy\, Aw\ \frac{187 \sqrt{k / Fy}}{h / tw}$$

$$Si\ h / tw > 234 \sqrt{k / Fy} \Rightarrow \varnothing Vn = \varnothing\, Aw\ \frac{26400\, k}{(h / tw)^2}$$

$$\frac{hc}{tw} = 128 > 234 \sqrt{\frac{k}{Fy}} = 87.2$$

$$\underline{Vn = 18 \left[\frac{26400\ (5)}{128^2} \right] = 145 \text{ kip}}$$

<u>*Para la sección b):*</u>

$$h / tw = 48 / 0.25 = 192 > \frac{970}{\sqrt{36}} = 161.7$$

entonces el alma es compacta

Pandeo lateral por torsión

$$Lb / rt = \frac{20 \times 12}{7.2} = 33.3 < \frac{300}{\sqrt{36}} = 50$$

entonces:

$$Fcr = Fy = 36 \text{ Ksi}$$

$$Rp_G = 1 - 0.0005\, ar \left(\frac{hc}{tw} - \frac{970}{\sqrt{Fcr}} \right) \leq 1.0$$

Rp_G = factor de reducción por pandeo del alma
ar = relación del área del alma y el área a compresión del patin
Fcr = esfuerzo de pandeo crítico:

$$\text{Si } \lambda \leq \lambda p \Rightarrow Fcr = Fy$$

$$\text{Si } \lambda < \lambda \leq \lambda r \Rightarrow Fcr = Cb\, Fy \left[1 - \frac{\lambda - \lambda p}{2(\lambda r - \lambda p)} \right] < Fy$$

$$\text{si } \lambda > \lambda r \Rightarrow Fcr = \frac{Cp_G}{\lambda^2}$$

Para el estado límite de pandeo lateral-torsional:

$$\lambda = \frac{Lb}{rt} \;;\; \lambda p = 300/\sqrt{Fy} \;;\; \lambda r = 756/\sqrt{Fy} \;;\; Cp_G = 286{,}000\, Cp$$

Para el pandeo local de los patines:

$$\lambda = bf/2tf \;;\; \lambda p = 65/\sqrt{Fy} \;;\; \lambda r = 150/\sqrt{Fy} \;;\; Cp_G = 11200 \;;\; Cb = 1.0$$

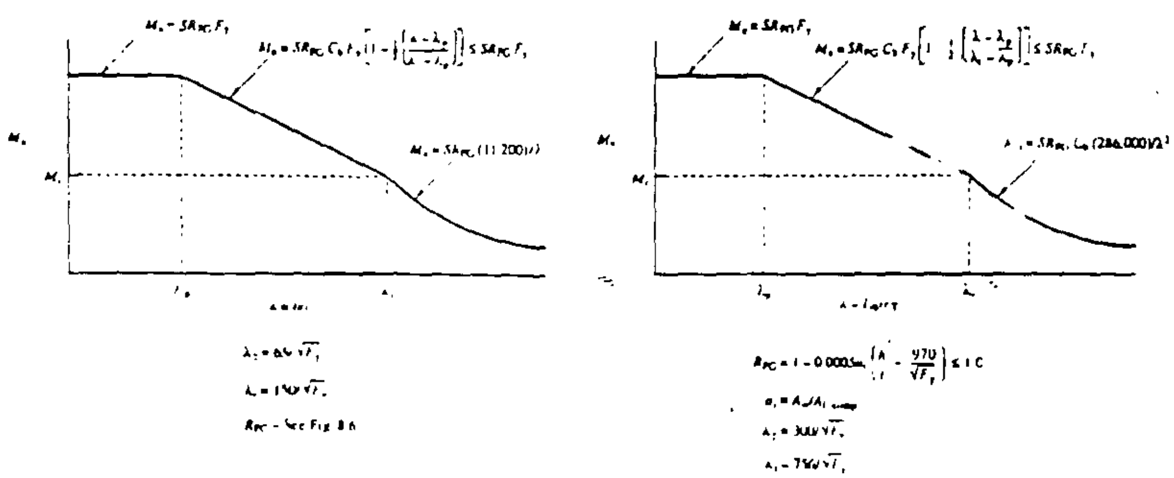

Así:

$$Rp_G = 1 - 0.0005 \left[\frac{48\,(0.25)}{26\,(0.875)} \right] (192 - 161.7) = 0.992$$

$$Mn = Sx\, Rp_G\, Fy = \frac{639\,(0.992)\,(36)}{12} = 1902 \text{ kip-pie}$$

Pandeo de los patines

$$bf / 2\, tf = 14.86 > \frac{65}{\sqrt{36}} = 10.8$$

$$< \frac{150}{\sqrt{36}} = 25$$

entonces:

$$Fcr = (1)\,(36)\,[\,1 - \frac{14.86 - 10.8}{2(25-10.8)}\,] = 30.85$$

$$Rp_G = 1 - 0.0005\,[\,\frac{48\,(0.25)}{26\,(0.875)}\,]\,(\,192 - \frac{970}{\sqrt{30.85}} = 0.995$$

$$Mn = \frac{639\,(0.995)\,(36)}{12} = 1907 \text{ kip-pie}$$

entonces:

$$\underline{Mn = 1902 \text{ kip-pie}}$$

Cortante:

$$hc / tw = 192 > 234\sqrt{k/Fy} = 87$$

$$\underline{Vn = 48\,(0.25)\,[\,\frac{26400\,(5)}{192^2}\,] = 43 \text{ kips}}$$

CONEXIONES

Ejemplo

Determinar el tamaño y número de remaches y pernos requeridos en la siguiente conexión. Usar remaches A502 grado 2 y pernos A490 de alta resistencia y acero A36.

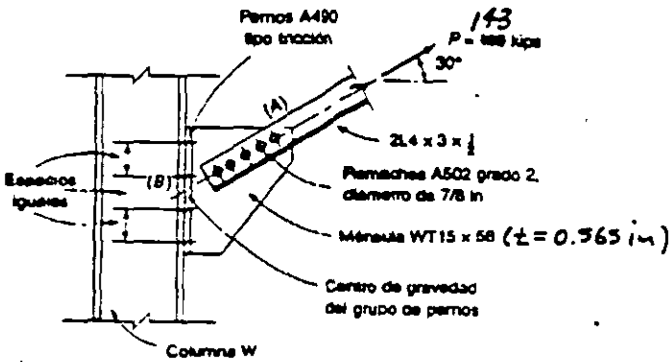

Remaches de 7/8 in de diámetro:

$$\text{núm. de remaches} = \frac{P_U}{2\phi F_v A_b} = \frac{143}{2(0.75)(33)(0.601)} = 4.8 \approx 5 \text{ remaches}$$

Resistencia al aplastamiento:

$\phi = 0.75$; $d = 7/8$ in ; $t = 0.565$ in (espesor ménsula)

$F_U = 58$ ksi ; $R_u = 2.4\, d t\, F_v = 68.8$ kips

$$\text{núm. de remaches} = \frac{P_U}{\phi R_n} = 2.7 < 5 \checkmark$$

Conexión con pernos ménsula-columna.

Suponiendo que la carga a tensión pasa por el centro de gravedad de los pernos, los componentes de tensión son:

tensión $\quad T = P\cos 30^\circ = 110 \times 0.866 = 95.3$ kips

cortante $\quad V = P\,\text{sen}\, 30^\circ = 110 \times 0.5 = 55$ kips

remaches con $d = 7/8$ in ; $A_b = 0.601\, in^2$; $F_v = 21$ Ksi ; $\phi = 1.0$; $T_b = 49$ kips (pre-tensión)

Para 8 pernos en cortante:

$$R_n = 8\phi F_v A_b \left(1 - \frac{T}{8T_b}\right) = 76.4 \text{ Kips}$$

$$\phi R_n = 76.4 \text{ Kips} > 55 \text{ kips} \checkmark$$

CONEXIONES

Ejemplo

Diseñar la conexión usando soldadura de filete de 7/16 in y electrodos E70.Resistencia de diseño de la soldadura qa=9.73 kips/in

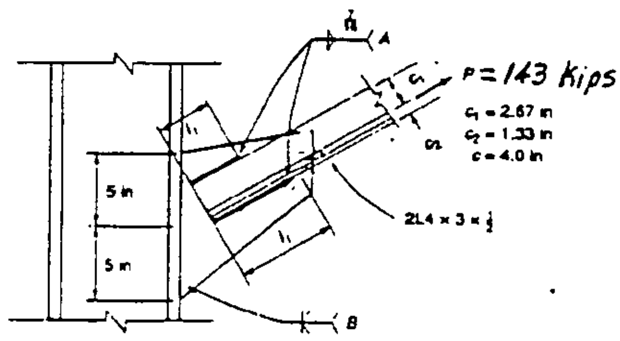

Longitud de la soldadura:

$$\ell = P/q_a = 143/2/9.73 = 7.35 \text{ in}$$

$$\ell_1 = C_2 \ell / C = 1.33 \times 7.35/4 = 2.44 \text{ in} \approx 2.5 \text{ in}$$

$$\ell_2 = C_1 \ell / C = 2.67 \times 7.35/4 = 4.91 \text{ in} \approx 5.0 \text{ in}$$

CONEXIONES

Ejemplo

Calcular el número y tamaño de pernos A325 de la mensula de la figura

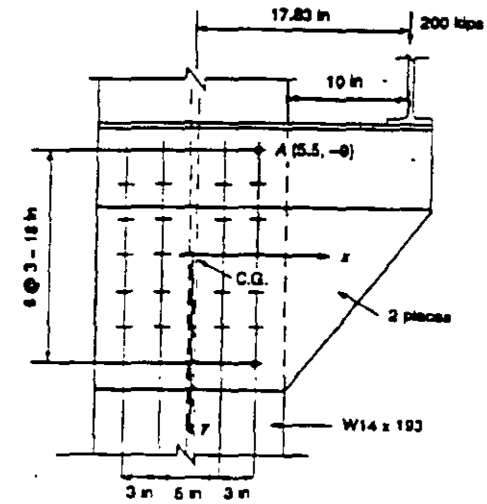

Suponiendo 7 pernos espaciados a cada 3 pulgadas en cada Línea vertical

$$P_x = 0 \; ; \; P_y = 200/2 = 100 \text{ Kips}$$
$$M = 100 \times 17.83 = 1783 \text{ Kips-in}$$
en cada placa
$$n = 7 \times 4 = 28 \text{ pernos}$$

El perno A es el más esforzado. Por estática, las componentes sobre el perno son:

$$R_x = 10.56 \text{ kips / perno}$$
$$R_y = 10.05 \text{ kips / perno}$$
$$R_A = \sqrt{R_x^2 + R_y^2} = 14.56 \text{ kips / perno}$$

Para pernos de 3/4 in :

$$\phi F_v A_b = 0.75(48)(0.442) = 15.9 \text{ kips / perno} > R_A \checkmark$$

BIBLIOGRAFIA

Barker R.M. y Puchett J.A. , " Desig of highway bridges ", Wiley Interscience, Nueva York, 1997.

Bresler B., Lin T.Y., y Scalzi J.B., "Design of steel structures", John Wiley and Sons, Nueva York, 1968

"Constructional steel desig, an international guide", Editado por Dowling P.J., Harding J.E., y Bjorhorde R., Elsevier Applied Science, 1992.

Geschwinder L., Disque R.O. y Bjorhorde R., "Load and resistence factor design for steel structures", Prentice Hall, 1994.

Kulak G.L., Fisher J.W., y Struik J.H.A., "Guide to design criteria for bolted and riveted joints", 2ª. Ed Wiley, Nueva York, 1987.

McGuire W., "Steel structures", Pretince Hall Inc, 1969.

Schnider J., "Introduction to safety and reliability of structures", IABSE, Structural Engineering Documents 5, 1997.

Strength Limit State—Noncomposite *I*-Sections in Positive and Negative Flexure $R_h = 1.0$

	Compact	Noncompact	Slender
Nominal flexural resistance	$M_n = M_p$	$F_n = R_b F_{yc}$	$F_n \le R_b F_{yc}$
Web slenderness	$\frac{2D_{cp}}{t_w} \le 3.76\sqrt{\frac{E}{F_{yc}}}$	Without longitudinal stiffeners $\frac{2D_c}{t_w} \le 6.77\sqrt{\frac{E}{f_c}}$ With longitudinal stiffeners $\frac{2D_c}{t_w} \le 11.63\sqrt{\frac{E}{f_c}}$	If $L_b > L_r$ $\frac{2D_c}{t_w} \le \lambda_b\sqrt{\frac{E}{F_{yc}}}$ (See Eq 8.81 for λ_b)
Compression flange slenderness	$\frac{b_f}{2t_f} \le 0.382\sqrt{\frac{E}{F_{yc}}}$	$\frac{b_f}{2t_f} \le 1.38\sqrt{\frac{E}{f_c\sqrt{\frac{2D_c}{t_w}}}}$	$\frac{b_f}{2t_f} \le 2.52\sqrt{\frac{E}{F_{yc}\sqrt{\frac{2D_c}{t_w}}}}$ (See [A6 10.5 6])
Compression flange bracing	$L_b \le \left[0.124 - 0.0759\left(\frac{M_l}{M_p}\right)\right]\left(\frac{r_y E}{F_{yc}}\right)$	$L_b \le L_p = 1.76 r_t\sqrt{\frac{E}{F_{yc}}}$	$L_r = \sqrt{\frac{2\pi^2 I_{yc} d}{S_{xc}}\frac{E}{F_{yc}}}$ $L_p < L_b \le L_r$ Use Eq 8 113 $L_b > L_r$ Use Eq 8 110

Nominal Shear Resistance of Stiffened Webs

	Compact	Noncompact
Nominal shear resistance	If $M_u \le 0.5\phi_f M_p$	If $f_u \le 0.75\phi_f F_y$
	$V_n = V_p\left[C + \frac{0.87(1-C)}{\sqrt{1+(d_o/D)^2}}\right]$	
	If $M_u > 0.5\phi_f M_p$	If $f_u > 0.75\phi_f F_y$
	$V_n = RV_p\left[C + \frac{0.87(1-C)}{\sqrt{1+(d_o/D)^2}}\right] \ge CV_p$	
Reduction factor	$R = 0.6 + 0.4\frac{(M_r - M_u)}{(M_r - 0.75\phi_f M_y)} \le 1.0$	$R = 0.6 + 0.4\frac{(F_r - f_u)}{(F_r - 0.75\phi_f F_y)} \le 1.0$

Ratio of Shear Buckling Stress to Shear Yield Strength

	No Buckling	Inelastic Buckling	Elastic Buckling
Web Slenderness	$\frac{D}{t_w} \le 1.10\sqrt{\frac{Ek}{F_{yw}}}$	$\frac{D}{t_w} \le 1.38\sqrt{\frac{Ek}{F_{yw}}}$	$\frac{D}{t_w} > 1.38\sqrt{\frac{Ek}{F_{yw}}}$
$C = \frac{\tau_{cr}}{\tau_y}$	$C = 1.0$	$C = \frac{1.10}{D/t_w}\sqrt{\frac{Ek}{F_{yw}}}$	$C = \frac{1.52}{(D/t_w)^2}\frac{Ek}{F_{yw}}$

Nominal Shear Resistance of Unstiffened Webs

	No Buckling	Inelastic Buckling	Elastic Buckling
Web slenderness	$\frac{D}{t_w} \leq 2.46\sqrt{\frac{E}{F_{yw}}}$	$\frac{D}{t_w} \leq 3.07\sqrt{\frac{E}{F_{yw}}}$	$\frac{D}{t_w} > 3.07\sqrt{\frac{E}{F_{yw}}}$
Nominal shear resistance	$V_n = V_p$	$V_n = 1.48t_w^2\sqrt{EF_{yw}}$	$V_n = \frac{4.55t_w^3E}{D}$

FACULTAD DE INGENIERIA U.N.A.M.
DIVISION DE EDUCACION CONTINUA

CURSOS ABIERTOS

INSTITUTO MEXICANO DEL TRANSPORTE

XXV CURSO INTERNACIONAL DE INGENIERÍA SÍSMICA

MÓDULO III. DISEÑO SÍSMICO DE PUENTES

TEMA :

DISEÑO SÍSMICO DE PUENTES
(ACERO. PARTE II)

EXPOSITOR: DR. JOSÉ ALBERTO ESCOBAR SÁNCHEZ
PALACIO DE MINERÍA
SEPTIEMBRE 1999

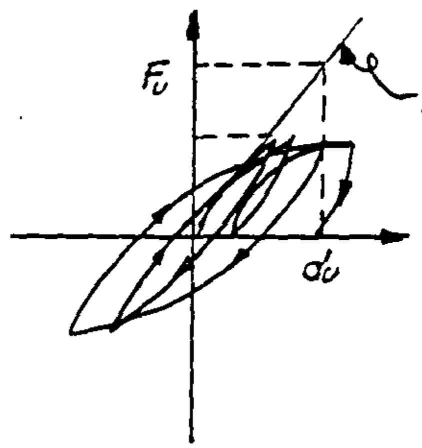

ANALISIS ELASTICO

- La solución satisface la condición de equilibrio
- Se basa en la rigidez de los elementos estructurales
- Como solución se obtiene:
  distribución de fuerzas y desplazamientos
  magnitud de fuerzas y desplazamientos

Fuentes de error
- estimación de la magnitud de las rigideces
- suposición de rigideces constantes

Observación: los resultados del análisis elástico deben ser utilizados con cuidado

ANALISIS NO LINEAL

Objetivo fundamental: Hacer una mejor modelación del comportamiento estructural para obtener una respuesta más realista.

NECESITAMOS EL ANALISIS NO LINEAL?

- Con análisis elástico → demanda de resistencia → diseño
- Con análisis no lineal → demanda de deformación → revisión del diseño

De gran utilidad para:

- investigación
- evaluación de estructuras después de grandes sismos
- revisión de estructuras de gran importancia (revisión del diseño)
- diseño estructural donde las no linealidades están bien definidas (estructuras con disipadores de energía, aisladores sísmicos, etc).
- cada vez más utilizado para el análisis y evaluación de estructuras convencionales.
- predicción de daño estructural
    - local
    - global

METODOS DE ANALISIS NO LINEAL

- Estático o cuasiestático (incremental al colapso)
  permite conocer la capacidad o demanda de deformación plástica

- Dinámico (paso a paso)
  permite determinar la historia de la respuesta sísmica de la estructura (desplazamientos, deformaciones, fuerzas, aceleraciones, etc) <u>ante registros sísmicos específicos</u>

ANALISIS PASO A PASO

Solución de la ecuación de equilibrio en análisis dinámico

$$m\ddot{x} + c\dot{x} + kx = f \qquad (1)$$

donde:

m, c, k son las matrices de masas, amortiguamiento y rigideces
f es la fuerza externa (aceleración del suelo)
$x, \dot{x}, \ddot{x}$ desplazamiento, velocidad y aceleración.

Métodos de integración directa $\rightarrow$ busca resolver un problema de valores iniciales discreto en el tiempo

Observación: si no fuera de valores iniciales sería de valores en la frontera

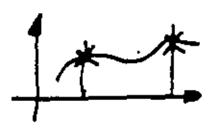

$\leftarrow$ condiciones en los extremos del intervalo de cálculo o integración

La solución buscada es la función

$$x(t)$$

para todo tiempo t que satisfaga la ec (1) y las condiciones iniciales

$$x(0) = d$$
$$\dot{x}(0) = v$$

donde los vectores d, v son datos.

Ejemplo: sistema de dos gdl acoplado

$$\begin{bmatrix} m_{11} & 0 \\ 0 & m_{22} \end{bmatrix} \begin{Bmatrix} \ddot{x}_1 \\ \ddot{x}_2 \end{Bmatrix} + \begin{bmatrix} c_{11} & c_{12} \\ c_{21} & c_{22} \end{bmatrix} \begin{Bmatrix} \dot{x}_1 \\ \dot{x}_2 \end{Bmatrix} + \begin{bmatrix} k_{11} & k_{12} \\ k_{21} & k_{22} \end{bmatrix} \begin{Bmatrix} x_1 \\ x_2 \end{Bmatrix} = \begin{Bmatrix} f_1 \\ f_2 \end{Bmatrix}$$

desarrollando:

$$\left.\begin{aligned} m_{11}\underline{\ddot{x}_1} + c_{11}\underline{\dot{x}_1} + c_{12}\underline{\dot{x}_2} + k_{11}\underline{x_1} + k_{12}\underline{x_2} &= f_1 \\ m_{22}\underline{\ddot{x}_2} + c_{21}\underline{\dot{x}_1} + c_{22}\underline{\dot{x}_2} + k_{21}\underline{x_1} + k_{22}\underline{x_2} &= f_2 \end{aligned}\right\} \text{en las dos ecuaciones intervienen los 2 gdl}$$

sistema de dos gdl desacoplado

$$\begin{bmatrix} m_{11} & 0 \\ 0 & m_{22}\end{bmatrix}\begin{Bmatrix}\ddot{x}_1\\ \ddot{x}_2\end{Bmatrix} + \begin{bmatrix} c_{11} & 0\\ 0 & c_{22}\end{bmatrix}\begin{Bmatrix}\dot{x}_1\\ \dot{x}_2\end{Bmatrix} + \begin{bmatrix}k_{11} & 0\\ 0 & k_{22}\end{bmatrix}\begin{Bmatrix}x_1\\x_2\end{Bmatrix} = \begin{Bmatrix}f_1\\f_2\end{Bmatrix}$$

desarrollando

$$m_{11}\underline{\ddot{x}_1} + c_{11}\underline{\dot{x}_1} + k_{11}\underline{x_1} = f_1$$

$$m_{22}\underline{\ddot{x}_2} + c_{22}\underline{\dot{x}_2} + k_{22}\underline{x_2} = f_2$$

Los métodos de integración directa se basan en las ideas siguientes:

① Se encuentra la solución en cada intervalo de tiempo Δt, buscándose el equilibrio para los puntos discretos en el tiempo t_i

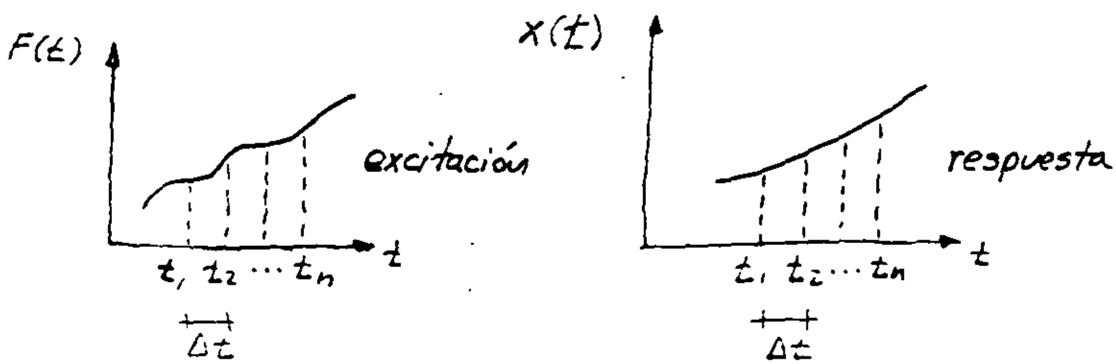

② La variación de los desplazamientos, velocidades y aceleraciones se calcula para cada intervalo de tiempo Δt, por lo que se tendrá una solución, esto es:

$$x = 0,\ \Delta t,\ 2\Delta t, \ldots\ t+\Delta t, \ldots\ t_{total}$$

③ La variación de la aceleración en cada intervalo de tiempo se supone lineal

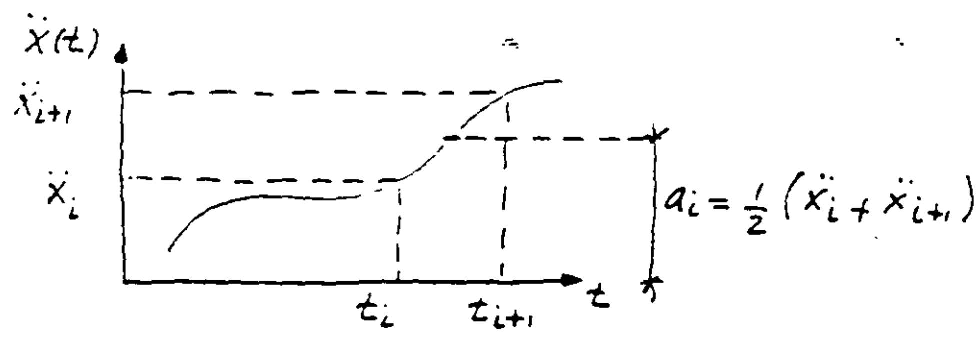

La aceleración en el intervalo t_i a t_{i+1} se toma como el promedio de los valores iniciales y finales, esto es:

$$\ddot{x}(t) = \frac{1}{2}(\ddot{x}_i + \ddot{x}_{i+1})$$

Integrando la ec. anterior:

$$\dot{x}_{i+1} = \dot{x}_i + \left(\frac{\Delta t_i}{2}\right)(\ddot{x}_i + \ddot{x}_{i+1})$$

$$x_{i+1} = x_i + \dot{x}_i \Delta t + \left(\frac{\Delta t_i^2}{4}\right)(\ddot{x}_i + \ddot{x}_{i+1})$$

haciendo:

$$x_{i+1} = x_i + \Delta x_i$$

$$\dot{x}_{i+1} = \dot{x}_i + \Delta \dot{x}_{i+1} \qquad (a)$$

$$\ddot{x}_{i+1} = \ddot{x}_i + \Delta \ddot{x}_{i+1}$$

sust. en las ecs. anteriores y combinándolas se obtiene:

$$\Delta \ddot{x}_i = \left(\frac{4}{\Delta t_i^2}\right)(\Delta x_i - \dot{x}_i \Delta t) - 2\ddot{x}_i \qquad (b)$$

$$\Delta \dot{x}_i = \left(\frac{2}{\Delta t}\right)\Delta x_i - 2\dot{x}_i \qquad (c)$$

En cada instante de tiempo t_i y t_{i+1} se debe cumplir el equilibrio, esto es:

$$m\Delta \ddot{x}_i + c\Delta \dot{x}_i + k\Delta x_i = \Delta f$$

sust. y agrupando en esta ec. se obtiene:

$$k_i^* \Delta x_i = \Delta f_i^* \qquad (d)$$

donde:

$$k_i^* = k + \left(\frac{2c}{\Delta t}\right) + \left(\frac{4m}{\Delta t^2}\right)$$

y:

$$\Delta f_i^* = \Delta f + \left[\left(\frac{4m}{\Delta t}\right) + 2c\right]\dot{x}_i + 2m\ddot{x}_i$$

Procedimiento

- obtener Δx_i de la ec. (d)
- obtener $\Delta \dot{x}_i$ de la ec. (c)
- obtener $\Delta \ddot{x}_i$ de la ec (b)
- actualizar x, $\dot{x}$ y $\ddot{x}$ en la ec. (a)

Método de Newmark
(integración constante)

DETERMINACION DEL TAMAÑO DEL PASO DE INTEGRACION Δt

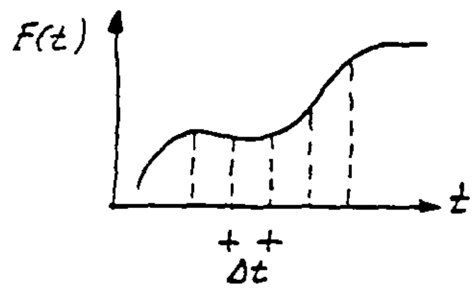

Se recomienda usar el menor valor del intervalo de digitización del registro sísmico (0.01 ó 0.02 s) o una fracción del periodo fundamental de vibración p.ej. $T/10$.

Observación

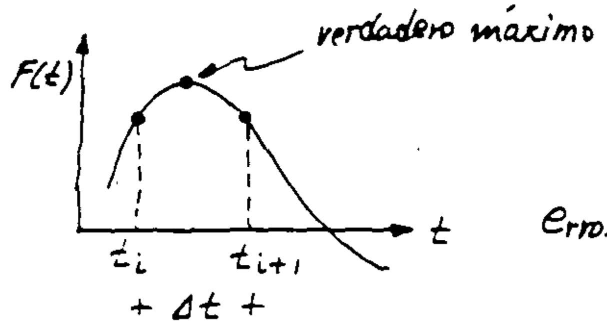

para una función aproximadamente senoidal:

$$error_{máx} = \left(1-\cos\frac{\pi\Delta t}{T}\right)\times 100$$

$\Delta t = T/10 \longrightarrow e_{máx} = 4.9\ \%$

$\Delta t = T/20 \longrightarrow e_{máx} = 1.2\ \%$

$\Delta t = T/40 \longrightarrow e_{máx} = 0.3\ \%$

además:

estabilidad → propagación de errores numéricos

convergencia → la solución linealizada tiende a la solución verdadera

En análisis no lineal además :

$$k(x(t))$$

Modelos histeréticos

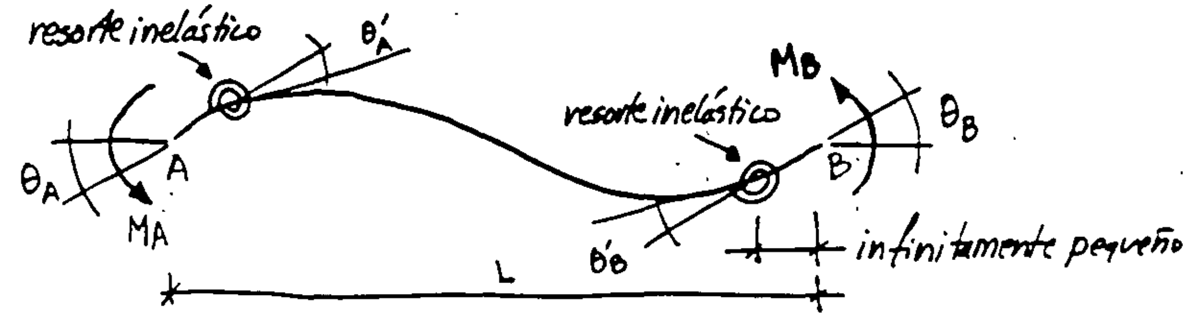

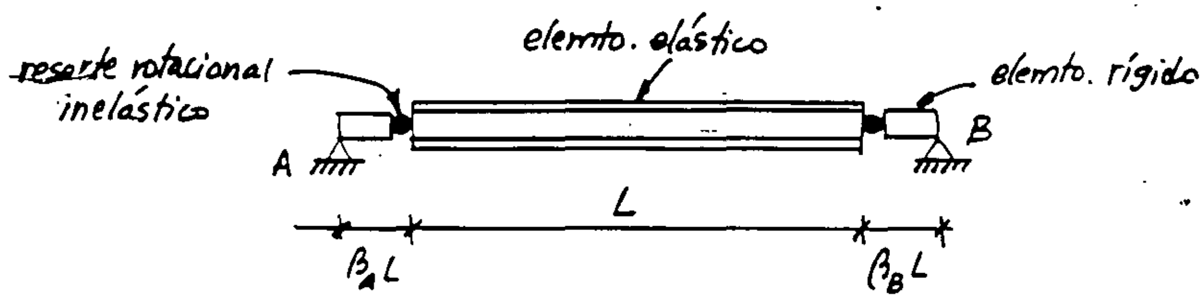

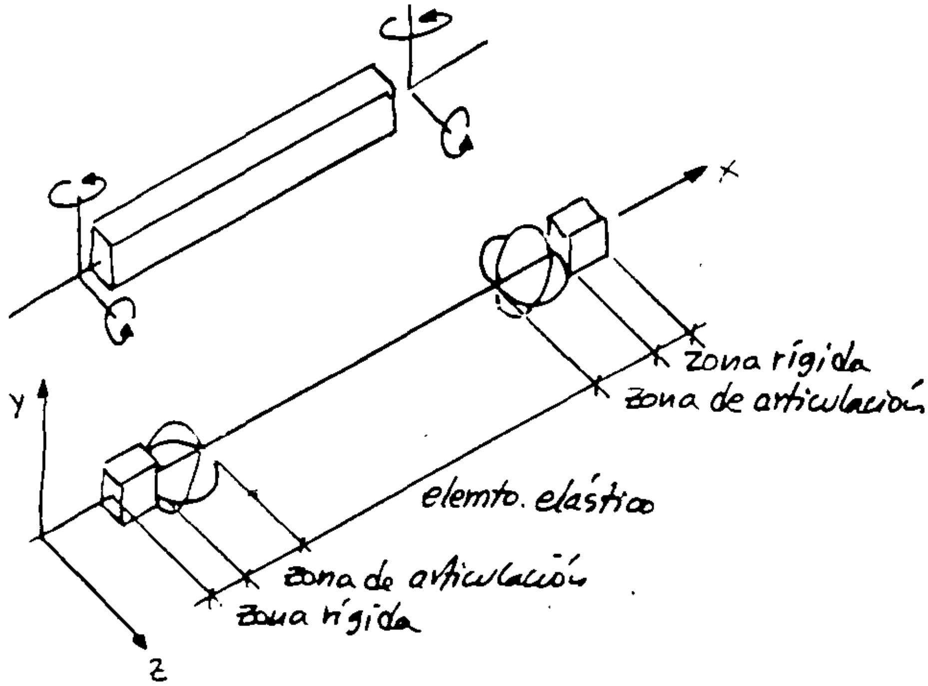

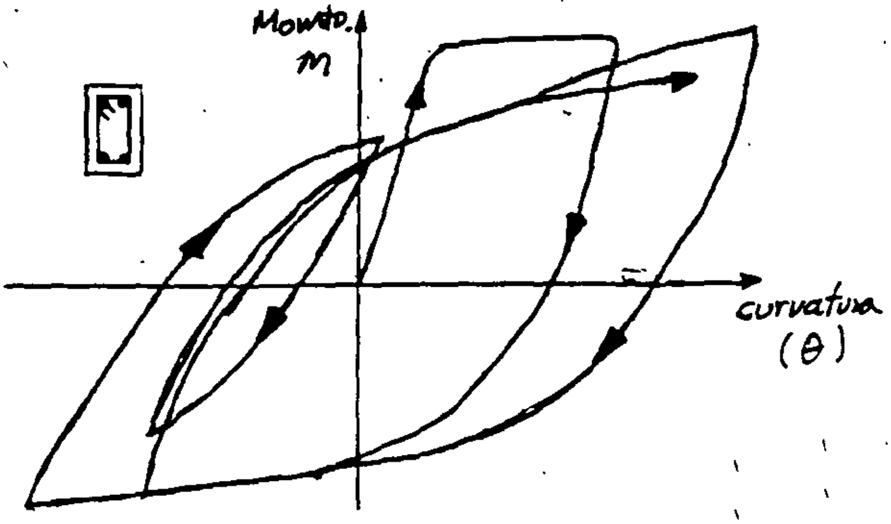

Momto.
M
curvatura
(θ)

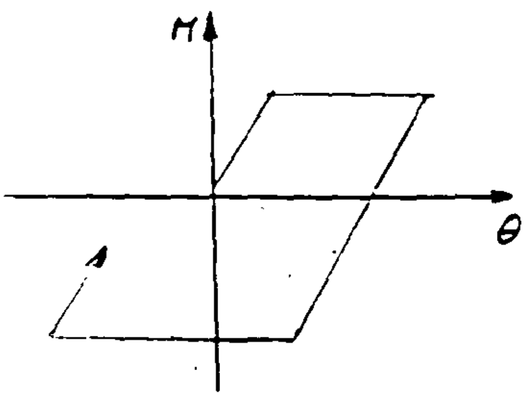

M
θ

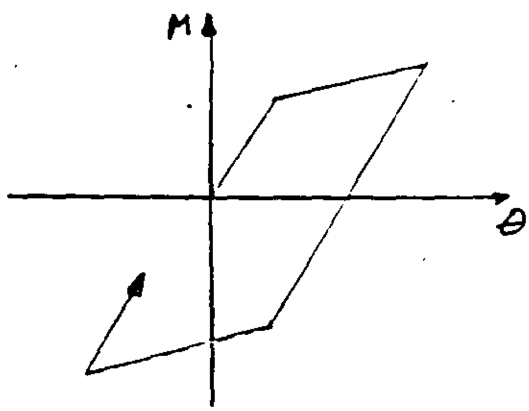

M
θ

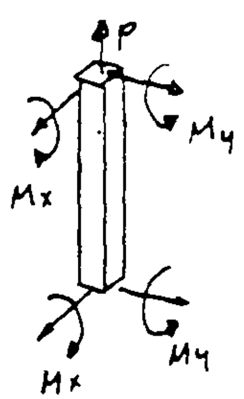

P
My
Mx
My
Mx

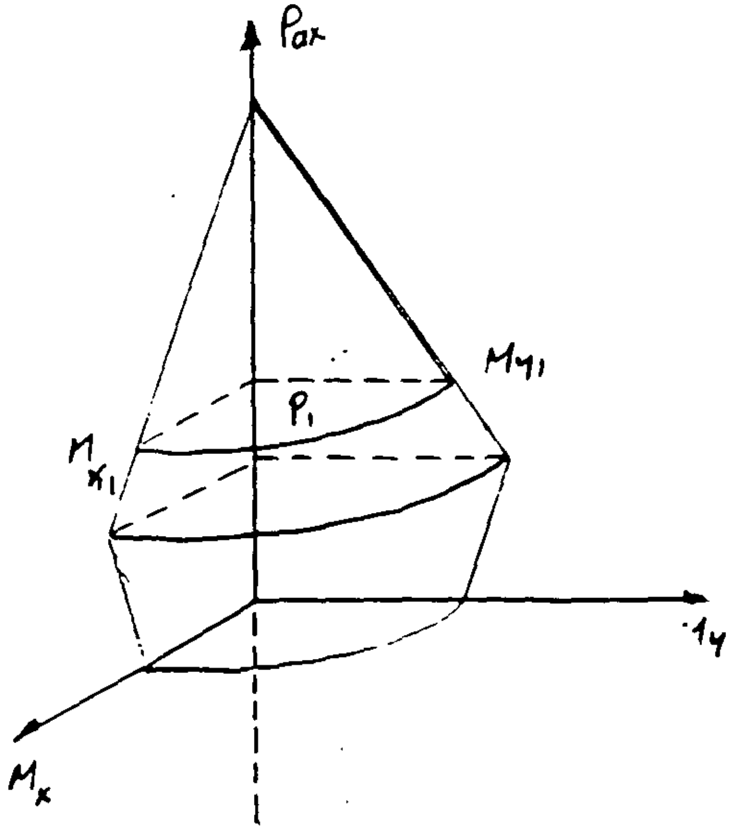

Pax
My1
P1
Mx1
Mx

4.3 Degrading Bilinear Model

Yielding stiffness:

Rule 2. $K_2 = \beta' K_0$, Rule 3: $K_3 = \beta K_1$

Where, β, β' are the stiffness factor after yielding.

Unloading stiffness:

Rule 4. $K_4 = K_0\left(\dfrac{d'_y}{d'_m}\right)^{\gamma}$, Rule 5. $K_5 = K_0\left(\dfrac{d_y}{d_m}\right)^{\gamma}$

Hysteresis parameter 1: γ, from 0 to 0.4.
Hysteresis parameter 2: dummy.

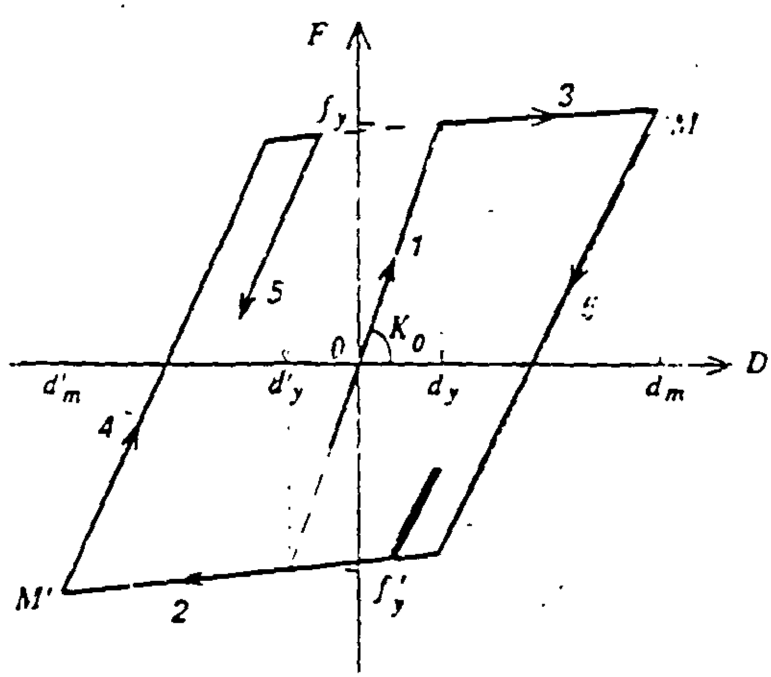

Fig.B-2 Degrading Bilinear Model

B.6 Takeda-Rule Bilinear Model

Rule 2,3 Yielding primary curve

$K_2 = \beta' K_0$, $K_3 = \beta K_0$, β, β': stiffness factor after yielding

Rule 4,5 Unloading curve

Unloading of outside loop: $K_4 = K_0\left(\frac{d'_y}{d'_m}\right)^{\gamma}$; $K_5 = K_0\left(\frac{d_y}{d_m}\right)^{\gamma}$.

Unloading of internal loop: $K'_4 = \xi \cdot K_4$, $K'_5 = \xi \cdot K_5$.

Hysteresis parameter 1: γ, from 0 to 0.4.
Hysteresis parameter 2: ξ, from 0.8 to 1.0.

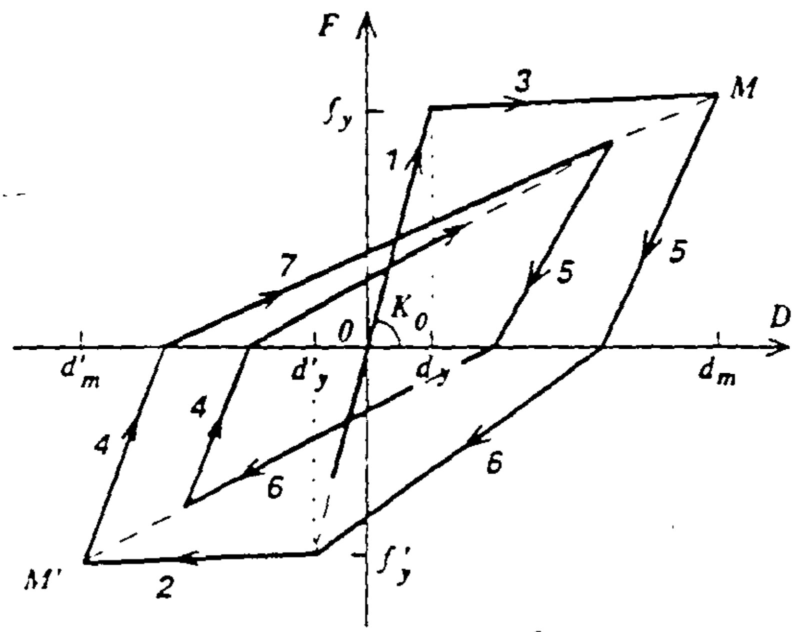

Fig.B-6 Takeda-Rule Bilinear Model

B.7 Takeda-Rule Trilinear Model

Rule 2.3: After cracking. $K_2 = \alpha' \cdot K_0$. $K_3 = \alpha \cdot K_0$. α, α' :cracking stiffness factor

Rule 6.7. Yielding. $K_6 = \beta' \cdot K_0$. $K_7 = \beta \cdot K_0$. β. β': yielding stiffness factor.

Rule 8.9.12.13. Unloading curve.

Unloading from primary curve before yielding:

$$K_8 = \begin{cases} K_5 & |f'_p| < |f_p| \\ \dfrac{f'_p - f_c}{d'_p - d_c} & |f'_p| \ge |f_p| \end{cases}; \qquad K_9 = \begin{cases} K_4 & |f_p| < |f'_p| \\ \dfrac{f_p - f'_c}{d_p - d'_c} & |f_p| \ge |f'_p| \end{cases}$$

Unloading from primary curve after yielding:

$$K_8, K_{12} = \frac{f'_y - f_c}{d'_y - d_c}\left(\frac{d'_y}{d'_m}\right)^{\gamma}; \quad K_9, K_{13} = \frac{f_y - f'_c}{d_y - d'_c}\left(\frac{d_y}{d_m}\right)^{\gamma}.$$

Unloading of interior loop: $K'_8 = \xi' \cdot K_8$; $K'_9 = \xi \cdot K_9$.

Hysteresis parameter 1: γ, from 0 to 0.4.
Hysteresis parameter 2: ξ, from 0.8 to 1.0.

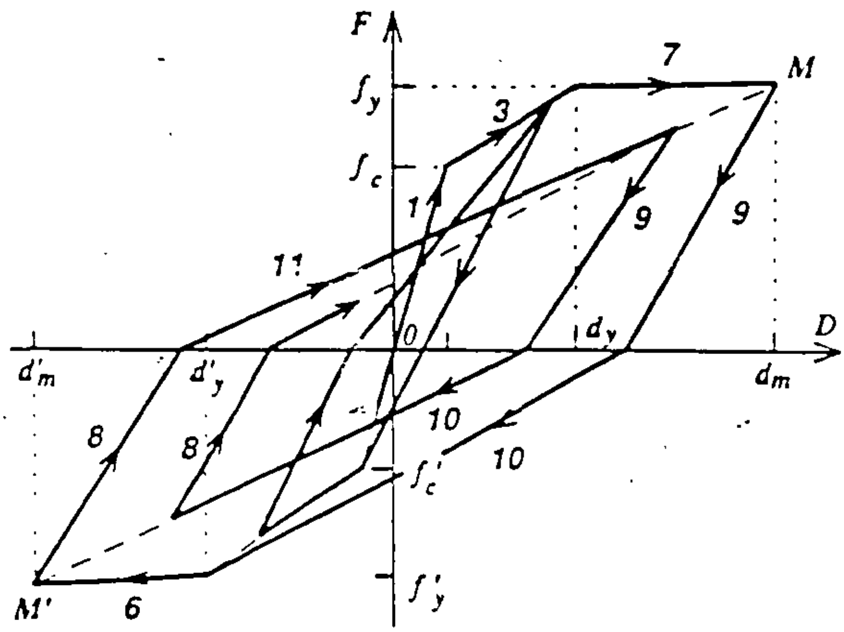

Fig.B-7 Takeda-Rule Trilinear Model

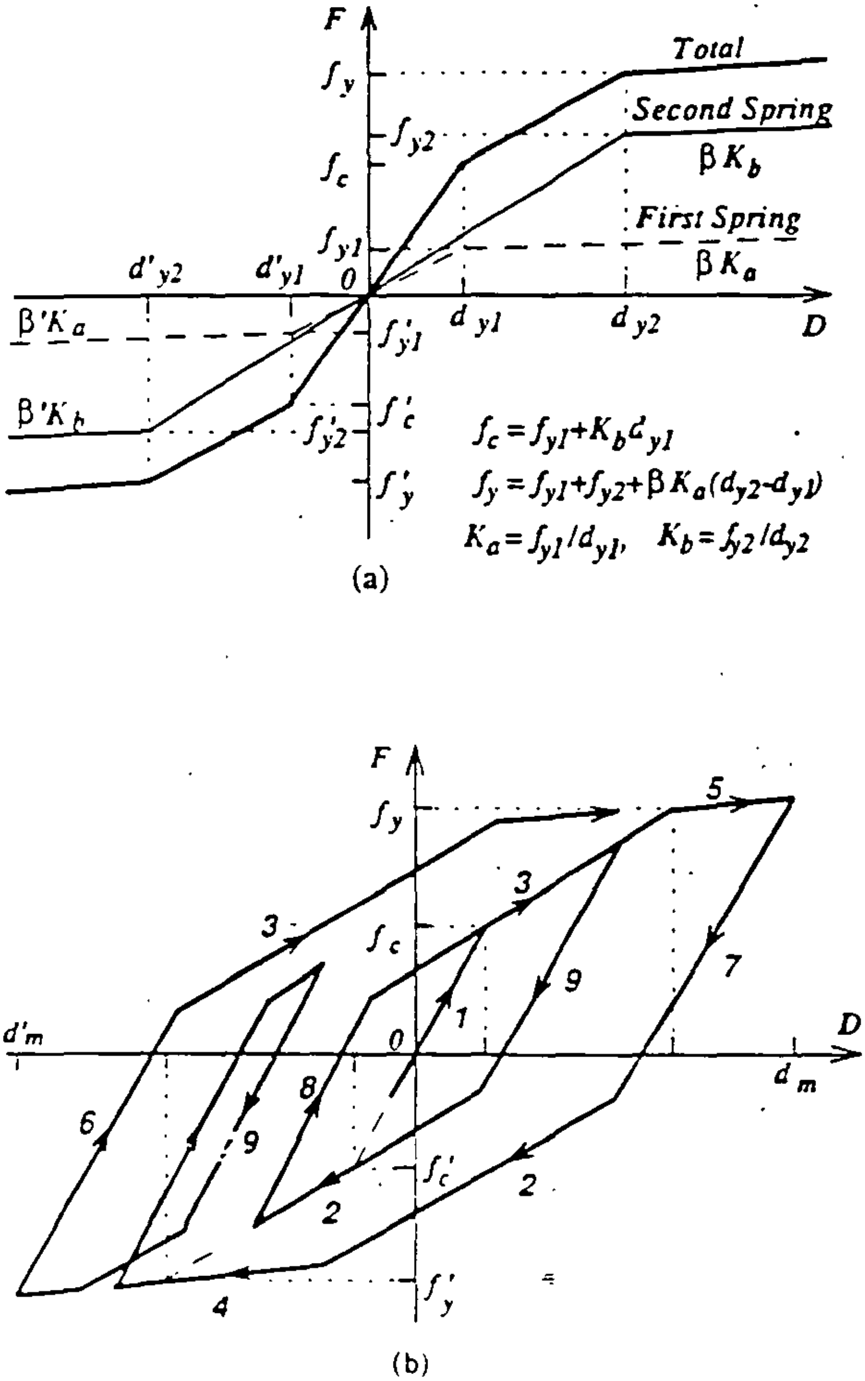

Fig. B-13 Double Degrading Bilinear Model

B.13 Axial Stiffness Model 1

Rule 1: Compression elastic stage.

Rule 2: Tension cracking. $K_2 = \alpha \cdot K_0$ (α: about 0.5).

Rule 3: Tension yielding. K_3 K_0 (β: about 0.001).

Rule 4.9: Tension unloading. $K_4 = \dfrac{f_c - f_m}{d_c - d_m}$, $K_9 = K_4$.

where, f_m, d_m: tensile peak point, f_c, d_c: oriented-point C for elastic loading under compression displacement, $f_c = \gamma \cdot |f_y|$, $d_c = f_c / K_0$.

Rule 5: Loading towards compression. $K_5 = \begin{cases} K_2 & |d_m| \le |d_y| \\ K_2 \dfrac{(f_c - f_m)(d_c - d_y)}{(f_c - f_y)(d_c - d_m)} & |d_m| > |d_y| \end{cases}$

Rule 6: Elastic compression. Loading pass through point C.

Rule 7: Loading towards tension. $K_7 = K_4$.

Rule 8: Tension reloading towards peak point (f_m, d_m).

Hysteresis parameter 1: γ about 2.0, to define point C.
Hysteresis parameter 2: dummy.

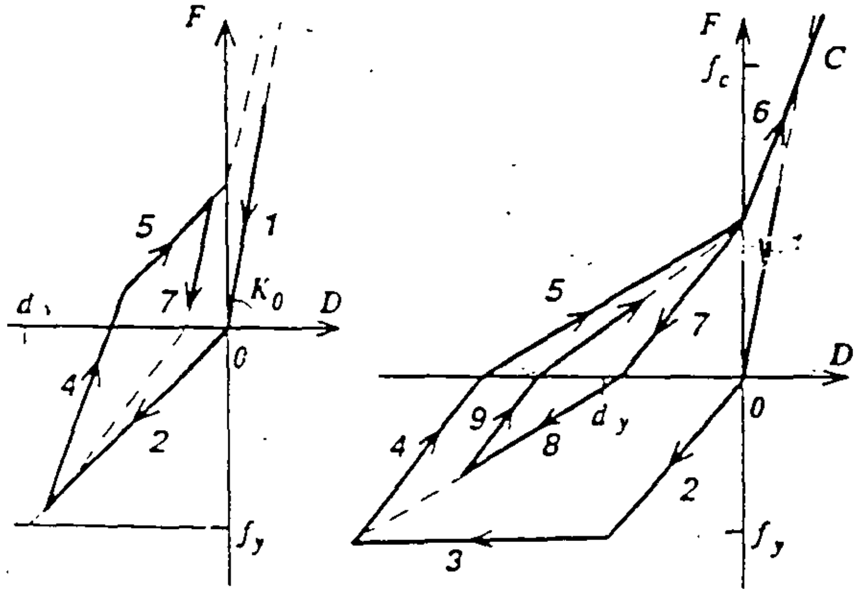

Fig. B-16 Axial Stiffness Model 1

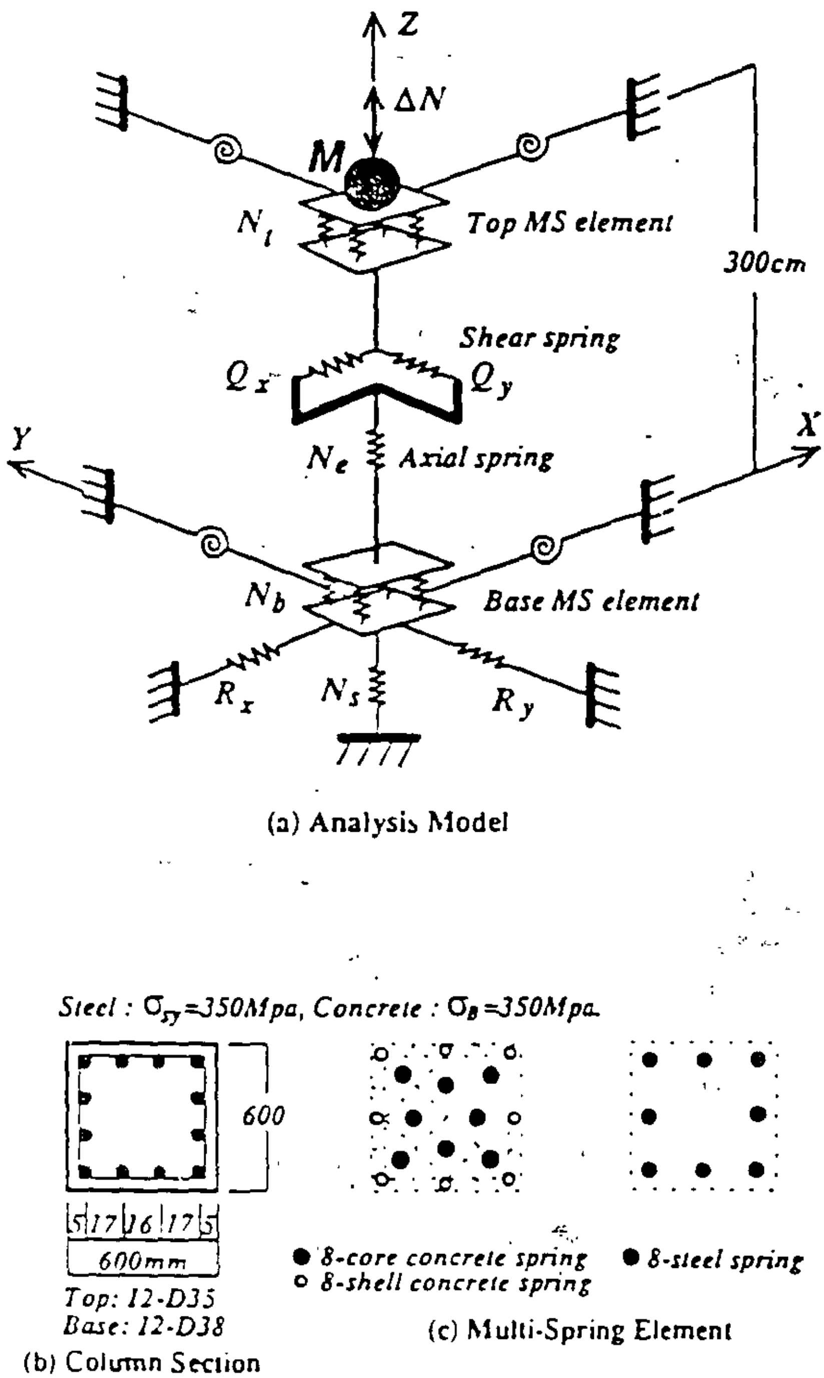

Fig. F-1 Example 1: Analysis Model of One-Column

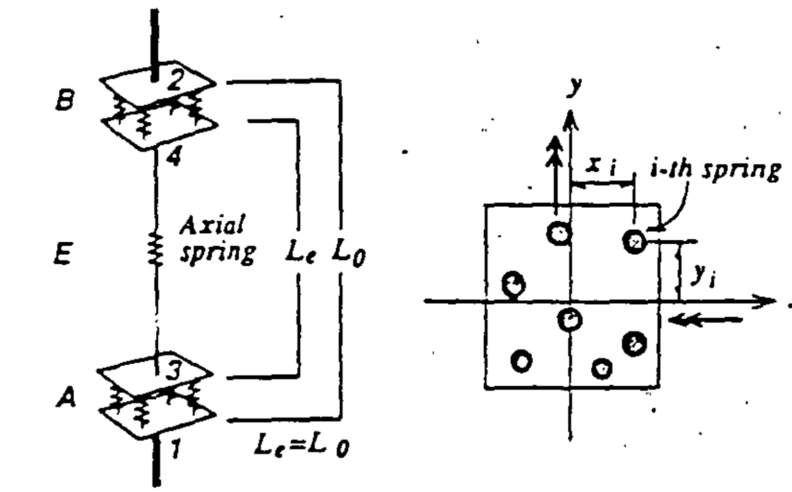

(a) Idealization of Column (b) Inelastic Element

A,B : Multi-spring inelastic elements;
E Elastic element with nonlienar axial spring

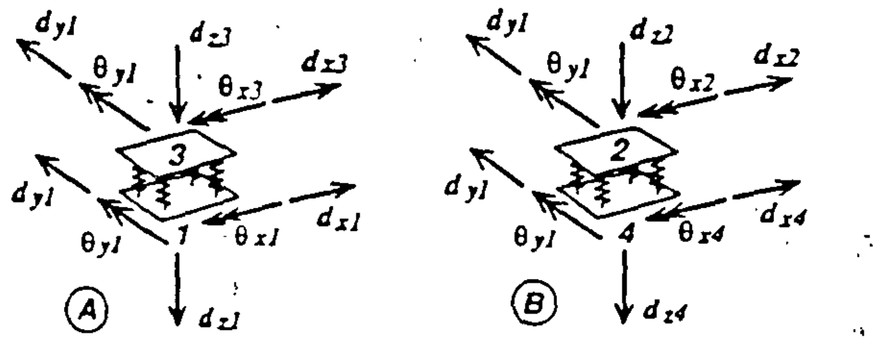

(c) Base Multi-spring Element (b) Top Multi-spring Element

Fig. C-1 Multi-Spring Model for Column Member

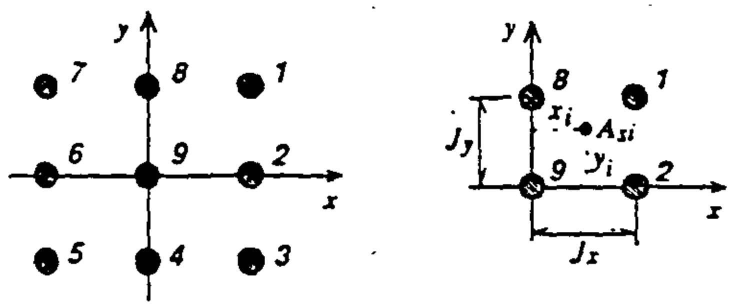

$$A_1 = \frac{X_i Y_i}{J_x J_y/4} A_{si}, \qquad A_8 = \frac{(J_y/2 - X_i)Y_i}{J_x J_y/4} A_{si},$$

$$A_2 = \frac{X_i (J_y/2 - Y_i)}{J_x J_y/4} A_{si}, \qquad A_9 = \frac{(J_x/2 - X_i)(J_y/2 - Y_i)}{J_x J_y/4} A_{si}.$$

(a) Steel Springs

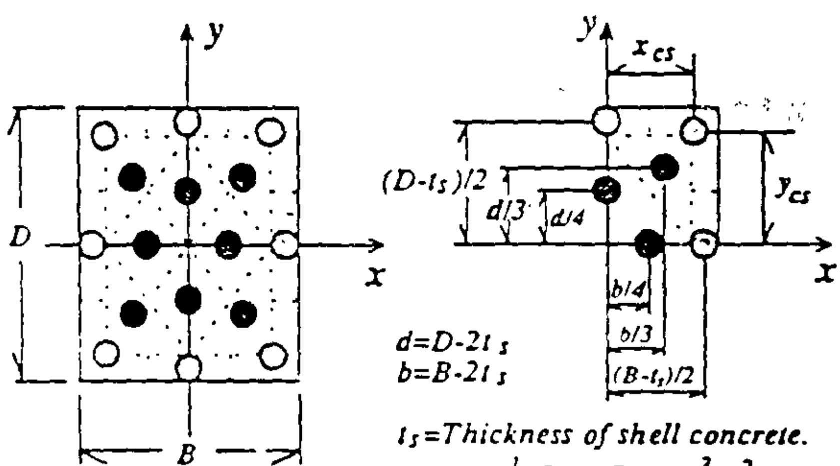

t_s=*Thickness of shell concrete.*

$$x_{cs} = \frac{\frac{1}{2}(B-t_s)(D-t_s) + \frac{3}{8}B^2}{B+D}$$

$$y_{cs} = \frac{\frac{1}{2}(B-t_s)(D-t_s) + \frac{3}{8}D^2}{B+D}$$

○ *Shell concrete spring*
● *Core concrete spring*

(b) Concrete Springs and Location

Fig. C-2 Division of Rectangular Symmetrical RC Section

RESULTADOS DE ANALISIS NO LINEAL

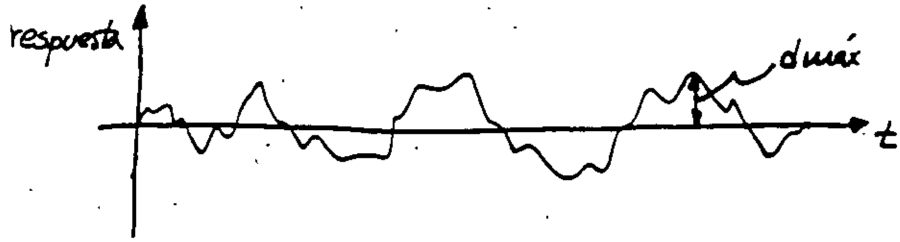

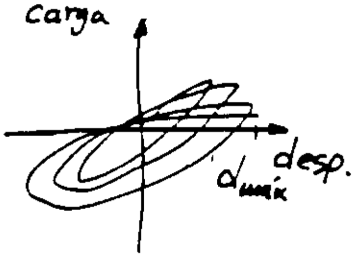

$$\mu = \frac{d_{máx}}{d_y}$$

Observación :

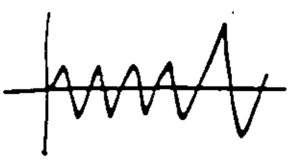

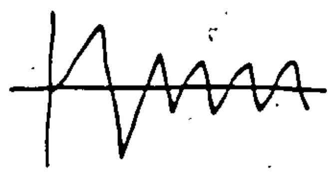

E_h = energía histerética

DAÑO ESTRUCTURAL, QUE ES?

aproximaciones:

i) demanda - capacidad

resistencia
desplazamiento / deformación
disipación de energía

2) degradación

rigidez
resistencia
disipación de energía